Design, Synthesis and Characterization of a Series of Self-assembling Polypeptides

by

Bushra Siddique

A thesis
Presented to the University of Waterloo
In fulfillment of the
Thesis requirement for the degree of
Doctor of Philosophy
in
Chemistry

Waterloo, Ontario, Canada, 2007

I hereby declare that I am the sole author of this thesis. This is a true copy of the thesis, including any required final revisions, as accepted by my examiners.

I understand that my thesis may be made electronically available to the public.

Abstract

A series of polypeptides with well-defined sequences, $(Asp_3Phe_1)_n$, $(Asp_2Phe_1)_n$, $(Asp_1Phe_1)_n$, $(Asp_1Phe_2)_n$, and $(Asp_1Phe_3)_n$, containing the hydrophilic amino acid, aspartic acid (Asp) and the hydrophobic amino acid, phenylalanine (Phe), were synthesized. Their behaviour in aqueous solution was investigated by performing fluorescence quenching and non-radiative energy transfer (NRET) experiments which were complemented by dynamic (DLS) and static (SLS) light scattering. The photophysical properties of the polypeptides were dependent on their Phe content. An increase in the Phe content led to an increase in the extinction coefficient, fluorescence quantum yield, and fluorescence average lifetime of the polypeptides. Circular dichroism experiments revealed that except for the $(Asp_1Phe_3)_n$ polypeptide, which adopts an α–helical conformation in aqueous solution, the other polypeptides did not adopt any known conformation in solution. The fluorescence quenching studies performed using molecular pyrene physically bound to the polypeptide via hydrophobic interactions resulted in protective quenching for the $(Asp_1Phe_1)_n$, $(Asp_1Phe_2)_n$, and $(Asp_1Phe_3)_n$ polypeptides, with some pyrenes having a lifetime of ~300 ns. Evidence for protective quenching was also observed in the polypeptides richer in Phe, when pyrene was covalently attached onto the polypeptides. However pyrene was found to be fully exposed to the quencher solution for the more hydrophilic polypeptides. The presence of NRET between a naphthalene labeled polypeptide and a pyrene labeled polypeptide for the $(Asp_1Phe_2)_n$ and $(Asp_1Phe_3)_n$ polypeptides and its absence for the $(Asp_3Phe_1)_n$, $(Asp_2Phe_1)_n$, and $(Asp_1Phe_1)_n$ polypeptides led to the conclusion that those polypeptides richer in Phe generate interpolymeric aggregates which provide protection to a hydrophobic cargo like molecular pyrene whereas the hydrophilic polypeptides exist predominantly as unimolecular micelles.

These results were confirmed by DLS and SLS experiments.

Acknowledgements

I would like to express my gratitude and appreciation to Professor Jean Duhamel, my supervisor for his guidance and help throughout the course of my graduate program. I will forever be grateful to him for the support and patience that he has given me.

I am indebted to the members of my thesis advisory committee, Professor Susan Mikkelsen, Professor France-Isabelle Azanneau, and Professor Mario Gauthier for their feedback and useful suggestions. Particular thanks are due to Professor Mario Gauthier for his valuable comments and suggestions which have been very helpful to the development of this project. I would also like to thank all the helpful people whom I have dealt with during my stay here. These include the Department secretarial staff, the technicians and the people at the Chemistry Stores.

I would like to acknowledge some of the funding agencies which have made it possible for me to come to Canada in the pursuit of higher education. The Ministry of Science and Technology, Government of Pakistan for providing me a TROSS scholarship for 4 years. To the University of Waterloo and the Department of Chemistry for granting me admission and use of their facilities and NSERC for their financial support. My employers back home who gave me a study leave and their blessing to improve my qualifications, which are greatly appreciated.

I take this opportunity to thank the members of the Duhamel group both past and present, especially Christine Keyes-Baig, Mark Ingratta and Howard Siu and to the co-op students, Thomas O'Brien and Jimmy De Leon, who assisted me in various aspects of my project, for creating a pleasant work environment. Their help and suggestions during my project have been greatly appreciated. It has been a pleasure to know them all as they have

made my stay here both pleasant and very informative. The members of the Gauthier group also deserve a special thank you.

Finally I would like to thank each and every member of my family. Without their love and encouragement it would not have been possible for me to get through these past five years. My sister, Naila, who helped me get settled here at the University and then took over the family responsibility back home, deserves my eternal gratitude. My mother and sister Asma both of whom passed away during my stay here are greatly missed.

To my late parents

and

sister Asma

Table of Contents

List of Tables

List of Schemes

List of Figures

List of Symbols and Acronyms

A	Acceptor molecule
A_2	Second virial coefficient obtained from light scattering measurements
AP	Amphiphilic polymers
Asp	Aspartic acid
a.u.	arbitrary units
CD	Circular dichroism
cmc	Critical micelle concentration
CTAB	Cetyl trimethylammonium bromide
D	Donor molecule
D	Translational diffusion coefficient
DCC	Dicyclohexylcarbodiimide
DCU	Dicyclohexyl urea
DDS	Drug delivery systems
DLS	Dynamic light scattering
DMF	*N*,*N*-Dimethylformamide
DMSO	Dimethylsuphoxide
EDC	1-Ethyl-3-(3-dimethylaminopropyl)carbodiimide
E_{ET}	Efficiency of energy transfer
ESI	Electrospray ionizer
f_a	Fraction of pyrenes accessible to the quencher
FRET	Fluorescence resonance energy transfer
GS	Ground state
HASE	Hydrophobically modified alkali-swellable emulsions
HEUR	Hydrophobically modified ethoxylated urethane
HHHs	Hexagonally packed hollow hoops

HMPE	Hydrophobically modified polyelectrolytes
HMWSPs	Hydrophobically modified water-soluble polymers
HOBt	1-Hydroxybenzotriazole
HOSu	*N*-Hydroxysuccinimide
I_0	Fluorescence intensity without the quencher
I_1	Fluorescence intensity of the first peak of the pyrene monomer
I_1/I_3	Ratio of the fluorescence intensity of the first-to-third peak
I_3	Fluorescence intensity of the third peak of the pyrene monomer
I_D	Fluorescence intensity of the donor in the presence of the acceptor
I_{D0}	Fluorescence intensity of the donor in the absence of the acceptor
I_E	Pyrene excimer fluorescence intensity
I_E/I_M	Excimer-to-monomer fluorescence intensity ratio
I_M	Pyrene monomer fluorescence intensity
I_{Np}	Fluorescence intensity of naphthalene
I_{Np}/I_{Py}	Ratio of naphthalene fluorescence intensity-to-pyrene fluorescence intensity
I_{Py}	Fluorescence intensity of pyrene
I_Q	Fluorescence intensity with the quencher
k	Rate constant of radiationless decay
k_{ET}	Energy transfer rate constant
k_Q	Collisional quenching rate constant
K_S	Static equilibrium constant
LCMs	Large compound micelles
LCVs	Large compound vesicles
MSA	Methane sulphonic acid
MW	Molecular weight
M_w	Weight-average molecular weight
NCAs	N-carboxyanhydrides

NMM	*N*-Methylmorpholine
NMR	Nuclear magnetic resonance
Np	Naphthalene
NRET	Non-radiative energy transfer
OD	Optical density
PCP	Pentachlorophenol
Phe	Phenylalanine
PNP	*p*-Nitrophenol
ppm	Parts per million
Py	Pyrene
Py^*	Excited pyrene
$(PyPy)^*$	Excited pyrene excimer
Q	Fluorescence quantum yield
$[Q]$	Quencher concentration
r	Distance between the donor and acceptor molecules
R_0	Förster radius
RES	Reticuloendothelial system
SANS	Small angle neutron scattering
SAXS	Small angle X-ray scattering
SDS	Sodium dodecylsulphate
SLS	Static light scattering
SMA	Styrene maleic anhydride copolymers
TEA	Triethylamine
TEM	Transmission electron microscopy
TFA	Trifluoroacetic acid
THF	Tetrahydrofuran
TLC	Thin layer chromatography

χ^2	Chi-square value evaluating the goodness of the fit of the fluorescence decays with a given equation
δ	Chemical shift
ε	Extinction coefficient
η	Viscosity
Γ	Emissive rate constant of chromophore
λ_{em}	Emission wavelength
λ_{ex}	Excitation wavelength
τ	Excited lifetime of chromophore
$<\tau>$	Average lifetime of chromophore
τ_0	Natural lifetime of chromophore
τ_D	Lifetime of donor molecule
τ_E	Lifetime of the excimer
τ_M	Lifetime of the monomer
τ_Q	Lifetime with the quencher
$[\theta]$	Molar ellipticity

Chapter 1
Introduction

The aim of this chapter is to give a short review of the basics of the self-assembly of macromolecules and of the resulting supramolecular structures. The first part of the chapter gives examples of molecules that are known to undergo self-assembly such as surfactants, block copolymers, hydrophobically modified polymers, and polypeptides. The synthesis of these molecules is also briefly described. This is followed by a discussion on structures generated by these self-assembling macromolecules in drug delivery, it being one of the most medically relevant applications of these systems. The next section outlines the various experimental techniques used in this study, with particular emphasis on fluorescence. The last two sections present the project objective and the thesis outline.

1.1. Self-assembly

In recent years, molecular self-assembly has attracted considerable attention for its use in the design and fabrication of nanostructures leading to the development of advanced materials.[1-4] The key to self-assembly lies in the design and synthesis of macromolecules that organize themselves into desired patterns and functions. Along with chemical composition and functionality, the molecular architecture of the macromolecules is the main factor that affects the resulting self-assembled structures.[5-9] In particular, systems that operate in aqueous media have been subject to intense research.[10-15] This is mostly because many devices must be biocompatible, which implies that they must function in aqueous solutions. Over the past few years, new approaches for mimicking cell surfaces or generating biocompatible and bioactive drug delivery systems have been developed.[16,17] One recent development takes advantage of polymeric systems with an enhanced biofunctionality, such as amphiphilic copolymers that can act as mimetics for biological membranes.[18] Because

there are virtually no limits to combinations of monomers, biological and synthetic building blocks, ligands, receptors and other proteins, polymer hybrid materials show a great promise for applications in biomedicine and biotechnology.[19,20] Thus the self-assembly of biomolecular building blocks plays an increasingly important role in the discovery of new materials and scaffolds with a wide range of applications in nanotechnology and medical technologies such as regenerative medicine and drug delivery.[21,22]

1.2. Self-assembling systems

Surfactants, lipids, and copolymers are self-assembling molecules whose assemblies exhibit a broad range of properties and applications which are under intense scrutiny.[3,23-26] These materials are used in various technological formulations such as paints, coatings, inks, foodstuff and drug delivery in the form of micelles, vesicles, and other types of dispersed aggregates. The importance of these systems for drug delivery applications has increased during the past decade as a result of many new candidate drugs being sparingly soluble in water.[26-29] Hence a solubilizing delivery system is frequently required to enable sufficient drug bioavailability and/or to facilitate clinical or even preclinical research and development.

1.2.1. Surfactants

Surfactant molecules are composed of a polar hydrophilic head, and a non polar hydrophobic tail.[30] This dual nature endows the surfactants with their unique solution and interfacial characteristics. In aqueous solution, surfactant molecules self-assemble to form aggregates via the association of their hydrophobic tails. Depending upon the type of surfactant and solution conditions, the aggregates may be spherical, globular or rodlike

micelles or spherical bilayers.[31,32] The closed aggregates with hydrophobic interiors are known as micelles whereas the spherical bilayers containing an encapsulated aqueous phase are called vesicles (Figure 1.1).

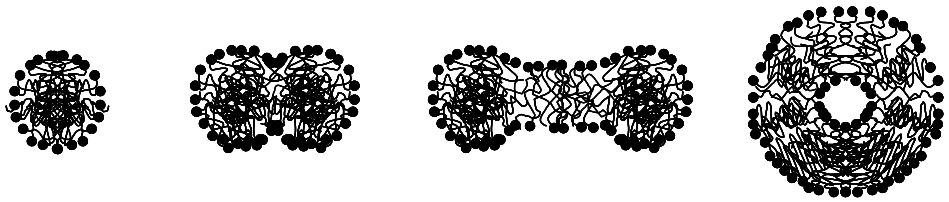

Figure 1.1. Schematic representation of surfactant aggregates in dilute aqueous solutions. From left to right: spherical, globular, spherocylindrical micelles and spherical bilayer vesicles.

Surfactants can be categorized as anionic, cationic, and nonionic surfactants depending on the charge present on the hydrophilic part of the molecule. The most investigated anionic surfactant is sodium dodecylsulfate (SDS), whose structure is given in Figure 1.2 along with some other well known surfactants.[31-33]

Surfactant	**Molecular structure**	**Type**
SDS $[C_{12}H_{25}OSO_3^-]\ Na^+$	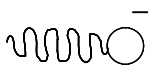	Anionic
CTAB $[C_{16}H_{33}N^+(CH_3)_3]\ Br^-$		Cationic
Triton X-100 $4–(C_8H_{17})C_6H_4(OCH_2CH_2)_{10}OH$	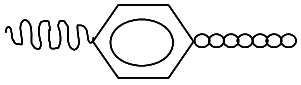	Nonionic
Gemini $[CH_3–N^+–(CH_2)_n–N^+–CH_3]_2Br^-$ $C_{16}H_{33}$ $C_{16}H_{33}$	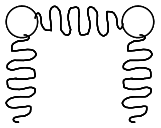	Dimeric

Figure 1.2. Structure of some common surfactants.

Numerous studies have been carried out to characterize the aggregates of surfactants.[34-39] The features of particular interest to describe surfactant aggregates are the critical micelle concentration (cmc)[30] which is the concentration at which the surfactant aggregates form, the average size and shape of the aggregates, and their polydispersity. One of the most important properties of aqueous surfactant solutions is their ability to enhance the solubility of hydrophobic solutes that have otherwise very low solubilities in water. This solubilization is enabled by the hydrophobic domains generated by the surfactant aggregates which can host the hydrophobic compounds to be solubilized. A successful surfactant enhances the solubility of a hydrophobic solute by several orders of magnitude compared to its solubility in aqueous solution in the absence of surfactant.[40]

Surfactants find numerous applications in the chemical industry, the formulation of pharmaceuticals, household products, agricultural chemicals, mineral processing technologies, and food processing industries.[30,31] Naturally occurring surfactants found in plants, animals and humans have important biological or physiological functions. The wide range of applications for surfactants is a consequence of the large number of variations that are possible in the types of head and tail building blocks constituting any surfactant. The variety of molecular structures found with surfactants allows for extensive variation of their solution and interfacial properties and hence, rationalizes the efforts being made to discover the link existing between the molecular structure of a surfactant and its self-assembling and solution properties, with the ultimate goal that surfactants be synthesized or selected specifically for a given application.[31,32,36,37]

1.2.2. Block copolymers

Macromolecules are particularly well suited for applications where different physical, chemical, and biological functions are required simultaneously. This observation has been particularly well understood by Nature which uses innumerable examples of biopolymers. Polymers have attracted a great deal of interest because they offer a unique platform for the development of materials in fields as diverse as biomedicine and packaging.[41,42] Improvements in the molecular and supramolecular control achieved by the chemistry used to synthesize macromolecules have enabled the preparation of macromolecules which exhibit a predicted physical and biological response.[43-47] Amphiphilic block copolymer systems with enhanced biofunctionality have been developed that have been shown to act as mimetics for biological membranes.[18,48] As the combinations of biological and synthetic building blocks are practically limitless, it is possible to develop polymeric materials for a large number of applications in biomedicine and biotechnology.

The self-assembly of amphiphilic block copolymers generates aggregates that have various morphologies in solutions. The most commonly observed morphology is that of the star-micelles.[49,50] Star micelles refer to micelles having a core-corona structure, where the core is small and the corona is large (Figure 1.3).

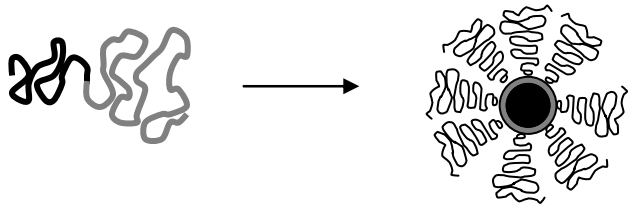

Figure 1.3. Self-assembly of a block copolymer into a "Star" micelle.[3]

Depending on the polarity of the solvent, micelles can be categorized as either regular micelles in a polar solvent or reverse micelles[51] in an apolar solvent. Recently much attention has been garnered by the self-assembly of highly asymmetric, amphiphilic block copolymers into aggregates for which the term "crew-cut" has been proposed by Halperin.[49] The block copolymers generating crew-cut micelles are constituted of a long hydrophobic block that forms the core of the aggregate and a short hydrophilic block that yields the corona. A variety of aggregate morphologies has been prepared by manipulating the relative block lengths and environmental conditions, such as solvent composition, presence of additives, and temperature.[3,52-55] Possible morphologies include spheres, rods, vesicles, lamellae, tubules, large compound micelles (LCMs), large compound vesicles (LCVs), and hexagonally packed hollow hoops (HHHs). The broad variety of self-organizing structures enabled by block copolymers is shown in Figure 1.4.

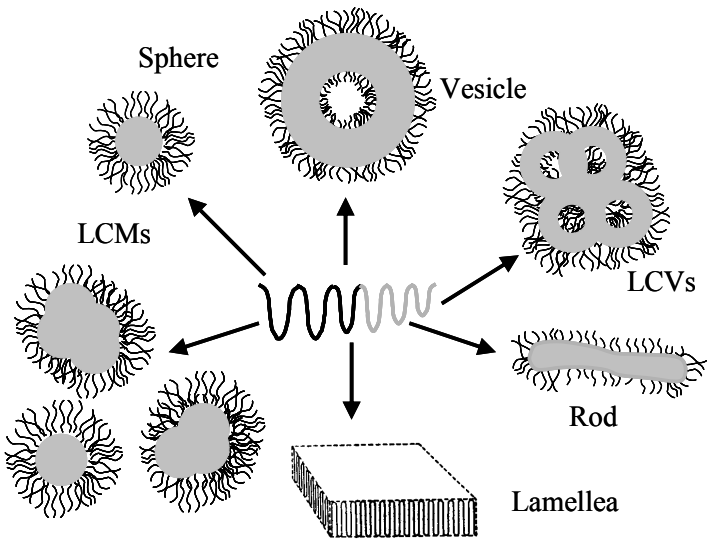

Figure 1.4. Self-organized structures of block copolymers: spherical micelles, vesicles, cylindrical micelles, lamellae, large compound vesicles (LCVs), and large compound micelles (LCMs).[3]

During the last decade, it has become possible to prepare block copolymers of various architectures, solubilities, and functionalities. Diblock,[53-55] triblock[52b] and multiblock[56] copolymers can have the different polymeric blocks arranged with a linear, star-like, or comb architecture. The solubilities of the various blocks can be adjusted to enable the solubilization of block copolymers in solvents ranging from polar solvents such as water to media with very low cohesion energies such as silicon oil or fluorinated solvents. The ability to control the functionality of specific blocks is extremely important to stabilize metallic,[57] semiconductors,[58] ceramic,[59] or biological systems.[17,18]

The different synthetic routes to prepare block copolymers are based on living polymerization using anionic, and more recently cationic, and radical polymerization. It is also possible to combine different polymerization techniques to further increase the variety of block copolymers. For instance, functional groups can be attached on a macromolecule to initiate the polymerization of the next polymer block (macroinitiators). Figure 1.5 shows an example of a block copolymer of a heterobifunctional PEO with end groups that allow for adjustment in the physicochemical properties of the resulting material as well as aid in the synthesis of hydrophilic/hydrophobic block copolymers.[60]

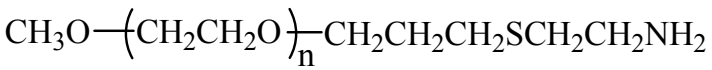

Figure 1.5. Structure of α-methoxy-ω-amino PEO

There exist a large number of published strategies for preparing block copolymers by living anionic polymerization.[41,42] Recent years have seen the development of new methods for living cationic and living radical polymerization.[3,42]

1.2.3. Hydrophobically modified polymers

Hydrophobically modified water–soluble polymers (HMWSPs) are polymers made up of well-defined hydrophilic and hydrophobic parts. When dissolved in water they often undergo aggregation.[61-67] There are two broad classes of HMWSPs. They can either have a high content of hydrophobic groups, as in the case of alternating copolymers of ionic and hydrophobic monomers such as polysoaps,[68] or a low content of hydrophobic groups, as for example in hydrophobically-modified cellulose ethers[69] or polyacrylamides.[70,71] The functions of these polymers are controlled by a number of factors, including the chemical structure and the electrostatic charge of the monomer units and the overall composition and the architecture of the macromolecule. In aqueous solutions of HMWSPs, intra– or intermolecular association of the hydrophobic segments competes with the solvation of the HMWSPs afforded by the hydrophilic segments. Therefore the hydrophilic/hydrophobic balance is an important factor to control the shape (star, flower, or networks) of the self-assembled structures.[72]

Amphiphilic derivatives of polyelectrolytes are of particular importance, as they tend to have a higher solubility in water, compared to that of neutral polymers. For hydrophobically modified polyelectrolytes (HMPE), the intramolecular association of the hydrophobes competes with electrostatic repulsion from the ionic groups. Therefore, the balance between the contents of the hydrophobic and charged units in the HMWSPs

constitutes a critical factor to determine whether or not self-organization occurs. For example, amphiphilic poly(carboxylic acids)[73,74] which adopt an extended chain conformation that favors intermolecular associations at high pH, collapse intramolecularly to form a compact conformation at low pH. On the other hand polysulphonic acids, which are "strong" polyelectrolytes show no such pH dependence of their conformation because they are fully ionized even at low pH.[71] Copolymers of styrene and maleic anhydride studied by Duhamel et al.[75] are an example of an HMPE where the hydrophobe-to-charge ratio can be controlled by adjusting the degree of ionization to either increase or decrease the hydrophobic character of the copolymer in aqueous solution. The extent of aggregation was also found to increase by having a styrene-to-maleic anhydride ratio greater than 1, which is typically encountered for this strongly alternating copolymer.

Low concentrations favor intramolecular hydrophobic associations which induce a contraction of the molecular dimensions of the modified polymer coil and disfavors intermolecular aggregation. Increasing the polymer concentration above the overlap concentration enables interchain association of the hydrophobic groups which leads to an enhancement of the solution viscosity. Figure 1.6 gives a glimpse of the type of HMWSPs that are able to undergo hydrophobic interactions in aqueous solution.

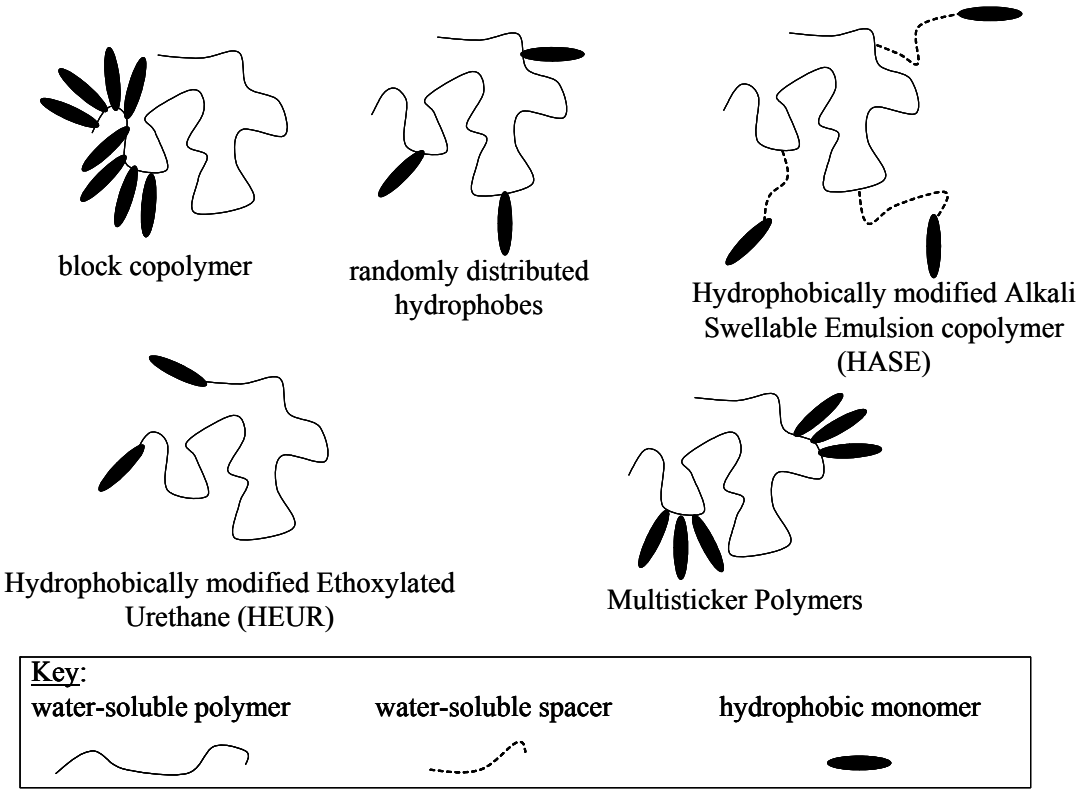

Figure 1.6. Various types of HMWSPs capable of undergoing hydrophobic associations.

1.2.4. Polypeptides

Polypeptides are a class of biopolymers composed of α-amino acids joined by peptide bonds. Polypeptides are biological materials with important therapeutic and clinical applications.[3] Their synthesis has been the subject of special attention.[76] In recent years, their ability to self-organize into nanostructures such as micelles, vesicles, and gels in aqueous solutions have offered new applications such as the encapsulation of therapeutic agents for drug/gene delivery, tissue engineering, and surface patterning to better understand the biological functions associated with cell adhesion, cell recognition, and various other actuator functions[3] (Figure 1.7).

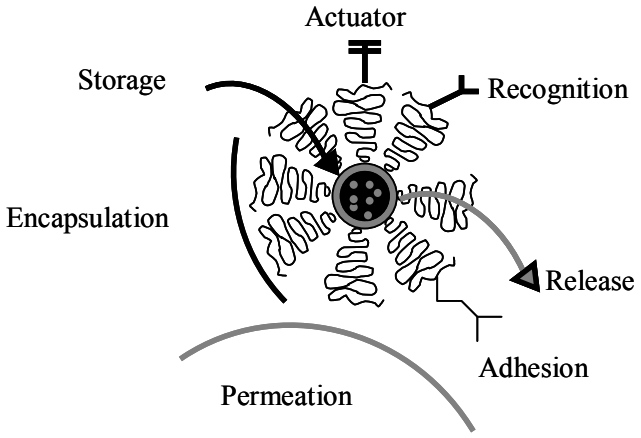

Figure 1.7. Schematic diagram of the biological functions enabled by the self-organization of polymeric structures.[3]

Although a number of synthetic methods are available for the synthesis of polypeptides,[76] no single method is considered the ideal method. Broadly speaking, most polypeptide syntheses fall into two major catogories, which are the classical, solution-phase syntheses[77-80] (explained in much more details in Chapter 2) and the more recently developed solid-phase syntheses.[81]

Leuches' anhydrides: A solution-phase method not mentioned in Chapter 2, which has received considerable attention for the synthesis of both homopolypeptides and random copolypeptides is the N-carboxyanhydrides (NCAs or Leuchs' anhydrides)[82-85] procedure. The NCAs are readily prepared by the reaction of an amino acid with phosgene in an aprotic solvent (Figure 1.8).

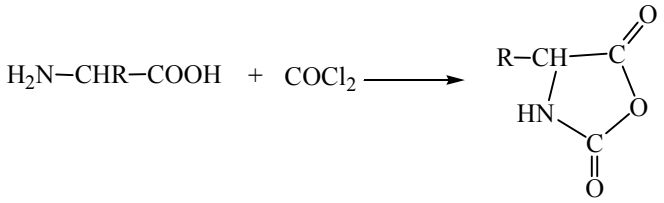

Figure 1.8. Formation of a N-carboxyanhydride (NCA)

Polycondensation to form the polypeptide can proceed through ring opening of the NCA by traces of water to yield a carbamic acid which loses carbon dioxide and regenerates the amino acid. The amino group of the amino acid then attacks the carbonyl group of a second NCA molecule and the coupling reaction is followed by decarboxylation to yield a dipeptide. The process continues and high molecular weight material is formed in this manner (Figure 1.9).

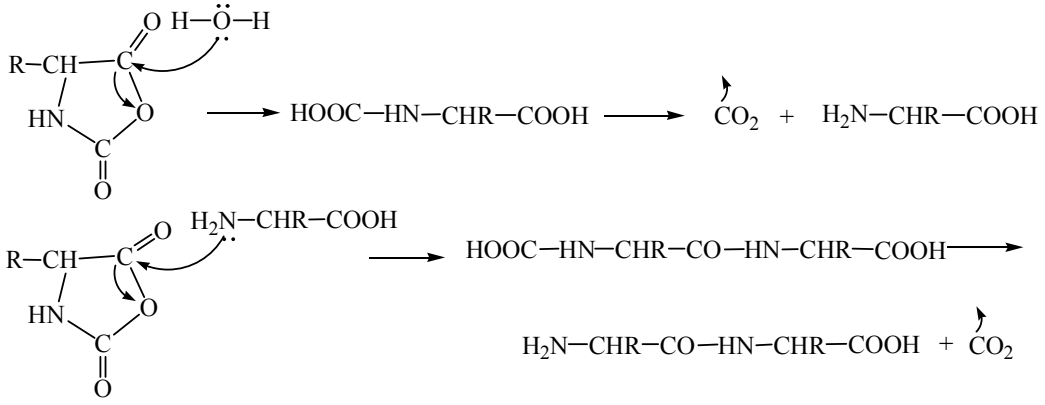

Figure 1.9. Polypeptide formation through successive additions of NCAs

This method is not applicable to heteropolypeptides with defined sequences containing specifically defined amino acids in predetermined positions in the peptide chain.

Solid-phase synthesis: Solid-phase peptide synthesis as described by Merrifield[81] has proven to be quite successful. In this method, the condensation of individual amino acids is performed on a solid support material (preferably slightly cross-linked polystyrene), until finally the finished polypeptide is cleaved from the support.

Some of the steps involved in the stepwise synthesis of a polypeptide using a solid support material using solid-phase synthesis are shown in Figure 1.10. The advantage of the Merrifield synthesis is that it is performed in heterogeneous phase, so that the reagents used in the peptide synthesis can be easily separated from the actual synthesis product bound to the support material.

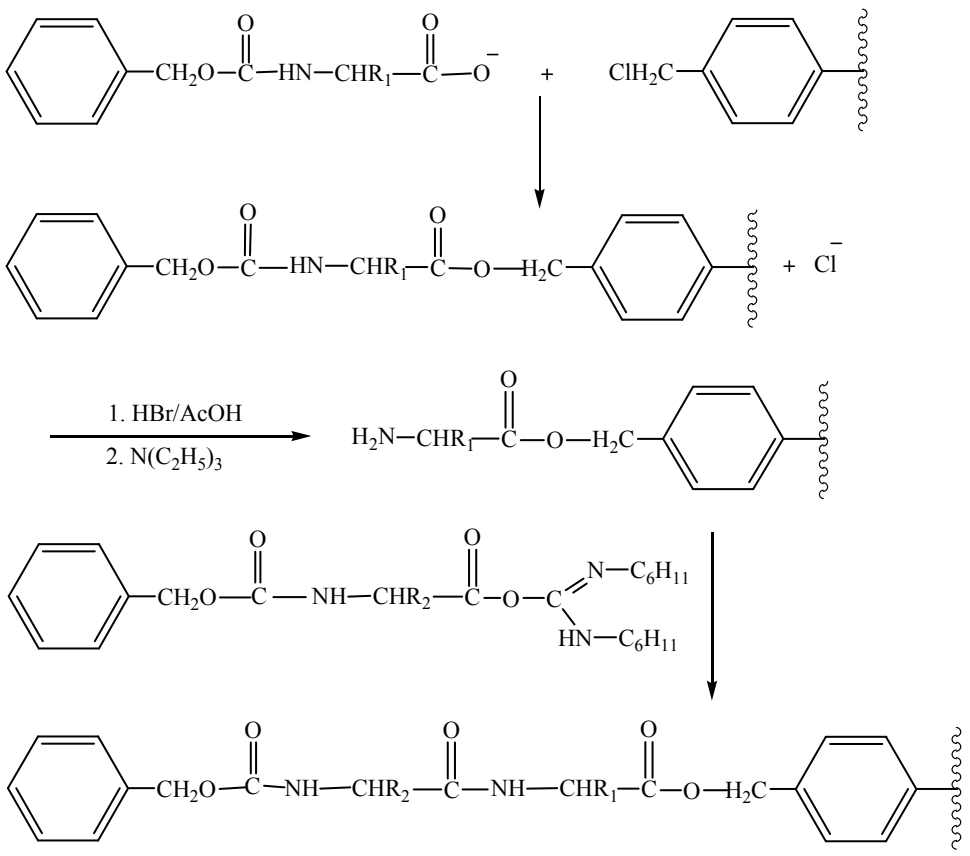

Figure 1.10. Solid phase peptide synthesis

The disadvantage of this synthesis is that the chemical reactions used for the sequential synthesis are not quantitative, so that to some extent, the reaction does not take place as desired and therefore unwanted peptides are synthesized simultaneously and can be separated only with considerable difficulty. In the case of longer amino acid sequences, i.e. those with 50 amino acids and more, even if the individual steps are 99 % effective, the multiplicity of the reactions involved results in a large number of by-products in addition to the targeted peptide, which may be shorter chains or peptides containing defects in the amino acid sequence. Biosynthesis through recombinant DNA[86,87] is another method by which polypeptides can be synthesized, and this method has the advantage of generating monodispersed polypeptides.

1.3. Drug delivery

Research in the field of drug delivery and drug targeting at the molecular level has increased exponentially due to progress made in biotechnology and immunology.[19-22] Drugs are susceptible to chemical or enzymatic degradation. They may also lose or change their biological functions as a result of, for example, aggregation and conformational changes following interactions with various compounds in the biological systems or in the formulation. For these types of drugs, carrier systems have been found to improve the drug stability and delivery.[17,88-92] It is therefore fortunate that the increased need in new and efficient delivery systems required for sparingly soluble drugs has been paralleled by the progresses made in understanding how surfactants, lipids, block and hydrophobically modified polymers self-assemble into stable structures. The improved solubilization of drugs is just one of the advantages of these self-assembled structures. Other advantages include

protection from hydrolysis and chemical and enzymatic degradation, reduction of toxicity, improvement of drug bioavailability, and controlled release.[19-22] The self-assembled carrier systems can incorporate a drug by either passive association[29,93-95] of the drug with the pre-assembled carrier, or by covalently attaching[30,96,97] the drug to the units constituting the carrier followed by their self-assembly. These two approaches are depicted in Figure 1.11. They have been implemented with block copolymers of poly(ethylene oxide)–*b*–poly(*β*–benzyl–L–aspartate) (PEO–*b*–PBLA).[30,96] The benzyl group was removed prior to attaching the drug in approach B.

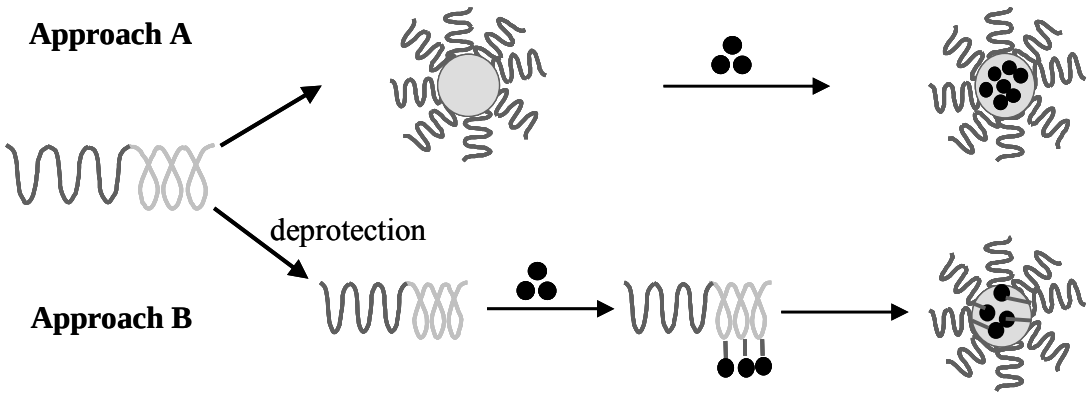

Figure 1.11. Block copolymers as drug carriers: Approach A: the drug is present as a free molecule. Approach B: the drug is attached covalently onto one block of the copolymer.

Depending on the properties of the drug, association of the drug with the self-assembled system might occur in the hydrophilic part, in the hydrophobic part, or at their interface. After the polymeric carriers have been brought to their target, the active agent, the drug, is released. This can take place either by induced degradation of the polymeric matrix or dissociation of the drug from the polymer induced by swelling of the polymer. For control

purposes, an actuator function may also be incorporated in the carrier to trigger the release of the drug depending on the local conditions such as salt concentration, temperature, and pH.

The idea of using block copolymer micelles as carriers for active agents was originally proposed by Ringsdorf and co-workers[98] who investigated micelles of poly(L–lysine)–*b*–poly(ethylene oxide) (PLys–*b*–PEO).[99] The active agent, i.e. the drug, can be covalently attached along the peptidic block of PLys–*b*–PEO via a covalent bond which is then broken by proteases present in increased concentration in many types of tumors. Anticancer drugs can also be physically solubilized in the micelle cores of poly(aspartic acid)–*b*–poly(ethylene glycol) (PAsp–*b*–PEG) as shown by Kataoka et al.[93b,100] PAsp solubilizes large quantities of drugs and, being a polypeptide, is biodegradable. PEG being both water soluble and chemically stable under physiological conditions, it reduces the antigen effect of the copolymer/agent conjugate (Figure 1.12).

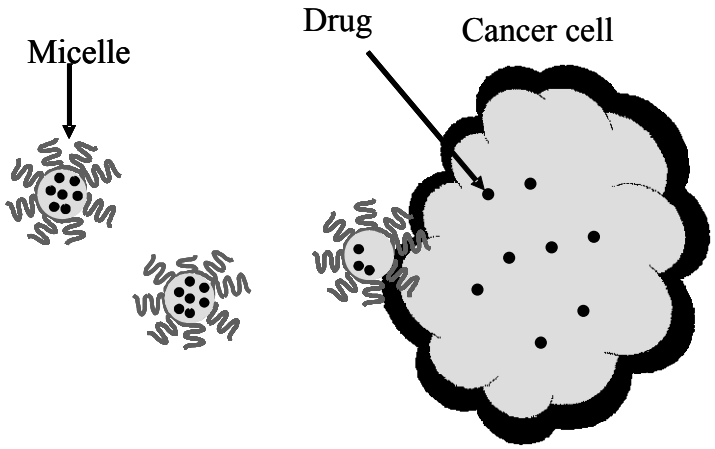

Figure 1.12. Chemotherapy with block copolymer micelles transporting a drug into the tumor cell.[3]

In aqueous solutions, the PAsp–*b*–PEG micelles prepared by Kataoka et al.[100] had a

diameter of approximately 60 nm. Their size prevented renal filtration and uptake by the reticuloendothelial system (RES). This feature increases the circulation time of these micelles in the blood stream. PEO–*b*–PPO–*b*–PEO micelles[101] conjugated with anthracyclin antibiotics (doxorubicin, Ruboxyl, EPI) have also been applied in chemotherapy resulting in a 15 % increase in life expectancy and a 90 % inhibition of the growth of the tumor. In some cases, the tumor disappeared completely.

There is a great need to develop polymeric biomaterials as drug carriers for specific applications and functions as most drug delivery systems have to be implanted directly at the site.[19,102-104] Such is the case for delivering chemotherapeutic agents to malignant gliomas, where a poly(anhydride)[105] is used as a delivery system. Since the majority of the cases require a controlled release of the drug, a delivery system is needed which can not only travel to the disease site, but also remain there for prolonged periods before undergoing degradation. The polymeric materials used should also be safe for the human body, by ensuring that they can easily leave the body once their job is done, or are biodegradable. There are a wide variety of polymers available to encapsulate a drug, either via passive association or chemical attachment of the drug. A comprehensive review of the broad spectrum of polymeric systems available for controlled drug delivery has been written by Uhrich.[88]

1.4. Methods

The characterization of the aggregates formed by self-assembling macromolecules is usually accomplished by a combination of several techniques such as fluorescence,[106-110] dynamic light scattering (DLS),[10,12,70,74] static light scattering (SLS),[66,68a,71c] small angle X-

ray scattering (SAXS),[12] small angle neutron scattering (SANS),[14,74] electron microscopy,[51,53-55] and NMR.[10,11,15] Among these techniques, fluorescence has been extensively used to gain structural information on the aggregates during the self-organization of polymeric systems. The techniques employed in this thesis are reviewed hereafter, with a detailed account on fluorescence, being the major analytical tool used in this thesis.

1.4.1. Circular dichroism

Circular dichroism (CD) is a valuable technique which has been extensively applied to characterize the structure of proteins and polypeptides and monitor changes in their conformation.[111] The CD spectra are very sensitive to any small alterations of the structure of the polypeptide backbone. It has been widely used for both quantitative and qualitative purposes to examine the binding of ligands to proteins, as well as to study the nature of the interactions taking place between proteins and other macromolecules. CD spectroscopy is a form of light absorption spectroscopy that measures the difference between the amount of right– and left–circularly polarized light being absorbed by a substance. The CD signal between 190 nm and 250 nm can be analyzed to determine the amounts of different secondary structures found in proteins such as α-helices, β-sheets, or random coils (Figure 1.13).[112]

The advantages of using CD for monitoring the conformational changes of biological macromolecules include the requirement of small sample quantities, the speed at which these experiments can be conducted, and the sensitivity of CD to probe alterations in the polypeptide backbone at the molecular level.

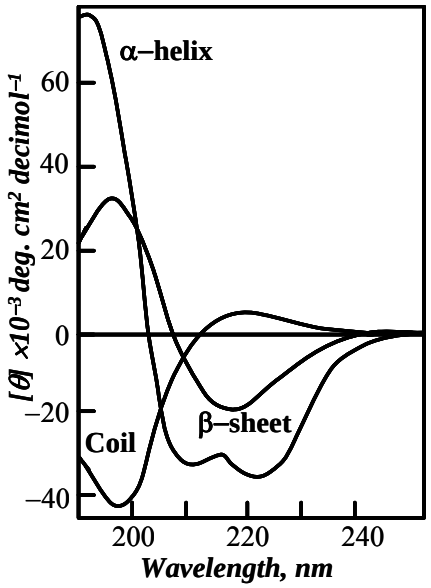

Figure 1.13. CD spectra of poly(L-lysine) illustrating its ability to adopt different secondary structures in different conditions; α-helix in basic, β-sheet in neutral, and random coil in acidic solution.[112]

Polypeptides that self-assemble in aqueous solutions are being used increasingly to carry drugs which are either insoluble or sparingly soluble under physiological conditions. In some cases, the drug has to be covalently attached onto the polypeptide backbone, with potential effect on the secondary structure of the polypeptide. If the retention of the secondary structure is important to maintain the desired properties of the carrier, it is then useful to obtain the CD spectra of the polypeptides before and after they have been modified.[113-115]

1.4.2. Dynamic light scattering

Over the years, dynamic light scattering (DLS) has become a powerful technique for the characterization of polymers and macromolecules in solution. DLS measures the time-

dependent fluctuations in the intensity of light scattered by particles undergoing Brownian motion in solution. The motion of the particles due to Brownian motion is characterized by a relaxation time that is related to the time taken by the species in solution to move in and out of the volume irradiated during a DLS experiment. In turn the relaxation time is related to the translational diffusion coefficient (D_Z). This diffusion coefficient can be converted into a particle size using the Stoke-Einstein equation and assuming a spherical shape for the particles.

The molecular structure, conformation and orientation of the polymer molecules can greatly affect the macroscopic properties of their solutions. It is therefore highly informative to determine the size of these polymers in solution.[116] For example, hydrophobically modified alkali swellable emulsion polymers (HASE)[117] and copolymers of sodium 2-(acrylamido)-2-methylpropanesulphonate and dodecyl methacrylate[118] exhibit a bimodal distribution of relaxation times referred to as the slow and the fast relaxation modes. The slow and fast components indicate the presence of polymeric aggregates and single chain unimers (unimolecular micelles), respectively. This observation confirms that unimers and aggregates (several polymer chains held together by interpolymeric hydrophobic interactions) coexist in solution.[117]

1.4.3. Fluorescence

Fluorescence techniques have been extensively used to characterize the aggregation of amphiphilic compounds such as self-assembling polymers and surfactants for more than three decades.[106-111] Due to its sensitivity and versatility, important information regarding the microstructure and molecular dynamics of macromolecules has been obtained. The time scale over which information on the dynamics of macromolecules is available depends on the time

window over which the chromophore remains excited. The fluorescence lifetime of a chromophore such as pyrene is usually in the 200-400 ns range. However, similar studies with phosphorescence can access timescales of the order of seconds to minutes. The experiments are usually set up in such a way that the luminescent chromophore is either physically bound to the polymer or covalently attached to the polymer or surfactant.

The combination of steady-state and time-resolved fluorescence enables one to attain quantitative information about the dynamic processes occurring in several photophysical processes such as in excimer formation, non-radiative energy transfer (NRET), or fluorescence quenching. These fluorescence experiments yield information about the compactness of the self-assembled clusters and their microviscosity. Fluorescence probe analysis is largely empirical in nature, but when applied with proper care and precautions, it can serve in mapping out the complex behaviour of microheterogeneous systems. Sustained efforts have been made in this area in order to characterize the dynamics and self-organization of many hydrophobically modified polymers.

1.4.3.1. Jablonski diagram

When a molecule is raised to its electronically excited state by the absorption of light, it can return to the ground state via several unimolecular pathways as shown by the Jablonski diagram[106] depicted in Scheme 1.1. After absorption of a photon by a chromophore, a very rapid relaxation ($\leq 10^{-12}$ sec) called internal conversion takes place leading to the lowest singlet excited state S_1. The chromophore in the singlet excited state S_1 can either return to the ground-state S_0 via nonradiative or radiative transitions (fluorescence), or undergo intersystem crossing to a triplet state. Due to the spin restrictions, the molecules in the triplet state slowly return to the ground-state S_0 again via a nonradiative or radiative transition

(phosphorescence).

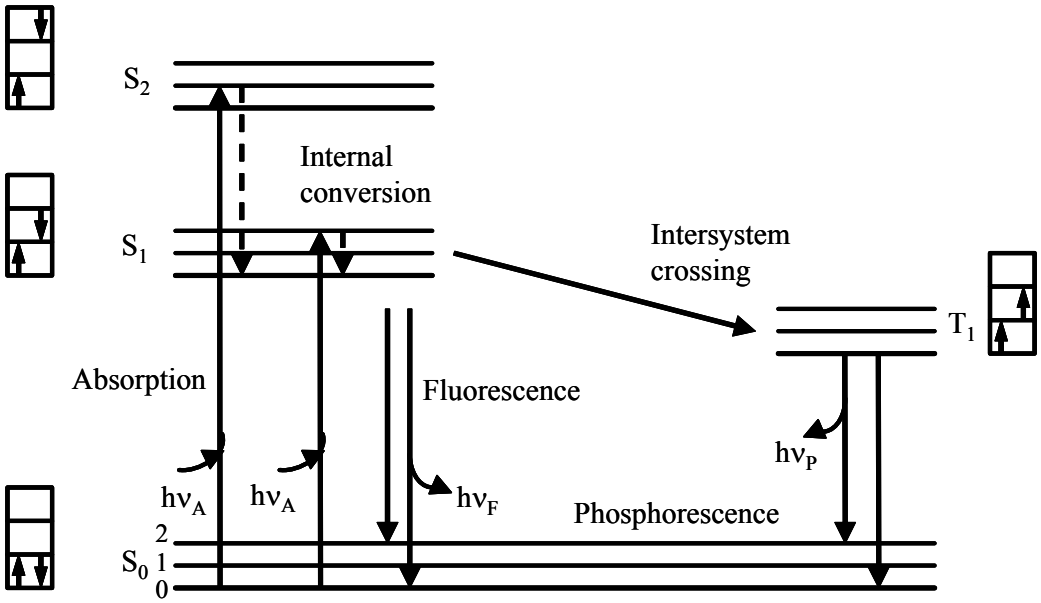

Scheme 1.1. Schematic representation of the various excited electronic states of an organic molecule, their energy level relationships, and interconversion processes.

From the above considerations, the absorption spectrum of molecules reflects the vibrational levels of the electronically excited states whereas the emission spectrum reflects the vibrational levels of the ground-state. Usually, electronic excitation does not greatly alter the spacing of the vibrational energy levels. As a result, the vibrational structures seen in the absorption and emission spectra are often mirror images of each others.[106]

1.4.3.3. Fluorescence lifetime and quantum yield

Fluorescence lifetimes and quantum yields are perhaps the most important characteristics of fluorescent substances. Substances with the largest quantum yields, approaching unity, display the brightest emission. The lifetime determines the time that the

fluorescing molecule remains excited.

The fluorescence quantum yield (Q) is the ratio of the number of photons emitted to the number of photons absorbed, and can be obtained from Equation 1.1,

$$Q = \frac{\Gamma}{(\Gamma + k)} \tag{1.1}$$

where Γ is the emissive rate constant of the chromophore, and k is the rate constant for radiationless decay of the excited chromophore to the ground-state (GS). The lifetime (τ) of the excited state is defined by the average time the molecule remains in the excited state prior to returning to the GS. Generally fluorescence lifetimes are around 10 ns and their expression is given by Equation 1.2.

$$\tau = \frac{1}{(\Gamma + k)} \tag{1.2}$$

The lifetime of the fluorophore in the absence of nonradiative processes is called the intrinsic or natural lifetime and is given by Equation 1.3.

$$\tau_i = \frac{1}{\Gamma} \tag{1.3}$$

Combining Equations 1.1 and 1.3 leads to a relationship between Q, τ_i, and τ given in Equation 1.4.

$$Q = \frac{\tau}{\tau_i} \qquad (1.4)$$

1.4.3.4. Chromophores

At present, thousands of chromophores are known.[106] Chromophores can be broadly divided into two main classes, intrinsic and extrinsic.[106] Intrinsic chromophores are those which are naturally present in a macromolecule such as the benzyl moieties of polystyrene or the aromatic amino acids tyrosine, tryptophan, flavins, and the derivatives of chlorophyll in a protein.

Extrinsic chromophores are those which are added to a sample to provide fluorescence when none exists. Extrinsic chromophores include compounds like pyrene, naphthalene, anthracene and phenanthrene, generally condensed aromatic compounds whose structures are shown in Figure 1.14. Among the fluorescent chromophores employed so far, pyrene is "by far the most frequently used chromophores in the fluorescence studies of labeled polymers".[109] Due to its long lifetime (150-350 ns), large extinction coefficient, and high quantum yield, pyrene is presently still the fluorescent chromophore of choice when it comes to using fluorescence to characterize polymeric systems.

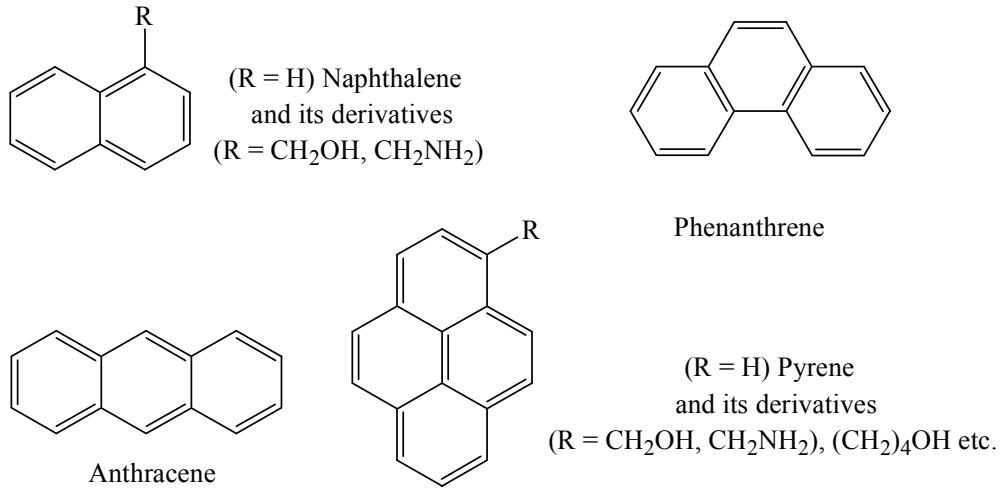

Figure 1.14. Structures of commonly used chromophores and their derivatives.

1.3.3.5. Pyrene excimer

Pyrene is one of the most widely used chromophores in the characterization of polymeric systems because of its spectral features (Figure 1.15).[109] It has a well-characterized long-lived excited state, it can undergo fluorescence quenching, its emission spectrum is sensitive to its microenvironment and most importantly, can form excimers.

Since pyrene is often used in this thesis to characterize polypeptide aggregates, the effect of excimer formation on the fluorescence spectrum of pyrene is being discussed in more detail. The steady-state fluorescence spectrum of pyrene shows two species in solution as illustrated in Figure 1.15, the excited pyrene monomer and, when the pyrene concentration is sufficiently large, the pyrene excimer. Sharp, well-resolved peaks between 370 nm and 400 nm are characteristic of the fluorescence of the pyrene monomer and a broad structureless fluorescence emission between 450-550 nm is characteristic of the excimer.

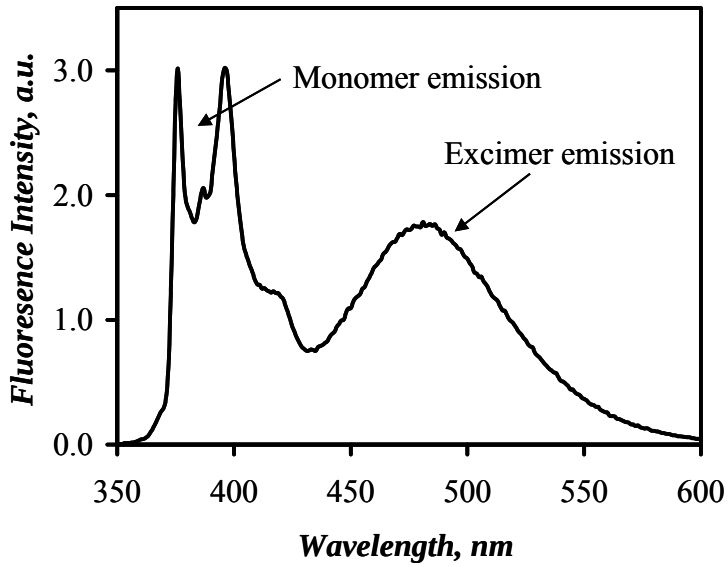

Figure 1.15. Steady-state fluorescence emission spectrum of pyrene randomly attached onto the alternating polypeptide $(Asp_1Phe_1)_n$ prepared in this thesis. [*Polypeptide*] = 0.80 g/L, [*Py*] = 4.14×10^{-5} M in 0.01 M Na_2CO_3 solution at pH 9, λ_{exc} = 346 nm.

The I_E/I_M ratio representing the ratio of the pyrene excimer to monomer fluorescence intensity is easily obtained from the steady-state emission spectrum of pyrene. The I_E/I_M ratio is usually determined from the area of the spectrum in a selected wavelength range under the emission bands of the excimer and the monomer to obtain the quantities I_E and I_M, respectively. The I_E/I_M ratio gives information about the probability of encounters between two pyrenes in solution when the pyrenes are attached onto a polymer. The I_E/I_M ratio is related to the dynamics of the polymer chain, the solvent quality for the polymer, the viscosity of the solvent, the presence of microheterogeneous environments, the polymer concentration, and the distance between two neighbouring pyrenes in the chain. The I_E/I_M ratio has been used to monitor different polymer systems as a function of pH, ionic strength, polymer concentration, hydrophobic content in the polymer chain, and the associations

between the pyrene labeled polymers and surfactants.[47,118,119]

An excimer, as defined by Birks,[120] is a dimer which is associated in the excited electronic state and which is dissociated in the ground-state. The formation of a pyrene excimer requires the encounter of an electronically excited pyrene (Py*) with a GS pyrene. The excimer state has been described theoretically by a configurational mixing of excitation-resonance states.[109] Based on crystal structure studies (Figure 1.16), a sandwich configuration for the pyrene excimer has been proposed in which the excimer is formed by the mutual approach of two pyrene molecules with their molecular planes parallel:

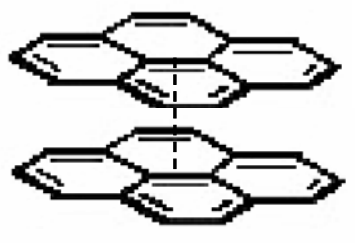

Figure 1.16. Theoretically expected geometrical arrangement between the two pyrene units constituting a pyrene excimer.

The interplanar distance has been calculated to be about 3.53 Å.[120] The changes in enthalpy for the dissociation of excimers equal 39.7 (± 4.0) kJ.[109] These numbers reflect a weak dissociation energy and a rigid configuration for the excimer.

The formation of the excimer can occur either by diffusion (dynamic excimer) according to the Birks' scheme, or fast rearrangement of pre-associated pyrenes which exist under certain conditions (static excimers).[109] The formation of a dynamic excimer is described by the Birks'[120] Scheme 1.2A, while excimer formation via the diffusional encounters of two pyrenes and direct excitation of a pyrene ground-state dimer is described

in Scheme 1.2B.

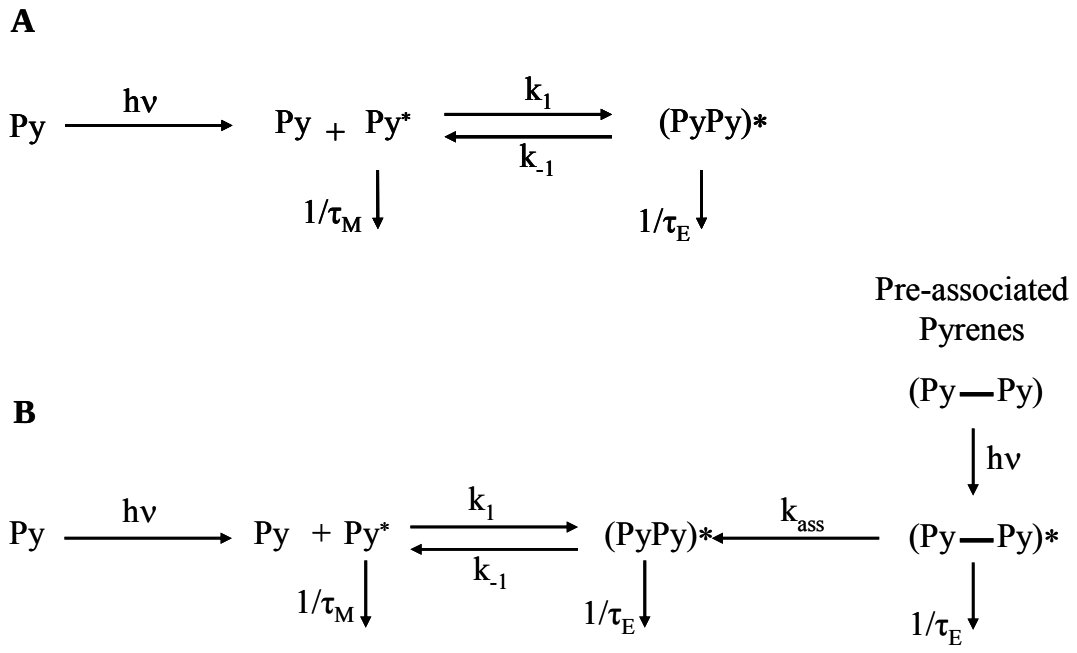

Scheme 1.2. Formation of pyrene excimer through diffusional encounter (Birks' scheme) (A) and through pre-formed pyrene aggregates (B).

1.4.3.6. Medium effects

The emission of molecules generally occurs at wavelengths longer than those where light absorption occurs. This loss of energy between absorption and emission is known as the Stokes' shift.[106] These energy losses can be due to the dissipation of vibrational energy, the redistribution of electrons in the surrounding solvent molecules induced by the dipole moment of the excited molecule, the reorientation of the solvent molecules and the excited state dipole, or to specific interactions between the excited molecule and the solvent. Hence the fluorescence emission spectra of many chromophores are sensitive to the polarity of their surrounding environment. Figure 1.17 shows the emission spectrum of a fluorescence probe, 6-propionyl–2–(dimethylamino) naphthalene (PRODAN),[121] in solvents of increasing

polarity. It can be seen that the emission spectrum shifts to longer wavelengths (Stoke' shifts) as the solvent polarity increases

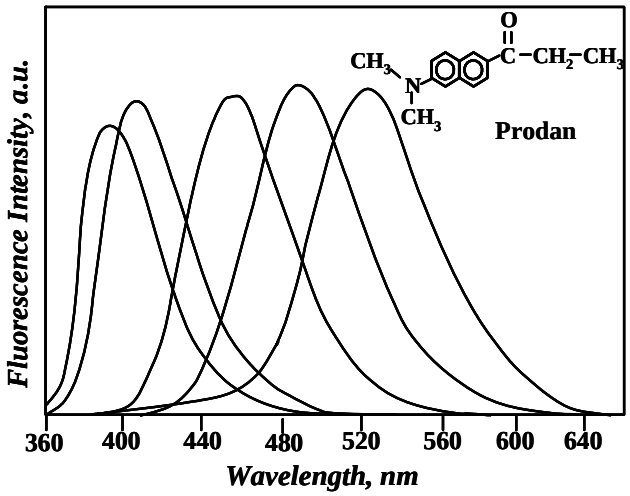

Figure 1.17. Fluorescence emission spectra of PRODAN. From left to right the solvents are cyclohexane, chlorobenzene, dimethylformamide, ethanol, and water.[121]

Besides polarity, the viscosity of the medium can also influence the emission of the probe in the medium. Duhamel et al.[75] have investigated the microviscosity of the hydrophobic microdomains generated by the oligomers of styrene and maleic anhydride (SMA) using dipyme as a chromophore. Dipyme is a molecule made of two 1-pyrenemethylene moieties connected by an ether linkage (Figure 1.18). At low dipyme concentration, excimer formation occurs intramolecularly and the amount of excimer formed with respect to the monomer yields information about the viscosity of the environment where dipyme is dissolved. A viscous solution will hinder excimer formation whereas a fluid solution will enable excimer formation (Figure 1.19).

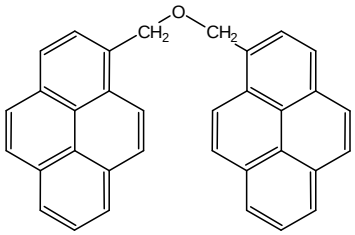

Figure 1.18. Chemical structure of dipyme

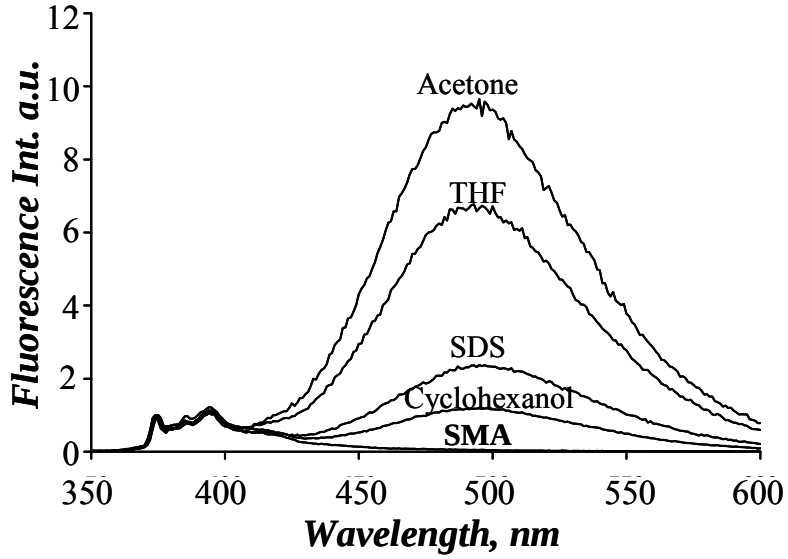

Figure 1.19. Emission spectra of dipyme in different solvents: acetone, η = 0.306 mPa.s at 25 ^{o}C; THF, η = 0.48 mPa.s at 25 ^{o}C; cyclohexanol, η = 41.07 mPa.s at 25 ^{o}C.[75]

The excimer-to-monomer ratio has been used to obtain qualitative information about the microviscosity of surfactant and polymeric micelles.[122] No excimer formation was observed for dipyme dissolved in any of the SMA solutions which were investigated.[75] This observation indicated that the interior of SMA aggregates is extremely rigid. Thus, solvents affect the emission of a chromophore in many different ways, either through specific solute-solvent interactions or via bulk effects such as solvent viscosity or polarity.

In microheterogeneous systems, changes in the nature of the environment

experienced by the probe upon transfer from the aqueous medium to the host, or migration from one region of the carrier to another are readily detected in the emission properties of the fluorescent probes. This is one of the reasons why fluorescence is widely applied to monitor partitioning of the probe between the hydrophobic domains generated by a given carrier and the aqueous solution.

Another interesting feature about the use of pyrene to study hydrophobic microdomains is the sensitivity of the vibrational band structure of its fluorescence emission spectrum to the polarity of the environment.[123,124] As the solvent polarity varies the relative intensities of the peaks in the emission spectrum undergo significant changes. In particular, the ratio of the intensity of the first peak (I_1) to that of the third peak (I_3), the I_1/I_3 ratio, increases with solvent polarity and hence can be used to probe the polarity of the microenvironment experienced by the probe (Figure 1.20). The I_1/I_3 ratio equals 0.58 in cyclohexane, while it equals 1.66-1.87 in water.[123,124] This feature enables the use of pyrene to probe the formation of surfactant micelles. At concentrations lower than cmc, pyrene is in water and the ratio I_1/I_3 equals that of pure water. At concentrations above the cmc, micelles are formed and the hydrophobic core of the micelles host pyrene, providing a less polar environment reflected by a lower value of the I_1/I_3 ratio. The surfactant concentration at which the I_1/I_3 ratio changes from a high to a low value is that of the cmc. For instance, the cmc of sodium dodecylsulphate (SDS) can be found to equal 8.0×10^{-3} mol/L by monitoring the fluorescence of pyrene as a function of SDS concentration.

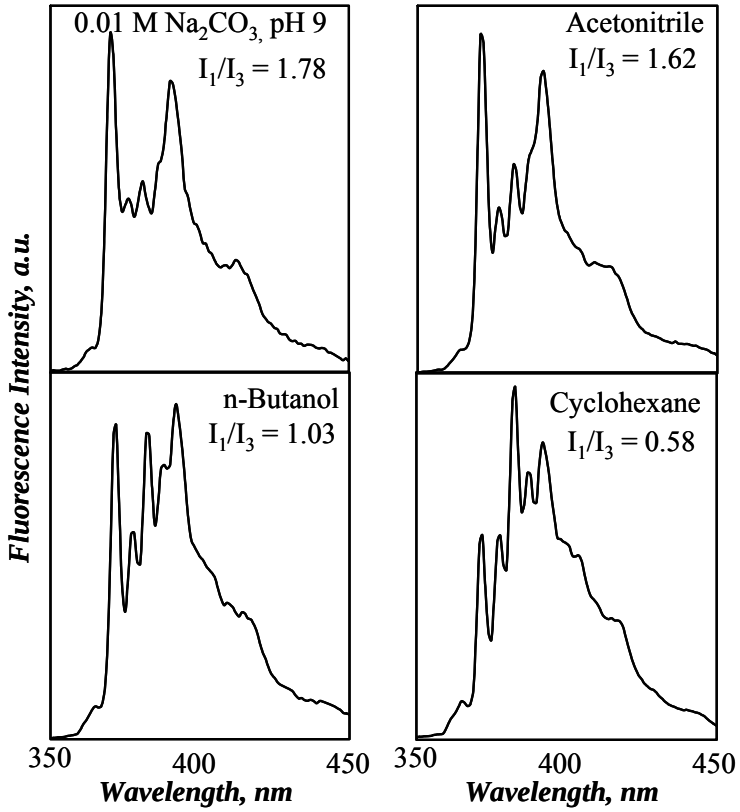

Figure 1.20. Solvent dependence of the vibronic band intensities of the pyrene monomer fluorescence at room temperature leading to different values of the I_1/I_3 ratio. (λ_{ex} = 338 nm).

The I_1/I_3 ratio has been used by Horiuchi et al.[65b] and Kumacheva et al.[125] to monitor the effect of polymer concentration and the degree of neutralization on the partition of the probe between the aqueous phase and the microdomains formed by the hydrophobic groups of the polymers under study. The effect of the ionic strength of the solution on this ratio has been studied by Magny et al.[126] and Morishima et al.[118] who have utilized the I_1/I_3 ratio of a pyrene-labeled polymer to study the interactions between other hydrophobic pendants attached to the chain.

1.4.3.7. Fluorescence quenching

Fluorescence quenching refers to any process which decreases the fluorescence intensity of a given chromophore such as pyrene via a non-radiative process.[106] There are a variety of processes which can result in quenching. Some occur over a certain distance, such as electron transfer or non-radiative energy transfer. Others occur upon direct contact with the quencher such as in collisional quenching. A decrease in the fluorescence of the chromophore can also take place by complex formation (static quenching). Different quenching scenarios are possible, depending on whether both the chromophore and the quencher are attached to the polymer, the chromophore is attached to the polymer and the quencher is free in solution, or the reverse situation where the quencher is attached to the polymer and the chromophore is free in solution. For pyrene, typical quenchers include ionic species such as iodide, copper, thallium, or alkylpyridinium ions, or neutral species such as nitromethane, dimethlybenzophenone, or acrylamide.[72,76,127-130]

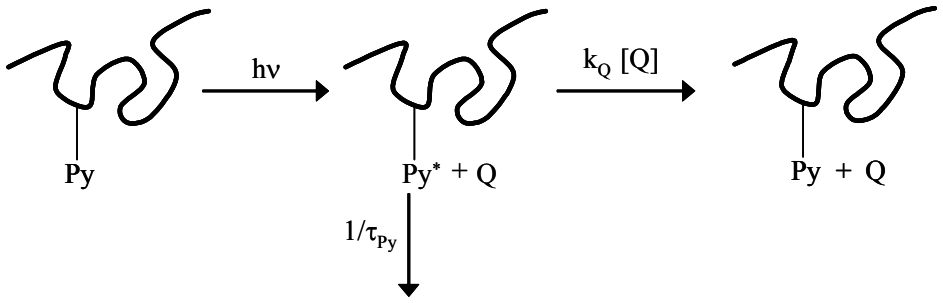

Scheme 1.3. Quenching of pyrene attached onto the polymer backbone by a free quencher molecule.

Both static and collisional quenching requires molecular contact between the quencher and the chromophore. In the case of collisional quenching, the quencher must

diffuse toward the chromophore during the lifetime of its excited state. The collision between the excited chromophore and the quencher induces the chromophore to return to the ground-state. In the case of static quenching, a complex is formed between the chromophore and the quencher. This complex is non−fluorescent. Whether the quenching is dynamic or static, the quencher and the chromophore must be in contact.

When an external quencher (i.e. not attached to the polymer) is added to a solution containing a polymer labeled with pyrene, the chromophore is quenched according to Scheme 1.3. A Stern-Volmer plot can be obtained using Equation 1.5 where τ_0 and τ_Q are the lifetime and decay time of the chromophore without and with quencher, respectively, and I_0 and I_Q are, respectively, the fluorescence intensities of the chromophore without and with quencher. k_Q is the collisional quenching rate constant and [Q] is the quencher concentration.

$$\frac{I_0}{I_Q} = \frac{\tau_0}{\tau_Q} = 1 + \tau_0 k_Q [Q] \qquad (1.5)$$

If the quenching is purely diffusional, the ratios τ_0/τ_Q and I_0/I_Q are equal and increase with the quencher concentration. A τ_0/τ_Q ratio lower than the I_0/I_Q ratio indicates the occurrence of static quenching. As already mentioned, collisional quenching of the chromophore occurs by diffusional encounters of the excited chromophore with the quencher. This means that the collisional quenching rate constant k_Q provides information about the rigidity of the medium surrounding the chromophore, since a more rigid environment will result in a smaller k_Q.

1.4.3.7.1. Protective quenching

In some quenching studies, the Stern-Volmer plot departs from linearity and reaches a plateau at higher quencher concentrations. In such a case, protective quenching takes place.[75] Such fluorescence experiments are very important to characterize polymeric systems where water-soluble polymers have been hydrophobically modified to generate hydrophobic microdomains in aqueous solution. These hydrophobic microdomains can encapsulate hydrophobic compounds such as drugs. If they exhibit protective quenching, these hydrophobic microdomains provide the drugs with some protection from the aqueous environment. A chromophore such as pyrene can be used as either a molecular probe which associates passively with hydrophobically modified water-soluble polymers (HMWSPs) or a label covalently attached to the backbone of the polymer. Pyrene being hydrophobic associates with the hydrophobic microdomains. If these microdomains are sufficiently rigid, only those pyrenes close to the surface of the microdomains are exposed to the aqueous environment and hence can be quenched by a water-soluble quencher. The fraction of pyrenes which are accessible to this quencher can be determined from Equation 1.6 which predicts that the $I_0/(I_0-I_Q)$ ratio increases linearly with $[Q]^{-1}$.

$$\frac{I_0}{I_0 - I_Q} = \frac{1}{f_a} + \frac{1}{f_a k_Q \tau_{Py}} \frac{1}{[Q]} \qquad (1.6)$$

In Equation 1.6, f_a is the fraction of pyrenes accessible to the quencher. It can be obtained from the intercept of a plot of $I_0/(I_0-I_Q)$ vs $1/[Q]$. The collisional quenching rate constant k_Q can be calculated from the slope.

1.4.3.8. Fluorescence resonance energy transfer

Fluorescence resonance energy transfer (FRET) has also been frequently used in studies of polymeric systems labeled with a donor (*D*) and an acceptor (*A*).[106,131] When the donor molecule is selectively excited at a wavelength where the acceptor molecule does not absorb, the excitation energy can be transferred non-radiatively to the acceptor molecule, which results in the acceptor becoming excited. Such a process is known as FRET (Scheme 1.4). Owing to the strong dependence of FRET on the distance separating the donor and the acceptor molecules, it has been frequently referred to as a "spectroscopic ruler"[131] and therefore has been widely used in the study of many polymeric and biological systems.

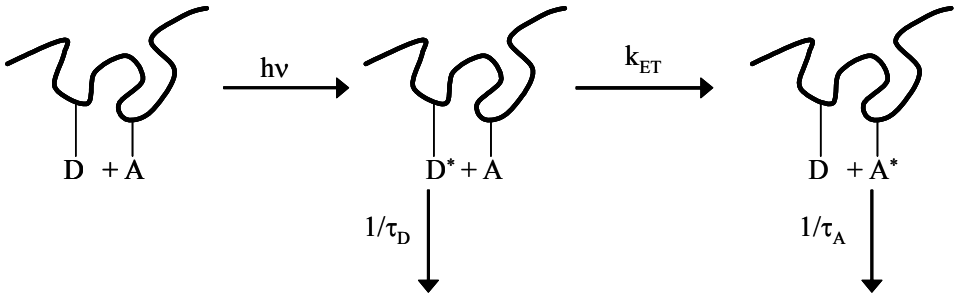

Scheme 1.4. Fluorescence energy transfer when both the donor and the acceptor are attached onto the same polymer chain.

Two very important parameters associated with FRET are the rate and efficiency of FRET. The rate of energy transfer from a donor to an acceptor is given by Equation 1.7.

$$k_{ET} = \frac{1}{\tau_D}\left(\frac{R_0}{r}\right)^6 \qquad (1.7)$$

In Equation 1.7, τ_D is the lifetime of the donor in the absence of acceptor, r is the distance between the donor and acceptor molecules, and R_o is the "Förster" radius, which depends on the extent of overlap between the absorption spectrum of the acceptor and the emission of the donor and the relative orientation of the donor and acceptor transition dipoles. The rate constant, k_{ET}, is proportional to r^{-6} which means that the rate constant of FRET is very sensitive to r. A small r would result in strong FRET whereas weak FRET would be observed for a large r.

The FRET efficiency (E_{ET}) can be calculated from Equation 1.8,

$$E_{ET} = \frac{I_D}{I_{D0}} = \frac{R_0^6}{R_0^6 + r^6} \qquad (1.8)$$

where I_{D0} and I_D represent the fluorescence intensity of the donor in the absence and presence of the acceptor, respectively. Similar to k_{ET}, E_{ET} depends strongly on r, the distance separating the donor and the acceptor molecules. When r is significantly smaller than R_0, E_{ET} is close to 1.0, indicating strong FRET. On the other hand when r is much larger than R_0, E_{ET} is closer to 0, resulting in weak FRET.

Naphthalene and pyrene, phenanthrene and anthracene, or fluorescein and rhodamine are common donor/acceptor probe pairs used in FRET experiments. R_0 has been determined to equal 2.9 nm[132,133] and 3.4 nm,[134] 2.5 nm,[132] and 4.9 nm[132] for the naphthalene/pyrene, phenanthrene/anthracene, and fluorescein/rodamine pairs, respectively. For the naphthalene/ pyrene pair, naphthalene is excited around 290 nm where pyrene absorbs little. The naphthalene emission, I_{Np}, is monitored at 330 nm, whereas that of pyrene, I_{Py}, is monitored at 375 nm. An estimate of E_{ET} is obtained from the ratio I_{Py}/I_{Np}. Efficient FRET yields a

small I_{Np} and a large I_{Py} resulting in a large I_{Py}/I_{Np} ratio. Inefficient FRET results in a small I_{Py}/I_{Np} ratio.

1.5. Project objectives

In view of the interest for self-assembling systems made up from macromolecules and their potential uses in various industries, it is advisable to develop new and improved polymeric building blocks which can be used for self-assembly. Most of the recent work done in the field of self-assembly, especially for self-assembled carriers used as drug delivery systems, makes use of either block copolymers, where one block is water soluble such as PEO and the other is either a poly(amino acid), (PEO–PAsp),[11,16,17] or poly(styrene) (PS),[12,50] or copolymers where cholesterol[15] moieties have been grafted onto the hydrophilic block. Not much research has been carried out in the use of alternating copolymers, where the hydrophobic and hydrophilic monomers are arranged in a repeating sequence. One such study carried out by Duhamel et al.[75] makes use of copolymers of styrene and maleic anhydride (SMAs). The aggregation behaviour of two SMAs, one of them having an alternating sequence, was investigated in alkaline aqueous solution. It was possible to vary the hydrophobic character of the SMA not only by changing the hydrophobic character of the copolymers, but also by adjusting the degree of ionization of each of the copolymers, thus enabling the manipulation of the degree of self-assembly of the system. The SMAs were found to self-assemble into nanostructures with diameters of approximately 2 nm with the core consisting of mainly styrene pendants stabilized in alkaline aqueous solution by the maleate anions. The hydrophobic microdomains thus generated were investigated by making use of various fluorescence techniques. From the I_1/I_3 ratio it was clear that pyrene was

located in a hydrophobic environment. It was also possible to load these microdomains with large amounts of pyrene, which showed their high capacity for solubilization of hydrophobic compounds. The absence of pyrene excimer revealed another interesting feature of these hydrophobic microdomains, namely that their local microviscosity was extremely large. This was confirmed by FRET with the donor/acceptor pair of phenanthrene/anthracene. This study demonstrated that the self-assembly of SMAs led to aggregates whose rigid hydrophobic cores could dissolve large quantities of hydrophobic compounds. This study suggested that SMA aggregates could be used as carriers when slow release of the hydrophobic cargo is required.

These exciting results made SMAs very interesting as potential drug carriers. Unfortunately, SMAs are not biocompatible. The monomers of SMA are however very similar to amino acids, such as phenylalanine (Phe) for styrene and aspartic acid (Asp) or glutamic acid (Glu) for maleic anhydride. The objective of this thesis was therefore to synthesize a series of polypeptides with different sequences using Phe and Asp as the two building blocks, and to investigate their association properties in aqueous solution. The polypeptides prepared were $(Asp_3Phe_1)_n$, $(Asp_2Phe_1)_n$, $(Asp_1Phe_1)_n$, $(Asp_1Phe_2)_n$, and $(Asp_1Phe_3)_n$ starting from a hydrophilic polypeptide to a polypeptide with a high hydrophobic character. Pyrene was used to investigate the hydrophobic microdomains of these polypeptides, first as a free molecule that would passively associate with the polypeptide aggregates, and second by randomly attaching pyrene onto the polypeptide at the aspartic acid sites. Fluorescence resonance energy transfer was used to determine whether the species present were polypeptide aggregates or unimolecular micelles. Fluorescence quenching with a water soluble quencher established the accessibility of pyrene to the surrounding. It was

expected that as the hydrophobicity of the polypeptides increased, their ability to encapsulate pyrene would also increase, and that this effect would be observed by both FRET and fluorescence quenching.

1.6. Thesis outline

This thesis is organized in the following manner. Chapter 1 provided a literature overview on self-assembling systems and a description of their importance with a special emphasis on their use for drug delivery. Various techniques used in this thesis to characterize the polypeptide aggregates were also described in Chapter 1. Chapter 2 gives a detailed description of the synthesis of the polypeptides used in this project. The intrinsic properties of the polypeptides in solution are investigated in Chapter 3. The association of the alternating polypeptide was characterized by DLS, fluorescence resonance energy transfer and fluorescence quenching and the results of this study are presented in Chapter 4. The effect of the Phe content of the polypeptides on the aggregation behaviour of the polypeptides in solution was investigated by DLS and fluorescence techniques in Chapter 5. The last chapter, Chapter 6, summarizes the results of the work and offers some recommendations for future work.

1.7. References:

1. Robinson, B. H. *Self-Assembly*, IOS Press: Tokyo: Ohmsha, 2003.
2. Lindoy, L. F. *Self-Assembly in Supramolecular Systems*, Royal Society of Chemistry: Cambridge, 2000.
3. Förster, S.; Plantenberg, T. *Angew. Chem. Int. Ed*. **2002**, *41*, 688-714.
4. Zhang, S. *Nature Biotechnology* **2003**, *21*, 1171-1178.
5. Klok, H.; Lecommandoux, S. *Adv. Mater*. **2001**, *13*, 1217-1229.
6. Harada, A.; Kataoka, K. *Science* **1999**, *283*, 65-67.
7. Ringsdorf, H.; Schlarb, B.; Venzmer, J. *Angew*. *Chem*. *Int*. *Ed*. *Engl*. **1988**, *27*, 113-158.
8. Lutz, J. *Polym*. *Int*. **2006**, *55*, 979-993.
9. Tu, R. S.; Tirrell, M. *Adv*. *Drug Deliv*. *Rev*. **2004**, *56*, 1537-1563.
10. Kukula, H.; Schlaad, H.; Antonietti, M.; Förster, S. *J. Am. Chem. Soc*. **2002**, *124*, 1658-1663.
11. Kwon, G.; Naito, M.; Yokoyama, M.; Okano, T.; Sakuri, Y.; Kataoka, K. *Langmuir* **1993**, *9*, 945-949.
12. Jada, A.; Hurtrez, G.; Siffert, B.; Riess, G. *Macromol. Chem. Phys*. **1996**, *197*, 3697-3710.
13. Gohy, J. F.; Creutz, S.; Garcia, M.; Mahltig, B.; Stamm, M.; Jerome, R. *Macromolecules* **2000**, *33*, 6378-6387.
14. Bonné, T. B.; Lüdtke; K.; Jordan, R.; Štěpánek, P.; Papadakis, C. M. *Colloid Polym. Sci*. **2004**, *282*, 833-843.
15. Nishikawa, T.; Akiyoshi, K.; Sunamoto, J. *Macromolecules* **1994**, *27*, 7654-7659.
16. Deming, T. J. *Adv*. *Drug Deliv. Rev*. **2002**, *54*, 1145-1155.
17. Kataoka, K.; Harada, A.; Nagasaki, Y. *Adv*. *Drug Deliv*. *Rev*. **2001**, *47*, 113-131.
18. a) Wright, E. R.; Conticello, V. P. *Adv*. *Drug*. *Deliv*. *Rev*. **2002**, *54*, 1057-1073. b) Wright, E. R.; Conticello, V. P.; Apkarian, R. P. *Microsc. Microanal*. **2003**, *9*, 171-182.
19. Karsa, D. R.; Stephenson, R. A. *Chemical aspects of drug delivery systems*, Royal Society of Chemistry Information Services: Cambridge, 1996.
20. Dinh, S. M.; DeNuzzio, J.D.; Comfort, A. R. *Intelligent materials for controlled*

drug release, ACS: Washington DC, 1999.

21. El-Nokaly, M.A.; Piatt, D. M.; Charpentier, B.A. *Polymeric delivery systems: Properties and applications*, ACS: Washington DC, 1993.
22. Tarcha, P. J. *Polymers for Controlled drug delivery*, CRC Press: Boca Raton, 1991.
23. Kwak, J. C. *Polymer-Surfactant Systems*, Surfactant Science Series 77; Marcel Decker; New York, 1998.
24. Rodrígruez-Hernández, J.; Chécot, F.; Gnanou, Y.; Lecommandoux, D. *Prog*. *Polym*. *Sci*. **2005**, *30*, 691-724.
25. Adams, M. L.; Lavasanifar, A.; Kwon, G. S. *J*. *Pharm*. *Sci*. **2003**, *92*, 1343-355.
26. Savić, R.; Luo, L.; Eisenberg, A.; Maysinger, D. *Science* **2003**, *300*, 615-618.
27. von Corswant, C.; Thorén, P. E. G. *Langmuir* **1999**, *15*, 3710-3717.
28. Jeong, Y-Il.; Cheon, J-B.; Kim, S-H.; Nah, J-W.; Lee, Y-M.; Sung, Y-K.; Akaike, T.; Cho, C-S. *J*. *Control*. *Rel*. **1998**, *51*, 169-178.
29. Li, Y.; Kwon, S. *Colloids Surf. B: Biointerfaces* **1999**, *16*, 217-226.
30. Jonsson, B. *Surfactants and Polymers in Aqueous Solution*, Wiley: New York, 1998.
31. Tundo, J. H. *Acc*. *Chem*. *Res*. **1984**, *17*, 3-8.
32. Karukstis, K. K.; McDonough, J. R. *Langmuir* **2005**, *21*, 5716-5721.
33. Goyal, P. S.; Aswal, V. K. *Curr*. *Sci*. **2001**, *80*, 972-979.
34. Siu, H.; Prazeres, T. J. V.; Duhamel, J.; Olesen, K.; Shay, G. *Macromolecules* **2005**, *38*, 2865-2875.
35. Narayanan, V. W.; Mendes, E.; Schosseler, F. *Langmuir* **2003**, *19*, 992-1000.
36. Santhana R.; Krishnan, G.; Thennarasu, S.; Mandal, A. B. *J*. *Phys*. *Chem*. *B* **2004**, *108*, 8806-8816.
37. Xu, J. –P.; Chen, W. –D.; Shen, J. –C. *Macromol*. *Biosci*. **2005**, *5*, 164-171.
38. Fan, Y.; Cao, M.; Yuan, G.; Wang, Y.; Yan, H.; Han, C. C. *J*. *Colloid Interface Sci*. **2006**, *299*, 928-937.
39. Jin, Y.; Tong, Li, Ai, P.; Li, M.; Hou, X. *Int*. *J*. *Pharm*. **2006**, *309*, 199-207.
40. Drew, M. *Surfactant Science and Technology*, VCH: New York, 1992.
41. Noshay, A. *Block Copolymers*: *Overview and Critical Survey*, Academic Press: New York, London, 1977.
42. Baltá-Calleja, F. J.; Rosłaniec, Z. *Block Copolymers*, Marcel Dekker: New York,

2000.

43. Hayashi, T.; Nakanishi, E.; Nakajima, A. *Polym. J.* **1987**, *9*, 1025-1032.
44. Nah, J-W, Jeong, Y-Il.; Cho, C-S. *Bull. Korean Chem. Soc*. **2000**, *21*, 383-388.
45. Chécot, F.; Lecommandoux, S.; Klok, H. –A.; Gnanou, Y. *Eur. Phys. J.* **2003**, *10*, 25-35.
46. Alexandridis, P.; Olsson, U.; Lindman, B. *Macromolecules* **1995**, *28*, 7700-7710.
47. Joralemon, M. J.; Murthy, K. S.; Remsen, E. E.; Becker, M. L.; Wooley, K. L. *Biomacromolecules* **2004**, *5*, 903-913.
48. a) Deming, T. J.; Nowak, A.; Yu, M.; Wyrsta, M. *Polymer Preprints* **2000**, *41*, 923. b) Pakstis, L. M.; Ozbas, B.; Hales, K. D.; Nowak, A. P.; Deming, T. J.; Pochan, D. *Biomacromolecules* **2004**, *5*, 312-318.
49. Halperin, A.; Tirrell, M.; Lodge, T. P. *Adv. Polym. Sci*. **1992**, *100*, 31-71.
50. a) Zhang, L.; Yu, K.; Eisenberg, A. *Science* **1996**, *272*, 1777-1779. b) Zhang, L.; Eisenberg, A. *J. Am. Chem. Soc*. **1996**, *118*, 3168-3181.
51. Desjardins, A.; Eisenberg, A. *Macromolecules* **1991**, *24*, 5779-5790.
52. a) Choucair, A. A.; Kycia, A. H.; Eisenberg, A. *Langmuir* **2003**, *19*, 1001-1008. b) Nardin, C.; Hirt, T.; Leukel, J.; Meier, W. *Langmuir* **2000**, *16*, 1035-1041. c) Opsteen, J. O.; Cornelissen, J. J. L. M.; van Hest, J. C. M. *Pure Appl. Chem*. **2004**, *76*, 1309-1319.
53. Shen, H.; Zhnag, L.; Eisenberg, A. *J. Am. Chem. Soc*. **1999**, *121*, 2728-2740.
54. Raez, J.; Manners, I.; Winnik, M.A. *J. Am. Chem. Soc*. **2002**, *124*, 10381-10395.
55. Jenekhe, S.; Chen, X. L. *Science* **1999**, *283*, 372-375.
56. Rathore, O.; Sogah, D. Y. *J. Am. Chem. Soc*. **2001**, *123*, 5231-5239.
57. a) Forster, S.; Antonietti, M. *Adv. Mater*. **1998**, *10*, 195-217. b) Antonietti, M.; Forster, S.; Hartman, J.; Oestreich, S. *Macromolecules* **1996**, *29*, 3800-3806.
58. a) Moffitt, M.; McMahon, L.; Oessel, V.; Eisenberg, A. *Chem. Mater*. **1995**, *7*, 1185-1192. b) Aizawa, M.; Buriak, J. *J. Am. Chem. Soc*. **2005**, *127*, 8932-8933.
59. a) Kamperman, M.; Garcia, C. B. W.; Du, P.; Ow, H.; Wiesner. *J. Am. Chem. Soc*. **2004**, *126*, 14708-14709. b) Jain, A.; Hall, L. M.; Garcia, C. B. W.; Gruner, S. M.; Wiesner, U. *Macromolecules* **2005**, *38*, 10095-10100.
60. a) Cammas, S.; Nagasaki, Y.; Kataoka, K. *Bioconj. Chem*. **1995**, *6*, 226-230. b)

Cammas, S.; Kataoka, K. *Macromol. Chem. Phys*. **1995**, *196*, 1899-1905.

61. *Polymers in Aqueous Media*: *Performance through Association*. Ed. J. E. Glass; ACS Advances in Chemistry Series 223; 1989.
62. *Hydrophilic Polymers*: *Performance with Environmental Acceptability* Ed. J. E. Glass; ACS Advances in Chemistry Series 248; 1996.
63. *Associative Polymers in Aqueous Media*. Ed. J. E. Glass; ACS Advances in Chemistry Series 765; 2000.
64. a) Duhamel, J.; Yekta, A.; Hu, Y. Z.; Winnik, M. A. *Macromolecules* **1992**, *25*, 7024-7030. b) Horiuchi, K.; Rharbi, Y.; Spiro, J. G.; Yekta, A.; Winnik, M. A.; Jenkins. R. D.; Bassett, D. R. *Langmuir* **1999**, *15*, 1644-1650.
65. a) Suwa, M.; Hashidzume, A.; Morishima, Y.; Nakato, T.; Tomida, M. *Macromolecules* **2000**, *33*, 7884-7892. b) Kang, H. S.; Yang, S. R.; Kim, J. -D.; Han, S. -H.; Chang, I. -S. *Langmuir* **2001**, *17*, 7501-7506.
66. Sato, Y.; Hashidzume, A.; Morishima, Y. *Macromolecules* **2001**, *34*, 6121-6130.
67. Garnier, G.; Duskova-Smrckova, M.; Vyhnalkova, R.; van de Ven, T. G. M.; Revol, J. *Langmuir* **2000**, *16*, 3757-3763.
68. a) Hu, Y.; Smith, G. L.; Richardson, M. F.; McCormick, C. L. *Macromolecules* **1997**, *30*, 3526-3537. b) Hu, Y.; Armentrout, S.; McCormick, C. L. *Macromolecules* **1997**, *30*, 3538-3546.
69. Lee, K. Y.; Jo, W. H.; Kwon, I. C.; Kim, Y.; Jeong, S. Y. *Macromolecules* **1998**, *31*, 378-383.
70. a) Barros, T. C.; Adronov, A.; Winnik, F. M.; Bohne, C. *Langmuir* **1997**, *13*, 6089-6094. b) Spafford, M.; Polozoya, A.; Winnik, F. M. *Macromolecules* **1998**, *31*, 7099-7102. c) Principi, T.; Goh, C. C.; Liu, R. C. W.; Winnik, F. M. *Macromolecules* **2000**, *33*, 2958-2966. d) Akiyoshi, K.; Kang, E-C, Kurumada, S.; Sunamoto, J.; Principi, T.; Winnik, F. M. *Macromolecules* **2000**, *33*, 3244-3249. e) Miyazawa, R.; Winnik, F. M. *Macromolecules* **2002**, *35*, 9536-9544.
71. a) Yamamoto, H.; Mizuskai, M.; Yoda, K.; Morishima, Y. *Macromolecules* **1998**, *31*, 3588-3594. b) Mizusaki, M.; Morishima, Y.; Winnik, F. M. *Macromolecules* **1999**, *32*, 4317-4326. c) Yusa, -S.; Kamachi, M.; Morishima, Y. *Langmuir* **1998**, *14*, 6059-6067. d) Sun, Q.; Ren, B.; Liu, X.; Zeng, F.; Liu, P.; Tong, Z. *Macromol. Symp*. **2003**,

192, 251-264.

72. a) Laflèche, F.; Durand, D.; Nicolai, T. *Macromolecules* **2003**, *36*, 1331-1340. b) Laflèche, F.; Nicolai, T.; Durand, D. *Macromolecules* **2003**, *36*, 1341-1348. c) Beaudoin, E.; Borisov, O.; Lapp, A.; Billon, L.; Hiorns, R. C.; François, J. *Macromolecules* **2002**, *35*, 7436-7447. d) Yekta, A.; Xu, B.; Duhamel, J.; Adiwidjaja, H.; Winnik, M. A. *Macromolecules* **1995**, *28*, 956-966.
73. a) Philippova, O. E.; Hourdet, D.; Audebert, R.; Khkhlov, A. R. *Macromolecules* **1997**, *30*, 8278-8285. b) Sato, Y.; Hashidzume, A.; Morishima. Y. *Macromolecules* **2001**, *34*, 6121-6130.
74. Lee, A. S.; Gast, A. P.; Bütün, V.; Armes, P. *Macromolecules* **1999**, *32*, 4302-4310.
75. Claracq, J.; Santos, S. F. C. R.; Duhamel, J.; Dumousseaux, C.; Corpart, J. *Langmuir* **2002**, *18*, 3829-3835.
76. Bodanszky, M. *Peptide Chemistry*: *A Practical Text Book 2nd Edition*; Springer: Verlag Berlin 1993.
77. a) Kovacs, J.; Giannotti, R.; Kapoor, A. *J. Am. Chem. Soc.* **1966**, *88*, 2282-2292. b) Kovacs, J.; Kapoor, A. *J. Am. Chem. Soc.* **1965**, *87*, 118-119. c) Kovacs, J.; Ballina, R.; Rodin, R. L. *J. Am. Chem. Soc.* **1965**, *87*, 119-120.
78. a) DeTar, D. F.; Gouge, M.; Honsberg, W.; Honsberg, U. *J. Am. Chem. Soc.* **1967**, *89*, 988-998. b) DeTar, D. F.; Vajda, T. *J. Am. Chem. Soc.* **1967**, *89*, 998-1004.
79. Amiya, T.; Itou, S.; Van, K.; Teramoto, A. *Int. J. Biol. Macromol*. **1981**, *3*, 218-224.
80. Seipke, G.; Arfmann, H.; Wagner, K. *Biopolymers* **1980**, *19*, 189-201.
81. Merrifield. R. B. *J. Am. Chem. Soc.* **1963**, *85*, 2149-2154.
82. Blout., E. R.; Karlson, R. H. *J. Am. Chem. Soc.* **1956**, *78*, 941-946.
83. Cheng, J.; Deming, T. J. *J. Am. Chem. Soc*. **2001**, *123*, 9457-9458.
84. a) Cheng, J.; Deming, T. J. *Macromolecules* **2001**, *34*, 4348-4354. b) Berzezinska, K.R.; Deming, T. J. *Macromolecules* **2001**, *34*, 5169-5174.
85. Higuchi, M.; Takizawa, A.; kinoshita, T.; Tsujita, Y.; Okochi, K. *Macromolecules* **1990**, *23*, 361-365.
86. McGrath, K. P.; Fournier, M. J.; Mason, T.L.; Tirrell, D. A. *J. Am. Chem. Soc*. **1992**, *114*, 727-733.
87. Won, J. -I.; Barron, A. E. *Macromolecules* **2002**, *35*, 8281-8287.

88. Uhrich, K. E. *Chem. Rev*. **1999**, *99*, 3181-3198.

89. Herrero-Vanrell, R.; Refojo, M. F. *Adv. Drug Deliv Rev*. **2001**, *52*, 5-16

90. Kwon, G. S.; Okano, T. *Adv. Drug Deliv*. *Rev*. **1996**, *21*, 107-116.

91. Gillies, E. R.; Fréchet, J. M. *J. Pure Appl. Chem*. **2004**, *76*, 1295-1307.

92. Lavasanifar, A.; Samuel, J.; Kwon, G. S. *Adv. Drug Deliv*. *Rev*. **2002**, *54*, 169-190.

93. a) Kidchob, T.; Kimura, S.; Imanishi, Y. *J. Control*. *Rel*. **1996**, *40*, 285-291. b) Yokoyama, M.; Fukushima, S.; Uehara, R.; Okamoto, K.; Kataoka, K.; Sakuri, Y.; Okano, T. *J. Control*. *Rel*. **1998**, *50*, 79-92. c) Kidchob, T.; Kimura, S.; Imamishi, Y. *J. Control*. *Rel*. **1998**, *51*, 241-248. d) Yokoyama, M.; Satoh, A.; Sakuri, Y.; Okano, T.; Matsumura, Y.; Kakizoe, T.; Kataoka, K. *J. Control*. *Rel*. **1998**, *55*, 219-229. e) Govender, T.; Stolnik, S.; Xiong, C.; Zhang, S.; Illum, L.; Davis, S. S. *J. Control*. *Rel*. **2001**, *75*, 249-258.

94. Jeong, B.; Bae, Y. H.; Kim. S. W. *Colloids Surf. B: Biointerfaces* **1999**, *16*, 185-193.

95. Asano, M.; Yoshida, M.; Kaetsu, I. *Makromol. Chem*. **1983**, *184*, 1761-1770.

96. Kwon, G. S.; Naito, M.; Kataoka, K.; Yokoyama, M.; Sakuri, Y.; Okano, T. *Colloids Surf. B: Biointerfaces* **1994**, *2*, 429-424.

97. Yokoyama, M.; Kwon, G. S.; Okano, T.; Sakuri, Y.; Seto, T.; Kataoka, K. *Bioconjugate Chem*. **1992**, *3*, 295-301.

98. Bader, J. H.; Ringsdorf, H.; Schmidt, B. *Agnew. Makromol. Chem*. **1984**, *123*, 457-485.

99. Pattern, M. K.; Lloyd, J. B.; *Makromol. Chem*. **1985**, *186*, 725-733.

100. Yokoyama, M.; Miyauchi, M.; Yamada, N.; Okano, T.; Sakuri, Y.; Kataoka, K.; Inoue, S. *J. Control*. *Rel*. **1990**, *11*, 269-278.

101. a) Batrakova, E. V.; Dorodnych, T. Y.; Klinski, E. Y.; Kliushnen-kova, E. N.; Shemchukova, O. B.; Goncharova, O.N.; Arjakova, S. A.; Alakhov, V. Y.; Kabanov, A. V. *Br*. *J. Cancer* **1996**, *74*, 1545. b) Alakhov, V.; Klinski, E.; Li, S.; Pietrzynski, G.; Venne, A.; Batrakova, E.; Bronitch, T.; Kabanov, A. *Colloids Surf. B: Biointerfaces* **1999**, *16*, 113-134. c) Malmsten, M. *Soft Matt*. **2006**, *2*, 760-769. d) Fusco, S.; Borzacchiello, A.; Netti, P. A. *J. Bioact. Compat*. *Polym*. **2006**, *21*, 149-164.

102. Mitra, A.; Mulholland, J.; Nan, A.; McNeill, E.; Ghanderhari, H.; Line, B. R. *J.*

Control. *Rel*. **2005**, *102*, 191-201.

103. Sawant, R. M.; Hurley, J. P.; Salmaso, S.; Kale, A.; Tolcheva, E.; Levchenko, T. S.; Torchilin, V. P. *Bioconj. Chem*. **2006**, *17*, 943-949.
104. Kopeček, J. Eur. *J*. *Pharm*. *Sci*. **2003**, *20*, 1-16.
105. Walter, K. A.; Tamargo, R.; Olivi, A.; Burger, P. C.; Brem, H. *Neurosurgery* **1995**, *37*, 1129-1145.
106. Lakowicz, J. R. *Principles of Fluorescence Spectroscopy, 2nd Ed*. Kluwer Academic/Plenum Publishers: New York, 1999.
107. Demas, J. N. *Excited State Lifetime Measurements*; Academic Press: New York, 1983.
108. Duhamel, J. in *Molecular Interfacial Phenomena of Polymers and Biopolymers*. Ed. P. Chen, CRC Press, 2005; pp 214-248.
109. Winnik, F. M. *Chem. Rev*. **1993**, *93*, 587-614.
110. Winnik, F. M.; Regismond, S. T. A. *Colloids Surf. A: Phys. Eng. Asp.* **1996**, *118*, 1-39.
111. a) Johnson, W. C. *Proteins: Structure, Function, and Genetics* **1990**, *7*, 205-214. b) Wallace, B. A. *Nature structural biology* **2000**, *7*, 708-709. c) Fasman, G. D.; Hoving, H.; Timasheff, S. N. *Biochemistry* **1970**, *9*, 3316-3324.
112. a) Greenfield, N.; Fasman, G. D. *Biochemistry* **1969**, *8*, 4108-4116. b) Saxena, V. P.; Wetlaufer, D. B. *Proc*. *Natl*. *Acad*. *Sci*. *USA* **1971**, *68*, 969-972.
113. McDiarmid, R.; Doty, P. *J*. *Phys*. *Chem*. **1966**, *70*, 2620-2627.
114. Sage, H. J.; Fasman, G. D. *Biochemistry* **1966**, *5*, 286-296.
115. a) Auer, H. E.; Doty, P. *Biochemistry* **1966**, *5*, 1708-1715. b) Auer, H. E.; Doty, P. *Biochemistry* **1966**, *5*, 1716-1725.
116. a) Dai, S.; Tam, K. C.; Jenkins, R. D.; Basset, D. R. *Macromolecules* **2000**, *33* 7021-7028. b) Islam, M. F.; Jenkins, D. R.; Ou-Yang, H. D. *Macromolecules* **2000**, *33*, 2480-2485.
117. Dai, S.; Tam, K. C.; Jenkins, R. D.; Basset, D. R. *Macromolecules* **2000**, *33*, 404-411.
118. Noda, T.; Morishima, Y. *Macromolecules* **1999**, *32*, 4631-4640.
119. a) Winnik, M. A.; Bystryak, S. M.; Siddiqui, J. *Macromolecules* **1998**, *31*, 6855-6864. b) Winnik, M. A.; Bystryak, S. M.; Siddiqui, J. *Macromolecules* **1999**, *32*, 624-

632.

120. Birks J. B. *Photophysics of Aromatic Molecules*; Wiley: New York, 1970; p351, p 317.
121. Weber, G.; Farris, F. J. *Biochemistry* **1979**, *18*, 3075-3078.
122. Yekta, A.; Duhamel, J.; Adiwidjaja, H.; Brochard, P.; Winnik, M. A. *Langmuir* **1993**, *9*, 881-883.
123. Kalyanasundaran, K.; Thomas, J. K. *J. Am. Chem. Soc.* **1977**, *99*, 2039-2044.
124. Dong, D. C.; Winnik, M. A. *Can. J. Chem*. **1984**, *62*, 2560-2565.
125. Kumzcheva, E.; Rharbi, Y.; Winnik, M. A.; Guo, L.; Tam, K. C.; Jenkins, R. D. *Langmuir* **1997**, *13*, 182-186.
126. Magny, B.; iliopoulus, I.; Audebert, R. *Macromlecules Complex in Chemistry & Biology*, Dubin, P.; Bock, J.; Davis, R. M.; Shulz, D. N.; Thies, C. Eds. Spring-verlag, Berlin, 1994.
127. Clark, M.D.; Hoyle, C. E.; McCormick, C. L. *Macromolecules* **1990**, *23*, 3124-3129.
128. Sun, Q.; Tong, Z.; Wang, C.; Liu, X.; Zeng, F. *Eur*. *Polym*. *J*. **2003**, *39*, 697-703.
129. Kawamoto, T.; Hashidzume, A.; Morishima, Y. *J*. *Coll*. *Interface Sci*. **2005**, *291*, 537-542.
130. Mizusaki, M.; Morishima, Y.; Winnik, F. M. *Polymer* **2001**, *42*, 5615-5624.
131. Stryer, L.; Haugland, R. P. *Proc*. *Natl*. *Acad*. *Sci*. *USA* **1967**, *58*, 719-726.
132. Berlman, I. B. *Energy Transfer Parameters of Aromatic Compounds*, Academic Press: New York, 1973.
133. Winnik, F. M. *Polymer* **1990**, *31*, 2125-2134.
134. Zhang, M.; Duhamel, J.; van Duin, M.; Meessen, P. *Macromolecules* **2004**, *37*, 1877-1890.

Chapter 2
Polypeptide Synthesis

2.1. Introduction

The synthesis of peptides via the condensation of amino acids has been the focus of numerous studies for the past five or six decades[1-7] and many approaches to accomplish this synthesis have been developed. The choice of a proper synthetic method depends on the amino acids that constitute the peptide. Some amino acids have side groups which can undergo unwanted reactions with the reagents used in the synthesis. Thus special attention must be paid to the structure of the amino acids used in the synthesis of a given peptide sequence. With the exception of proline which is a cyclic amino acid, all amino acids have the structure shown in Figure 2.1.

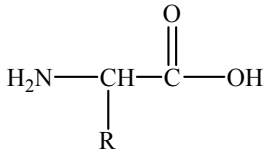

Figure 2.1. Chemical structure of an amino acid

Nineteen of the twenty essential amino acids differ only by the R group that is attached to the central carbon atom. Common amino acids include glycine (R = CH_3) and valine (R = isopropyl). Amino acids contain side groups which can have aromatic, basic, or acidic character. Out of the twenty essential amino acids, only proline has a secondary amine group, as shown in Figure 2.2.

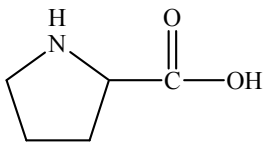

Figure 2.2. Chemical structure of proline.

All natural amino acids are found in the L-configuration and have a chiral carbon except for glycine for which the substituent R in Figure 2.1 is hydrogen. In nature, peptide synthesis is accomplished by the condensation reaction of an amine with an acid shown in Figure 2.3 which results in the formation of an amide bond and a water molecule. By driving the water out of the system, the reaction can be thermodynamically driven to the right. However the relative inefficiency of the process led scientists to devise new synthetic methods.

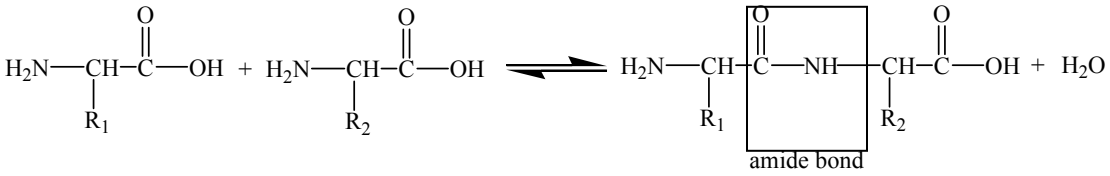

Figure 2.3. Amide bond formation between two amino acids

Almost all coupling reactions between two amino acids involve the protection of the amine function of one amino acid and the activation of its carboxylic acid. Nevertheless these more efficient syntheses are not without drawbacks. Countless papers involving peptide synthesis report difficulties in maintaining the chiral purity of the protected/activated amino acids during synthesis.[8] Unprotected amino acids are less prone to undergo racemization because the amine functionality hinders acidic catalysis and the carboxylic group hinders alkaline catalysis of racemization.

Figure 2.4 represents a typical mechanism by which an amino acid bearing a protected amine and an activated acid can undergo racemization. The mechanism depicted in Figure 2.4 occurs to varying degrees with each amino acid, depending on the steric hindrance

and electronic effects provided by the various side chains. No synthetic method has been found to be completely free of racemization, but many have been recognized to minimize its influence.

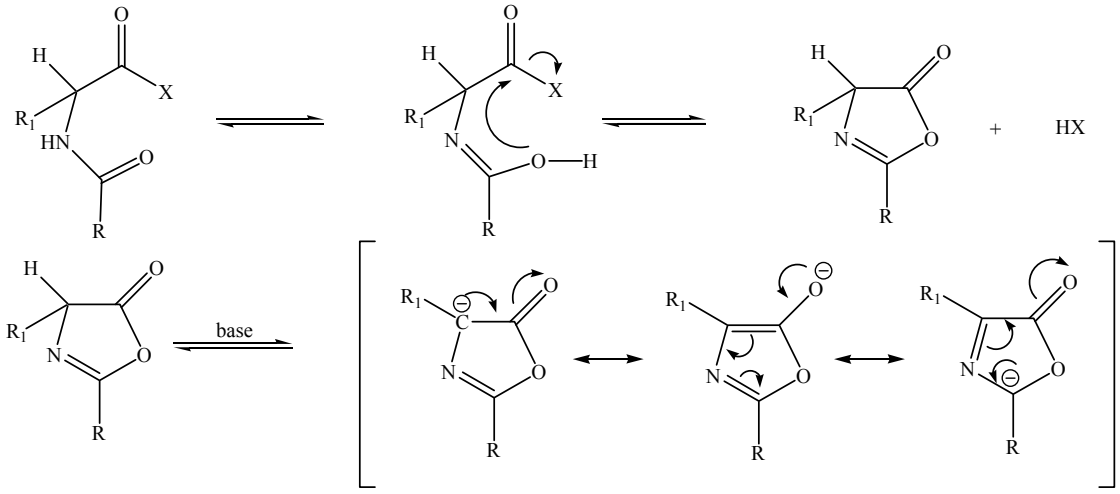

Figure 2.4. Racemization through an azlactone route: R_1 is the side chain for the amino acid, X is the activating/protecting group for the acid side of the amino acid and R is the alkyl group on the protecting group on the amino side of the amino acid.

The azlactone formation shown in Figure 2.4 occurs via a resonance stabilized cyclic intermediate and is generally accepted as a major pathway for racemization.[1] The cyclic intermediate is formed by the attack of the nucleophilic oxygen carboxyl carbon which has been made more electropositive by the presence of the activating group. In the presence of a base, de-protonation of the chiral center can take place. Re-protonation can occur on either side of the ring structure, thus resulting in a mixture of L- and D-isomers. The occurrence of D-isomers in a polypeptide must be minimized, because they can disrupt the secondary structure and thus the behavior of the polypeptide in solution. The uncontrolled incorporation of D-isomers in an otherwise all L-polypeptide complicates the characterization of the

polypeptide and weakens the conclusions drawn for the structure-property relations of a polypeptide.

2.1.1. Coupling methods

There are several factors, other than the sensitivity to side groups that need to be optimized when choosing a coupling method. These factors are the yield, the inertness of the protecting groups during the reaction, the minimization of side reactions and racemization, and the relative ease of synthesis.

The majority of coupling methods gives satisfactory results with respect to the first three considerations but often yield racemic mixtures. Many of them are difficult to handle and some require that the synthesis be conducted under inert atmosphere. All of them involve the activation of the carboxyl acid through an electron withdrawing substituent to produce a more highly electrophilic center for acylation. These methods include the use of acid chlorides,[9] acid azides[10] and anhydrides,[11] N-acyl derivatives[12] as well as carbodiimide coupling agents and active esters.[13] For example, coupling reactions involving acid chlorides require careful handling because they are very moisture sensitive and must be performed at low temperatures. Cyclic anhydride intermediates[1] and difficult to remove by-products are produced during the reactions. The acid chloride method also leads to extensive racemization.

In the azide method, the protected methyl ester of an amino acid is transformed into a hydrazide, which is then converted into an acid azide.[14] Although this procedure is still much in use, the major side reaction referred to as the Curtius rearrangement and shown in Figure 2.5 produces a toxic isocyanate by-product. This by-product is very reactive, forms a urea

linkage with the free amino acid groups in solution, and generates compounds which are very difficult to separate from the mixture. The advantage of this method is the presence of very low amounts of racemates. Unfortunately the reaction also produces very toxic hydrozoic acid as a by product.

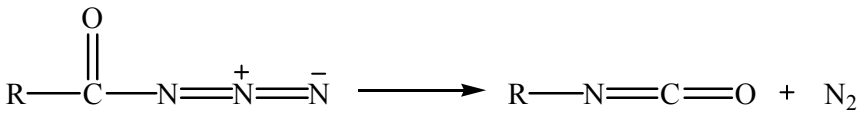

Figure 2.5. Curtius rearrangement: Formation of an isocyanate.

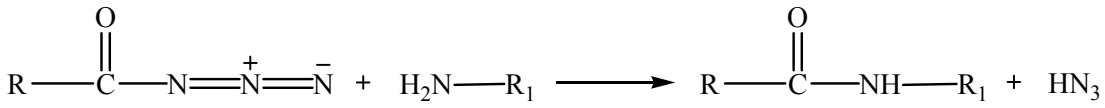

Figure 2.6. Formation of a peptide bond and hydrozoic acid.

Peptides have also been synthesized using alkyl mixed anhydrides. These have the advantage of generating easily removable by-products such as carbon dioxide and alcohol. The acid anhydride method has been the method of choice of Urry and Tamburro in the synthesis of artificial elastin.[15]

The reagent most commonly used by peptide chemists to create a mixed anhydride is isobutyl chloroformate.[16] As an anhydride, it exhibits two electrophilic sites that can react with the nucleophile, typically an amine. The main advantage of the method is that the bulky isobutyl side group minimizes potential side reactions and the amine attacks preferentially the A carbonyl group, as depicted in Figure 2.7. The main disadvantage of the method arises when dealing with an amino acid bearing a side chain of size comparable to that of isobutyl. For amino acids with bulky side chains like phenylalanine, isoleucine or valine, the

nucleophilic amine can react at either carbonyl A or B. This results in a by–product which is difficult to separate from the reaction mixture.

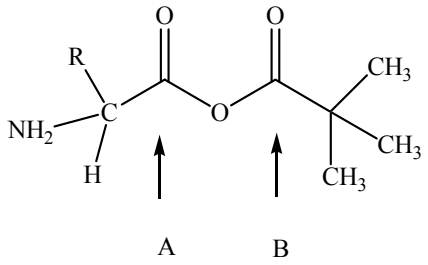

Figure 2.7. Mixed anhydride reactive sites: A is the preferred reaction site at the carboxyl of the amino acid, B is a sterically hindered second site by a t-Bu in this case.

Two of the most widely used methods for coupling today are carbodiimide and activated ester coupling. Both methods activate the free C-terminal carboxyl group on one amino acid to allow for faster coupling with the free N-terminal group on the second amino acid. The carbodiimide method is performed by activating the carboxyl group, and coupling and purifying the coupled amino acids in a single step[1] (Figure 2.8). The most commonly used carbodiimide in peptide synthesis is dicyclohexylcarbodiimide (DCC). It is fairly inexpensive and its by-product, dicyclohexyl urea (DCU) can be isolated and removed from the solution. However significant racemization can occur depending on the solvent used for coupling. The extent of racemization can be lowered by the addition of a catalyst, 1–hydroxybenzotriazole (HOBt), and copper salts such as $CuCl_2$.[17] HOBt is an excellent acylating agent which is also a weak acid that minimizes the removal of the hydrogen from the chiral carbon and its subsequent racemization.

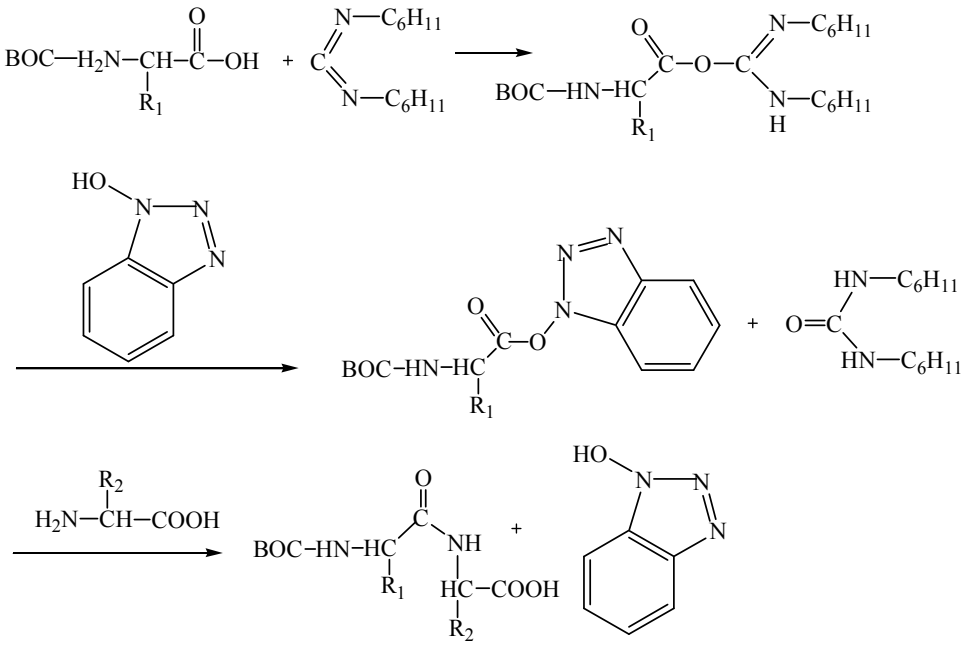

Figure 2.8. DCC/HOBt activation reaction

In the active ester method, DCC is used to activate the carboxyl group of an amino acid which is then reacted with HOBt, a strong electron withdrawing group that is easily crystallized and isolated before the addition of the next amino acid. Each electron withdrawing activating ester has different benefits and drawbacks. Three of the most widely used activating groups are *p*–nitrophenol (PNP),[18] *N*–hydroxysuccinimide (HOSu),[19] and pentachlorophenol (PCP).[20,21] They are shown in Figure 2.9. PCP is known to be the most reactive activated ester, reacting approximately 20 times faster than PNP,[22] but it also results in the largest steric hindrance as it contains many large chlorine groups close to the active site. HOSu is often used because it is water-soluble which makes it easily removable.[1,23]

There are many other coupling agents found in the literature that are reported to produce good yields and low racemization. They include 1–ethoxycarbonyl–2–ethoxy–1,2-

dihydroquinoline (EEDQ), 1−isobutylcarbonyl−2−isobutyloxy−1,2−dihydroquinoline (HDQ) used for mixed anhydrides,[24] benzotriazoyl N−oxytri-dimethyl-phophonium hexafluorophosphate chloride (BOP-Cl),[25] O−benzotriazolyl-tetramethyl-isouronium hexafluorophosphate (HBTU) and 1−ethyl−3−(3−dimethylaminopropyl) carbodiimide (EDC) to name but a few.

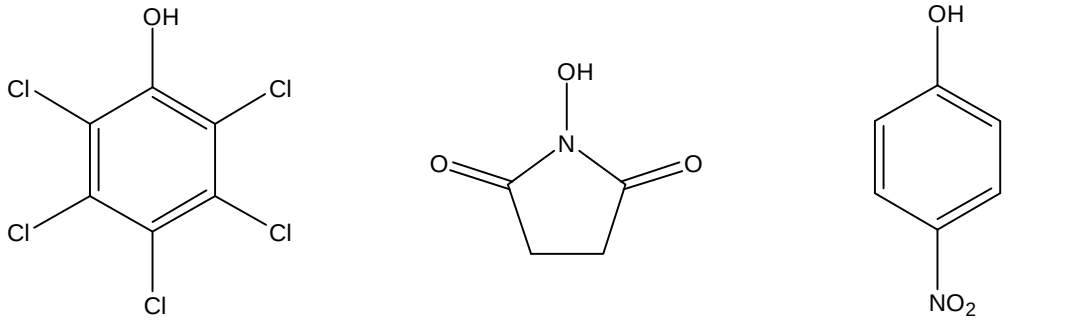

Pentachlorophenol (PCP) *N*-Hydroxysuccinimide (HOSu) *p*-Nitrophenol (PNP)

Figure 2.9. Common activating groups

2.1.2. Protecting groups

Most amino acids exhibit more than two reactive functional groups which complicates the specific coupling reaction of two amino acids. Accordingly protecting groups are used to minimize or completely eliminate side reactions. In the present work, the synthesis of the polypeptides has been carried out using two amino acids, phenylalanine and aspartic acid, the former being bifunctional whereas the latter is trifunctional. The chemical structures of these amino acids are shown in Figure 2.10. Consequently, the discussion of protective groups will focus on those most suitable for these two amino acids.

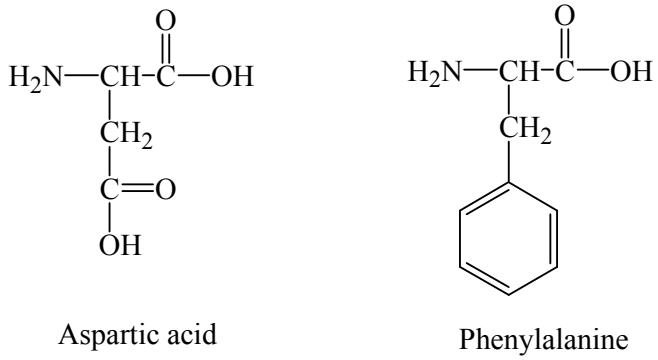

Figure 2.10. Chemical structure of trifunctional aspartic acid and bifunctional phenylalanine

The most commonly used amino protecting groups in peptide synthesis are the carbobenzoxycarbonyl (Z or CBz), *t*-butoxycarbonyl (*t*-Boc), and 9-fluorenylmethyloxycarbonyl (Fmoc), while *t*-butyl (*t*-Bu) and benzoxycarbonyl (Bz)[26-28] are used as protecting groups of the amino acid carboxylic group. Their structure is given in Figure 2.11.

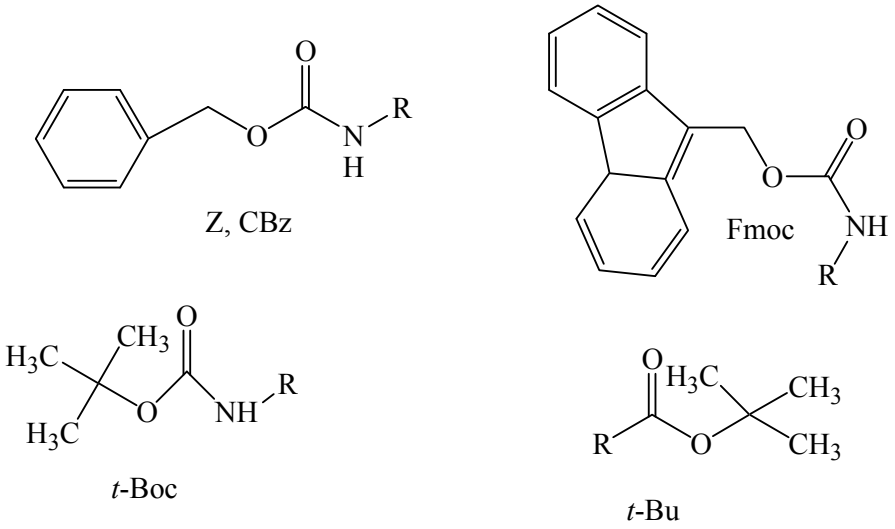

Figure 2.11. Common protecting groups in peptide synthesis

A well thought-out synthetic strategy must be applied to deprotect the desired group while leaving the others untouched.[29-31] Table 2.1 lists the conditions under which each group can be removed or remains stable. This list is by no means exhaustive, but accounts for those protecting groups most frequently used in peptide synthesis.

Table 2.1 Stability of peptide protecting groups

Protecting groups	Stable conditions	Removal conditions
Z, CBz	Basic	Hydrogenation, Acidic
t-Boc, *t*-Bu	Basic	Mild Acidic
Bz	Basic	Acidic
Methyl Ester	Acidic	Strong Basic
Fmoc	Acidic	Mild Basic

2.1.3. Polymerization

Polypeptides with well-defined repeating sequence can only be synthesized by preparing first a peptide referred to as a monomer which is then polymerized. To achieve high molecular weight polypeptides, the carboxyl group of the monomer must be activated using an active ester such as PCP, HOSu, or PNP. These active esters are more stable in solution than the intermediates produced using a coupling agent such as DCC, and thus live longer and continue to react over long periods of time to produce longer chain polypeptides.

After the required sequence has been synthesized, it is de-protected at the N-terminal of the monomer with a dilute solution of HCl or trifluroacetic acid (TFA) resulting in a chloride or trifluoroacetate ammonium salt. A hindered tertiary base such as triethylamine

(TEA) or *N*–methylmorpholine (NMM) is used to free the amine and begin the polymerization. Dimethylsulphoxide (DMSO) or *N*, *N*–dimethylformamide (DMF) are used as solvents for the polymerization reaction to ensure that the product remains soluble during the polymerization. Other common solvents such as ethyl acetate and methylene chloride commonly used during the monomer synthesis are unable to solubilize the growing chains. Also higher concentrations of monomer are used to produce higher molecular weight (MW) polypeptides.

Depending on the reactivity of the monomer and the desired MW, the polymerization reaction can go on for 1 to 14 days before completion. The workup of the polypeptides is carried out by successive washes with large portions of ether, water, and methanol to remove the solvent and any small molecules such as PCP and TFA as well as any undesirable low MW oligomeric material. These steps can be followed by dialysis, where the pore size of the dialysis tubing is chosen to remove low molecular weight polypeptides.

2.1.4. Monomer synthesis

In this work, the monomer refers to a sequence of 3-4 amino acids which will be polymerized to give a polypeptide with a well-defined repeating sequence. The strategy is followed to prepare five polypeptides made up of aspartic acid (Asp) and phenylalanine (Phe) in varying proportions, $(Asp_3Phe_1)_n$, $(Asp_2Phe_1)_n$, $(Asp_1Phe_1)_n$, $(Asp_1Phe_2)_n$, and $(Asp_1Phe_3)_n$, affording a range of hydrophilic and hydrophobic character. The synthesis was designed to use a minimal number of steps and to yield the greatest amount of pure polypeptide.

Solution phase synthesis was chosen to produce the monomer because it generates

large quantities (grams) of material. Alternate method would have been to produce the monomer using solid phase synthesis. However solid phase synthesis is more commonly used to generate small amounts of oligopeptides in quantitative yield and the cost involved in obtaining gram scale quantities of such materials is quite high.

Schemes 2.1 and 2.2 illustrate two of the synthetic routes that were tried and found to be unsuccessful. By convention, the left and right hand side represents the N- and C-terminal of the amino acids, respectively. The *β*-carboxylic side chain of the aspartic acid is projected into the page and is shown as being either protected (Bz or *t*-Bu) or a free acid (OH). A horizontal line between two amino acids is a peptide linkage, while the reaction conditions for their coupling is described directly above the line.

Scheme 2.1. Synthesis of H–Asp(OBzl)Phe–PCP

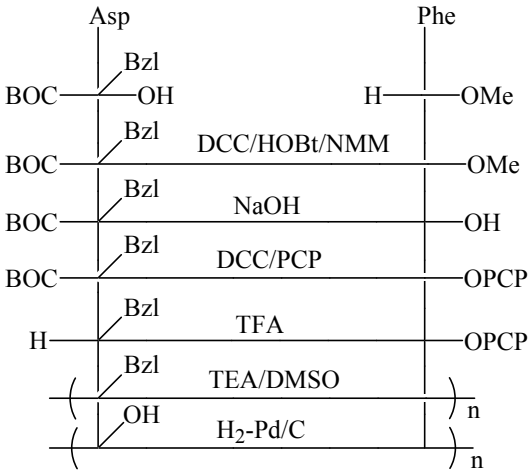

The route depicted in Scheme 2.1 was stopped due to the intermolecular cyclization of the dipeptide which occurred during the second step of the reaction scheme and whose mechanism is shown in Figure 2.12. This resulted in the removal of the Bzl protecting group

from the β–carboxylic acid on the aspartic acid as well as the desired elimination of the methyl group from the α–carboxylic acid of phenylalanine. Earlier studies have established that strong acidic or basic conditions induce cyclization when the β- or γ-carboxylic acid of, respectively, the aspartic or glutamic acid is protected by an n-alkyl or aryl group.[1]

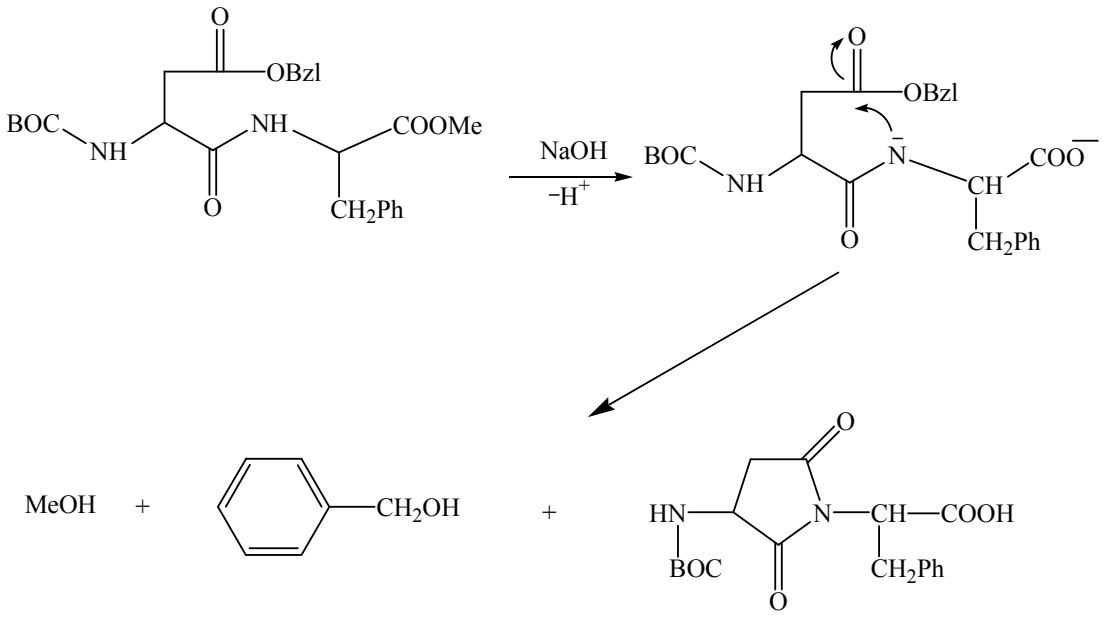

Figure 2.12. Mechanism for the cyclization reaction of the dipeptide resulting in the removal of the Bzl protecting group.

The second proposed route was discarded because of problems encountered with the hydrogenation of the monomer in the fifth step of Scheme 2.2. The activating group (PCP) was also being removed along with the CBz group which meant that low yields of the desired product were obtained.

Scheme 2.2 Synthesis of H–Asp(OBu^t)Phe–PCP

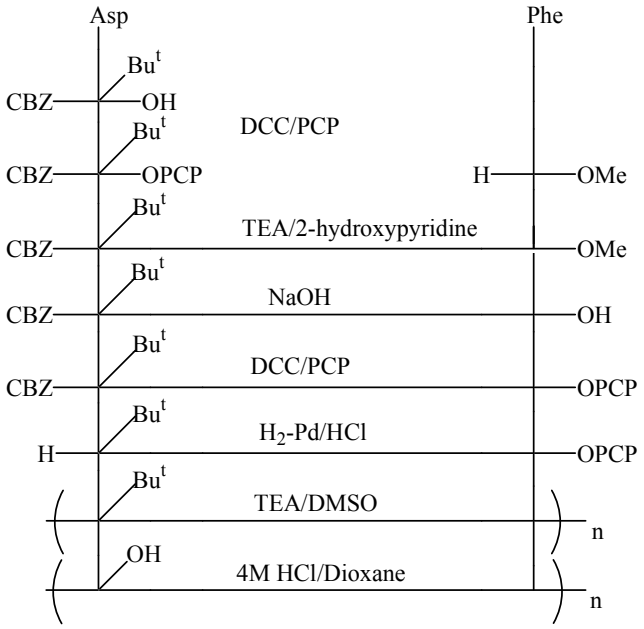

These unsuccessful synthetic schemes are examples of the difficulties encountered during the synthesis of the polypeptides used in this project. The successful syntheses are now reported.

2.2. Experimental

Materials and methods

Tert–butyloxycarbonyl–L–phenylalanine and *tert*–butyloxycarbonyl–L–*β*–benzyl-aspartic acid were obtained from Bachem. Phenylalanine and other chemicals used were purchased from Sigma-Aldrich. Solvents of spectrograde quality (acetone, ethyl acetate, methanol, THF, DMF, and diethyl ether) were bought from VWR or Caledon. All solvents were used as received unless otherwise stated. Milli–Q water, with a resistivity of over 18 MΩ.cm, was used in all preparatory steps.

All melting points are uncorrected and were taken on a Mel-Temp apparatus. The reactions were followed by chromatography and the solvent mixture used for TLC was chloroform:methanol:acetic acid (85:10:5). ^{1}H NMR spectra were acquired on a 300 MHz, Bruker Instrument in deutrated DMSO. The NMR spectra of all peptides and polypeptides prepared during this work are presented in the Appendix. All spectra exhibit two peaks at 2.4 and 3.3 ppm due to the presence of DMSO, the solvent, and residual water in the solvent, respectively. The NMR spectra show that some racemization does take place as indicated by the presence of extra NH peaks in the intermediates prepared during the synthesis of the monomer. There are extra NH peaks observed in the NMR spectra of the polypeptides which also indicate a small amount of racemization. Mass spectra were acquired on a Waters/Micromass QTOF Ultima Global mass spectrometer using positive ion nanoelectrospray (ESI) equipped with an electrospray ionizer and a quadrupole time-of-flight (QTOF) detector. Samples were infused at a rate of 2 μL/min in a 1:1 acetonitrile:water mixture. Typical operating conditions consisted of a source temperature of 80 ^{o}C, a capillary voltage of 3.5 kV, a cone voltage of 60-160 V, and a mass resolution of ~9000.

2.3. Peptide synthesis

2.3.1. Synthesis of poly(Asp_1Phe_1)

For polymerization purposes, a tetrapeptide active ester was chosen as the monomer since a dipeptide active ester would be expected to yield the diketopiperazine[1] in addition to the polymer, whereas the tripeptide would not give the desired alternating sequence. As shown in Scheme 2.3, the peptide was extended from its amino end by the reaction of the Boc-Asp(OBzl)-OSu ester with the free H-Phe-OH using $NaHCO_3$ for the coupling reaction.

The Boc protecting group was removed by using trifluoroacetic acid (TFA). The tripeptide and the tetrapeptide were prepared similarly. Each amino acid addition goes through an activation, a coupling and a deprotection step. This procedure ensures minimum racemization throughout the synthesis because the unwanted cyclization of the activated amino acid is reduced thanks to the bulkiness of the Boc group and also by the use of *N*-hydroxy succinimide (HOSu) which acts both as the activating group and as an auxiliary nucleophile providing competition in the abstraction of the proton from the carbon atom of the intermediate activated with dicyclohexylcarbodiimide (DCC). The Boc tetrapeptide was then activated with HOSu and the Boc group removed before polymerization. The polymerization was carried out in DMSO using triethylamine (TEA) as the base. The benzyl protecting group was finally removed after completing the polymerization using methane sulphonic acid in the presence of thioanisole.

Scheme 2.3 Synthesis of the alternating poly(Asp_1Phe_1)

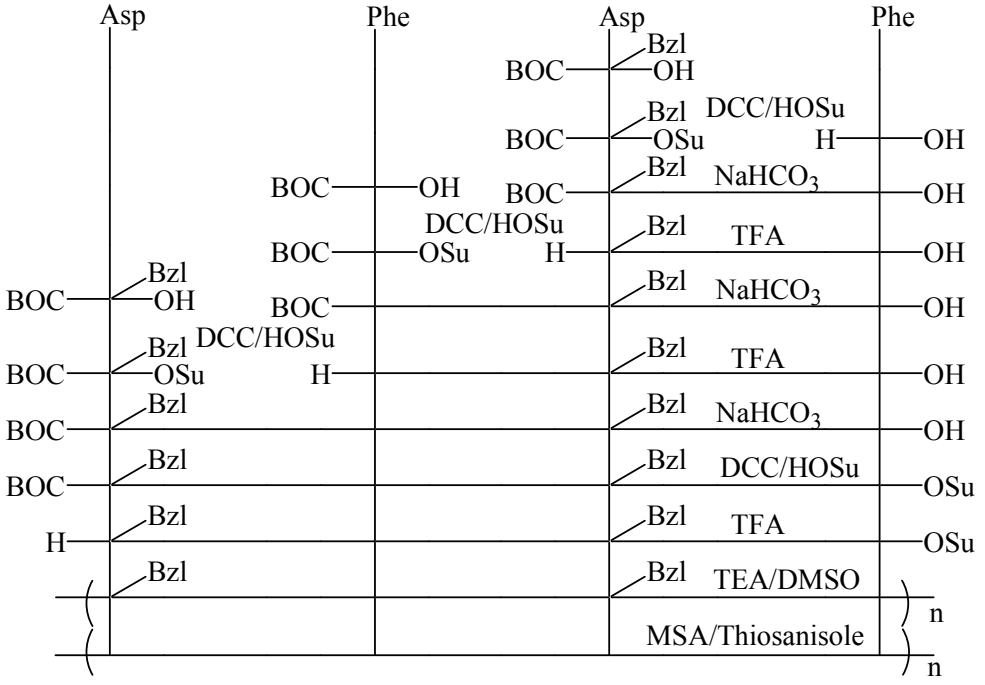

Boc-Asp(OBzl)-OSu (1)

To a solution of *tert*-butyloxycarbonyl-L-*β*-benzyl-aspartic acid (Boc-Asp(OBzl)-OH) (25 g, 0.077 mole) and *N*-hydroxy succinimide (HOSu, 9.8 g, 0.085 mole) in ethyl acetate (200 mL) at -5 ^{o}C, dicyclohexylcarbodiimide (DCC, 17.5 g, 0.085 mole) was added.[32] The mixture was stirred for 5 h at -5 ^{o}C and then left to stand overnight in a refrigerator. The excess DCC was decomposed by adding glacial acetic acid (3 mL). The dicyclohexyl urea thus produced was filtered off and the filtrate was concentrated under vacuum using a rotary evaporator. The viscous oil obtained was redissolved in ethyl acetate and more urea was filtered off. The ethyl acetate solution was successively washed with 40 mL of 0.5 M sodium carbonate, water, 0.5 M hydrochloric acid, and water. After drying of the ethyl acetate layer over anhydrous sodium sulphate and removal of the solvent under reduced pressure, the white solid of **1** was obtained which was crystallized in isopropanol.

Yield: 88 % (28.6 g), m.p. 98-99 ^{o}C

300 MHz, ^{1}H NMR: δ (dmso-d_6) ppm 1.34 (s, 9H, C(CH_3)$_3$-Boc), 2.76 (s, 4H, CH_2-Su), 2.81-3.0 (m, 2H, CH_2-pendent), 4.70-4.77 (q, 1H, CH-backbone), 5.09 (s, 2H, CH_2-Bzl), 7.32 (5H, Ar-H), 7.68-7.71 (d, 1H, NH)

Boc-Asp(OBzl)-Phe-OH (2)

A solution of **1** (16 g, 0.038 mole) in tetrahydrofuran (THF, 200 mL) was added to a solution of phenylalanine (5.9 g, 0.036 mole) and sodium bicarbonate (6.0 g, 0.71 mole) in THF (200 mL) and water (200 mL).[33] After the solution had been stirred at room temperature for 24 h, the reaction mixture was concentrated by removing THF with the rotary evaporator, acidified with 0.5 M hydrochloric acid, and extracted with ethyl acetate (500 mL). The organic layer was then washed with water three times (200 mL), dried over anhydrous

sodium sulphate, filtered, and the solvent was removed under reduced pressure. Addition of petroleum ether (bp 30-60 ^{o}C) to the oily concentrate resulted in the precipitation of the dipeptide **2** which was filtered.

Yield: 92 % (15.5 g), m.p. 115-116.5 ^{o}C

300 MHz, ^{1}H NMR: δ (dmso-d_6) ppm 1.33 (s, 9H, C(CH_3)$_3$-Boc), 2.47-2.71 (m, 2H, CH_2-pendent), 2.77-3.03 (m, 2H, CH_2-pendent), 4.29-4.38 (m, 2H, CH-backbone), 5.0-5.09 (s, 2H, CH_2-Bzl), 7.10-7.32 (m, 10H, Ar-H), 7.89-7.95 (d, 1H, NH)

Boc-Phe-OSu (3)

To a solution of *tert*-butyloxycarbonyl-L-phenylalanine (Boc-Phe-OH) (15 g, 0.057 mole) and HOSu (7.2 g, 0.062 mole) in methylene chloride (CH_2Cl_2, 120 mL) at -5 ^{o}C, DCC (12.8 g, 0.062 mole) was added. The mixture was stirred for 5 h at -5 ^{o}C and then left to stand overnight in a refrigerator. The reaction was worked up as mentioned above for **1**. A white solid of **3** was obtained which was crystallized in isopropanol.

Yield: 82 % (16.8 g), m.p. 138-138.5 ^{o}C

300 MHz, ^{1}H NMR: δ (dmso-d_6) ppm 1.27 (s, 9H, C(CH_3)$_3$-Boc), 2.78 (s, 4H, CH_2-Su), 2.92-3.17 (m, 2H, CH_2-pendent), 4.48-4.56 (m, 1H, CH-backbone), 7.19-7.30 (m, 5H, Ar-H), 7.61-7.64 (d, 1H, NH)

H-Asp(OBzl)-Phe-OH.CF_3COOH (4)

The dipeptide **2** (5 g, 0.011 mole) was dissolved in trifluoroacetic acid, (TFA, 12 mL) and the reaction mixture was stirred for 45 min at room temperature.[33] After removal of TFA under reduced pressure, anhydrous ether was added to the residue to obtain white crystals of **4** in quantitative yield.

m.p. 73-76 ^{o}C

300 MHz, ^{1}H NMR: δ (dmso-d_6) ppm 2.74-3.11 (m, 4H, CH_2-pendent), 4.0-4.1 (m, 1H, CH-backbone), 4.4-4.5 (m, 1H, CH-backbone), 5.08 -5.16 (t, 2H, CH_2-Bzl), 7.20-7.36 (m, 10H, Ar-H), 8.19 (br, 3H, NH_3), 8.7-8.8 (d, 1H, NH)

Boc-Phe-Asp(OBzl)-Phe-OH (5)

Into a solution of **4** (5 g, 0.0103 mole) and sodium bicarbonate (2.6 g, 0.031 mole) in a mixture of THF (60 mL) and water (60 mL) was added a solution of **3** (4.5 g, 0.124 mole) in THF (65 mL). The solution was left to stir at room temperature for 24 h. The reaction mixture was concentrated by removing the THF with a rotary evaporator, acidified with 0.5 M hydrochloric acid, and extracted with ethyl acetate (200 mL). The organic layer was then washed three times with water (50 mL), dried over anhydrous Na_2SO_4, and filtered. The solvent was removed under vacuum. Petroleum ether (bp 30-60 ^oC) was added and the precipitate thus formed was collected by filtration and dried to give the tripeptide.

Yield: 95 % (6.05 g), m.p. 99-100 ^oC

300 MHz, ^{1}H NMR: δ (dmso-d_6) ppm 1.23 (s, 9H, $C(CH_3)_3$-Boc), 2.52-2.99 (m, 6H, CH_2-pendent), 4.05-4.18 (m, 1H, CH-backbone), 4.37-4.41 (m, 1H, CH-backbone), 4.6-4.75 (m, 1H, CH-backbone), 5.05-5.08 (t, 2H, CH_2-Bzl), 6.87-6.89 (d, 1H, NH), 7.11-7.34 (m, 15H, Ar-H), 8.08-8.10 (d, 1H, NH), 8.2-8.3 (d, 1H, NH)

H-Phe-Asp(OBzl)-Phe-OH.CF_3COOH (6)

A solution of **5** (6.0 g, 0.01 mole) in TFA (10 mL) was stirred for 45 min. After removing TFA with the rotary evaporator, the product was precipitated by adding anhydrous ether. The crystals obtained were filtered off.

Yield: 83 % (5.1 g), m.p. 77-79 ^oC

300 MHz, ^{1}H NMR: δ (dmso-d_6) ppm 2.47-3.06 (m, 6H, CH_2-pendent), 3.93-3.95 (m, 1H,

CH-backbone), 4.38-4.43 (m, 1H, CH-backbone), 4.65-4.75 (m, 1H, CH-backbone), 5.0-5.1 (s, 2H, CH_2-Bzl), 7.13-7.34 (m, 15H, Ar-H), 8.35-8.45 (d, 1H, NH), 8.8-8.9 (d, 1H, NH)

Boc-Asp(OBzl)-Phe-Asp(OBzl)-Phe-OH (7)

A solution of **1**, (5.6 g, 0.0133 mole) in THF (100 mL) was added to a solution of **6** (7.0 g, 0.011 mole) in a mixture of THF (90 mL) and water (90 mL) containing $NaHCO_3$ (2.77 g, 0.033 mole). After the solution was stirred at room temperature for 24 h, the reaction mixture was concentrated, acidified with 0.5 M HCl and extracted with ethyl acetate (200 mL). The organic layer was then washed with water three times (60 mL), dried over anhydrous Na_2SO_4, filtered and the solvent was removed under vacuum using a rotary evaporator. Upon addition of petroleum ether (bp 30-60 ^oC), a white precipitate of the tetrapeptide was formed which was collected.

Yield: 95 % (8.7 g), m.p. 145-146.6 ^oC

300 MHz, ^1H NMR: δ (dmso-d_6) ppm 1.31 (s, 9H, $C(CH_3)_3$-Boc), 2.49-2.98 (m, 8H, CH_2-pendent), 4.28-4.42 (m, 3H, CH-backbone), 4.6-4.7 (m, 1H, CH-backbone), 4.95-5.1 (s, 4H, CH_2-Bzl), 7.15-7.31 (m, 20H, Ar-H), 7.75-7.89 (d, 1H, NH), 8.01-8.15 (d, 1H, NH), 8.3-8.43 (d, 1H, NH)

Boc-Asp(OBzl)-Phe-Asp(OBzl)-Phe-OSu (8)

To a solution of **7** (8.0 g, 0.0097 mole) and HOSu (2.24 g, 0.0194 mole) in a 1:1 mixture of ethyl acetate:dioxane (80 mL) at -5 ^oC, DCC (3.0 g, 0.015 mole) was added. The mixture was stirred for 5 h at -5 ^oC and then left to stand overnight in a refrigerator. The excess DCC was decomposed by adding glacial acetic acid (2 mL). The dicyclohexyl urea thus produced was filtered off and the filtrate was concentrated under vacuum using a rotary evaporator. The viscous oil obtained was dissolved in ethyl acetate (100 mL) and more urea

was filtered off. The ethyl acetate solution was washed successively with 20 mL of 0.5 M sodium carbonate, water, 0.5 M hydrochloric acid, and water. After drying of the ethyl acetate layer over anhydrous Na_2SO_4 and removal of the solvent under reduced pressure, a white solid was obtained which was crystallized in isopropanol.

Yield: 86 % (7.7 g), m.p. 74-78 ^oC

300 MHz, ^1H NMR: δ (dmso-d_6) ppm 1.31 (s, 9H, $C(CH_3)_3$-Boc), 2.50-3.16 (m, 8H, CH_2-pendent), 2.77 (s, 4H, CH_2-Su), 4.25-4.32 (m, 1H, CH-backbone), 4.35-4.42 (m, 1H, CH-backbone), 4.65-4.75 (m, 1H, CH-backbone), 4.82-4.90 (m, 1H, CH-backbone), 4.98-5.10 (s, 4H, CH_2-Bzl), 7.14-7.30 (m, 20H, Ar-H), 7.72-7.80 (d, 1H, NH), 8.35-8.45 (d, 1H, NH), 8.65-8.75 (d, 1H, NH)

H-Asp(OBzl)-Phe-Asp(OBzl)-Phe-OSu.CF_3COOH (9)

The activated tetrapeptide **8** (7.5 g, 0.0082 mole) was dissolved in TFA (21 mL) and the reaction mixture was stirred for 45 min at room temperature to remove the BOC group. TFA was removed under reduced pressure. The solid was dissolved in anhydrous ether and white crystals of **9** were obtained.

Yield: 95 % (7.2 g), m.p. 145-147 ^oC

300 MHz, ^1H NMR: δ (dmso-d_6) ppm 2.55-3.17 (m, 8H, CH_2-pendent), 2.77 (s, 4H, CH_2-Su), 3.98-4.10 (m, 1H, CH-backbone), 4.45-4.55 (m, 1H, CH-backbone), 4.65-4.75 (m, 1H, CH-backbone), 4.8-4.9 (m, 1H, CH-backbone), 4.98-5.20 (m, 4H, CH_2-Bzl), 7.14-7.36 (m, 20H, Ar-H), 8.1-8.2 (br, 3H, NH_3), 8.45-8.55 (d, 1H, NH), 8.55-8.65 (d, 1H, NH), 8.75-8.85 (d, 1H, NH)

Mass: expected: 819, obtained: (ESI), 820 $[M+1]^+$ -TFA group.

Poly(Asp(OBzl)-Phe-Asp(OBzl)-Phe) (10)

To a solution of **9** (7 g, 0.0075 mole) in DMSO (9.0 mL), triethyl amine (TEA, 2.1 mL, 0.0145 mole) was added. The reaction mixture was stirred at room temperature and turned pale yellow and viscous within 2 days. After the mixture had been allowed to react at room temperature for 7 days, the mixture was triturated with ether. The precipitate was washed with water, methanol, and ether, and dried.

Yield: 60 % (3.2 g).

300 MHz, ^{1}H NMR: δ (dmso-d_6) ppm 2.72 (br, 2H, CH_2-pendent), 2.93 (br, 2H, CH_2-pendent), 4.42 (br, 1H, CH-backbone), 4.62 (br, 1H, CH-backbone), 4.98 (br, 2H, CH_2-Bzl), 7.12-7.40 (br, 10H, ArH), 7.90-8.3 (br, 2H, NH)

Poly(Asp(OH)-Phe-Asp(OH)-Phe) (11)

The protected polymer **10** (1 g, 0.0014 mole) was treated with 9 mL of methane sulphonic acid (MSA) [31,33] in the presence of thioanisole (0.9 mL) at room temperature for 1 hour and the mixture was triturated with ether to give a whitish precipitate. The solid was washed with methanol and ether and dried.

Yield: 70 % (0.5 g)

300 MHz, ^{1}H NMR: δ (dmso-d_6) ppm 2.93 (br, 4H, CH_2-pendent), 4.38 (br, 1H, CH-backbone), 4.73 (br, 1H, CH-backbone), 7.15 (br, 5H, ArH), 8.55 (br, NH)

2.3.2. Synthesis of poly(Asp_3Phe_1)

The sequence of this polypeptide required starting the synthesis with a tetrapeptide. The synthetic pathway of the tetrapeptide is illustrated in Scheme 2.4 and the synthetic steps are described below. Those steps which have already been described in the synthesis of the

alternating polypeptide have been omitted.

Scheme 2.4. Synthesis of poly(Asp_3Phe_1)

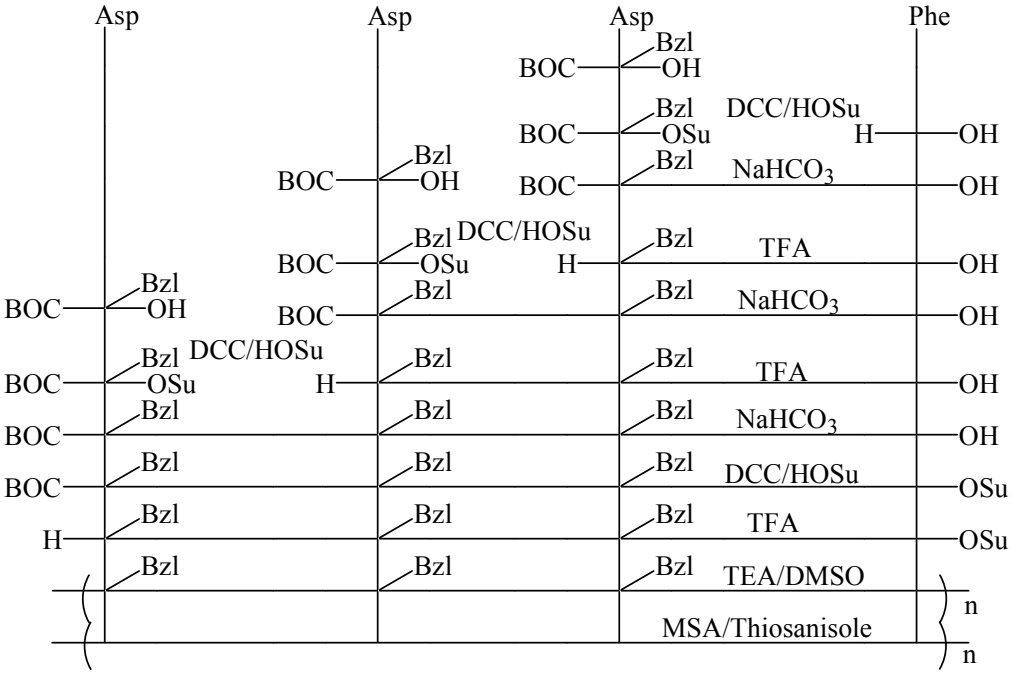

Boc-Asp(OBzl)-Asp(OBzl)-Phe-OH (12)

Into a solution of **4** (6.58 g, 0.0134 mole) and $NaHCO_3$ (3.45 g, 0.041 mole) in a mixture of THF (75 mL) and water (75 mL) was added a solution of **1** (6.3 g, 0.015 mole) in THF (70 mL). The resulting solution was left to stir at room temperature for 24 h. The reaction mixture was concentrated, acidified with 0.5 M hydrochloric acid and extracted with ethyl acetate (200 mL). The organic layer was then washed three times with water (50 mL), dried over anhydrous Na_2SO_4, and filtered. The solvent was removed under vacuum. Petroleum ether (bp 30-60 ^oC) was added and the precipitate formed was collected by filtration and dried.

Yield: 93 % (8.5 g), m.p. 81.5-83 ^{o}C

300 MHz, ^{1}H NMR: δ (dmso-d_6) ppm 1.33 (s, 9H, C(CH_3)$_3$-Boc) 2.46-2.98 (m, 6H, CH_2-pendent), 4.25-4.40 (m, 2H, CH-backbone), 4.60-4.70 (m, 1H, CH-backbone), 4.98-5.15 (s, 4H, CH_2-Bzl), 7.13-7.45 (m, 15H, ArH), 7.90-8.10 (d, 1H, NH), 8.15-8.20 (d, 1H, NH)

H-Asp(OBzl)-Asp(OBzl)-Phe-OH.CF_3COOH (13)

The tripeptide **12** (5.5 g, 0.0081 mole) was dissolved in TFA (12 mL) and the reaction mixture was stirred for 45 min at room temperature. TFA was removed under reduced pressure and white crystals were obtained upon the addition of anhydrous ether.

Yield: 75 % (4.2 g), m.p. 145.5-146.5 ^{o}C

300 MHz, ^{1}H NMR: δ (dmso-d_6) ppm 2.56-3.04 (m, 6H, CH_2-pendent), 3.89-3.99 (m, 1H, CH-backbone), 4.3-4.4 (m, 1H, CH-backbone), 4.6-4.7 (m, 1H, CH-backbone), 5.00-5.15 (s, 4H, CH_2-Bzl), 7.11-7.35 (m, 15H, ArH), 8.15-8.21 (d, 1H, NH), 8.58-8.70 (br, 3H, NH_3)

Boc-Asp(OBzl)-Asp(OBzl)-Asp(OBzl)-Phe-OH (14)

A solution of **1** (3.7 g, 0.009 mole) in THF (45 mL) was added to a solution of **13** (3.1 g, 0.0045 mole) in a mixture of THF (45 mL) and water (45 mL) containing $NaHCO_3$ (1.13 g, 0.0134 mole). After the solution was stirred at room temperature for 24 h, the reaction mixture was concentrated, acidified with 0.5 M hydrochloric acid, and extracted with ethyl acetate (200 mL). The organic layer was then washed three times with water (60 mL), dried over anhydrous Na_2SO_4, filtered and the solvent was removed under vacuum using a rotary evaporator. Upon addition of petroleum ether (bp 30-60 ^{o}C) a white precipitate of the tetrapeptide was formed which was collected.

Yield: 95 % (3.8 g), m.p. 80.3-82 ^{o}C

300 MHz, ^{1}H NMR: δ (dmso-d_6) ppm 1.32 (s, 9H, C(CH_3)$_3$-Boc), 2.47-2.99 (m, 8H, CH_2-

pendent), 4.25-4.36 (m, 2H, CH-backbone), 4.55-4.68 (m, 2H, CH-backbone), 5.01-5.10 (m, 6H, CH_2-Bzl), 7.10-7.34 (m, 20H, ArH), 7.9 (d, 1H, NH), 8.1 (d, 1H, NH), 8.21 (d, 1H, NH)

Boc-Asp(OBzl)-Asp(OBzl)-Asp(OBzl)-Phe-OSu (15)

N-methyl morpholine (NMM) (0.55 mL, 0.0051 mole) was added to a solution of **14** (4.5 g, 0.0051 mole), HOSu (1.17 g, 0.0102 mole) and DCC (1.5 g, 0.0073 mole) in a 1:1 ethyl acetate:dioxane mixture (50 mL) at -5 ^oC. The mixture was stirred for 5 h at -5 ^oC and then left to stand overnight in a refrigerator. The excess DCC was decomposed by adding glacial acetic acid (1 mL). DCU was filtered off and the filtrate was concentrated under vacuum. The solid obtained was dissolved in ethyl acetate and more urea was filtered off. The ethyl acetate solution was washed with 20 mL of water, 0.5 M HCl solution, and water successively. After drying of the ethyl acetate layer over anhydrous Na_2SO_4 and removal of the solvent under reduced pressure, a white solid was obtained which was crystallized in isopropanol.

Yield: 80 %, (4.0 g) m.p. 99-101 ^oC

300 MHz, ^1H NMR: δ (dmso-d_6) ppm 1.31 (s, 9H, $C(CH_3)_3$-Boc), 2.51-3.17 (m, 8H, CH_2-pendent), 2.75 (s, 4H, CH_2-Su), 4.25-4.35 (m, 1H, CH-backbone), 4.50-4.65 (m, 2H, CH-backbone), 4.72-4.85 (m, 1H, CH-backbone), 4.95-5.05 (s, 6H, CH_2-Bzl), 7.14-7.31 (m, 20H, ArH), 8.1-8.2 (br, 3H, NH), 8.48-8.55 (d, 1H, NH).

H-Asp(OBzl)-Asp(OBzl)-Asp(OBzl)-Phe-OSu.CF_3COOH (16)

A solution of **15** (4.0 g, 0.0041) in TFA (10 mL) was stirred for 45 min. After removing TFA, the product was precipitated by adding anhydrous ether. The crystals obtained were filtered off.

Yield: 89 % (3.6 g), m.p. 105-107 ^oC

300 MHz, ^{1}H NMR: δ (dmso-d_6) ppm 2.51-3.15 (m, 8H, CH_2-pendent), 2.76 (s, 4H, CH_2-Su), 4.02-4.12 (m, 1H, CH-backbone), 4.51-4.68 (m, 2H, CH-backbone), 4.71-4.81 (m, 1H, CH-backbone), 4.96-5.11 (s, 6H, CH_2-Bzl), 7.13-7.34 (m, 20H, ArH), 8.18 (br, 3H, NH_3), 8.25-8.31 (d, 1H, NH), 8.59-8.65 (d, 1H, NH), 8.75-8.80 (d, 1H, NH)

Mass: expected, 877, obtained: (ESI), 878 $[M+1]^+$, -TFA group

Poly(Asp(OBzl)-Asp)OBzl)-Asp(OBzl)-Phe) (17)

To a solution of tetrapeptide active ester **16** (3.6 g, 0.0036 mole) in dimethyl sulphoxide (3.6 mL), triethyl amine (TEA) (1.1 mL, 0.0072 mole) was added. The reaction mixture was stirred at room temperature and turned yellow and viscous within 2 days. After standing at room temperature for 7 days, the mixture was triturated with ether. The precipitate was washed with water, methanol, ether, and dried.

Yield: 56.3 % (1.6 g)

300 MHz, ^{1}H NMR: δ (dmso-d_6) ppm 2.55-3.4 (br, 8H, CH_2-pendent), 4.30-5.30 (br, 1H, CH-backbone), 4.62-4.82 (br, 1H, CH-backbone), 5.00-5.10 (br, 6H, CH_2-Bzl), 5.10-5.32 (br, 1H, CH-backbone), 7.18-7.32 (br, 20H, ArH), 8.80 (br, NH)

Poly(Asp(OH)-Asp)OH)-Asp(OH)-Phe) (18)

The protected polymer **17** (1 g, 0.0013 mole) was treated with 4.3 mL of methane sulphonic acid (MSA) in the presence of thioanisole (0.43 mL) at room temperature for 1 hour and the mixture was triturated with ether to give a whitish precipitate. The solid was washed with methanol and ether and dried.

Yield: 68 % (0.4 g)

300 MHz, ^{1}H NMR: δ (dmso-d_6) ppm 2.63 (br, 4H, CH_2-pendent), 2.99 (br, 4H, CH_2-pendent), 4.39 (br, 1H, CH-backbone), 4.71 (br, 1H, CH-backbone), 4.90-5.18 (br, 2H, CH-

backbone), 7.12-7.25 (br, 5H, ArH), 8.79 (br, NH)

2.3.3. Synthesis of poly(Asp_2Phe_1)

The desired polypeptide sequence required a tripeptide to be synthesized. The synthetic pathway is illustrated in Scheme 2.5 and the synthesis is described below.

Scheme 2.5. Synthesis of poly(Asp_2Phe_1)

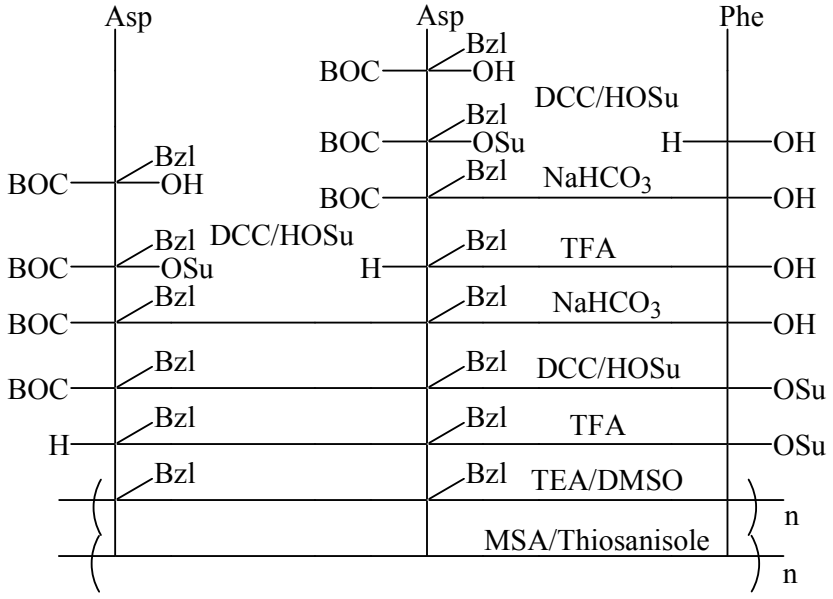

Boc-Asp(OBzl)-Asp(OBzl)-Phe-OSu (19)

To a solution of **12** (5.0 g, 0.0074 mole) and HOSu (1.28 g, 0.011 mole) in methylene chloride (30 mL) at -5 ^{o}C, DCC (1.83 g, 0.0089 mole) was added. The mixture was stirred for 5 h at -5 ^{o}C and then left to stand overnight in a refrigerator. Glacial acetic acid (1 mL) was added to decompose the excess DCC. The solution was filtered and the filtrate was

concentrated under vacuum. The solid was dissolved in ethyl acetate (80 mL) and more urea was filtered off. The ethyl acetate solution was washed successively with (20 mL) water, a 0.5 M HCl solution, and water. After drying of the ethyl acetate layer over anhydrous Na_2SO_4 and removal of the solvent under reduced pressure, the white solid obtained was crystallized in isopropanol.

Yield: 75.4 % (4.3 g), m.p. 95-98 ^oC

300 MHz, ^1H NMR: δ (dmso-d_6) ppm 1.33 (s, 9H, $C(CH_3)_3$-Boc), 2.52-2.73 (m, 4H, CH_2-pendent), 2.77 (s, 4H, CH_2-Su), 3.01-3.20 (m, 2H, CH_2-pendent), 4.28-4.35 (m, 1H, CH-backbone), 4.59-4.70 (m, 1H, CH-backbone), 4.75-4.85 (m, 1H, CH-backbone), 4.98-5.09 (s, 4H, CH_2-Bzl), 7.10-7.33 (m, 15H, ArH), 8.1-8.2 (d, 1H, NH), 8.58-8.65 (d, H, NH)

H-Asp(OBzl)-Asp(OBzl)-Phe-OSu.CF_3COOH (20)

A solution of **19** (4.31 g, 0.0056 mole) in TFA (12 mL) was stirred for 45 min. After removing TFA with a rotary evaporator, the product was precipitated by adding anhydrous ether. The pale yellow crystals obtained were filtered off.

Yield: 91 % (4.0 g), m.p. 143-146 ^oC

300 MHz, ^1H NMR: δ (dmso-d_6) ppm 2.53-3.38 (m, 6H, CH_2-pendent), 2.77 (s, 4H, CH_2-Su), 4.00-4.12 (m, 1H, CH-backbone), 4.60-4.70 (m, 1H, CH-backbone), 4.80-4.90 (m, 1H, CH-backbone), 5.00-5.14 (s, 4H, CH_2-Bzl), 7.16-7.36 (m, 15H, ArH), 8.10-8.30 (br, 3H, NH_3), 8.75-8.97 (d, 2H, NH)

Mass: expected 672, obtained: (ESI), 673 $[M+1]^+$, -TFA group

Poly(Asp(OBzl)-Asp(OBzl)-Phe) (21)

To a solution of the tripeptide active ester **20** (4.0 g, 0.0051 mole) in dimethyl sulphoxide (3.8 mL), triethyl amine (TEA) (1.2 mL, 0.0078 mole) was added. The reaction

mixture turned yellow immediately and was stirred at room temperature for 7 days. The mixture was triturated with ether and the precipitate was washed with water, methanol, and ether.

Yield: 58.3 % (1.7 g)

300 MHz, ^{1}H NMR: δ (dmso-d_6) ppm 2.98 (br, 6H, CH_2-pendent), 4.50 (br, 1H, CH-backbone), 4.62-4.85 (br, 1H, CH-backbone), 5.03 (br, 4H, CH_2-Bzl), 5.13 (br, 1H, CH-backbone), 7.16-7.48 (15H, ArH), 8.66-8.80 (br, NH)

Poly(Asp(OH)-Asp(OH)-Phe) (22)

The protected polymer **21** (0.8 g, 0.0014 mole) was treated with 4.7 mL of methane sulphonic acid (MSA) in the presence of thioanisole (0.47 mL) at room temperature for 1 hour and the mixture was triturated with ether to give a whitish precipitate. The solid was washed with methanol and ether and dried.

Yield: 64.8 % (0.4 g)

300 MHz, ^{1}H NMR: δ (dmso-d_6) ppm 2.98 (br, 6H, CH_2-pendent), 4.50 (br, 1H, CH-backbone), 4.76 (br, 1H, CH-backbone), 5.04-5.14 (br, 1H, CH-backbone), 7.1-7.23 (br, 5H, ArH), 8.60 (br, NH)

2.3.4. Synthesis of poly(Asp_1Phe_2)

A tripeptide was prepared to synthesize this polypeptide. The synthetic pathway is illustrated in Scheme 2.6 and the synthesis is described below.

Scheme 2.6. Synthesis of poly (Asp_1Phe_2)

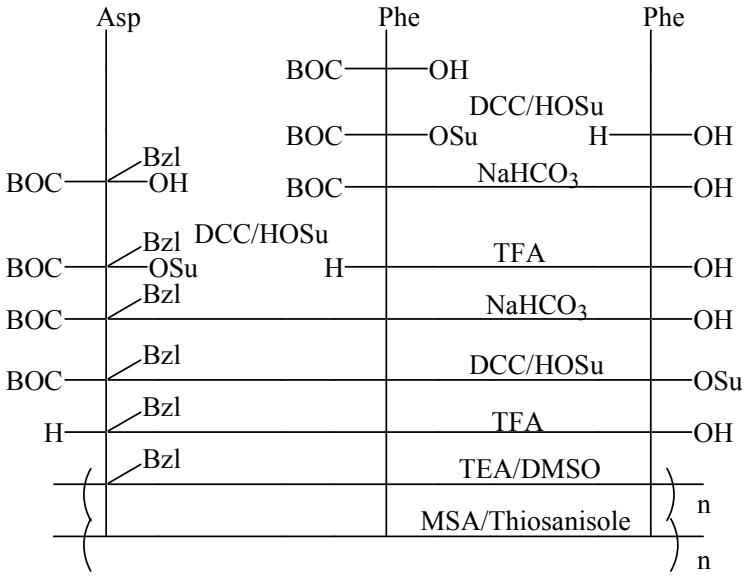

Boc-Phe-Phe-OH (23)

A solution of **3** (8.0 g, 0.022 mole) in THF (100 mL) was added to phenylalanine (3.32 g, 0.02 mole) dissolved in a mixture of THF (90 mL) and water (90 mL) containing sodium bicarbonate (3.38 g, 0.04 mole). After the solution was stirred at room temperature for 24 h, the reaction mixture was concentrated, acidified with 0.5 M hydrochloric acid and extracted with ethyl acetate (500 mL). The organic layer was then washed three times with water (200 mL), dried over anhydrous sodium sulphate, filtered, and the solvent was removed under vacuum using a rotary evaporator. Addition of petroleum ether (bp 30-60 ^oC) to the viscous oil resulted in the precipitation of the dipeptide **23** which was filtered.

Yield: 95 % (7.9 g), m.p. 124-125.3 ^oC

300 MHz, ^1H NMR: δ (dmso-d_6) ppm 1.24 (s, 9H, $C(CH_3)_3$-Boc), 2.58-3.07 (m, 4H, CH_2-pendent), 4.05-4.18 (m, 1H, CH-backbone), 4.35-4.48 (m, 1H, CH-backbone), 6.82-6.85 (d, 1H, NH), 7.13-7.27 (m, 10H, ArH), 8.07-8.09 (d, 1H, NH)

H-Phe-Phe-OH.CF_3COOH (24)

The Boc group was removed by stirring a solution of **23** (7.0 g, 0.017 mole) in TFA (14 mL) for 45 min at room temperature. After removal of TFA under vacuum, the product was precipitated by the addition of anhydrous ether. The white crystals were collected in a quantitative yield.

m.p. 77-78.5 ^oC

300 MHz, ^1H NMR: δ (dmso-d_6) ppm 2.87-3.12 (m, 4H, CH_2-pendent), 3.9-4.0 (m, 1H, CH-backbone), 4.42-4.50 (m, 1H, CH-backbone), 7.2-7.5 (m, 10H, ArH), 7.9-8.15 (br, 3H, NH_3), 8.83-8.86 (d, 1H, NH)

Boc-Asp(OBzl)-Phe-Phe-OH (25)

To a solution of **24** (3 g, 0.007 mole) and $NaHCO_3$ (1.77 g, 0.021 mole) in a mixture of THF (30 mL) and water (30 mL), a solution of **1** (3.25 g, 0.00774 mole) in THF (40 mL) was added. The reaction mixture was stirred for 24 h at room temperature. The solution was concentrated under vacuum and acidified with 0.5 N HCl solution (40 mL), extracted in ethyl acetate (150 mL) and washed 3 times with water (50 mL). After drying the organic layer over anhydrous Na_2SO_4, the solvent was removed and the solid was obtained by adding petroleum ether.

Yield: 92 % (4.0 g), m.p. 81-83.6 ^oC

300 MHz, ^1H NMR: δ (dmso-d_6) ppm 1.31 (s, 9H, $C(CH_3)_3$-Boc), 2.55-3.04 (m, 6H, CH_2-pendent), 4.2-4.3 (m, 1H, CH-backbone), 4.35-4.55 (m, 2H, CH-backbone), 5.03-5.06 (s, 2H, CH_2-Bzl), 7.08-7.32 (m, 15H, ArH), 7.65-7.75 (d, 1H, NH), 8.25-8.35 (d, 1H, NH)

Boc-Asp(OBzl)-Phe-Phe-OSu (26)

DCC (1.4 g, 0.0068 mole) was added to a solution of **25** (3.5 g, 0.0057 mole) and

HOSu (0.98 g, 0.0085 mole) in methylene dichloride (35 mL) at -5 ^{o}C. The reaction mixture was stirred at -5 ^{o}C for 5 h and then left overnight in a refrigerator. The reaction was worked up as mentioned above for **19**. The active ester was obtained as a white solid.

Yield: 84 % (3.4 g), m.p. 72-75 ^{o}C

300 MHz, ^{1}H NMR: δ (dmso-d_6) ppm 1.23 (s, 9H, C(CH_3)$_3$-Boc), 2.52-3.21 (m, 6H, CH_2-pendent), 2.73 (s, 4H, CH_2-Su), 4.12 (m, 1H, CH-backbone), 4.71 (m, 1H, CH-backbone), 4.8 (m, 1H, CH-backbone), 4.99-5.10 (s, 2H, CH_2-Bzl), 6.8 (d, 1H, NH), 7.16-7.32 (m, 15H, ArH), 8.25 (d, 1H, NH), 8.71-8.73 (d, 1H, NH)

H-Asp(OBzl)-Phe-Phe-OSu.CF_3COOH (27)

A solution of **26** (3.4 g, 0.0048 mole) in TFA (10 mL) was stirred for 45 min. After removing TFA, the product was precipitated by adding anhydrous ether and filtered.

Yield: 85 % (3.0 g), m.p. 85-87 ^{o}C

300 MHz, ^{1}H NMR: δ (dmso-d_6) ppm 2.55-3.19 (m, 6H, CH_2-pendent), 2.77 (s, 4H, CH_2-Su), 4.01 (m, 1H, CH-backbone), 4.53 (m, 1H, CH-backbone), 4.88 (m, 1H, CH-backbone), 5.07-5.17 (s, 2H, CH_2-Bzl), 7.17-7.37 (m, 15H, ArH), 8.01 (br, 3H, NH_3), 8.60-8.66 (d, 1H, NH), 8.90-8.96 (d, 1H, NH)

Mass: expected, 614, obtained: (ESI), 615 $[M+1]^{+}$, -TFA group

Poly(Asp(OBzl)-Phe-Phe) (28)

To a solution of tripeptide active ester **27** (2.95 g, 0.0041 mole) in DMSO (4 mL), TEA (1.2 mL, 0.0078 mole) was added. The reaction mixture turned pale yellow immediately and was stirred at room temperature for 7 days. The mixture was triturated with ether and the precipitate was washed with water, methanol, and ether.

Yield: 72.7% (1.5 g)

300 MHz, ^{1}H NMR: δ (dmso-d_6) ppm 2.69 (br, 4H, CH_2-pendent), 2.88 (br, 2H, CH_2-pendent), 4.45-4.61 (br, 3H, CH-backbone), 4.95-5.05 (br, 2H, CH_2-Bzl), 7.09-7.29 (br, 15H, ArH), 7.86 (br, 1H, NH), 8.10 (br, 1H, NH), 8.30 (br,1H, NH)

Poly(Asp(OH)-Phe-Phe) (29)

The protected polymer **28** (0.8 g, 0.0016 mole) was treated with 5.3 mL of MSA in the presence of thioanisole (0.53 mL) at room temperature for 1h and the mixture was triturated with ether to give a whitish precipitate. The solid was washed with methanol and ether and dried.

Yield: 63.0 % (0.4 g)

300 MHz, ^{1}H NMR: δ (dmso-d_6) ppm 2.69 (br, 2H, CH_2-pendent), 2.88 (br, 4H, CH_2-pendent), 4.47 (br, 3H, CH-backbone), 7.16 (br, 10H, ArH), 7.68 (br, 1H, NH), 8.07 (br, 1H, NH), 8.22 (br, 1H, NH)

2.3.5. Synthesis of poly(Asp_1Phe_3)

A tetrapeptide was prepared for this polypeptide. The synthetic pathway is illustrated in Scheme 2.7 and the synthesis is described below.

Scheme 2.7. Synthesis of poly(Asp_1Phe_3)

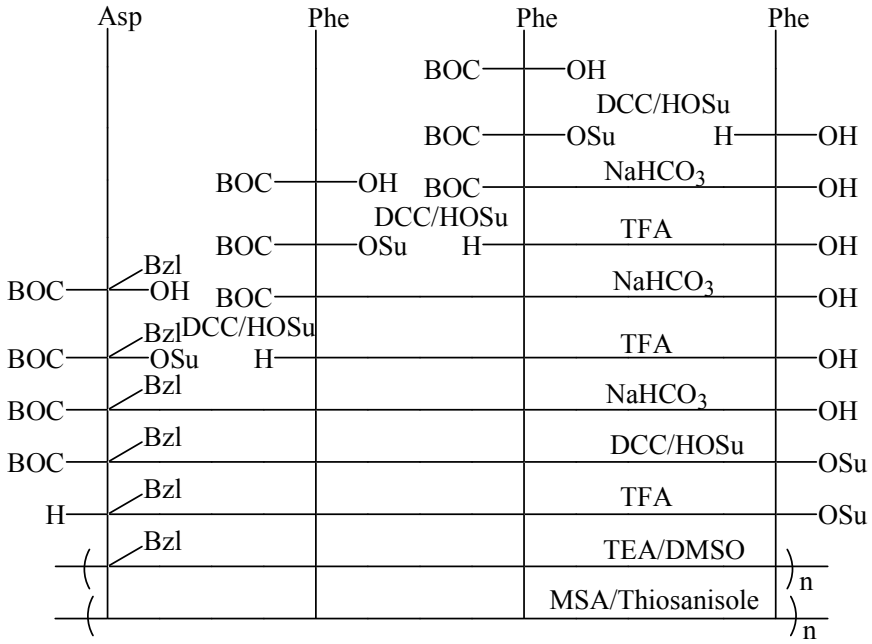

Boc-Phe-Phe-Phe-OH (30)

A solution of **3** (6.7 g, 0.0185 mole) in THF (97 mL) was added to a solution of **24** (7.24 g, 0.017 mole) and $NaHCO_3$ (4.28 g, 0.051 mole) in a mixture of THF (97 mL) and water (97 mL). After the reaction mixture had been stirred for 24 h, it was concentrated under vacuum, acidified with 0.5 M HCl (30 mL), and extracted with ethyl acetate (200 mL). The organic layer was washed three times with water (50 mL) and then dried over anhydrous Na_2SO_4. The tripeptide was obtained as a white solid after removal of the solvent and precipitation in petroleum ether.

Yield: 85 % (8.1 g), m.p. 168-170.3 ^oC

300 MHz, ^1H NMR: δ (dmso-d_6) ppm 1.22 (s, 9H, $C(CH_3)_3$-Boc), 2.50-3.02 (m, 6H, CH_2-pendent), 4.05 (m, 1H, CH-backbone), 4.44 (m, 1H, CH-backbone), 4.55 (m, 1H, CH-

backbone), 6.81-6.84 (d, 1H, NH), 7.10-7.25 (m, 15H, ArH), 7.86-7.88 (d, 1H, NH), 8.33-8.36 (d, 1H, NH)

H-Phe-Phe-Phe-OH.CF_3COOH (31)

A mixture of **30** (7 g, 0.0125 mole) in TFA (20 mL) was stirred at room temperature for 45 min. The solvent was removed under pressure and the product was precipitated after the addition of anhydrous ether.

Yield: 89 % (6.4 g), m.p. 125.0-126.5 ^oC

300 MHz, ^1H NMR: δ (dmso-d_6) ppm 2.72-3.09 (m, 6H, CH_2-pendent), 3.9-4.0 (m, 1H, CH-backbone), 4.4-4.5 (m, 1H, CH-backbone), 4.55-4.65 (m, 1H, CH-backbone), 7.10-7.22 (m, 15H, ArH), 7.85-8.05 (br, 3H, NH_3), 8.45-8.55 (d, 1H, NH), 8.65-8.75 (d, 1H, NH)

Boc-Asp(OBzl)-Phe-Phe-Phe-OH (32)

To a solution of **31** (6.4 g, 0.011 mole) and $NaHCO_3$ (2.8 g, 0.033 mole) in a mixture of THF (85 mL) and water (85 mL) at room temperature, a solution of **1** (7.2 g, 0.017 mole) in THF (85 mL) was added. The reaction was worked up as mentioned for **30** to obtain the tetrapeptide.

Yield: 85 % (7.3 g), m.p. 147.4-150.0 ^oC

300 MHz, ^1H NMR: δ (dmso-d_6) ppm 1.30 (s, 9H, $C(CH_3)_3$-Boc), 2.53-3.06 (m, 8H, CH_2-pendent), 4.2-4.3 (m, 1H, CH-backbone), 4.35-4.52 (m, 2H, CH-backbone), 5.02 (s, 2H, CH_2-Bzl), 7.09-7.30 (m, 20H, ArH), 7.6-7.7 (d, 1H, NH), 8.09-8.18 (d, 1H, NH), 8.28-8.38 (d, 1H, NH)

Boc-Asp(OBzl)-Phe-Phe-Phe-OSu (33)

To a solution of **32** (4.56 g, 0.0060 mole) and HOSu (1.37 g, 0.012 mole) in a 1:2 mixture of ethyl acetate:dioxane (110 mL) at -5 ^oC, DCC (1.84 g, 0.009 mole) and 4-methyl

morpholine (NMM) (0.65 mL, 0.006 mole) was added. The mixture was stirred for 5 h at –5 ^{o}C and then left to stand overnight in a refrigerator. The excess DCC was decomposed by adding glacial acetic acid (1 mL). DCU was filtered off and the filtrate was concentrated under vacuum. The solid obtained was dissolved in ethyl acetate (70 mL) and more urea was filtered off. The ethyl acetate solution was washed successively with 0.5 M $NaHCO_3$ (25 mL), water, 0.5 M HCl, and water. After drying of the ethyl acetate layer over anhydrous Na_2SO_4, and removal of the solvent under reduced pressure, a white solid was obtained which was crystallized in isopropanol.

Yield: 85 % (4.4 g), m.p. 127-128 ^{o}C

300 MHz, ^{1}H NMR: δ (dmso-d_6) ppm 1.30 (s, 9H, $C(CH_3)_3$-Boc), 2.55-3.24 (m, 8H, CH_2-pendent), 2.79 (s, 4H, CH_2-Su), 4.15-4.25 (m, 1H, CH-backbone), 4.30-4.45 (m, 1H, CH-backbone), 4.45-4.60 (m, 1H, CH-backbone), 4.80-4.98 (m, 1H, CH-backbone), 5.02 (s, 2H, CH_2-Bzl), 7.05-7.35 (m, 20H, ArH), 7.55-7.65 (d, 1H, NH), 8.25-8.35 (d, 1H, NH), 8.8-8.9 (d, 1H, NH)

H-Asp(OBzl)-Phe-Phe-Phe-OSu.CF_3COOH (34)

The activated tetrapeptide **33** (6.5g, 0.0082 mole) was dissolved in TFA (21 mL) and the reaction mixture was stirred for 45 min at room temperature. After removal of TFA under reduced pressure, anhydrous ether was added to obtain the product as a white crystal.

Yield: 90 % (6.0 g), m.p. 86-89 ^{o}C

300 MHz, ^{1}H NMR: δ (dmso-d_6) ppm 2.55-3.20 (m, 8H, CH_2-pendent), 2.79 (s, 4H, CH_2-Su), 3.92-4.05 (m, 1H, CH-backbone), 4.4-4.6 (m, 2H, CH-backbone), 4.80-4.92 (m, 1H, CH-backbone), 5.11 (t, 2H, CH_2-Bzl), 7.09-7.35 (m, 20H, ArH), 8.0-8.2 (br, 3H, NH_3), 8.3-8.4 (d, 1H, NH), 8.5-8.6 (d, 1H, NH), 8.85-8.98 (d, 1H, NH)

Mass: expected 761, obtained: (ESI), 762 $[M+1]^+$, -TFA group

Poly(Asp(OBzl)-Phe-Phe-Phe) (35)

To a solution of the tripeptide active ester **34** (6.0 g, 0.0069 mole) in DMSO (7.0 mL), TEA (2.0 mL, 0.013 mole) was added. The reaction mixture turned pale yellow immediately and was stirred at room temperature for 7 days. The mixture was triturated with ether and the precipitate was washed with water, methanol, and ether.

Yield: 74.5% (3.3 g)

300 MHz, ^{1}H NMR: δ (dmso-d_6) ppm 2.68 (br, 2H, CH_2-pendent), 2.90 (br, 2H, CH_2-pendent), 4.3-4.7 (br, 4H, CH-backbone), 5.00 (br, 2H, CH_2-Bzl), 7.06-7.28 (br, 20H, ArH), 7.85-8.30 (br, NH)

Poly(Asp(OH)-Phe-Phe-Phe) (36)

The protected polymer **35** (2.0 g, 0.0016 mole) was treated with 10.3 mL of MSA in the presence of thioanisole (1.03 mL) at room temperature for 1 hour and the mixture was triturated with ether to give a whitish precipitate. The solid was washed with methanol and ether and dried.

Yield: 74.3 % (1.3 g)

300 MHz, ^{1}H NMR: δ (dmso-d_6) ppm 2.68 (br, 2H, CH_2-pendent), 2.89 (br, 2H, CH_2-pendent), 4.50 (br, 4H, CH-backbone), 7.00-7.25 (br, 15H, ArH), 7.72-8.26 (br, NH)

2.4. Results and Discussion

Each of the five peptide monomers was prepared in a similar manner in THF/water mixtures where $NaHCO_3$ had been added. A Boc protected amino acid activated with *N*–hydroxysuccinimide is added to phenylalanine with a free α-carboxylic acid to insure

minimum racemization. DCC has been used to synthesize *N*-hydroxysuccinimide active esters, which are white/colourless crystalline compounds with good stability.[19,23] The *β*-carboxylic acid of the aspartic acid was protected with the benzyl group. The Boc group was removed selectively by using TFA and the benzyl group was eliminated after polymerization of the polypeptide by treatment with MSA in the presence of thioanisole.[31,33] The polypeptides were obtained in their protonated form.

The polymerization of polypeptides having a well-defined sequence of repeat units of amino acids is typically achieved by a self-condensation of monomer peptide active esters. For polymerization purposes, the peptide monomers were activated at the C-terminal by conversion of the carboxylic acid to its succinimide ester. All of the intermediates and the peptide monomers were generally obtained in good yield and purity as shown by a sharp melting point and single spots in chromatography. Chemical shift values obtained from ^{1}H NMR spectra for each intermediate and the peptide monomers agreed well with those expected suggesting a purity of at least 95 % for all intermediates since NMR spectroscopy gives a purity within a ± 5 %. The molecular weight values of the peptide monomers obtained by mass spectrometry were also those expected. These results indicated that all monomer were sufficiently pure to proceed with the polymerization.

The polymerization was carried out in DMSO in the presence of triethylamine after removing the Boc group of the activated esters using TFA. After the completion of polycondensation, the resulting polypeptides were isolated by precipitation from the reaction upon addition of diethyl ether. All signals of the ^{1}H NMR spectra of the polypeptides broadened due to slower tumbling of the molecules after polymerization. The Bzl groups of the protected polypeptides were removed by MSA in the presence of thioanisole. The ^{1}H

NMR confirmed the disappearance of the signals assigned to the protecting group after the cleavage reaction. Extra peaks for the NH protons observed for both the intermediates and the polypetides in the ^{1}H NMRs are a direct indication that racemic forms of these compounds are also present. The extent of racemization was found to be too little for most of intermediates to determine accurately through integration of the ^{1}H NMR spectra whereas for some it was found to be in the range of 10-15 %.

Appendix A contains the ^{1}H NMR spectra of all the intermediates, the monomer peptides, and the polypeptides. It also contains the mass spectra obtained for the monomer peptides before polymerization. Characterization of the behavior of these polypeptides in basic aqueous solutions is carried out in the following chapters.

2.5. References:

1. Bodanszky, M. *Peptide Chemistry*: *A Practical Text Book 2nd Edition*; Springer: Verlag Berlin 1993.
2. Ledger, R.; Stewart, F. H. C. *Aus. J. Chem.* **1967**, *20*, 2509-2516.
3. a) DeFar, D. F.; Gouge, M.; Honsberg, W.; Honesberg, U. *J. Am. Chem. Soc.* **1967**, *89*, 988-998. b) DeFar, D. F.; Vajda, T. *J. Am. Chem. Soc.* **1967**, *89*, 998-1004.
4. Johnson, B. J. *J. Chem. Soc.* (C) **1969**, 1412-1416.
5. Bell, J. R.; Boohan, R. C.; Jones, J. H.; Moore, R. M. *Int. J. Pept. Prot. Res.* **1975**, *7*, 227-234.
6. Fujino, M.; Wakimasu, M.; Shinagawa, S.; Kitada, C.; Yajima, H. *Chem. Pharm. Bull.* **1978**, *26*, 539-548.
7. a) Brack, A.; Caille, A. *Int. J. Pept. Prot. Res.* **1978**, *11*, 128-139. b) Barbier, B.; Caille, A.; Brack, A. *Biopolymers* **1984**, *23*, 2299-2310.
8. a) Benoiton, N.; Lee, Y.; Steinaur, R.; Chen, F. *Int. J. Pept. Prot. Res.* **1992**, *40*, 559-566. b) Meienhofer, J. *Biopolymers* **1981**, *20*, 1761-1784.
9. Fischer, E. *Ber. Dtsch. Chem. Ges.* **1903**, *36*, 2094-2106.
10. Curtius, T. *Ber. Dtsch. Chem. Ges.* **1902**, *35*, 3226-3228.
11. a) Chantrenne, H. *Nature* **1947**, *160*, 603-604. b) Boissonnas, R. A. *Helv. Chim. Acta* **1951**, *34*, 874-879. c) Vaughan, J. R. *J. Am. Chem. Soc.* **1951**, *73*, 3547.
12. Leuchs, H. *Ber. Dtsch. Chem. Ges.* **1906**, *69*, 857-861.
13. a) Schwyzer, R.; Iselin, B.; Feuer, M. *Helv. Chim. Acta* **1955**, *38*, 69-79. b) Bodanzky, M. *Nature* **1955**, *175*, 685. c) Kupriszewski, G. *Rocz. Chem.* **1961**, *35*, 595-600. d) Aderson, G. W.; Zimmermann, J. E.; Callahan, E. M. *J. Am. Chem. Soc.* **1963**, *85*, 3039. e) Kovacs, J.; Kisfaludy, L; Ceprini, M. Q. *J. Am. Chem. Soc*. **1967**, *89*, 183-184.
14. a) Hojo, K.; Maeda, M.; Smith, T.; Kawasaki, K. *Chem. Pharm. Bull.* **2002**, *50*, 140-142. b) Patil, B. S.; Vasanthakumar, G.; Babu, V. S. *J. Org. Chem.* **2003**, *68*, 7274-7280.
15. a) Rapaka, R. S.; Urry, D. W. *Int. J. Pept. Prot. Res.* **1978**, *11*, 97-108. b) Urry, D. W.; Harris, R. D.; Long, M. M.; Prasad, K. U. *Int. J. Pept. Prot. Res.* **1986**, *28*, 649-660.

16. Prasad, K.; Iqbal, M.; Urry, D. *Int. J. Pept. Prot. Res.* **1985**, *25*, 408-413.
17. a) Miyazawa, T.; Otomatsu, T.; Fukui, Y.; Yamada, T.; Kuwata, S. *J. Chem. Soc. Chem. Commun.* **1988**, 419. b) Miyazawa, T.; Otomatsu, T.; Fukui, Y.; Yamada, T.; Kuwata, S. *Int. J. Pept. Prot. Res.* **1992**, *39*, 237-244. c) Miyazawa, T.; Otomatsu, T.; Fukui, Y.; Yamada, T.; Kuwata, S. *Int. J. Pept. Prot. Res.* **1992**, *39*, 308-314.
18. a) Stewart, F. H. C. *Aust. J. Chem.* **1965**, *18*, 887-901. b) Stewart, F. H. C. *Aust. J. Chem.* **1965**, *18*, 1095-1103.
19. Laufer, D. A.; Blout, E. R. *J. Am. Chem. Soc.* **1967**, *89*, 1246-1249.
20. a) Kovacs, J.; Ballina, R.; Rodin, R. L.; Balasubramanian, D.; Applequist, J. *J. Am. Chem. Soc.* **1965**, *87*, 119-120. b) Kovacs, J.; Ceprini, M. Q.; Dupraz, C. A.; Schmit, G. N. *J. Org. Chem.* **1967**, *32*, 3696-3698.
21. Vommina, V. Babu, S.; Ananda, K.; Mathad, M. I. *Lett. Pept. Sci*, **2000**, *7,* 239-242.
22. Kovacs, J.; Giannotti, R.; Kapoor, A. *J. Am. Chem. Soc.* **1966**, *88*, 2282-2292.
23. Anderson, W.; Zimmerman, J.; Callahan, M. *J. Am. Chem. Soc.* **1964**, *86*, 1839-1842.
24. Belleau, B.; Malek, G. *J. Am. Chem. Soc.* **1968**, *90*, 1651-1652.
25. Diago-Meseguer, J.; Palomo, A.; Fernandez-Lizarbe, J.; Zugaza-Bibao, A. *Synthesis* **1980**, *7*, 547-551.
26. Anderson, G. W.; McGregor, A. C. *J. Am. Chem. Soc.* **1957**, *79*, 6180-6183.
27. Kenner, G. W.; Seely, J. H. *J. Am. Chem. Soc.* **1972**, *94*, 3259-3260.
28. Deboves, H. J. C.; Montalbetti, C. A. G. N.; Jackson, R. F. W. *J. Chem. Soc. Perkin Trans. I*, **2001**, 1876-1884.
29. Kovacs, J.; Rodin, R. L. *J. Org. Chem.* **1968**, *33*, 2418-2420.
30. Felix, A. M. *J. Org. Chem.* **1974**, *39*, 1427-1429.
31. Suzuki, K.; Endo, N. *Chem. Pharm. Bull.* **1978**, *26*, 2269-2274.
32. Nakajima, K.; Okawa, K. *Bull. Chem. Soc. Japan.* **1973**, *46*, 1811-1816.
33. Fukushima, Y. *Polym. Bull.* **2000**, *45*, 237-244.

2.6. Appendix

^{1}H NMR Spectra of intermediates, monomer peptides and polypeptides

Mass Spectra of the monomer peptides

BocAsp(OBzl)-OSu (1)

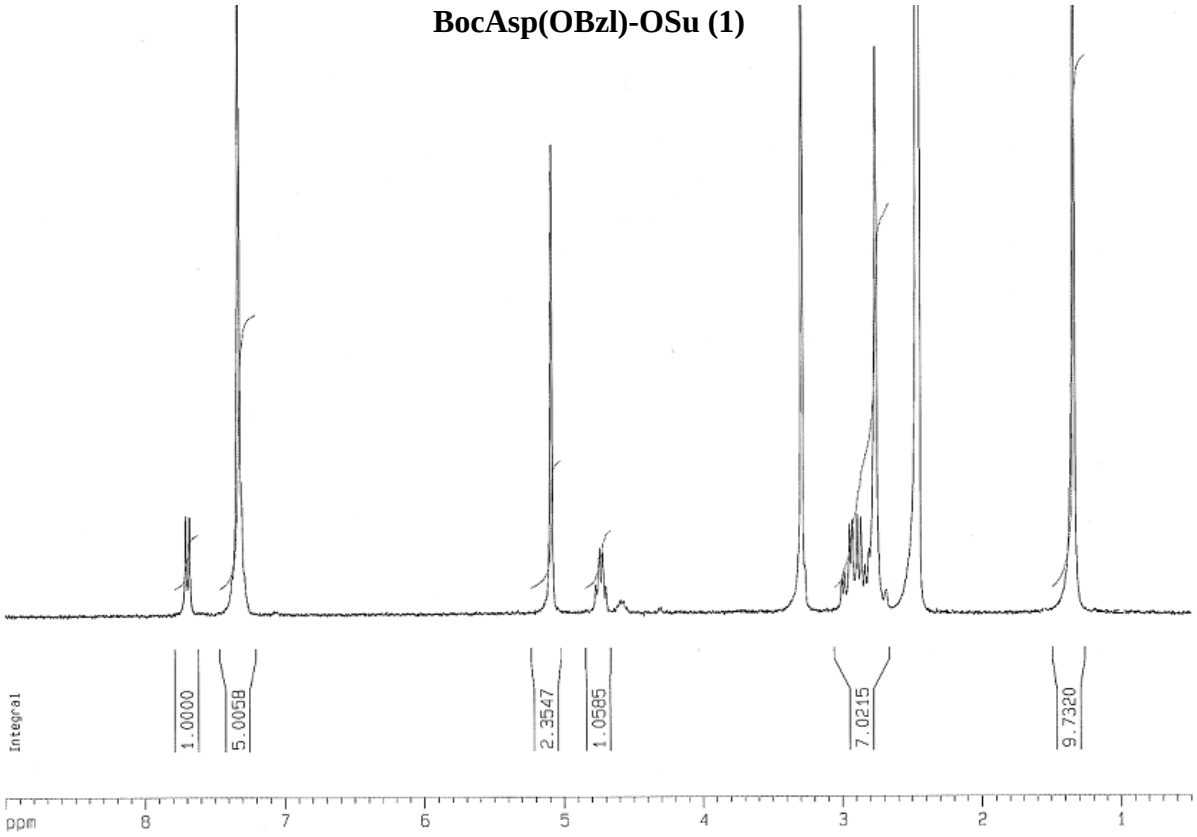

Boc-Asp(OBzl)-Phe-OH (2)

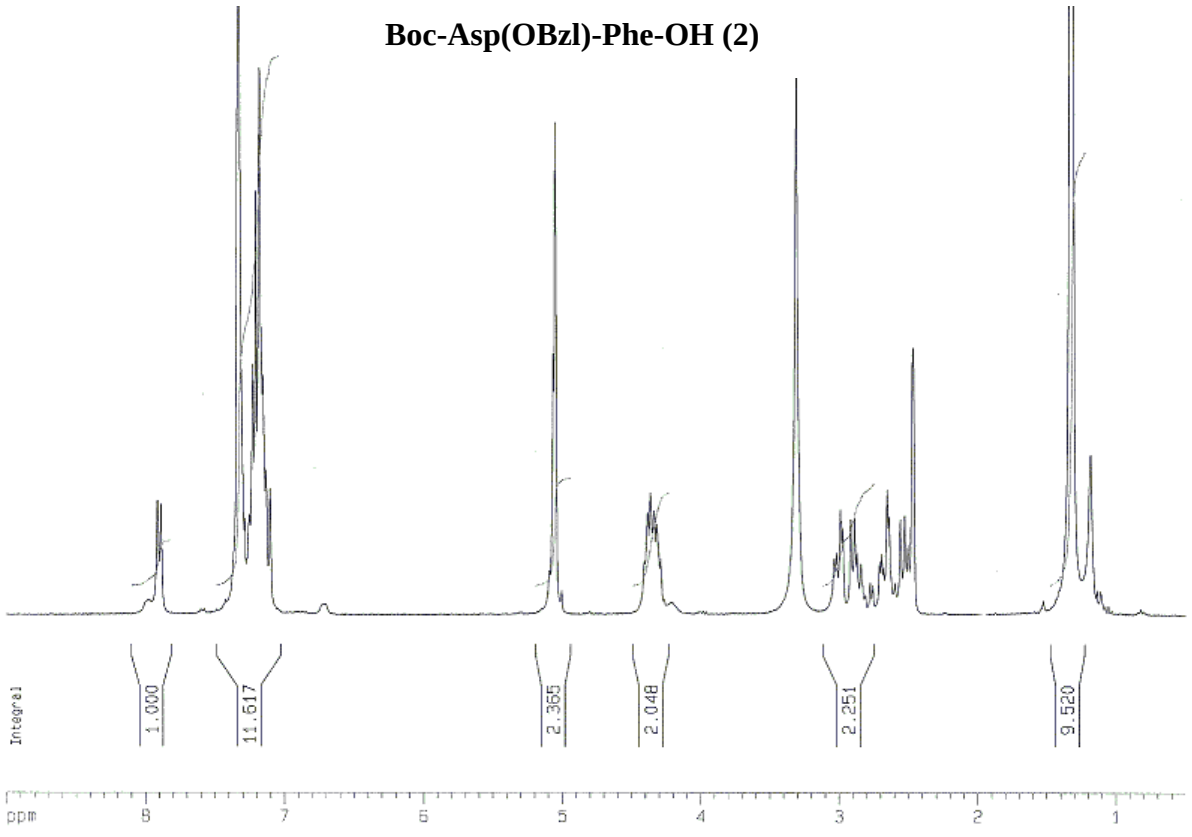

Boc-Phe-OSu (3)

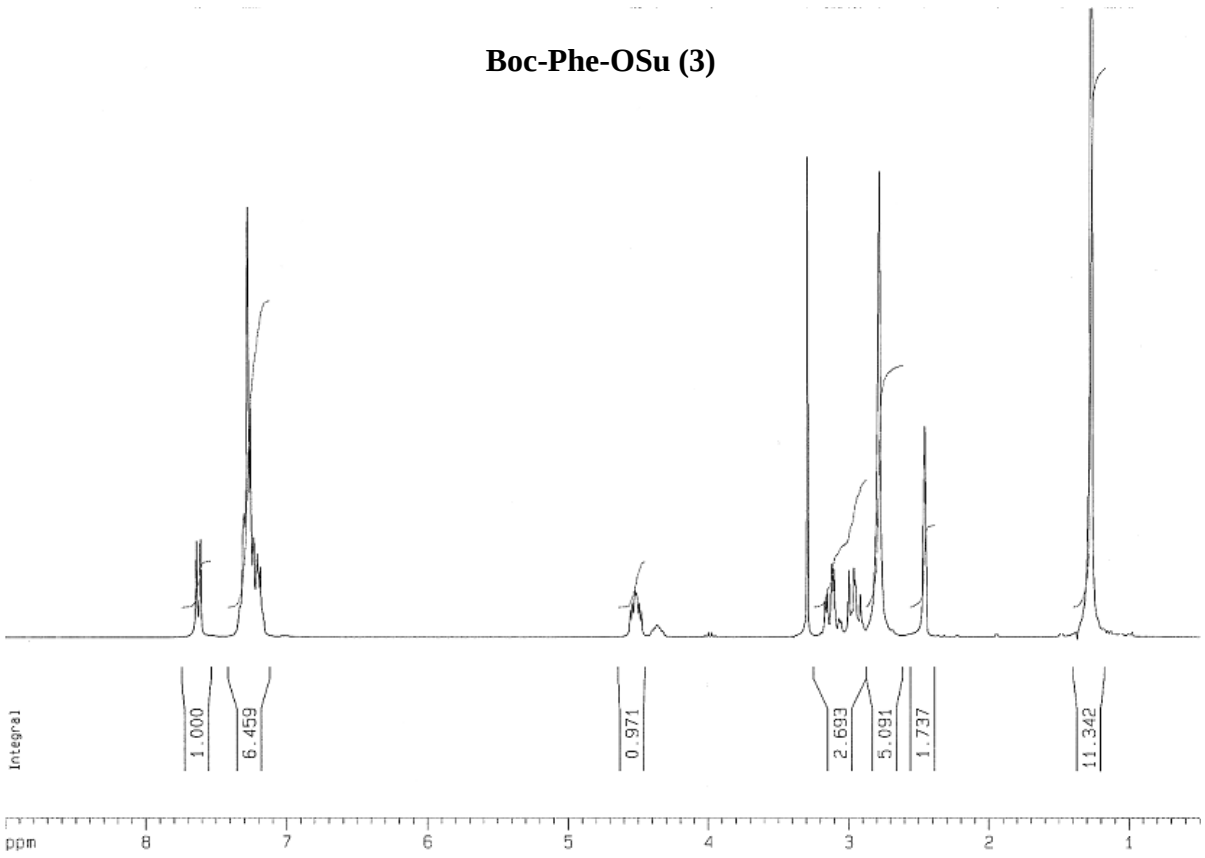

H-Asp(OBzl)-Phe-OH.CF_3COOH (4)

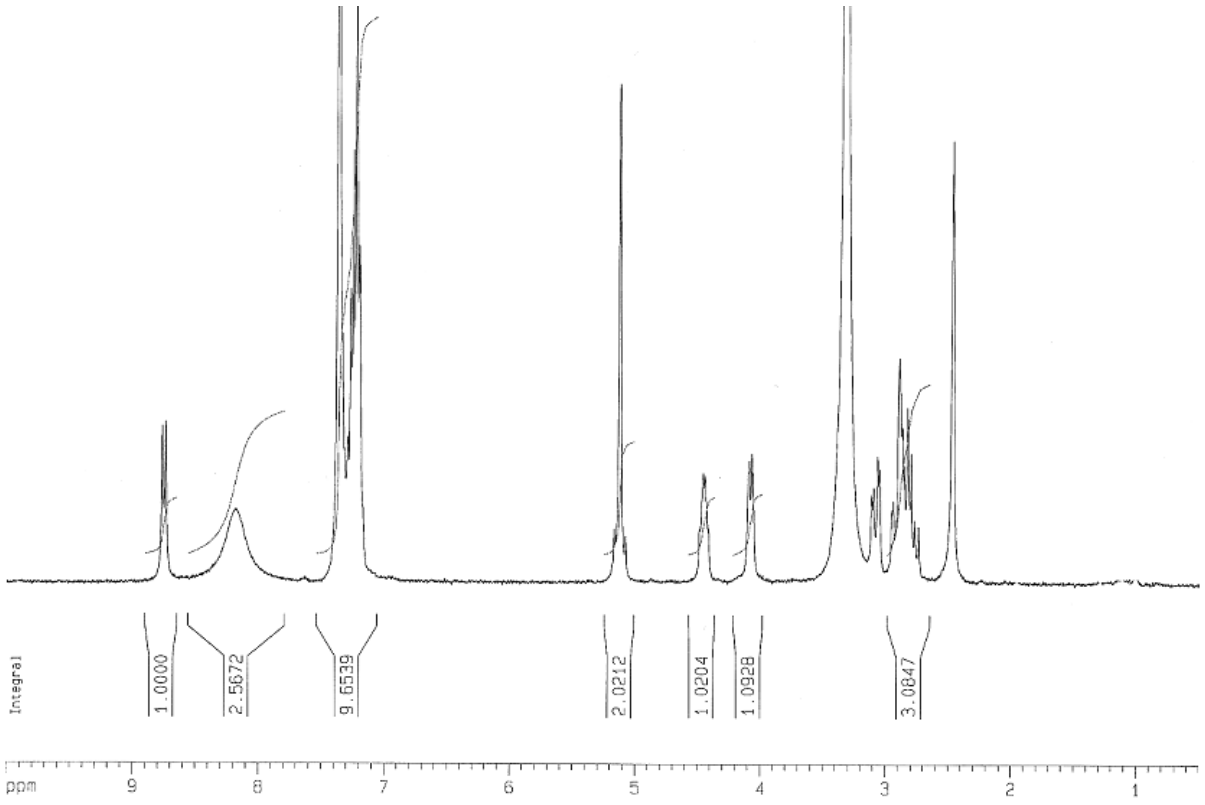

Boc-Phe-Asp(OBzl)-Phe-OH (5)

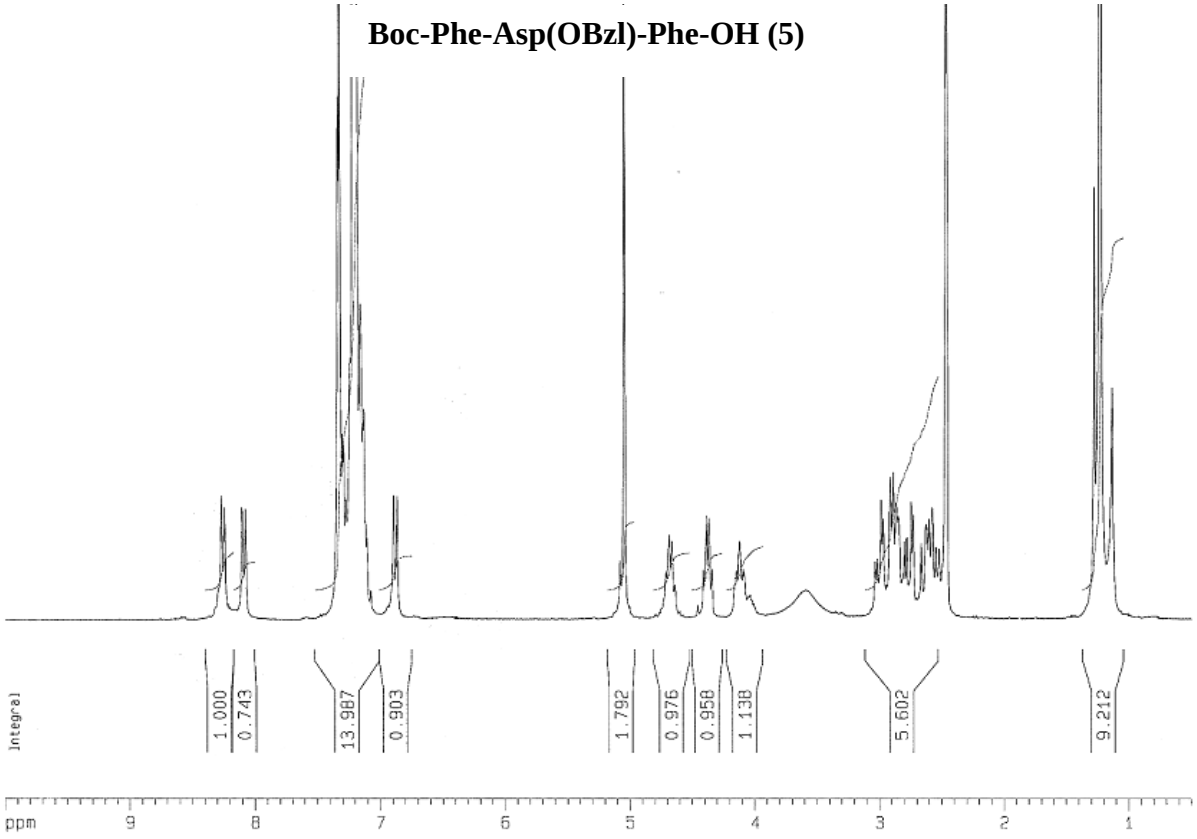

H-Phe-Asp(OBzl)-Phe-OH.CF_3COOH (6)

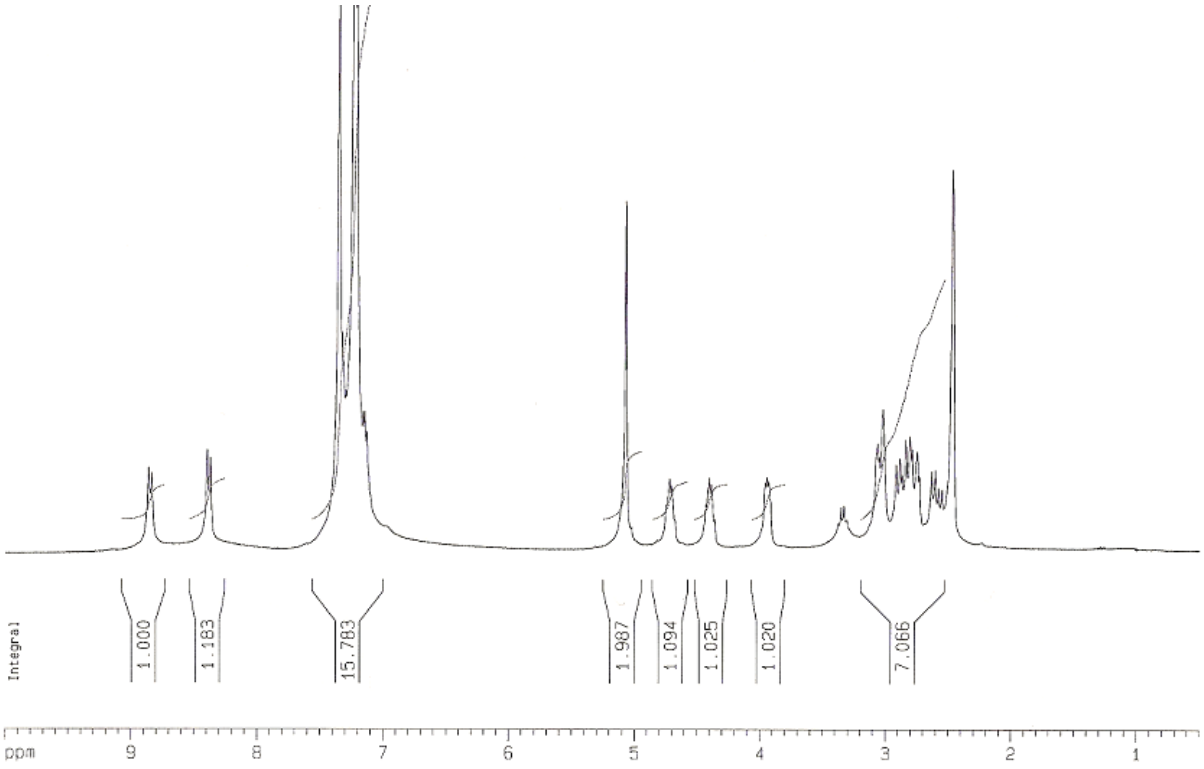

Boc-Asp(OBzl)-Phe-Asp(OBzl)-Phe-OH (7)

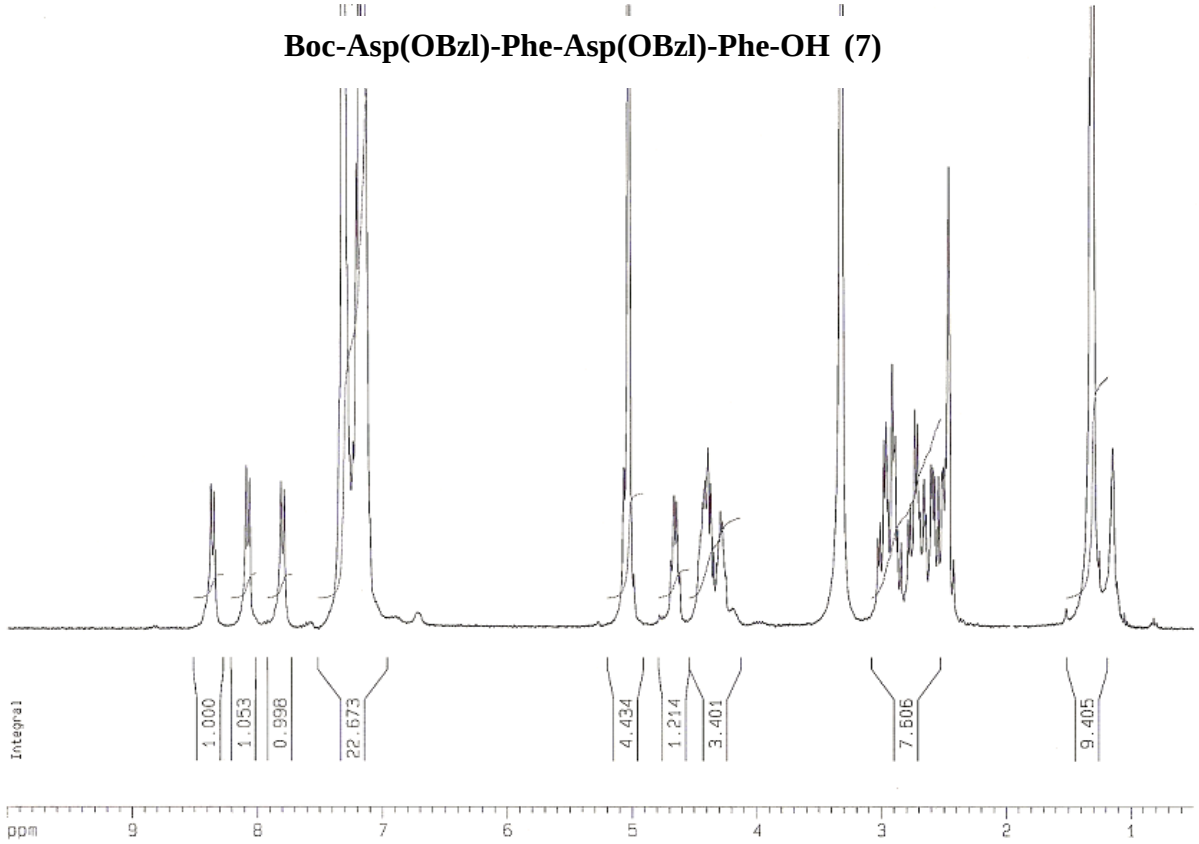

Boc-Asp(OBzl)-Phe-Asp(OBzl)-Phe-OSu (8)

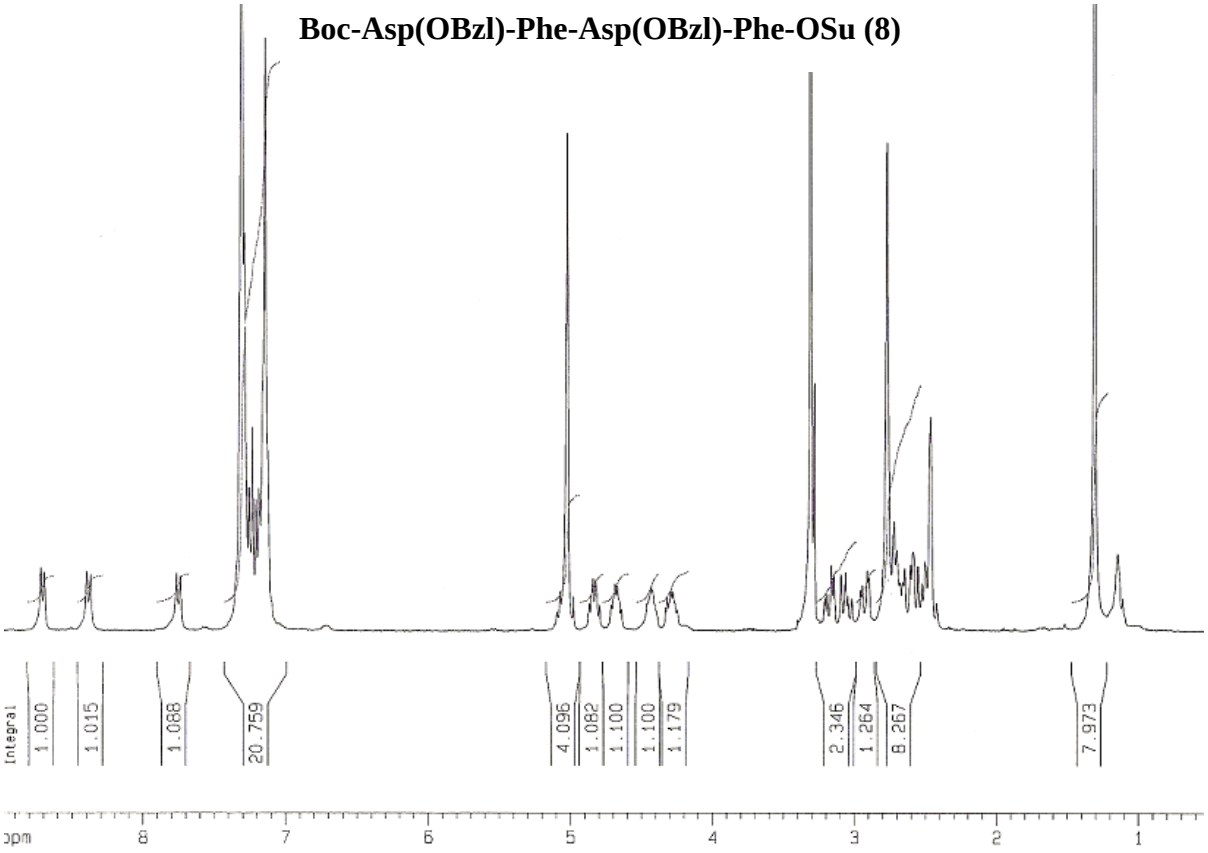

H-Asp(OBzl)-Phe-Asp(OBzl)-Phe-OSu.CF_3COOH (9)

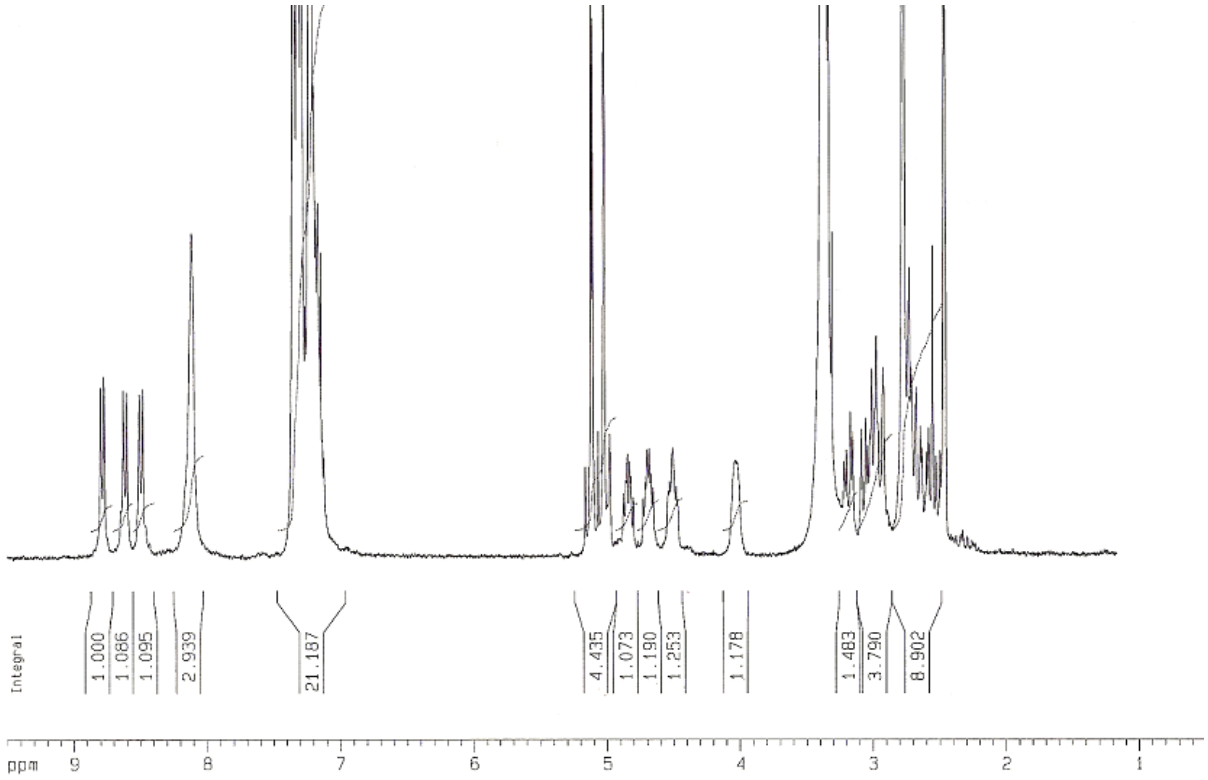

Poly(Asp(OBzl)-Phe-Asp(OBzl)-Phe) (10)

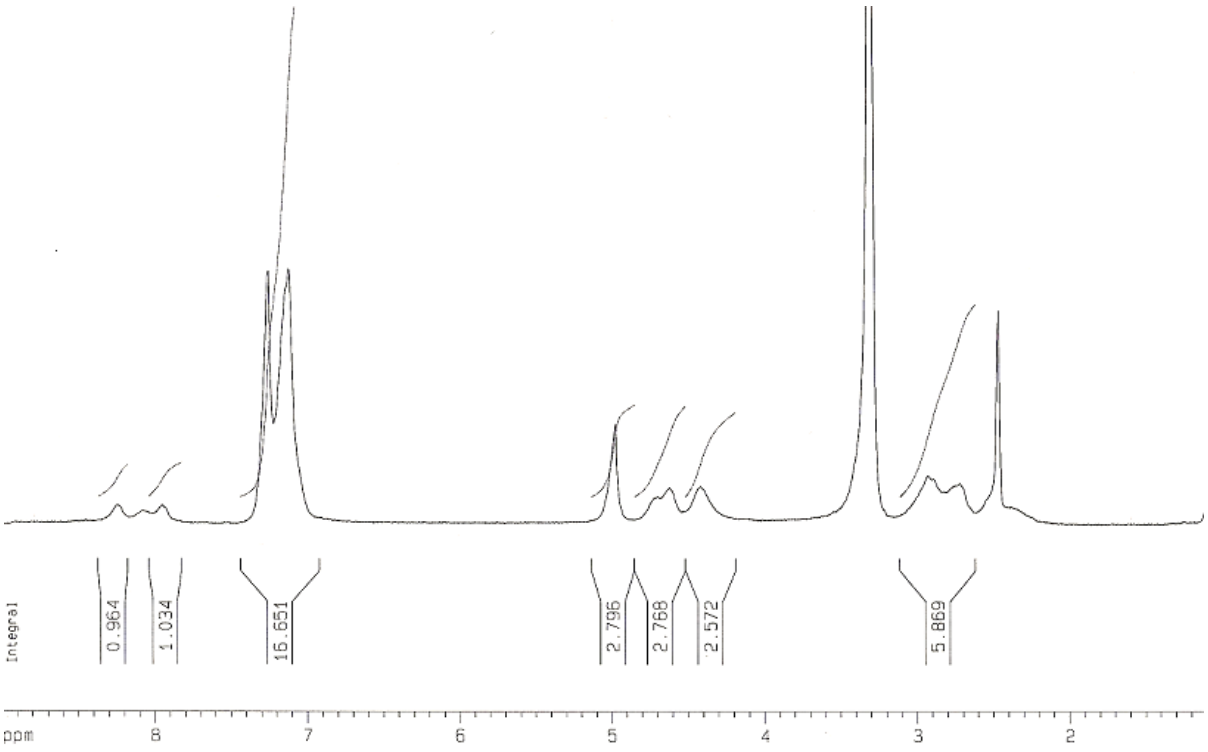

Poly(Asp(OH)-Phe-Asp(OH)-Phe) (11)

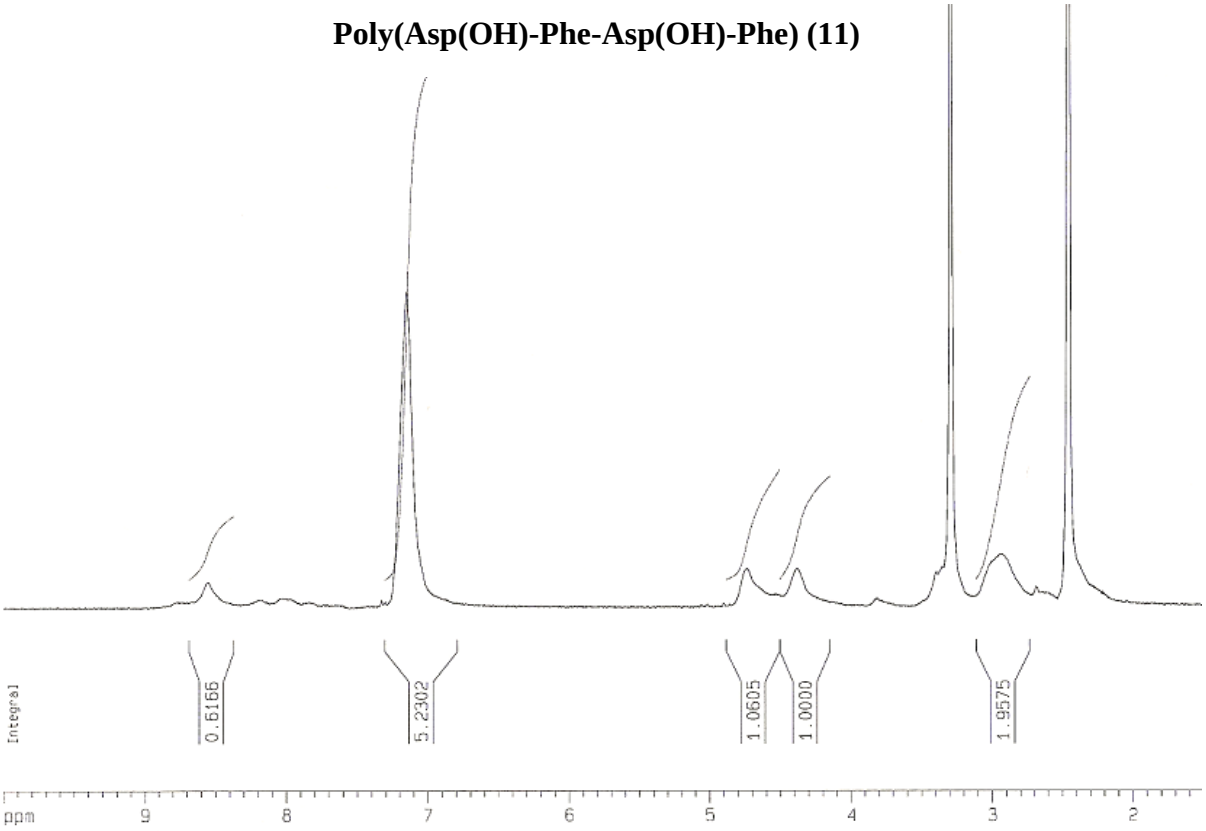

Boc-Asp(OBzl)-Asp(OBzl)-Phe-OH (12)

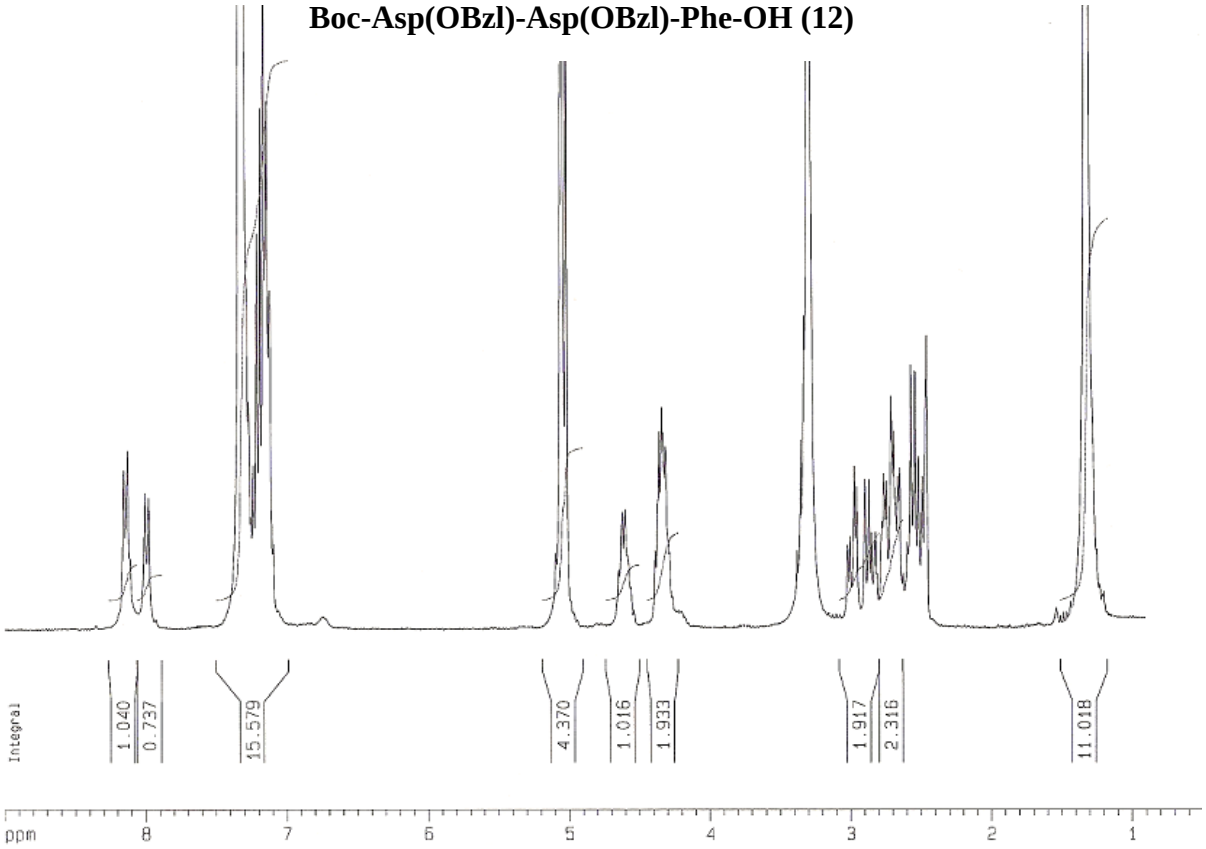

H-Asp(OBzl)-Asp(OBzl)-Phe-OH.CF_3COOH (13)

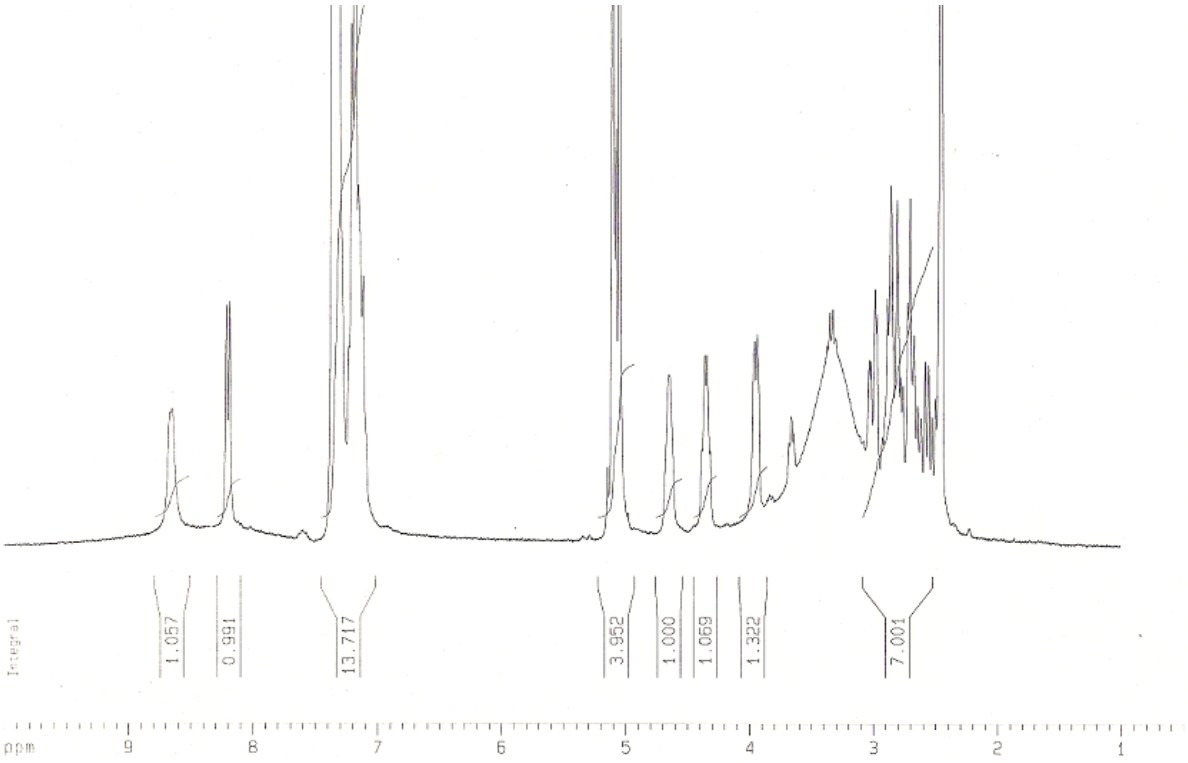

Boc-Asp(OBzl)-Asp(OBzl)-Asp(OBzl)-Phe-OH (14)

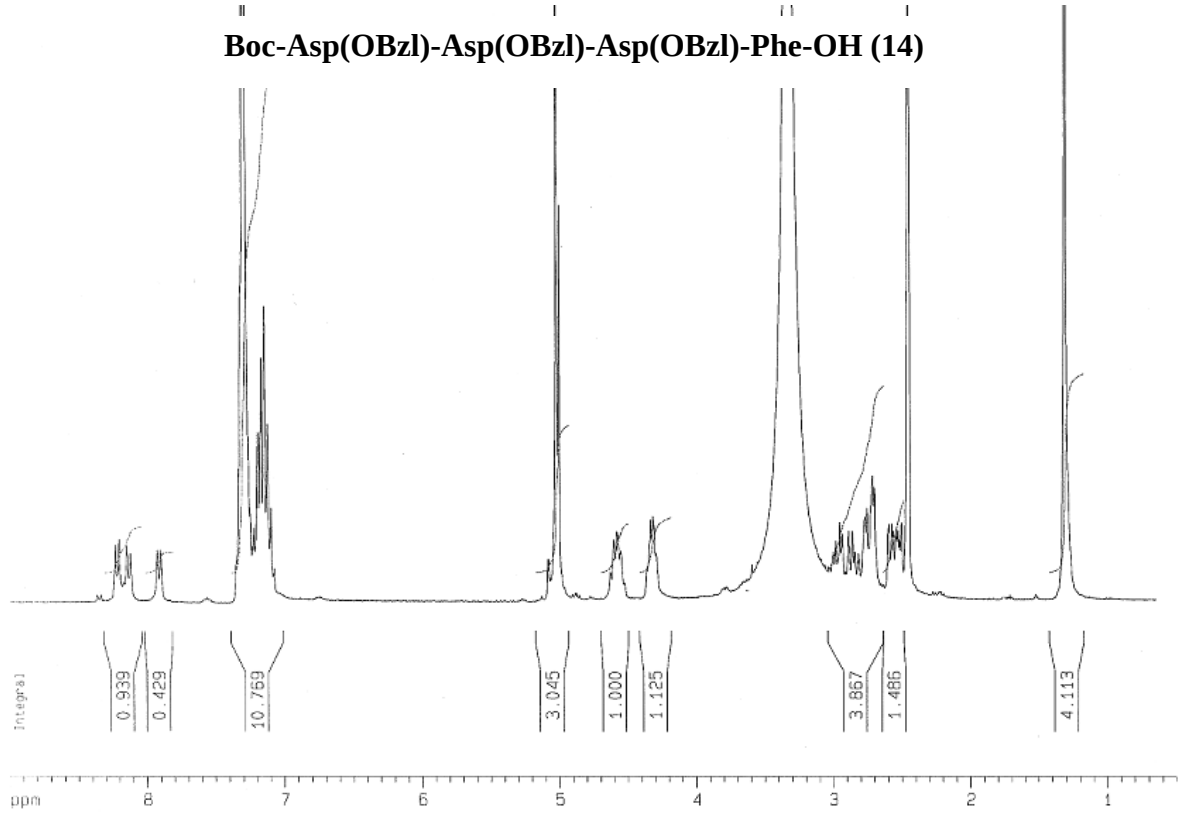

Boc-Asp(OBzl)-Asp(OBzl)-Asp(OBzl)-Phe-OSu (15)

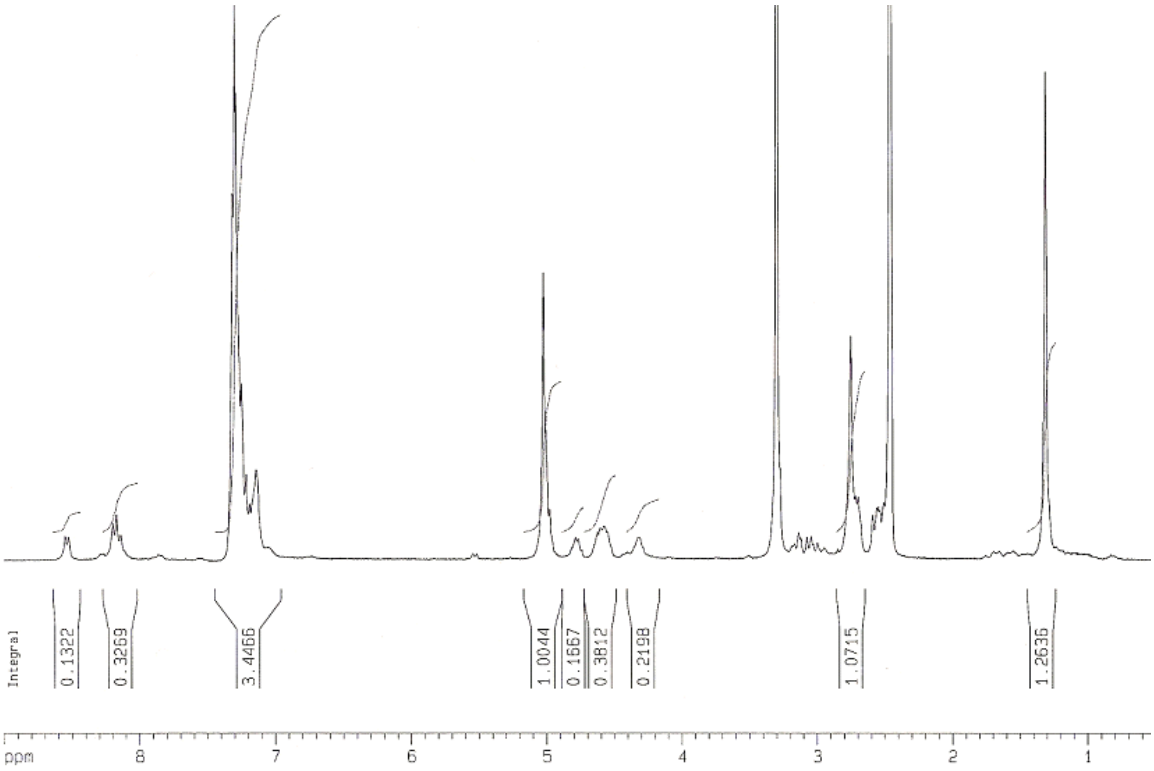

H-Asp(OBzl)-Asp(OBzl)-Asp(OBzl)-Phe-OSu.CF_3COOH (16)

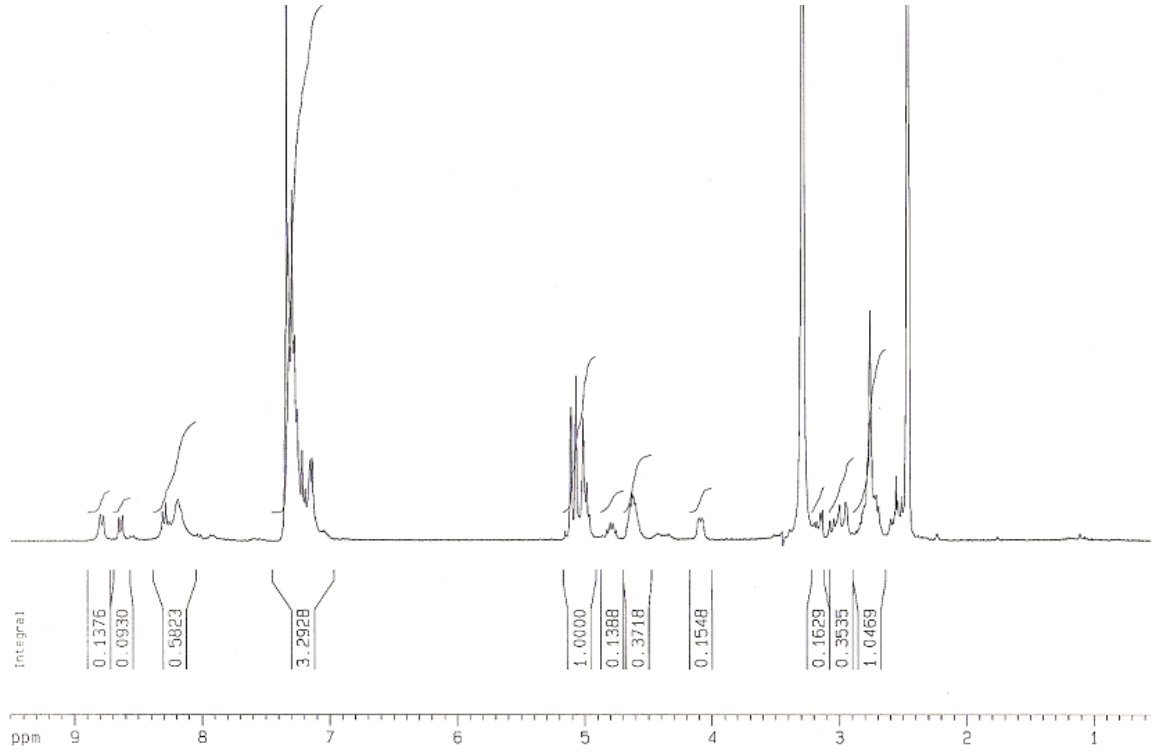

Poly(Asp(OBzl)-Asp(OBzl)-Asp(OBzl)-Phe) (17)

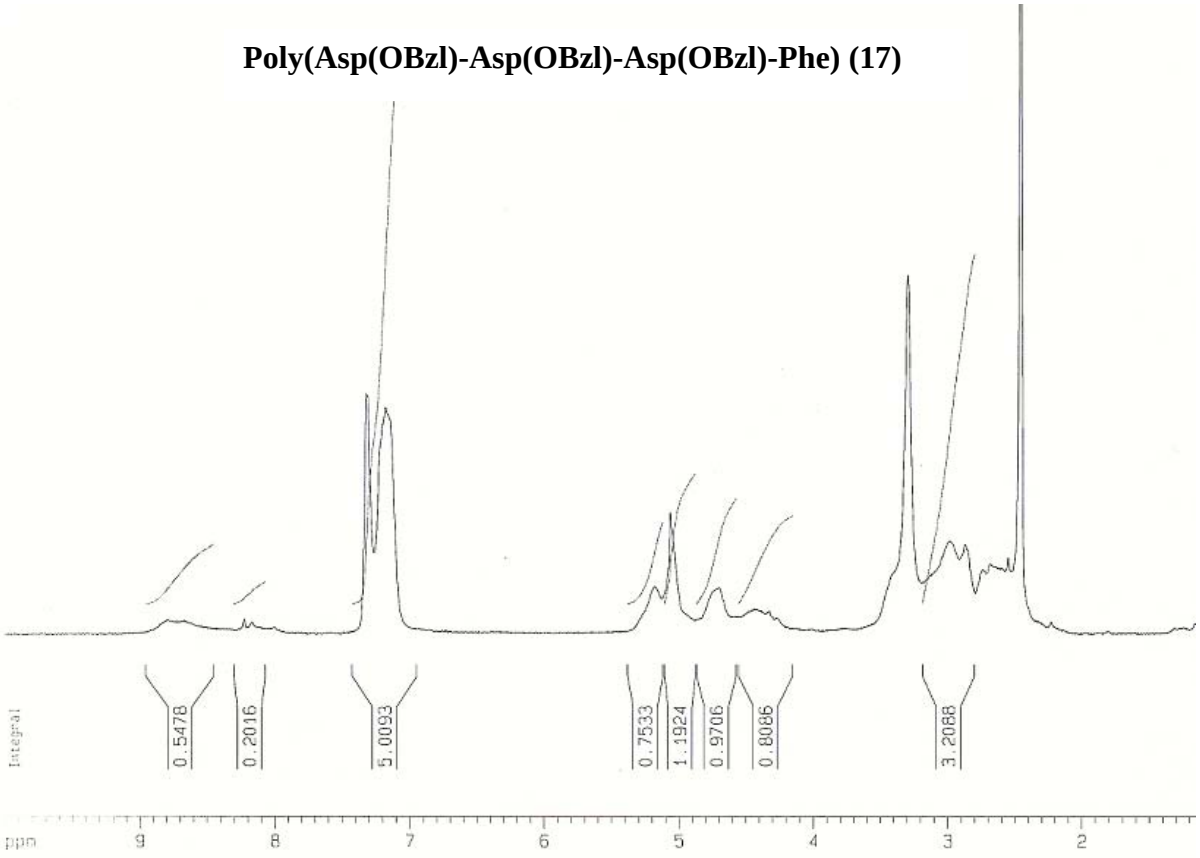

Poly(Asp(OH)-Asp(OH)-Asp(OH)-Phe) (18)

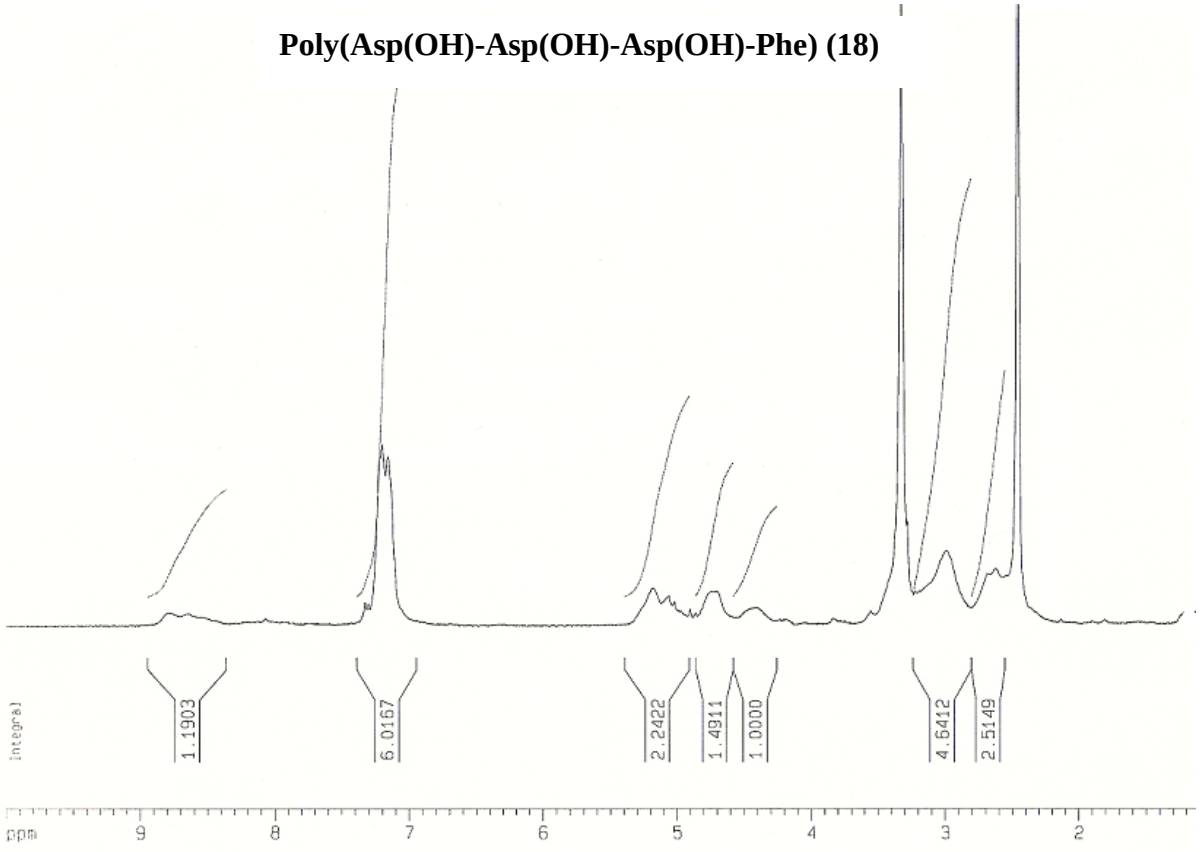

Boc-Asp(OBzl)-Asp(OBzl)-Phe-OSu (19)

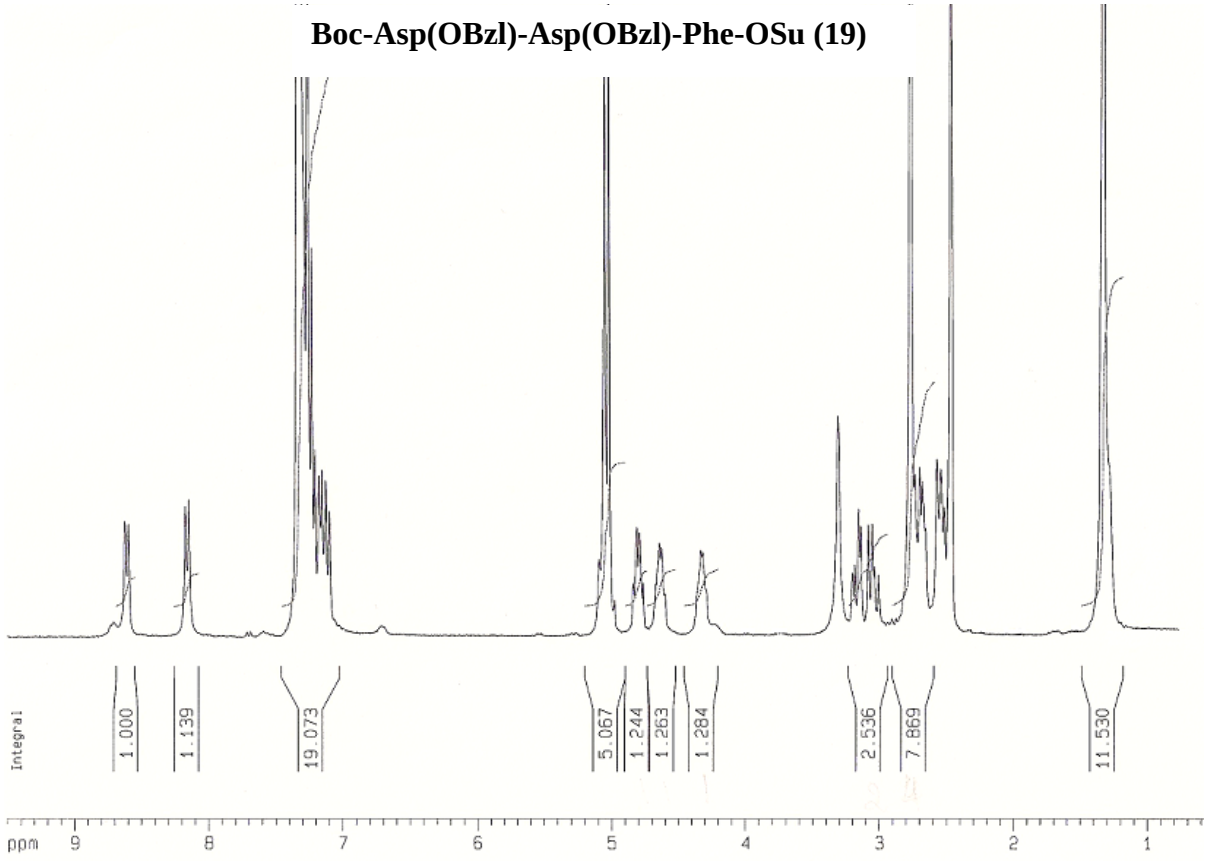

H-Asp(OBzl)-Asp(OBzl)-Phe-OSu.CF_3COOH (20)

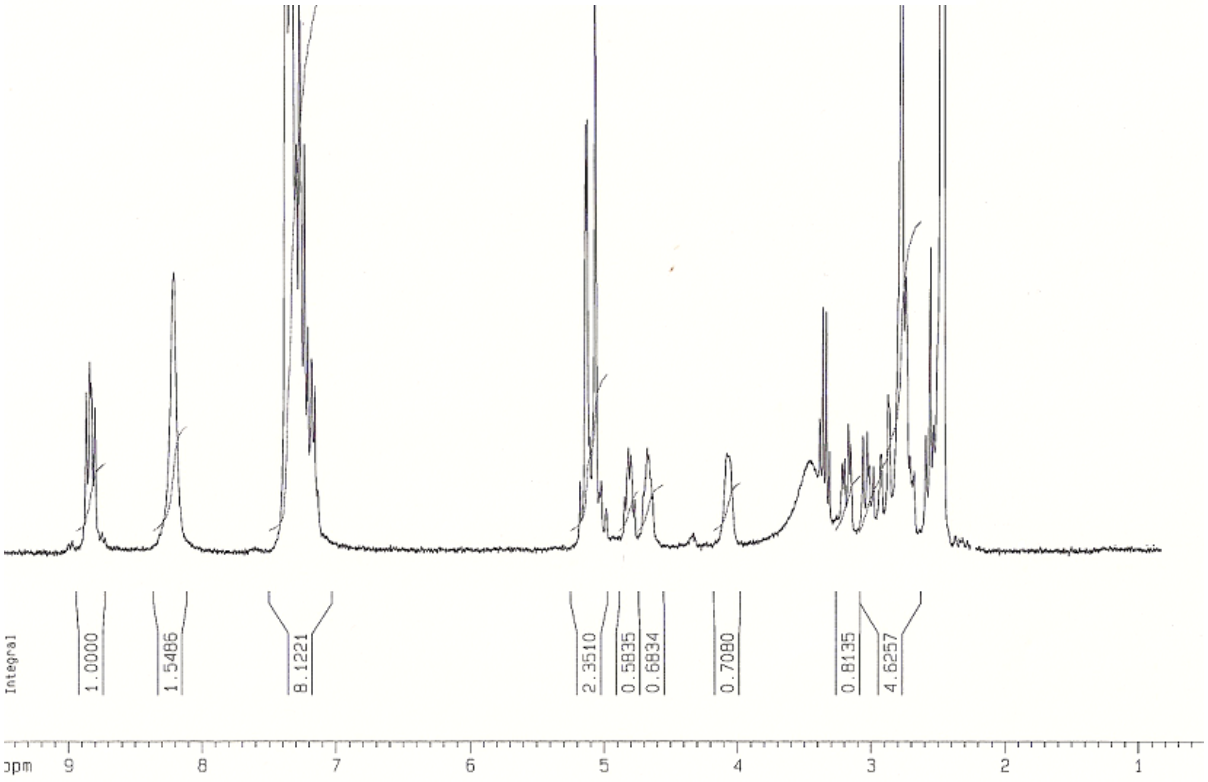

Poly(Asp(OBzl)-Asp(OBzl)-Phe) (21)

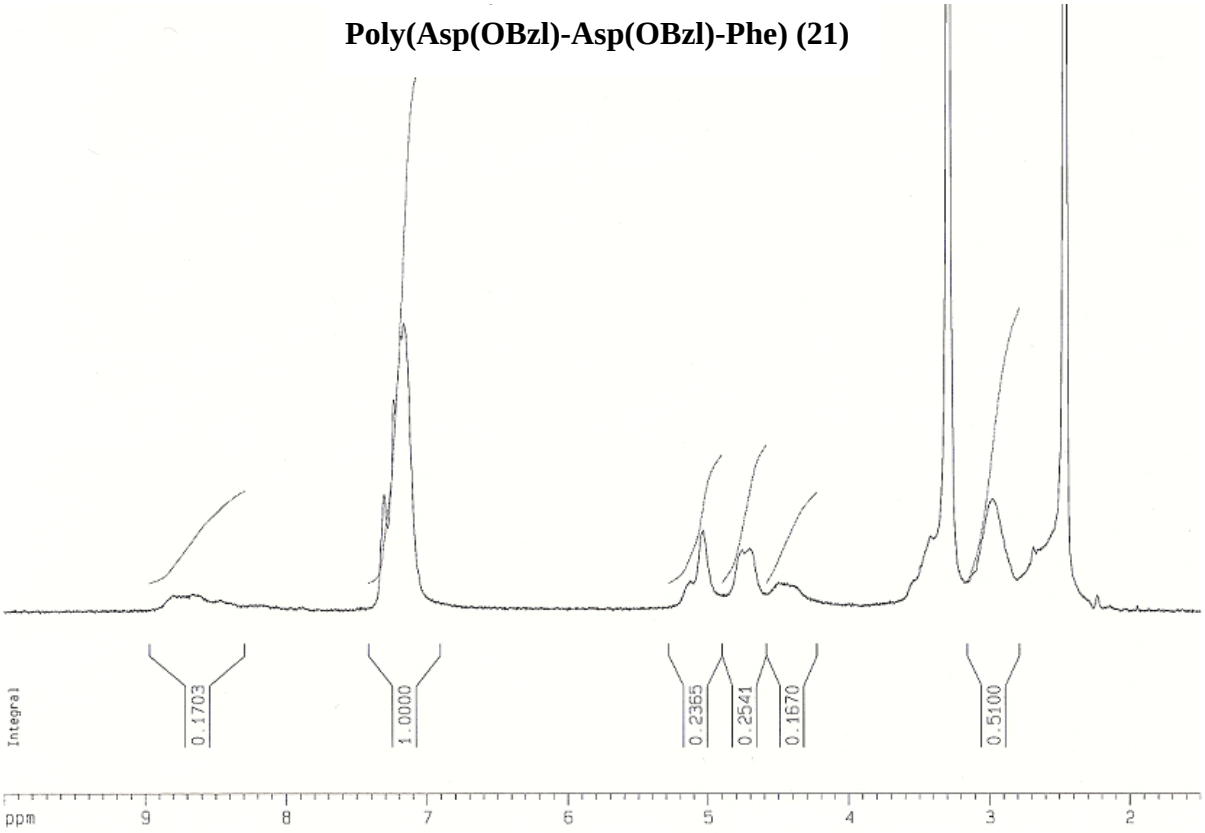

Poly(Asp(OH)-Asp(OH)-Phe) (22)

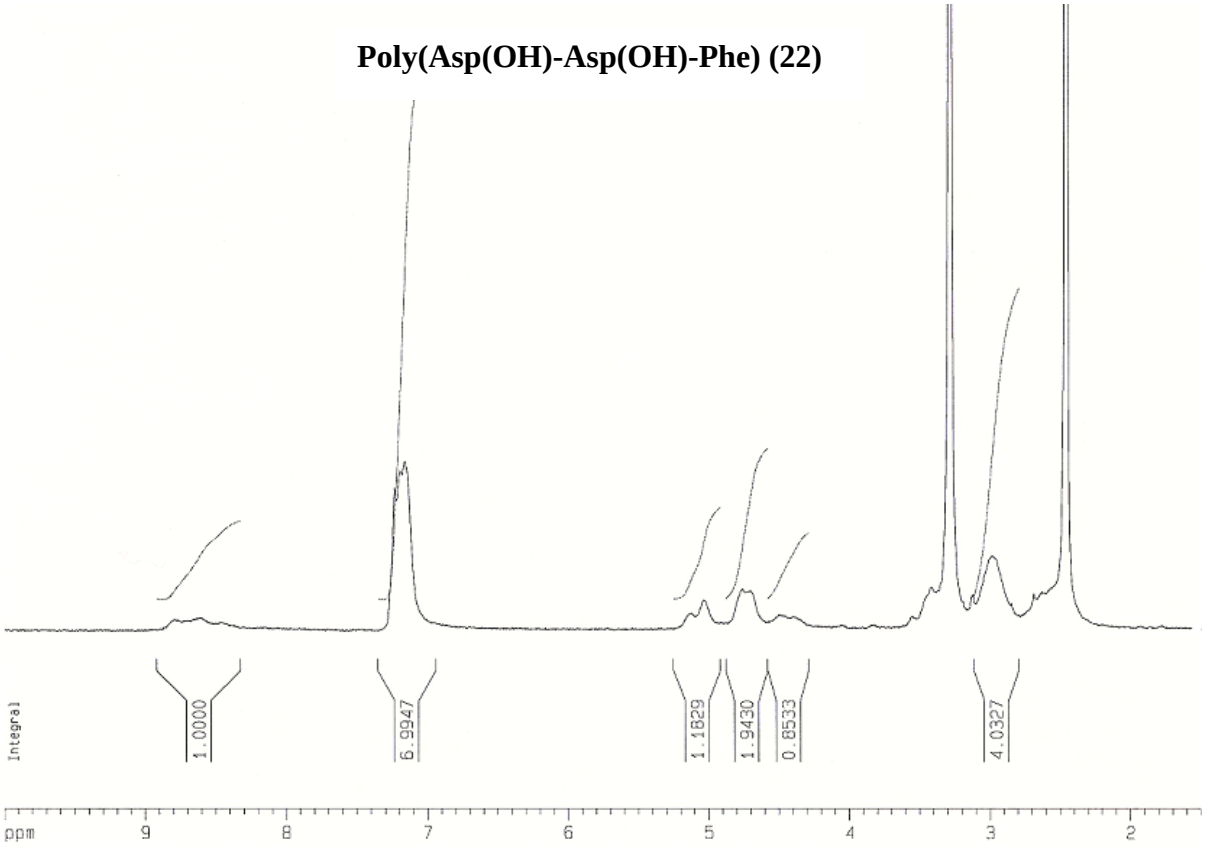

Boc-Phe-Phe-OH (23)

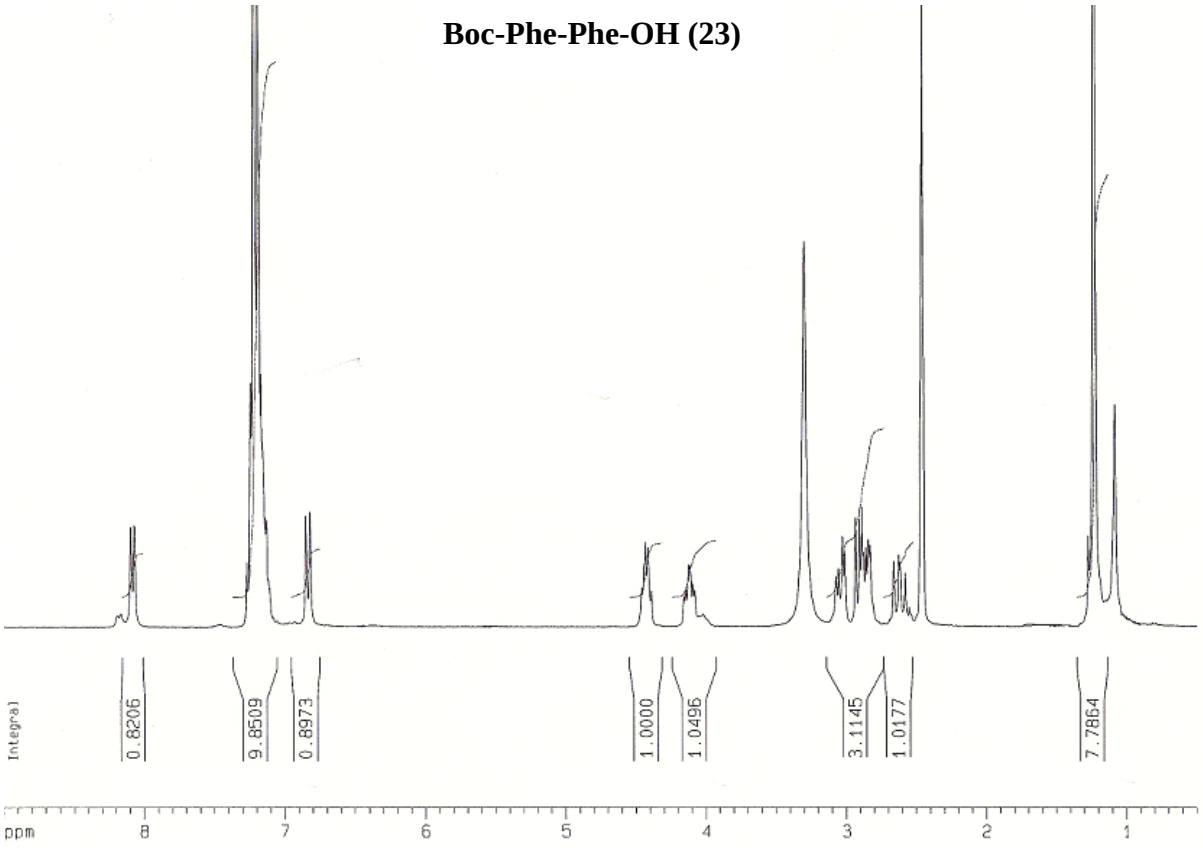

H-Phe-Phe-OH.CF_3COOH (24)

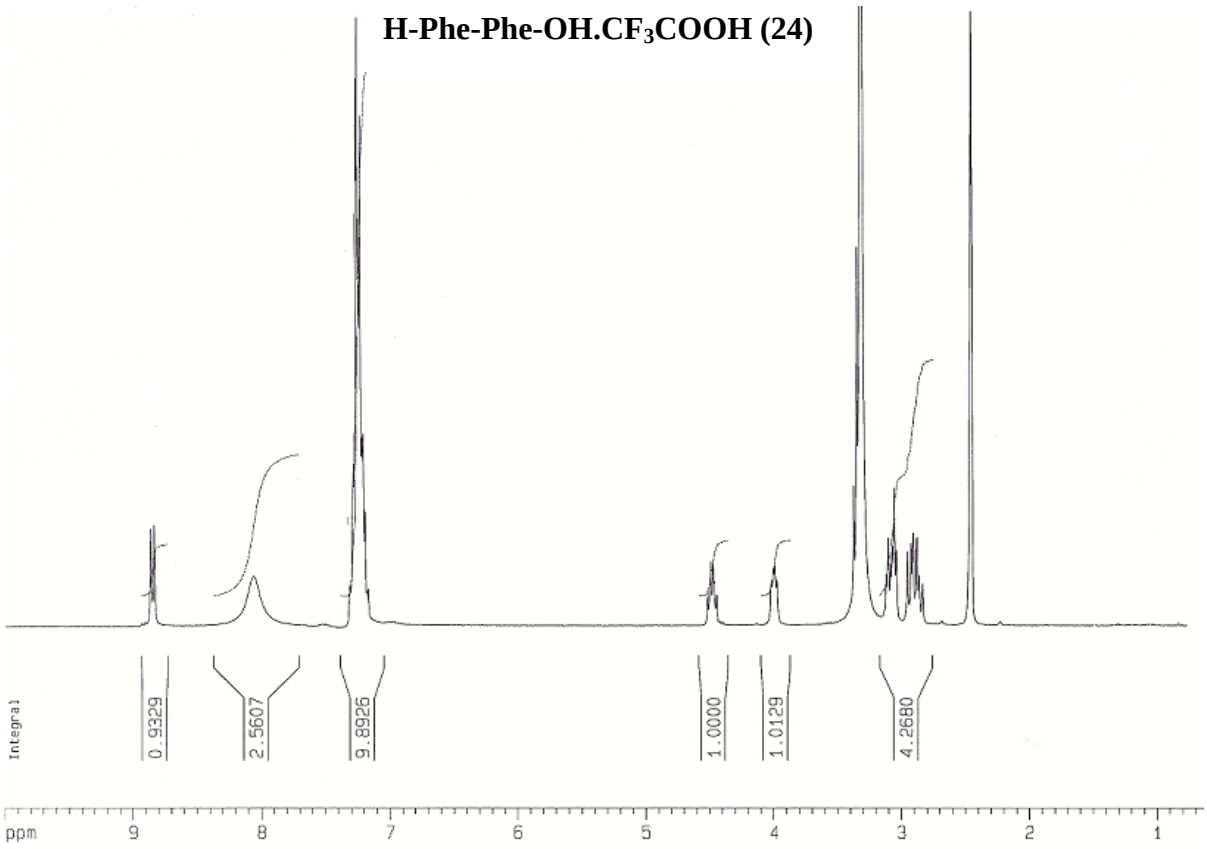

Boc-Asp(OBzl)-Phe-Phe-OH (25)

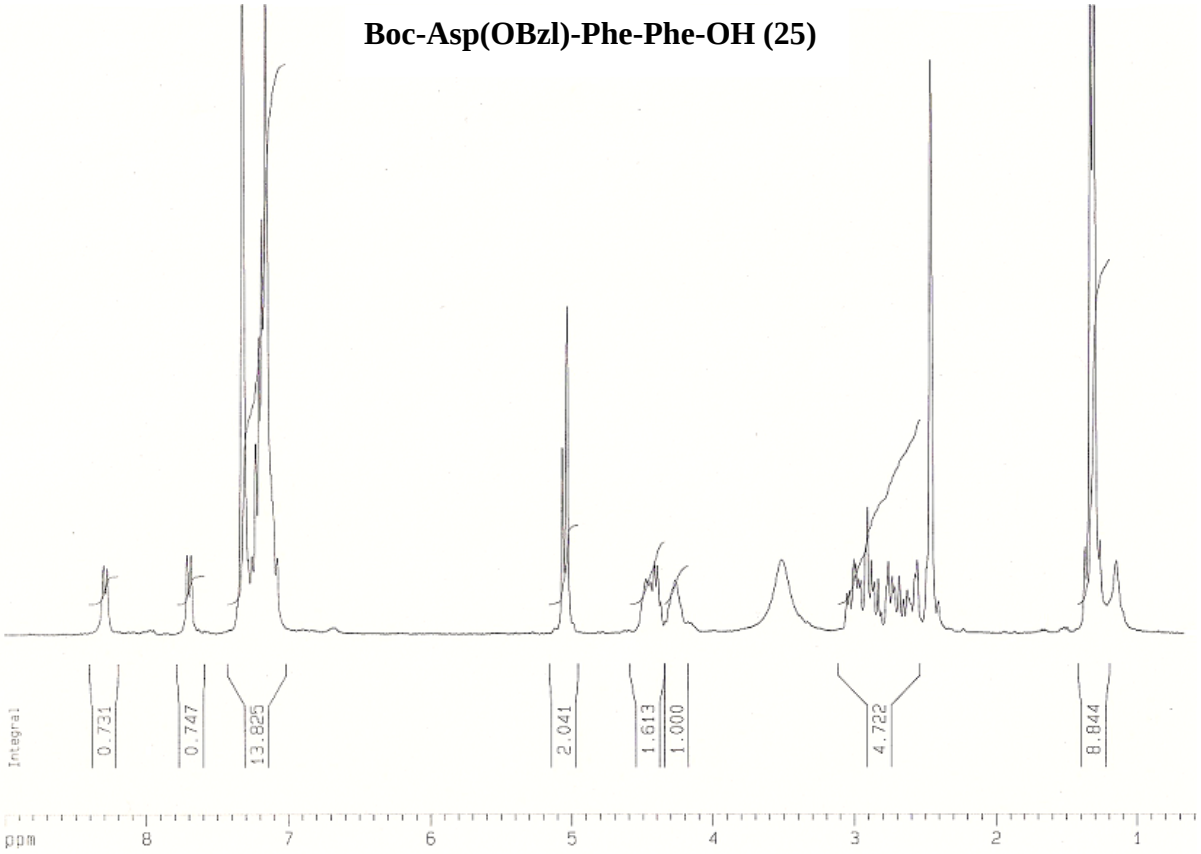

Boc-Asp(OBzl)-Phe-Phe-OSu (26)

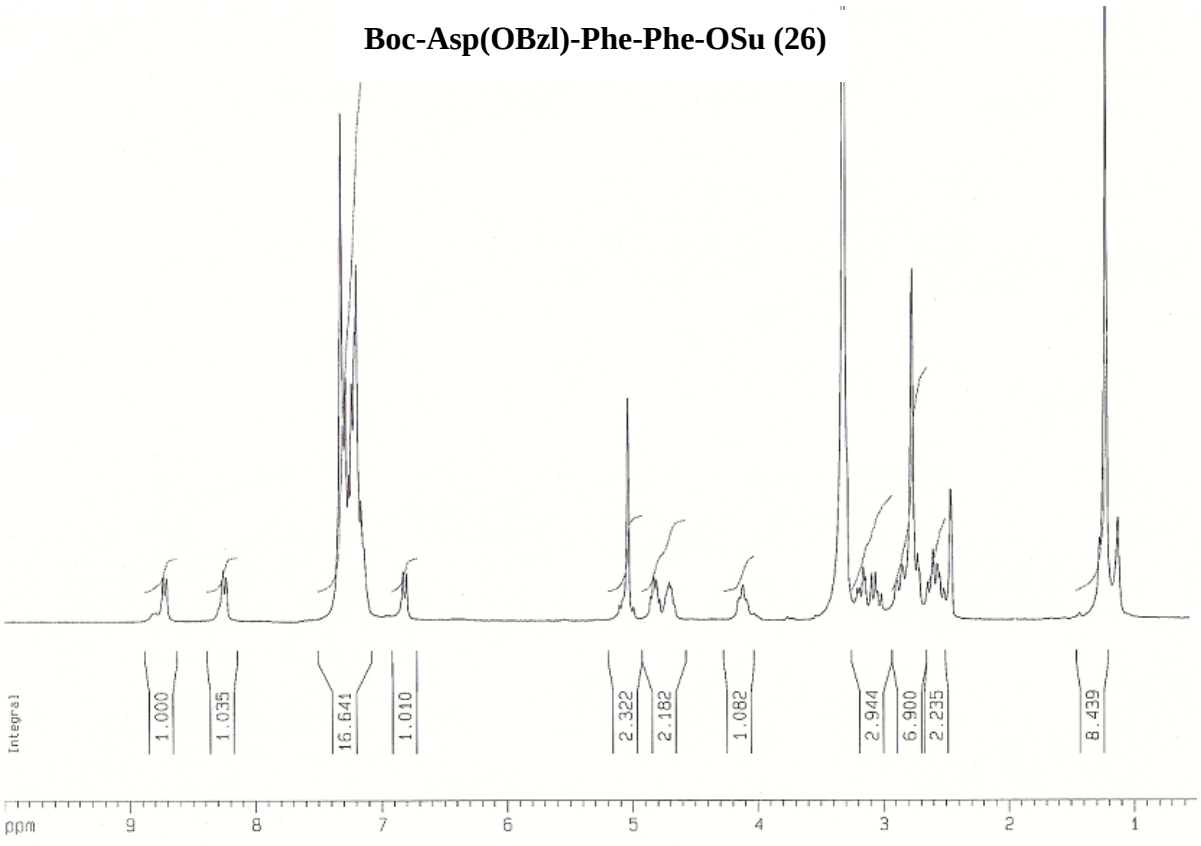

H-Asp(OBzl)-Phe-Phe-OSu.CF_3COOH (27)

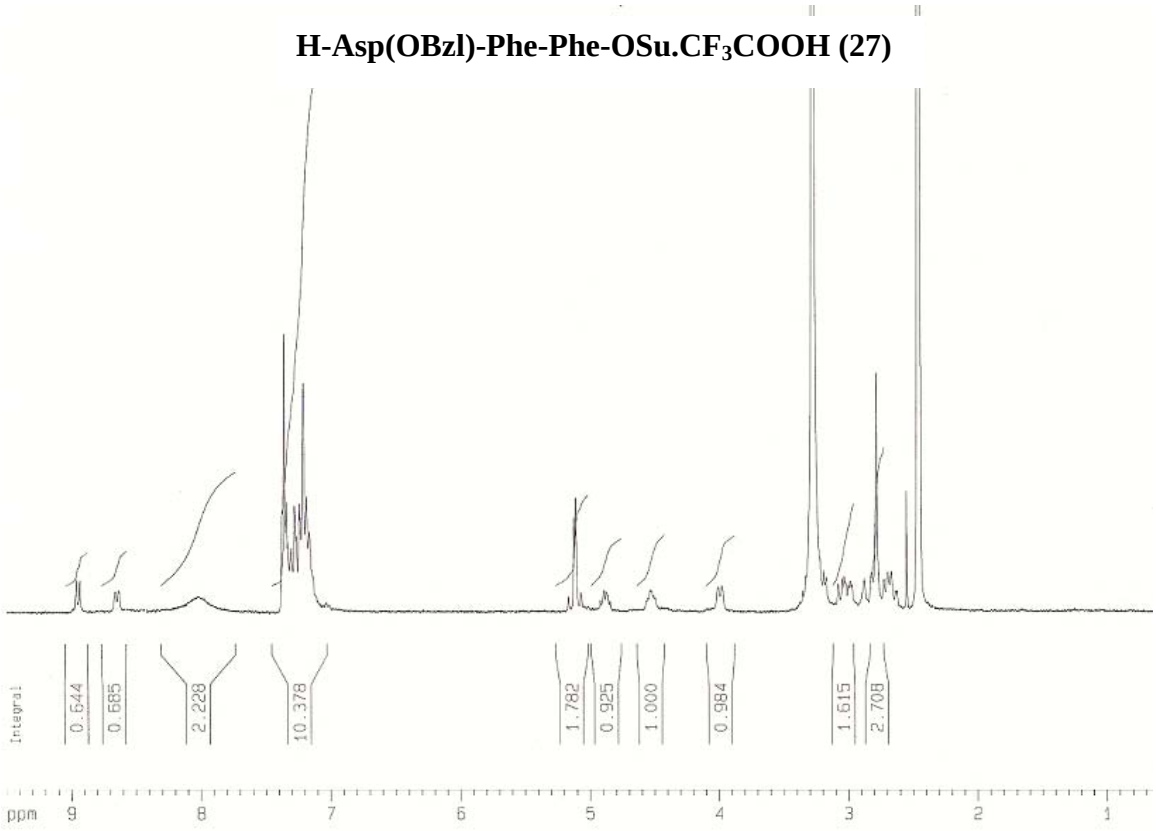

Poly(Asp(OBzl)-Phe-Phe) (28)

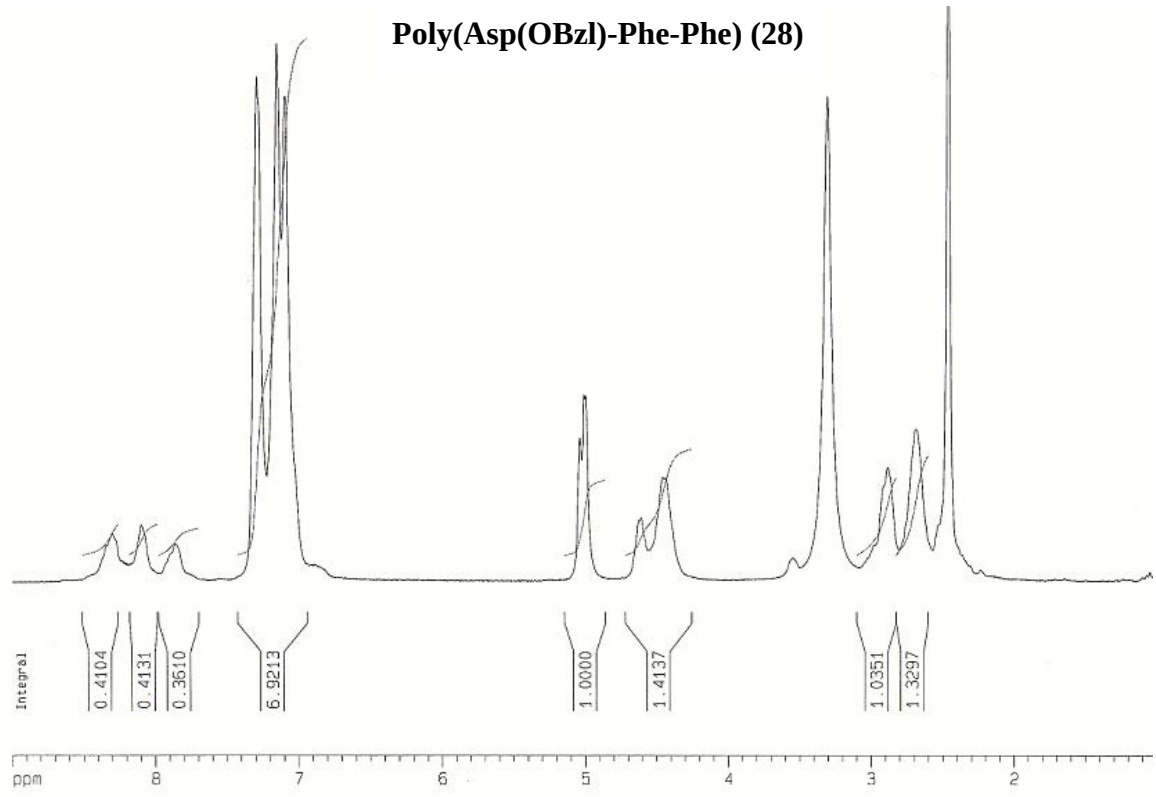

Poly(Asp(OH)-Phe-Phe) (29)

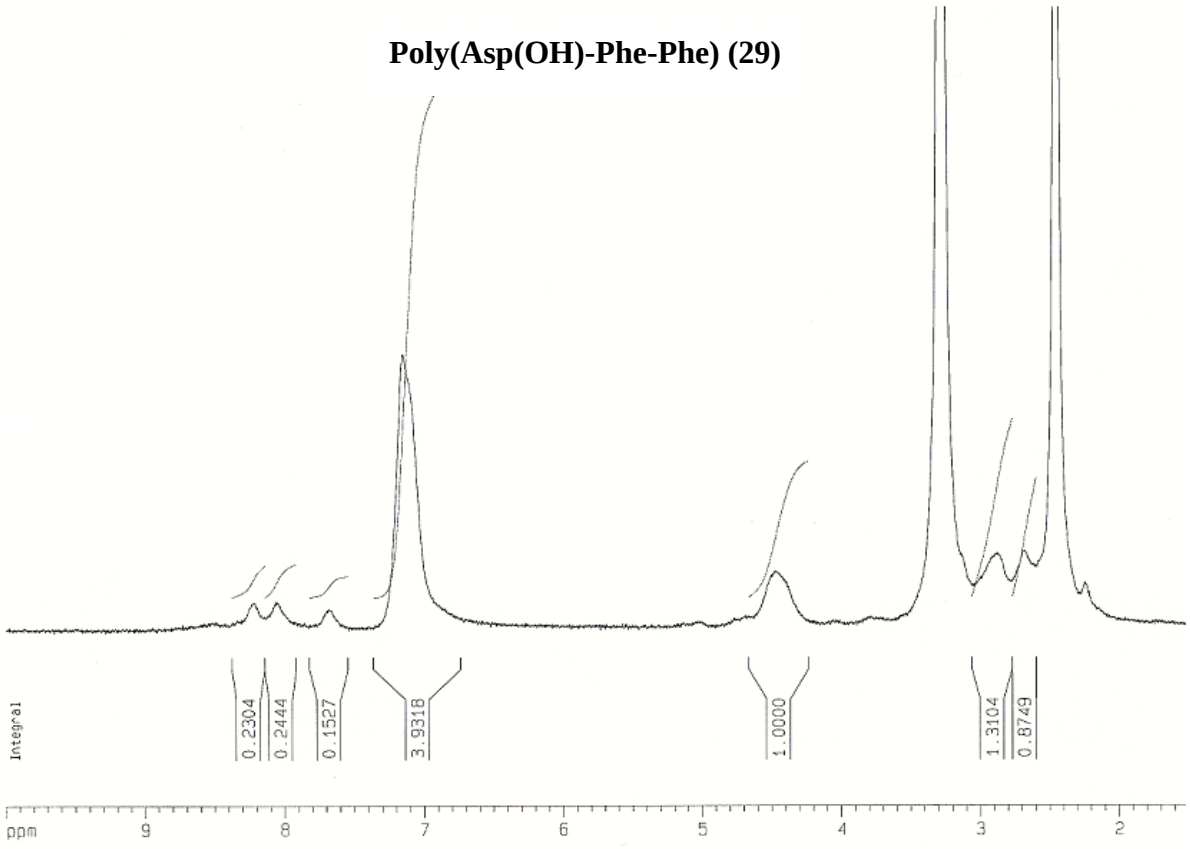

Boc-Phe-Phe-Phe-OH (30)

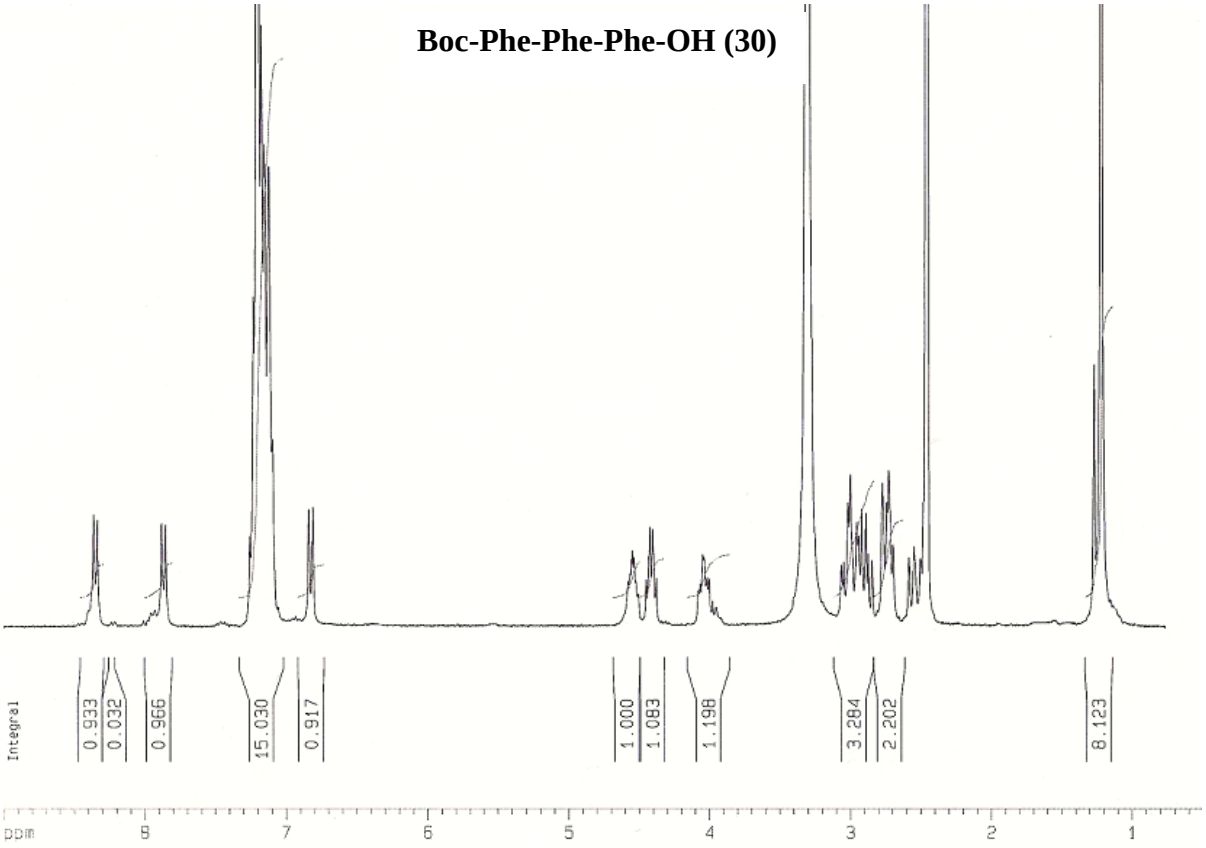

H-Phe-Phe-Phe-OH.CF_3COOH (31)

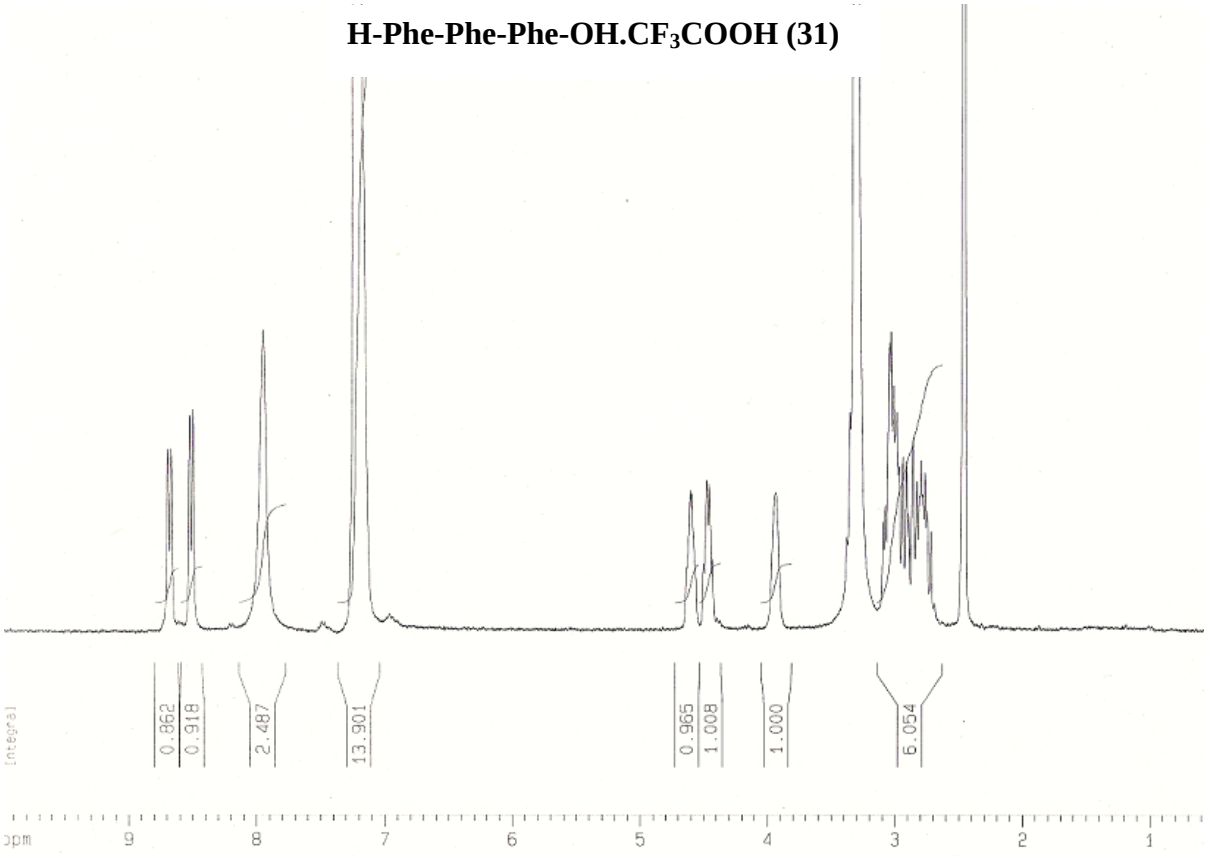

Boc-Asp(OBzl)-Phe-Phe-Phe-OH (32)

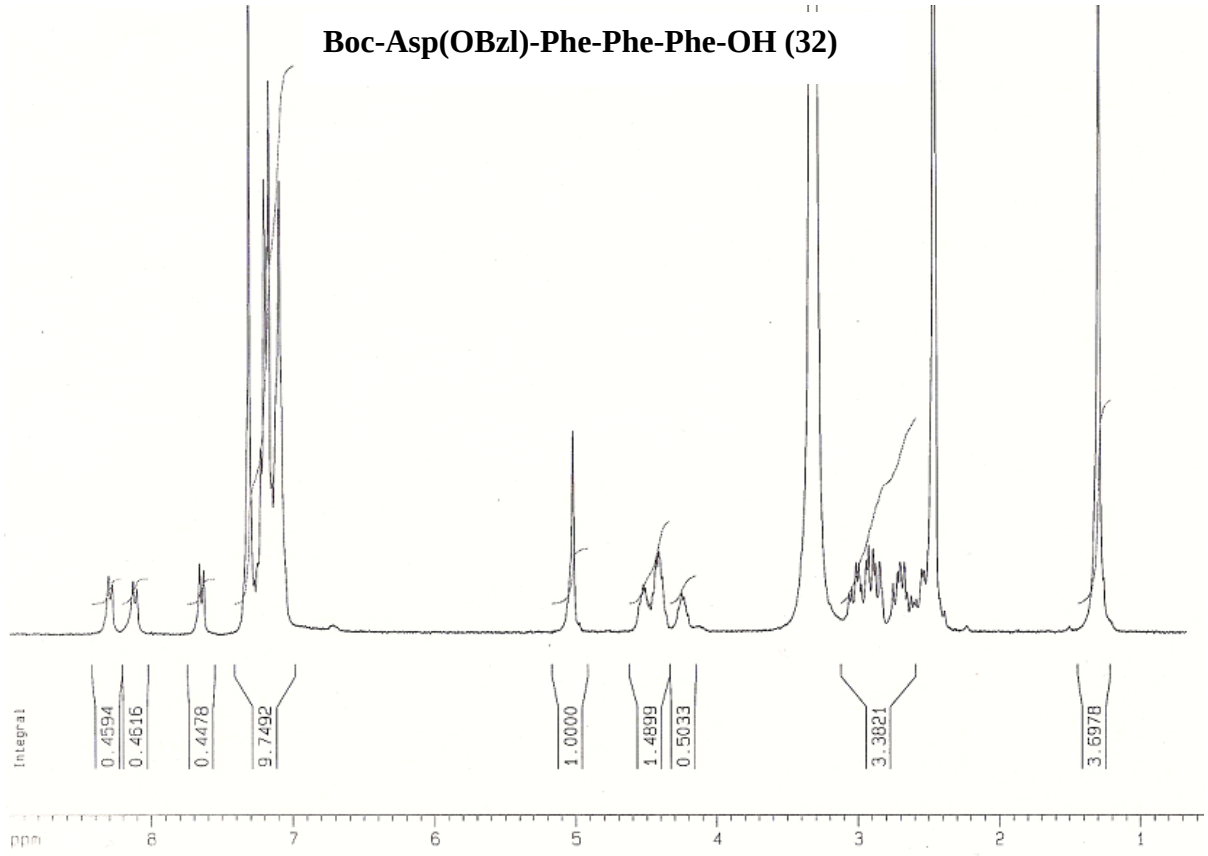

Boc-Asp(OBzl)-Phe-Phe-Phe-OSu (33)

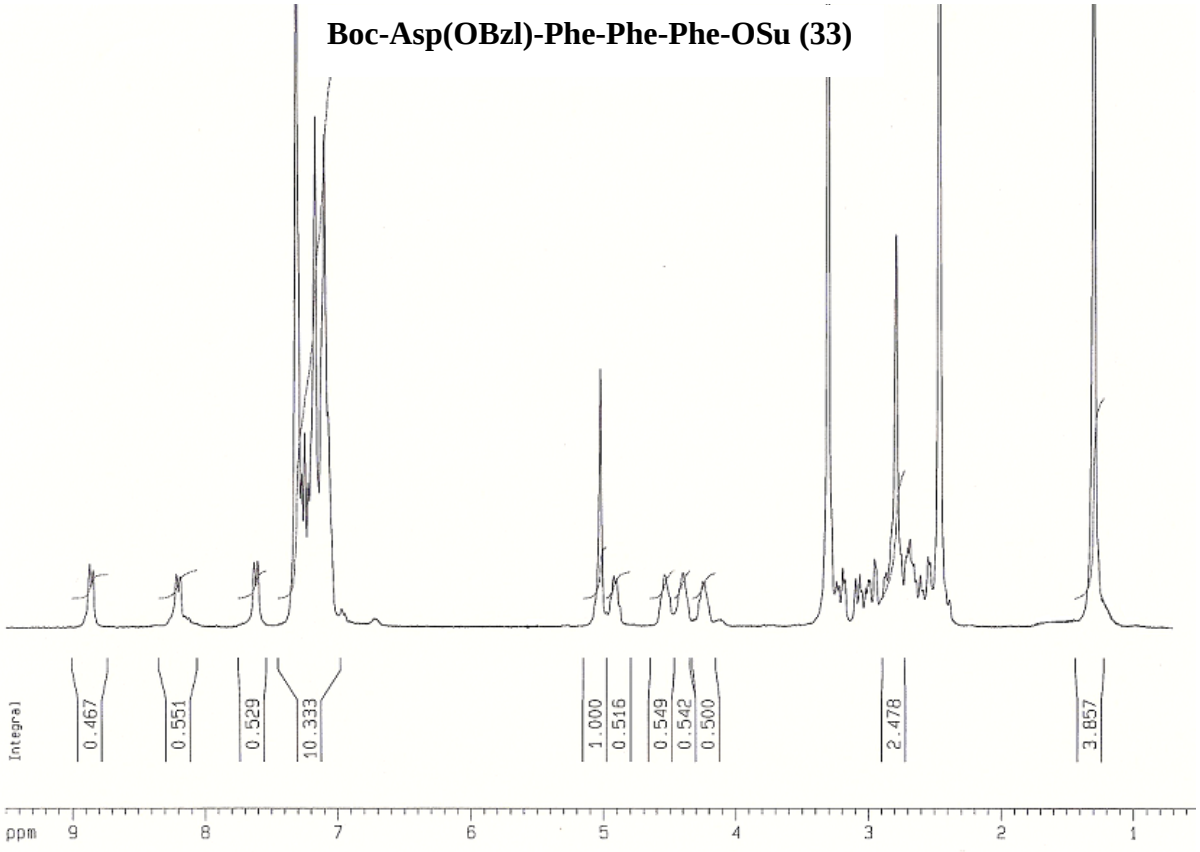

H-Asp(OBzl)-Phe-Phe-Phe-OSu.CF_3COOH (34)

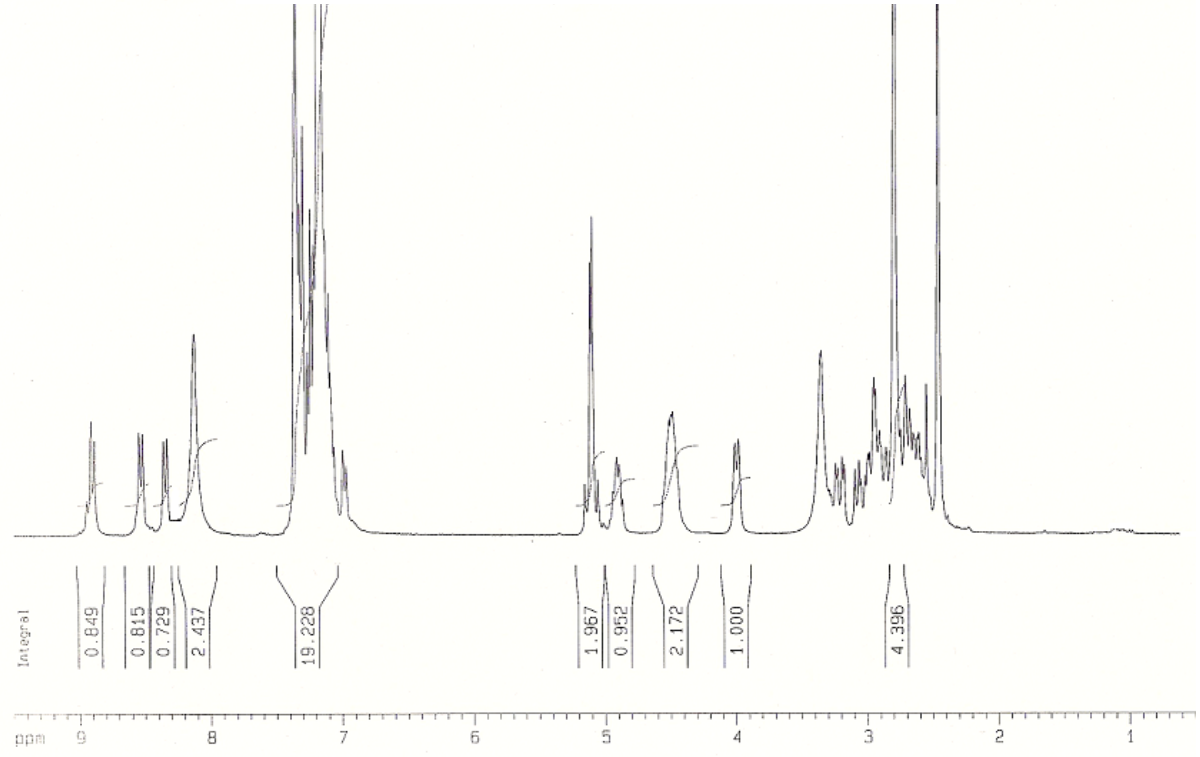

Poly(Asp(OBzl)-Phe-Phe-Phe) (35)

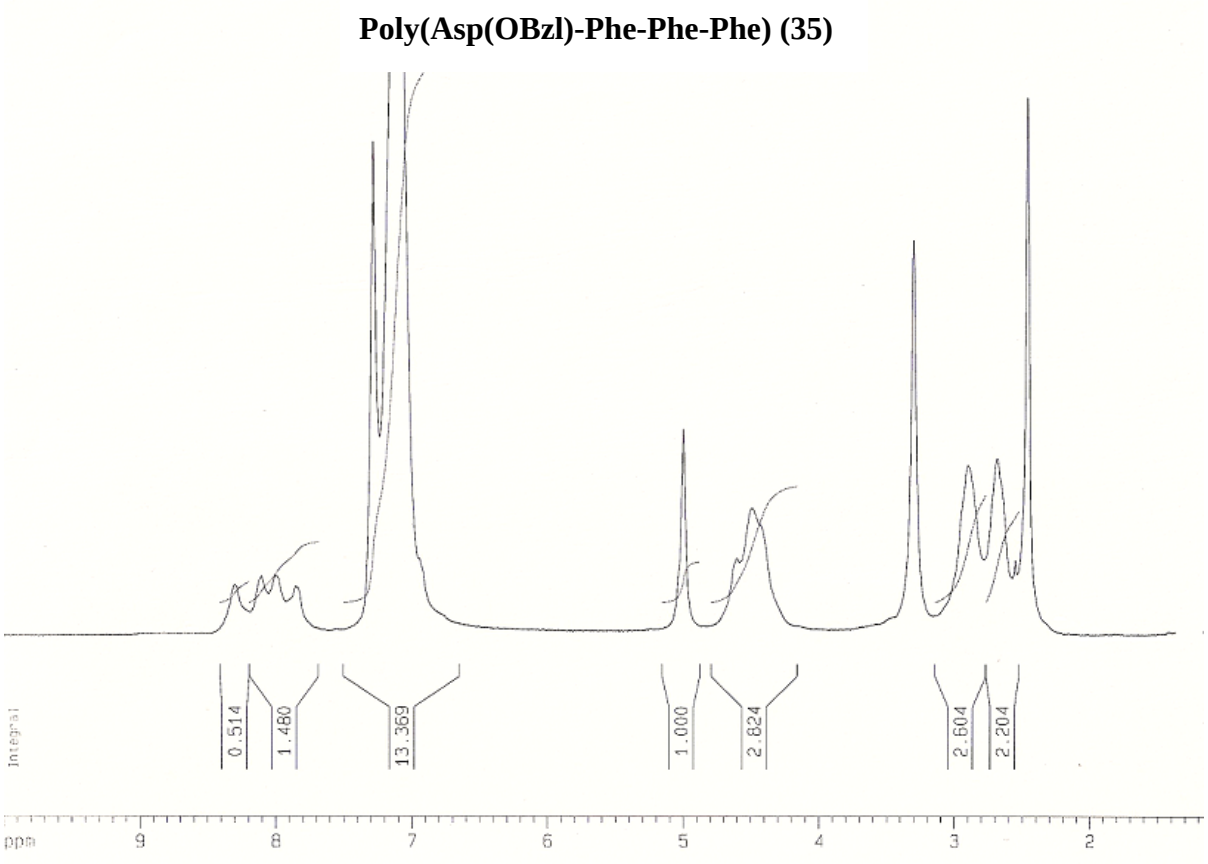

Poly(Asp(OH)-Phe-Phe-Phe) (36)

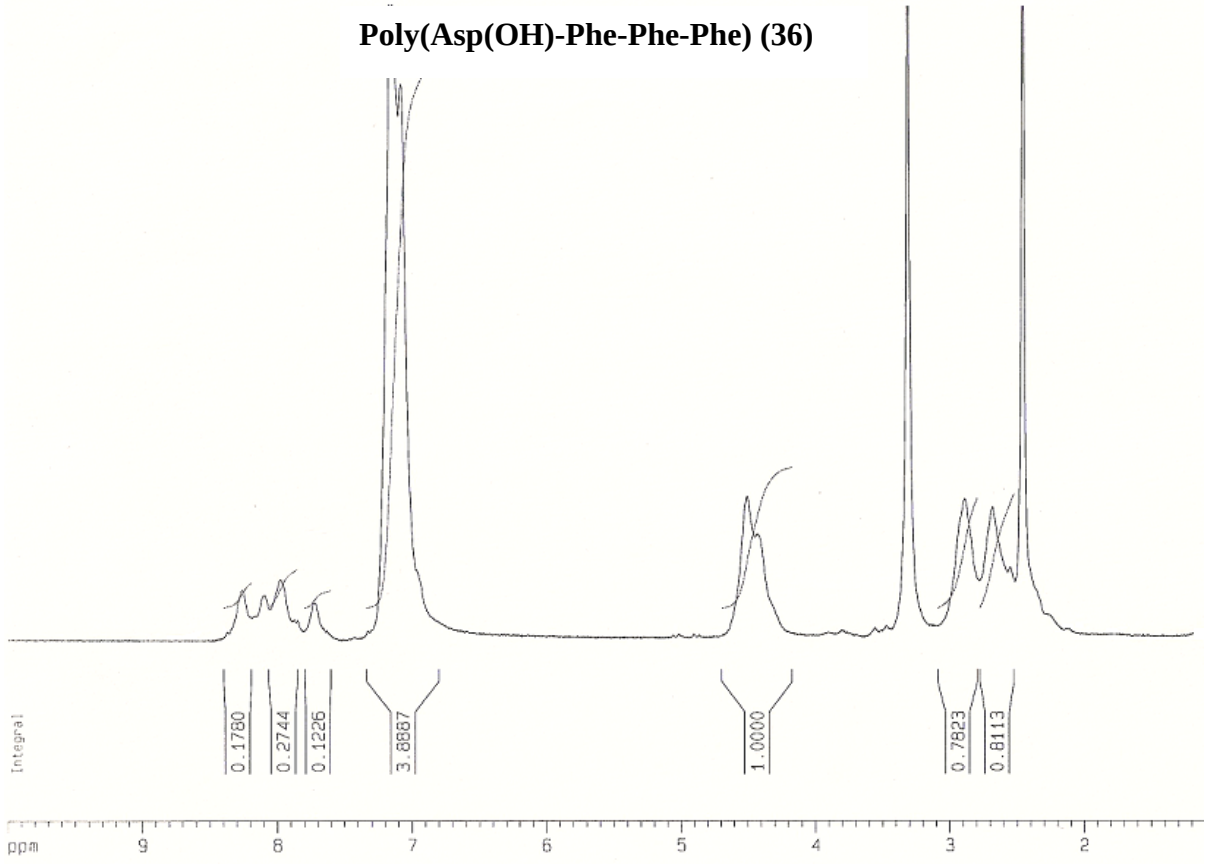

H-Asp(OBzl)-Phe-Asp(OBzl)-Phe-OSu.CF_3COOH

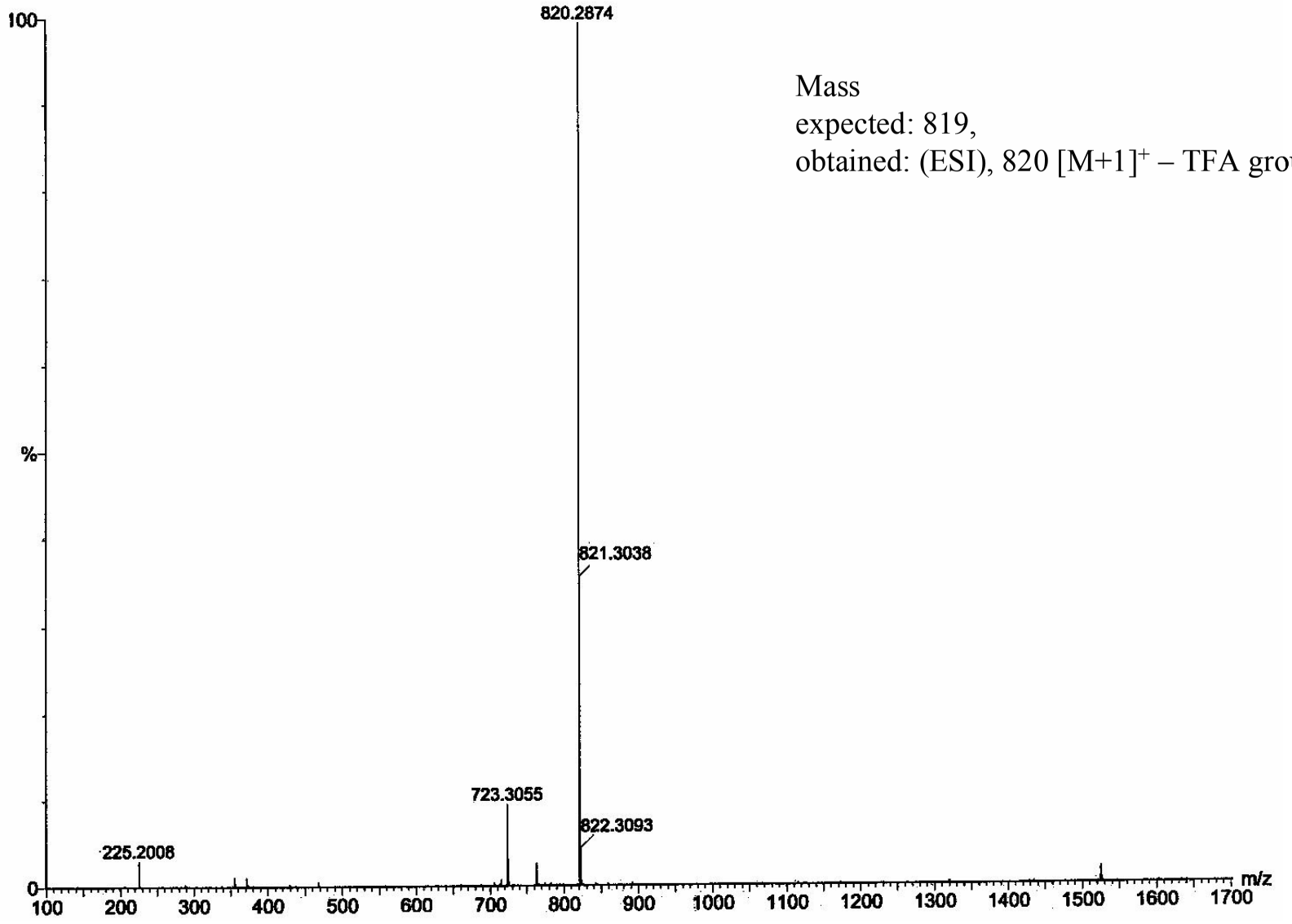

Mass
expected: 819,
obtained: (ESI), 820 $[M+1]^+$ – TFA group

H-Asp(OBzl)-Asp(OBzl)-Asp(OBzl)-Phe-OSu.CF_3COOH

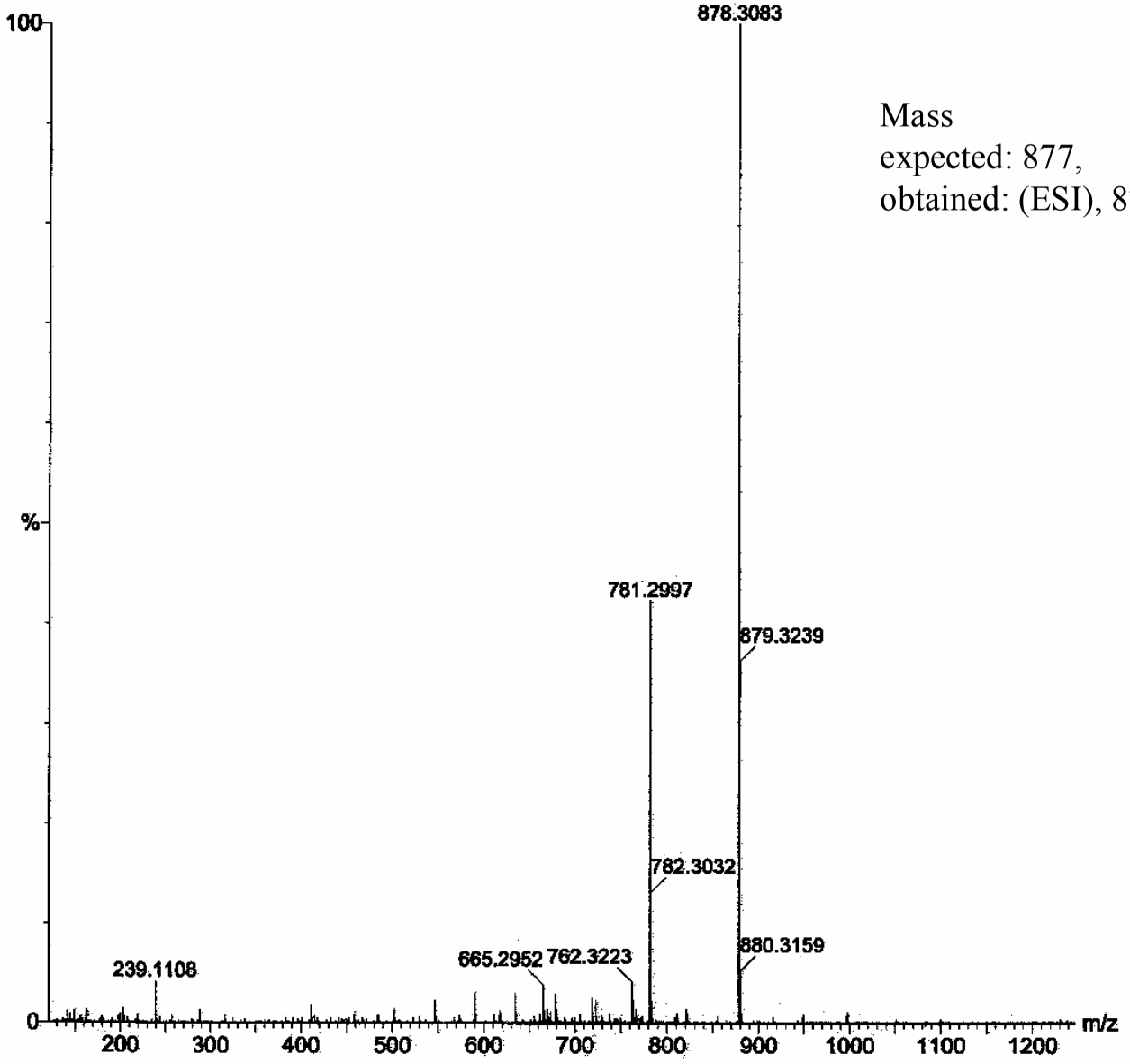

Mass
expected: 877,
obtained: (ESI), 878 $[M+1]^+$ – TFA group

H-Asp(OBzl)-Asp(OBzl)-Phe-OSu.CF_3COOH

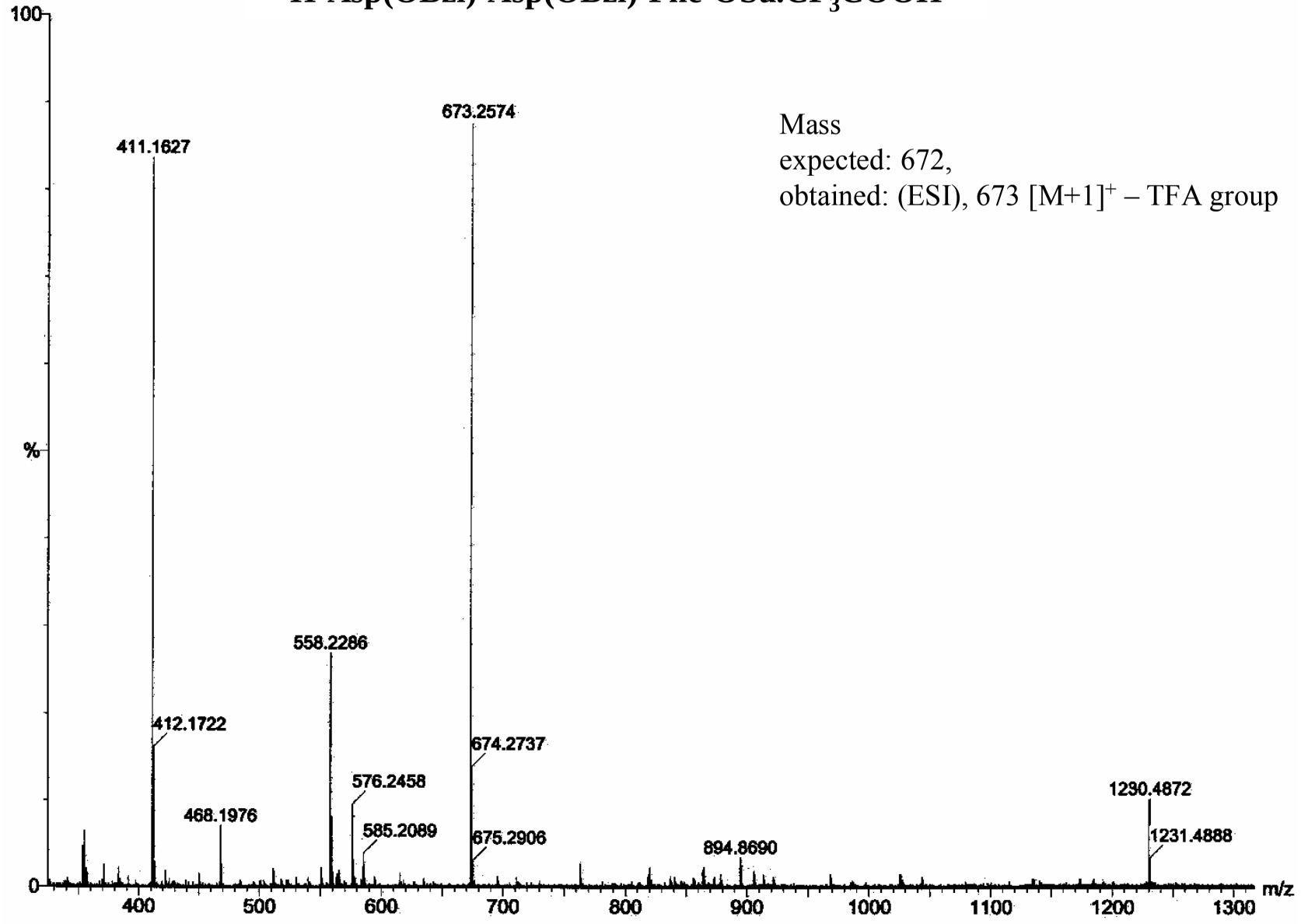

Mass
expected: 672,
obtained: (ESI), 673 $[M+1]^+$ – TFA group

H-Asp(OBzl)-Phe-Phe-OSu.CF_3COOH

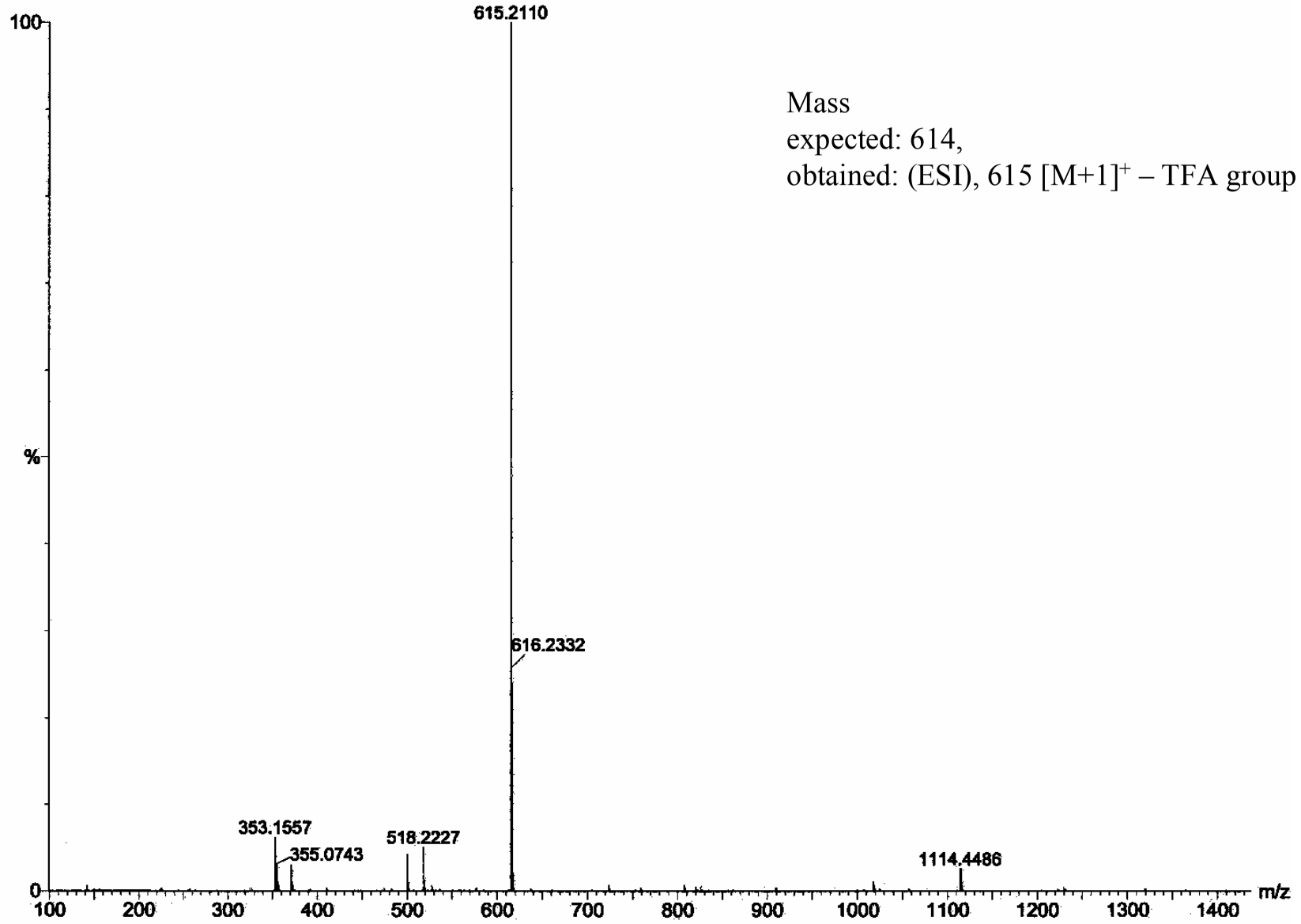

Mass
expected: 614,
obtained: (ESI), 615 $[M+1]^+$ – TFA group

H-Asp(OBzl)-Phe-Phe-Phe-OSu.CF_3COOH

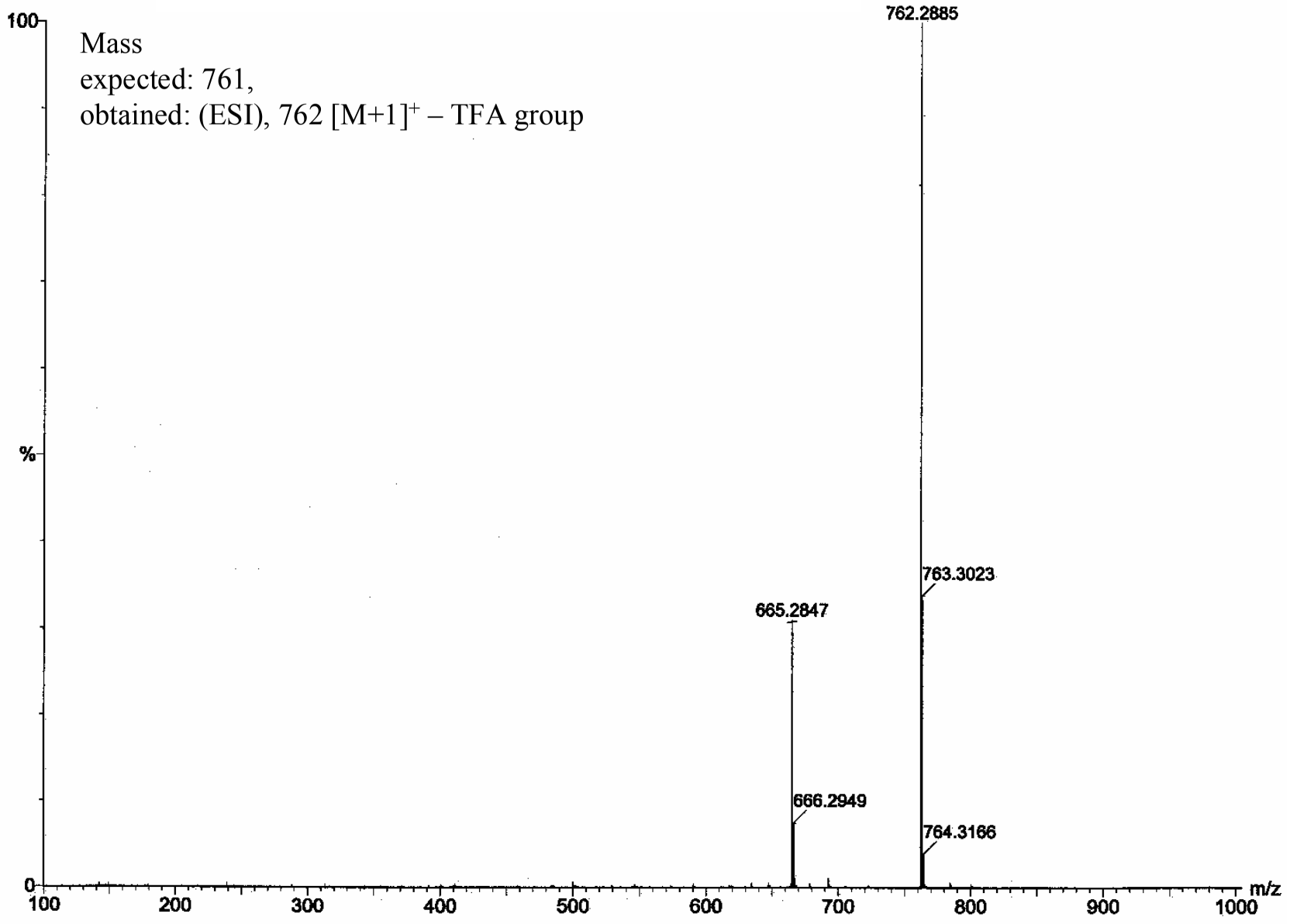

Chapter 3
Characterization of the Polypeptides
Photophysical Properties

3.1. Abstract

Five polypeptides were synthesized and their photophysical properties in solution were studied. These polypeptides had a well-defined repeating sequence and their composition was $(Asp_xPhe_y)_n$ with all combinations of x=1-3 and y=1 or x=1 and y=1-3. All experiments aiming at characterizing the photophysical properties of the polypeptides were carried out at pH 9.0 to ensure that they would be fully ionized. The photophysical properties of the polypeptides were found to depend on their phenylalanine (Phe) content. Increasing the Phe content led to a linear increase of the extinction coefficient, fluorescence emission intensity, and fluorescence average lifetime of the polypeptides. The fine structure of the fluorescence spectra of Phe is lost for the polypeptides, and the emission is shifted to higher wavelength suggesting the formation of Phe excimer or ground-state dimers. Circular dichroism spectra suggest that all polypeptides except $(Asp_1Phe_3)_n$ did not adopt any known structure in solution. On the other hand, $(Asp_1Phe_3)_n$ was found to be an α–helix in solution.

3.2. Introduction

Hydrophobically modified water-soluble polymers (HMWSPs) can generate hydrophobic microdomains in aqueous solution which can host hydrophobic drugs. For this reason, their use as drug delivery systems (DDSs) has been under intense scrutiny,[1-5] contributing another chapter to the use of polymers in drug delivery applications and leading some to suggest that present times are *The Dawning Era of Polymer Therapeutics*.[6] In the majority of cases, block copolymer-type HMWSPs have been considered for DDSs.[1,2,5,7] Block copolymers used for DDS consist of a hydrophilic and hydrophobic block joined together at one end. These block copolymers self-assemble into polymeric micelles[1,2,5,7] or vesicles[8] whose hydrophobic core is stabilized by the hydrophilic corona. Poly(ethylene oxide) (PEO) is the hydrophilic block of choice because of its high water-solubility, low toxicity, and "stealth" properties towards the reticuloendothelial system.[1] Poly(benzyl-L-aspartate) or poly(caprolactone) are examples of apolar polymers used as the hydrophobic block. A water-soluble block copolymer made of a PEO and poly(glutamic acid) (PGA) has also been modified into a HMWSP by attaching a hydrophobic drug such as doxorubicin onto the PGA moiety which induces PGA to turn hydrophobic upon sufficient drug attachment.[9] The modified PEO-*b*-PGA block copolymer can then self-assemble into block copolymer micelles where the hydrophobic core hosts the drug and the assembly is stabilized by the PEO chain.

HMWSPs where the hydrophobes are distributed throughout the polymer backbone are much less common examples of HMWSPs studied for drug delivery applications. The final structure of these copolymers falls into two main categories depending on the level of control achieved over the distribution of the hydrophobes along the chain. Random

incorporation of the hydrophobes along the chain can be achieved by covalently linking a hydrophobic pendant onto a water-soluble polymer substrate[10,11] or random copolymerization of a hydrophobic monomer with a hydrophilic monomer.[12,13] Incorporation of a hydrophobe at specific positions along the backbone, say every 3 monomer units, can only be achieved with polypeptides. Such polypeptides can be synthesized chemically by preparing a well-defined peptide sequence of a few amino acids which is then polymerized,[14,15] or via DNA recombinant technology.[16,17]

The ability of alternating styrene-maleic anhydride copolymers (SMA) to form small micelles ~2 nm in diameter that host large amounts of hydrophobic molecules and deliver them in a controlled manner by adjusting the ionization level of the polymer[18] triggered the interest of this laboratory to search for biocompatible SMA analogs that might be used for drug delivery applications. Alternating SMAs fall into the family of HMWSPs where the hydrophobes are distributed in a controlled manner along the chain. The requirement of biocompatibility combined with the alternating structure and chemical motives of SMAs led to the synthesis of polypeptides made of phenylalanine (Phe) and aspartic acid (Asp). The benzene ring of Phe and the acid functionality of Asp were expected to mimic the structural motives of the styrene and maleic acid monomers found in SMA, respectively. In these polypeptides, Phe and Asp play the part of the hydrophobic and hydrophilic monomers, respectively. To adjust the hydrophobic-to-hydrophilic ratio, five polypeptides were synthesized where the Phe content was increased according to the composition sequence $(Asp_3Phe_1)_n$, $(Asp_2Phe_1)_n$, $(Asp_1Phe_1)_n$, $(Asp_1Phe_2)_n$, and $(Asp_1Phe_3)_n$. This report describes the solution properties of the $(Asp_xPhe_y)_n$ polypeptides. Their associative properties are presented in Chapters 4 and 5.

3.3. Experimental

Reagents. Poly(aspartic acid) was purchased from Sigma-Aldrich with a M_w of 24 kg.mol^{-1}. NaOH (BDH) and HCl (reagent ACS grade) were supplied by Fischer and sodium carbonate anhydrous (ACS grade) was obtained from EMD. Milli-Q water with a resistivity of over 18 MΩ.cm was used to make all the aqueous solutions. Spectra/Por® 7 regenerated cellulose dialysis membranes having a cut-off value of 3,500 g/mol were used for dialysis.

Preparation of the polypeptide aqueous solutions. All polypeptide solutions were prepared in a 0.01 M Na_2CO_3 solution at pH 9. Due to the poor solubility of the polypeptides in aqueous solution, the samples could not be prepared by directly dissolving the polypeptides into the 0.01 M Na_2CO_3 solution at pH 9. Therefore, all aqueous solutions of the polypeptides were prepared according to the following protocol.[19] A known amount of the polypeptide (~ 50 mg) was dissolved in 10 mL of DMF. To this an aqueous solution of 0.1 M NaOH was added at a rate of one drop every 4 s with vigorous stirring. The solution turned cloudy as the polypeptide precipitated into stable aggregates. The addition of the NaOH solution was continued until the solution contained 30 wt% of the NaOH solution. The NaOH solution was used to ensure that all aspartic acids in the polypeptide were ionized. The resulting solution was dialyzed against a solution of 0.01 M Na_2CO_3 at pH 9 for 2 days. The 0.01 M Na_2CO_3 solution at pH 9 was renewed every 8 hours to remove the DMF.

UV-Vis absorption. All UV-Vis absorption spectra were obtained with a Hewlett Packard 8452A diode array spectrophotometer using a spectrometer cell with a 1 cm path length. The spectrophotometer measures the absorption as a function of wavelength with 2 nm increments.

Massic extinction coefficients of polypeptides. To determine the actual polypeptide concentration in the 0.01 M Na_2CO_3 aqueous solution at pH 9 prepared through dialysis, the massic extinction coefficient of the polypeptides was determined. The concentration of a polypeptide stock solution was determined by weighing three aliquots of the polypeptide stock solution and three similar aliquots of the 0.01 M Na_2CO_3 solution at pH 9. These samples were dried under a gentle flow of nitrogen. To remove any residual traces of water, the vials were left overnight in a vacuum oven at 60 ^{o}C. The vials were weighed and the average masses of the dried samples were obtained. The concentration of the polypeptide solution was determined by taking the difference between the solid contents of the polypeptide solution and that of the Na_2CO_3 solution.

Several samples were prepared by diluting the polypeptide stock solution of known concentration in g/L and their absorption spectrum was obtained. These spectra were baseline corrected for light scattering. The part of the absorption spectrum where Phe did not absorb (284-500 nm) was fitted with a quadratic polynomial equation which was substracted from the polypeptide UV-Vis spectrum. The massic extinction coefficient of each polypeptide expressed in $g^{-1}.L.cm^{-1}$ was retrieved from the slope of the straight line drawn by plotting the absorption at 260 nm versus the polypeptide concentration. These were then used to determine the concentration of any new polypeptide solutions prepared through dialysis.

Circular dichroism. CD spectra were acquired on a J 715 CD spectropolarimeter (Jasco) at 25 ^{o}C with a 0.1 cm path length cell, a 100 nm/min scan rate, and a 2 nm bandwidth. Spectra were an average of 10 scans from 190 to 250 nm.

Static light scattering. The absolute weight-average molecular weight, M_w, of the five polypeptides was determined using static light scattering. The refractive index increments

(*dn/dc*) were measured at room temperature using a Brice-Phoenix differential refractometer equipped with a 510 nm band-pass interference filter. A Brookhaven BI-200 SM light scattering goniometer equipped with a Lexel 2 W argon ion laser operating at 514.5 nm was used for the static light scattering measurements. All light scattering experiments were done in DMF except for $(Asp_3Phe_1)_n$ for which acetone was used. The SLS tubes (VWR) were flamed beforehand to remove eventual scratches in the glass and then washed for 30 minutes in an acetone fountain to remove dust. The weight-average molecular weight was determined by Zimm extrapolation to zero angle and zero concentration for a series of measurements for 8-9 solutions between 0.5 and 5.0 g/L at angles ranging from 45° to 145°. The samples were filtered through 0.45 μm Teflon filters prior to light scattering measurements. Table 3.1 lists the *dn/dc* values used to obtain the M_w, and the second virial coefficients, A_2, of the polypeptides by static light scattering.

Table 3.1. Values for *dn/dc*, M_w, and A_2 obtained for the polypeptides. All *SLS* experiments were done in DMF except for $(Asp_3Phe_1)_n$ where acetone was used.

Polypeptide	*dn*/*dc* mL.g^{-1}	M_w g/mol	A_2 cm^3 mol/gm^2
$(Asp_3Phe_1)_n$	0.142	8,500	0.0116
$(Asp_2Phe_1)_n$	0.119	9,500	-0.00441
$(Asp_1Phe_1)_n$	0.117	11,400	0.00711
$(Asp_1Phe_2)_n$	0.124	10,200	0.00779
$(Asp_1Phe_3)_n$	0.144	8,300	0.0119

Steady-state fluorescence measurements. The steady-state fluorescence spectra were obtained using a Photon Technology International LS-100 steady-state fluorometer with a continuous

xenon lamp. A fluorescence cell (VWR) with an inner cross section of 10×10 mm^2 was used in the right angle geometry and the samples were not deoxygenated. The emission spectra were acquired by exciting the polypeptide solutions at 245 nm.

Time-resolved fluorescence measurements. The fluorescence decay profiles were obtained by a time-correlated single photon counter manufactured by IBH Ltd. using a 5000F coaxial nanosecond flash lamp filled with H_2 gas. Samples were excited at 245 nm and the emission wavelength was set at 290 nm. The samples were placed in a 10×10 mm^2 fluorescence cell (VWR). All decays were collected with the right angle geometry over 200-800 channels with a minimum of 20,000 counts taken at the decay maximum to ensure a high signal-to-noise ratio. A light scattering standard was used for the lamp profile. Analysis of the decays was performed by convoluting the lamp profile with a sum of typically 3 exponentials (Equation 3.1) and comparing the convolution result with the experimental decay.

$$i_x(t) = a_1\exp(-t/\tau_1) + a_2\exp(-t/\tau_2) + a_3\exp(-t/\tau_3) \quad (3.1)$$

The parameters in Equation 3.1 were optimized using the Marquardt-Levenberg algorithm. The quality of the fits was established from the χ^2 values (<1.30) and the random distribution around zero of the residuals and of the autocorrelation function of the residuals.

3.4. Results and Discussion

The synthesis of the polypeptides was described in Chapter 2. It involves the elongation of an oligopeptide made of n ($n \geq 1$) amino acids (aa_n) by one amino acid (*a.a.*) at the time according to the following sequence of synthetic steps: 1) activation with

hydroxysuccinimide of one *a.a.* protected at the *N*-terminal with a *t*-BOC group, 2) coupling of the activated *a.a.* with aa_n to yield an oligopeptide of length $n + 1$ (aa_{n+1}), and 3) deprotection of the *N*-terminal of aa_{n+1}. The oligopeptide aa_{n+1} can then be extended by another *a.a.* by iterating steps 1-3. Polymerization of the oligopeptide activated with hydroxysuccinimide was conducted over several days yielding polypeptides with M_w in the 8-12 kg.mol^{-1} range (Table 3.1). These M_w values were determined by static light scattering with polypeptide solutions in DMF, except for $(Asp_3Phe_1)_n$ which was studied in acetone.

The solution behavior of weak polyelectrolytes or polyacids such as the polypeptides, poly(L-glutamic acid), poly(L-aspartic acid) is controlled by the solution pH.[20] Polyacids dissociate over a limited pH range.[21] As a result, the total charge of the chain can be tuned by adjusting the pH of the solution. In turn, this effect leads to an inhomogeneous charge distribution along the backbone. The chain ends are predicted to bear a larger charge than the center of the macromolecule because the monomer density being lower towards the ends is less disfavorable from an energy point of view.[21] As the charge density evolves with pH, so does the conformation of the polyacid. In the case where the polyacid contains some hydrophobic monomers such as the $(Asp_xPhe_y)_n$ polypeptides, the following sequence of conformations is expected as a function of pH.[22] When the backbone exhibits few charges, the polymer coil is a collapsed globule. As more charges are added onto the backbone, the polymer adopts a pearl-necklace conformation where collapsed neutral stretches of the polyelectrolyte are separated by stretches of charged monomers. When the polyelectrolyte is fully charged and if the electrostatic repulsion overcomes the van der Waals associations between the hydrophobic monomers, the polyacid adopts a stretched rod-like conformation. In view of this, all experiments were performed at pH 9 to ensure that the polypeptides of

$(Asp_xPhe_y)_n$ series would be all in the same fully ionized conditions.[20]

Although the small extinction coefficient (ε_{Phe} = 200 $M^{-1}.cm^{-1}$ at 258 nm)[23,24] and low quantum yield ($\phi_F(Phe)$ = 0.04)[24] of Phe make it almost impossible to detect by fluorescence in proteins that contain other aromatic amino acids,[25] the large Phe content of the $(Asp_xPhe_y)_n$ polypeptides implies that their photophysical properties reflect those of the Phe residues. Consequently the absorption and fluorescence of $(Asp_xPhe_y)_n$ solutions were characterized. The absorption spectra of polypeptides in 0.01 M Na_2CO_3 solution at pH 9 were acquired for 10 polypeptide concentrations ranging from 0.1 to 1.2 g/L. Typical absorption spectra of the polypeptide solutions are shown in Figure 3.1 for a polypeptide concentration of 0.5 g/L. As the Phe content of the polypeptide increases, so does its absorption. This result is reasonable since the Phe monomer absorbs at 260 nm, but not the Asp residue. Interestingly, the general features of the absorption spectrum of Phe are also observed for the polypeptides, but shifted by about 2 nm (also the resolution of the spectrophotometer). Phe exhibits absorption maxima at 252, 258, and 264 nm whereas the polypeptide solutions have absorption maxima at 254, 260, and 266 nm. At wavelengths smaller than 245 nm, the amides of the polypeptide backbone absorb strongly and dominate the absorption.

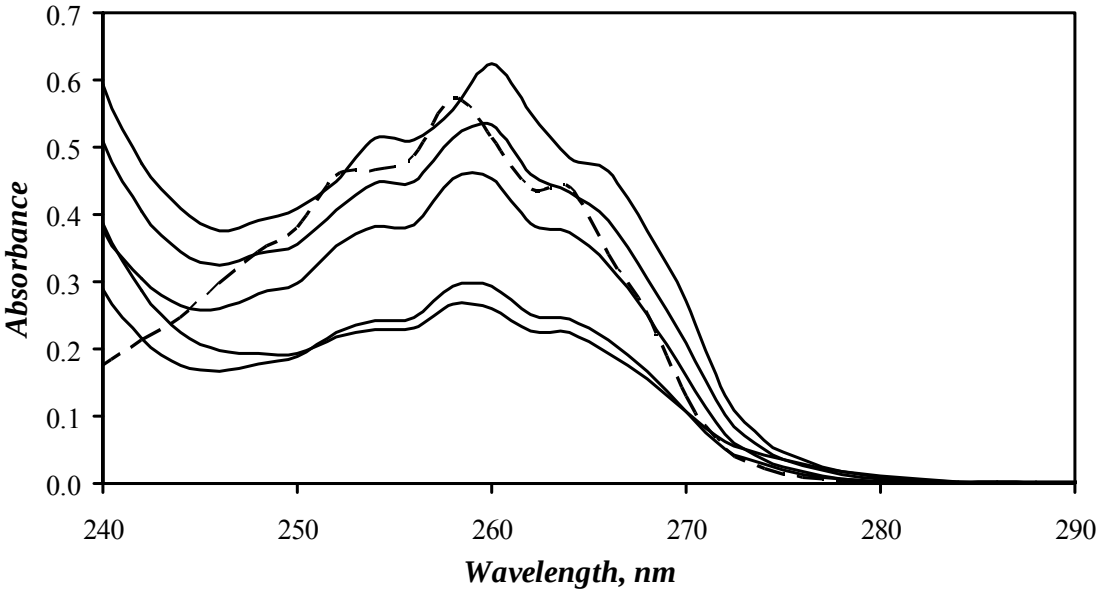

Figure 3.1. Absorption spectra of the 0.05 g/L polypeptide solutions in 0.01 M Na_2CO_3 solution at pH 9. Solid lines from bottom to top: $(Asp_3Phe_1)_n$, $(Asp_2Phe_1)_n$, $(Asp_1Phe_1)_n$, $(Asp_1Phe_2)_n$, and $(Asp_1Phe_3)_n$. Dashed line is for L-phenylalanine monomer ([*Phe*] = 2.8×10^{-3} mol.L^{-1}).

A plot of the absorption at 260 nm as a function of polypeptide concentration in g.L^{-1} for a given polypeptide resulted in a straight line passing through the origin. The slope of this straight line yielded the massic extinction coefficient of the polypeptides, ε_m, expressed in L.g^{-1}.cm^{-1}. As the Phe content of the polypeptide increased in the sequence $(Asp_3Phe_1)_n$, $(Asp_2Phe_1)_n$, $(Asp_1Phe_1)_n$, $(Asp_1Phe_2)_n$, and $(Asp_1Phe_3)_n$, ε_m increased taking values of 0.52, 0.59, 0.91, 1.07, and 1.25 g.L^{-1}, respectively. If x represents the mole fraction of Phe in the polypeptide, the relationship given in Equation 3.2 is expected to hold between the massic, ε_m, and molar, ε_M, extinction coefficients.

$$\varepsilon_m = \frac{x}{M_{Phe}\times x + M_{Asp}\times(1-x)}\times\varepsilon_M = \xi\times\varepsilon_M \qquad (3.2)$$

In Equation 3.2, ξ represents the Phe content of the polypeptides expressed in moles of Phe per grams of polypeptide. A plot of ε_m as a function of ξ is shown in Figure 3.2. A straight line is obtained whose slope yields the molar extinction coefficient equal to 230 ± 15 $L.mol^{-1}.cm^{-1}$. This extinction coefficient is in the range expected for Phe found to equal 202 $L.mol^{-1}.cm^{-1}$ in a 0.1 M NaCl solution.[23] The difference in extinction coefficient might be due to the presence of ground-state Phe dimers in the polypeptide aqueous solutions induced by the high local concentration of hydrophobic Phe residues. The ε_M value of 230 ± 15 $L.mol^{-1}.cm^{-1}$ agrees with that of 224 $L.mol^{-1}.cm^{-1}$ found for random copolymers of Phe and Glu.[13]

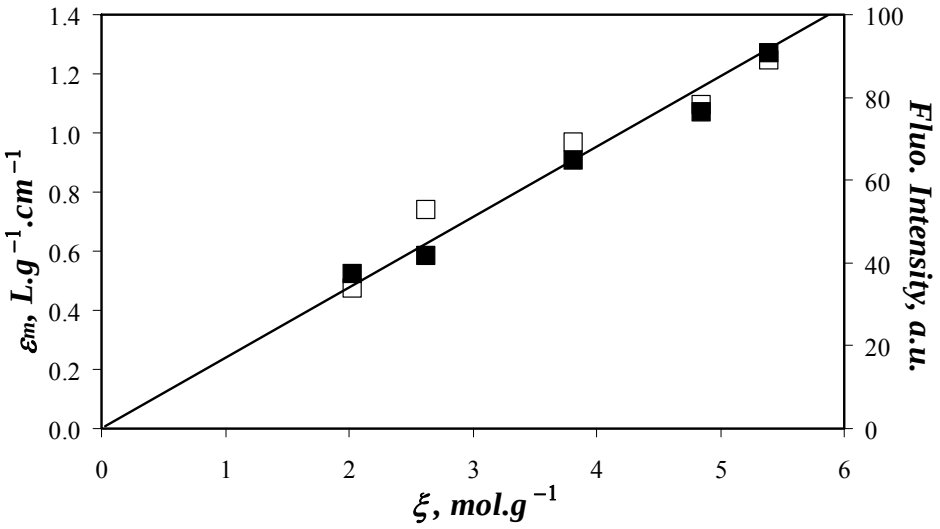

Figure 3.2. Massic extinction coefficient, ε_m, (■, left) and fluorescence intensity (□, right) of the polypeptides as a function of phenylalanine content, ξ.

Although the polypeptide solutions absorb most strongly at 260 nm, the fluorescence spectra and decays were acquired by exciting the solutions at 245 nm. This absorption wavelength was selected to minimize light scattering leaking into the fluorescence signal through the slits of the monochromator when the solutions were excited at 260 nm. The

fluorescence spectra are shown in Figure 3.3 for 0.05 g/L polypeptide samples in 0.01 M Na_2CO_3 solution at pH 9. The low polypeptide concentration ensured that the inner filter effect could be neglected (OD < 0.07).

The data shown in Figure 3.3 indicate that as the Phe content of the polypeptide increases, so does the fluorescence intensity at 290 nm. The fluorescence spectra of the polypeptides have lost the fine resolution of the fluorescence spectrum of Phe with peaks at 275, 281, and 288 nm. They also appear to have shifted to higher wavelengths with a maximum around 290 nm compared to 281 nm for Phe. At wavelengths larger than 340 nm where Phe does not emit, all polypeptides emit. These observations suggest that a Phe excimer or ground-state dimer is present in solution. The excimer of an aromatic molecule emits usually at wavelengths longer than those of the monomer fluorescence.[26]

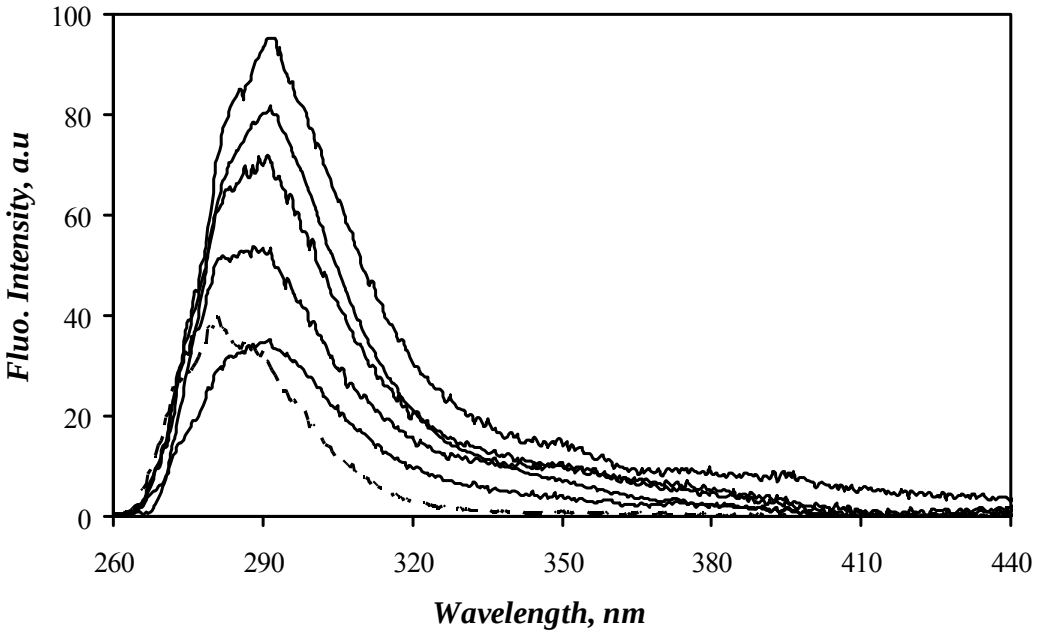

Figure 3.3. Solid lines: fluorescence spectra of 0.05 g/L polypeptide solutions in 0.01 M Na_2CO_3 solution at pH 9. From bottom to top: $(Asp_3Phe_1)_n$, $(Asp_2Phe_1)_n$, $(Asp_1Phe_1)_n$, $(Asp_1Phe_2)_n$, and $(Asp_1Phe_3)_n$. Dashed line is for L-phenylalanine ([*Phe*] = 2.8×10^{-3} mol.L^{-1}). λ_{ex} = 245 nm.

The intensity of the polypeptide fluorescence spectra shown in Figure 3.3 was integrated over 287-289 nm. If the increase in the fluorescence intensity, I_F, is the result of the increased Phe content, then I_F is expected to increase linearly with the molar concentration of Phe. If m is the polypeptide concentration in g/L, then I_F should be proportional to [*Phe*] in mol.L^{-1} with a proportionality constant α according to Equation 3.3:

$$I_F = \alpha \times [Phe] = \alpha \times m \times \frac{x}{M_{Phe} \times x + M_{Asp} \times (1-x)} = \alpha \times m \times \xi \qquad (3.3)$$

ξ is the Phe content of the polypeptide expressed in mol.g^{-1}. A plot of I_F versus ξ is given in Figure 3.2. According to Figure 3.2, both the extinction coefficient and the fluorescence intensity of the polypeptides increase linearly with the Phe content of the polypeptides.

The fluorescence decays of 0.5 g/L polypeptide samples in 0.01 M Na_2CO_3 solution at pH 9 were acquired using excitation and emission wavelengths of 245 and 290 nm, respectively. The decays of $(Asp_3Phe_1)_n$, $(Asp_2Phe_1)_n$, $(Asp_1Phe_1)_n$, $(Asp_1Phe_2)_n$, and Phe are shown in Figure 3.4. The inset of Figure 3.4 shows the decays of $(Asp_1Phe_1)_n$, $(Asp_1Phe_2)_n$, and $(Asp_1Phe_3)_n$. Phe in 0.01 M Na_2CO_3 solution at pH 9 exhibits a biexponential decay with a number-average lifetime of 4.8 ns. Phe is shorter-lived than any of the polypeptides. All polypeptides display a multiexponential decay which required three exponentials to fit. The decay times, pre-exponential factors, and χ^2 obtained from the analysis of the decays are listed in Table 3.2. The early part of the polypeptide decay is similar to that of Phe suggesting that some Phe monomers remain isolated on the polypeptide. However the fluorescence decays of all polypeptides indicate that a longer-lived species is present in

solution, and that the contribution of that species increases with Phe content up to $(Asp_1Phe_2)_n$. (Asp_1Phe_3) exhibits a fluorescence decay which is slightly shorter-lived than $(Asp_1Phe_2)_n$ (see inset in Figure 3.4), but still longer-lived than $(Asp_1Phe_1)_n$ and the polypeptides with a smaller Phe content. This longer-lived species is attributed to the presence of a Phe excimer or ground-state dimer.

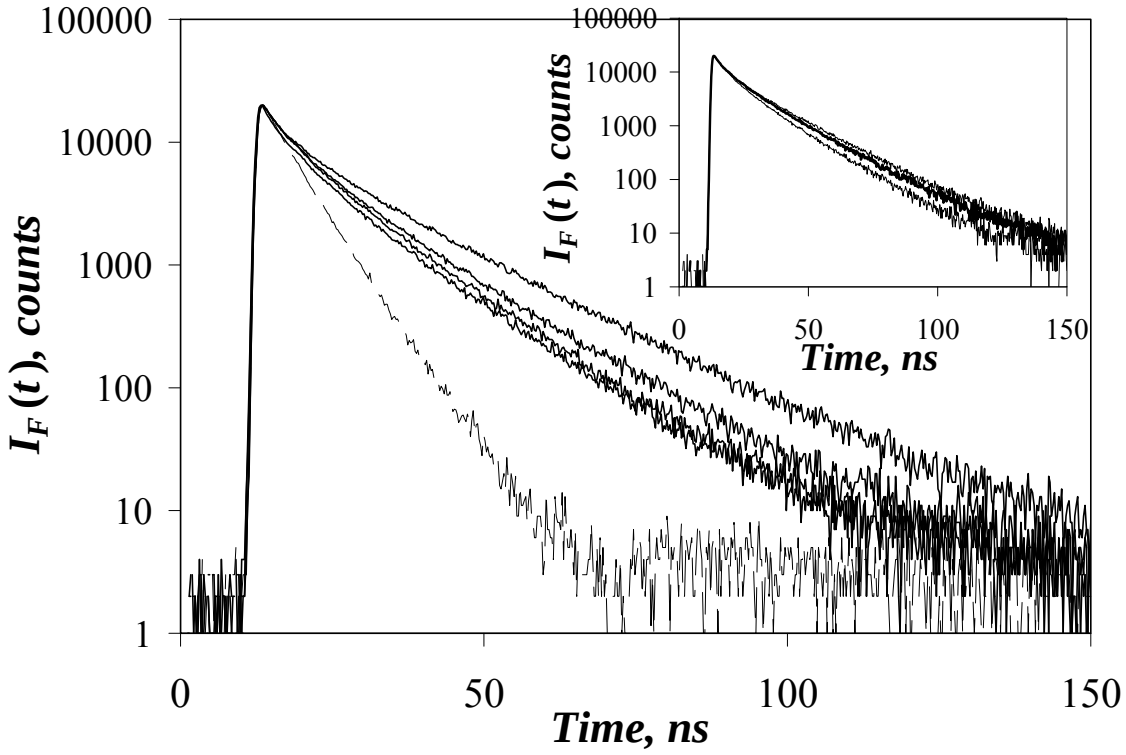

Figure 3.4. Solid lines: Fluorescence decays of 0.5 g/L polypeptide solutions in 0.01 M Na_2CO_3 solution at pH 9. From bottom to top: $(Asp_3Phe_1)_n$, $(Asp_2Phe_1)_n$, $(Asp_1Phe_1)_n$, and $(Asp_1Phe_2)_n$. Dashed line is for L-phenylalanine ([*Phe*] = 2.8×10^{-3} mol.L^{-1}). Inset: From bottom to top: Fluorescence decays of $(Asp_1Phe_1)_n$, $(Asp_1Phe_3)_n$, and $(Asp_1Phe_2)_n$. λ_{ex} = 245 nm.

Table 3.2. Pre-exponential factors, decaytimes, and χ^2 values obtained from the fit of the fluorescence decays with Equation 3.1.

Sample	τ_1 (ns)	a_1	τ_2 (ns)	a_2	τ_3 (ns)	a_3	$<\tau_0>$ (ns)	χ^2
L-Phe	2.6	0.29	5.8	0.71	–	–	4.8	1.20
$(Asp_3Phe_1)_n$	1.0	0.32	5.6	0.39	13.2	0.28	6.2	1.06
$(Asp_2Phe_1)_n$	1.4	0.23	5.6	0.41	13.1	0.36	7.3	1.16
$(Asp_1Phe_1)_n$	1.5	0.26	6.0	0.42	14.8	0.33	7.8	1.16
$(Asp_1Phe_2)_n$	1.5	0.32	6.4	0.32	17.6	0.36	8.8	1.30
$(Asp_1Phe_3)_n$	1.8	0.27	7.2	0.38	16.9	0.34	9.0	1.20

A plot of the number-average lifetime of the polypeptides, $<\tau>$, versus Phe content is shown in Figure 3.5. As expected from Figure 3.4, $<\tau>$ increases with increasing ξ. It intercepts the Y-axis at a $<\tau>$ value of 4.8 ± 0.3 ns. This value is the number-average lifetime of the Phe monomer found to equal 4.8 ns. As expected, the polypeptides with lower Phe content reflect the behavior of the Phe monomer.

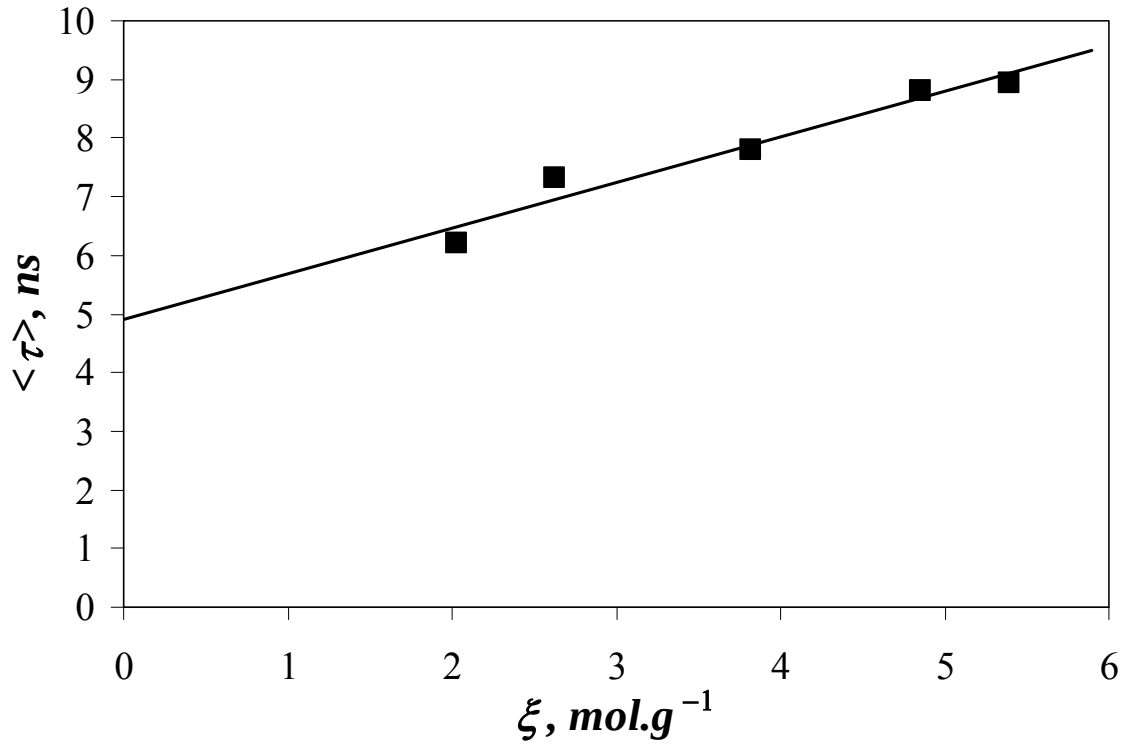

Figure 3.5. Number-average lifetime of the polypeptides in 0.01 M Na_2CO_3 solution at pH 9 as a function of Phe content.

The CD spectra of the polypeptide solutions were acquired from 195 to 250 nm. The CD spectra of the $(Asp_3Phe_1)_n$, $(Asp_2Phe_1)_n$, $(Asp_1Phe_1)_n$, $(Asp_1Phe_2)_n$ polypeptides did not yield any of the characteristic features of a β–sheet (minimum at 220 nm)[27] or α–helix (minima at 208 and 222 nm, maximum at 192 nm).[28] They did not exhibit the features of a random coil conformation (small maximum at 215 nm, minimum at 197 nm).[27] At this stage, the structure of these polypeptides in solution remains unknown. On the other hand, the CD spectrum of $(Asp_1Phe_3)_n$ displays the features of an α–helix with minima at 205 and 217 nm. Poly(aspartic acid) which should adopt a random coil conformation at pH 9[20] had a minimum at 203 nm.

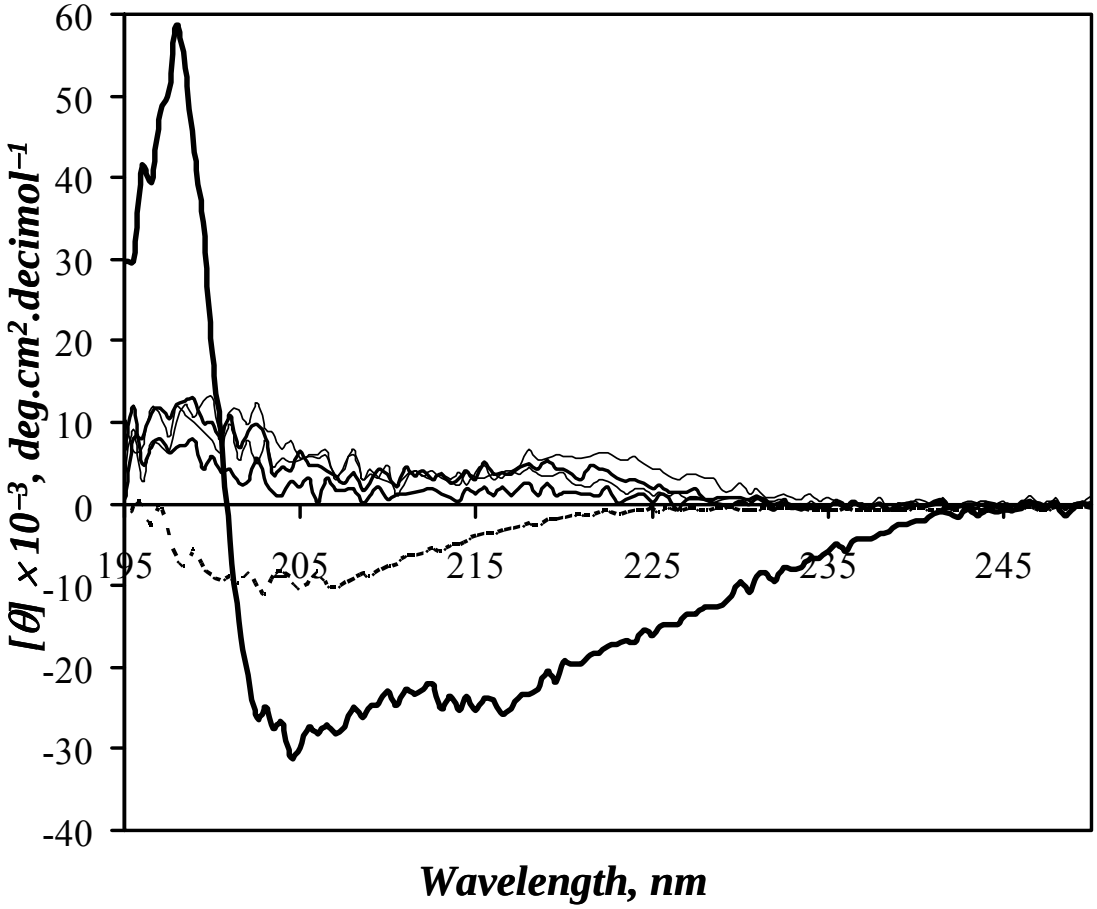

Figure 3.6. Circular dichroism spectra of the polypeptides in 0.01 M Na_2CO_3 solution at pH 9. Thin solid lines: $(Asp_3Phe_1)_n$, $(Asp_2Phe_1)_n$, $(Asp_1Phe_1)_n$, $(Asp_1Phe_2)_n$. Thick solid line: $(Asp_1Phe_3)_n$. Dashed line: Poly(Asp).

Whereas contiguous stretches of Phe induce α–helix formation,[29-31] poly(Asp) adopts a random coil conformation in basic aqueous solution.[20] The incorporation of Phe and Asp inside a same polypeptide provides a means to compare the strength of Phe to induce α–helix formation against the strength of Asp to induce a random coil formation. According to the CD spectra shown in Figure 3.6, a Phe to Asp ratio of 3:1 is necessary to induce α–helix formation. Lower Phe:Asp ratios result in CD responses which demonstrate the absence of

α–helix. The study of polypeptides having a larger Phe:Asp ratio is complicated by the increased hydrophobicity of the polypeptide which limits its solubility in aqueous solution.

3.5. Conclusions

The synthesis (in Chapter 2) and the solution properties of a series of polypeptides have been presented. The polypeptides consist of well defined repeating sequences of Phe and Asp with Phe:Asp ratios of 0.33, 0.5, 1.0, 2.0, and 3.0. Phe being hydrophobic and Asp being hydrophilic in basic aqueous solutions, these polypeptides are amphiphilic polymers and their associative properties in basic aqueous solutions will be described in Chapters 4 and 5. In Chapter 3, the photophysical properties of the polypeptides were investigated. They were found to depend strongly on the Phe content of the polypeptide. Molar extinction coefficient (Figure 3.2), fluorescence emission intensity (Figure 3.2), and fluorescence average lifetime (Figure 3.5) increased linearly with the Phe content of the polypeptides. The fluorescence spectra of the polypeptides were shifted to the red when compared to the fluorescence spectrum of Phe. The polypeptides were longer-lived than Phe. These observations suggest that the high local Phe concentration inside the polypeptide coils induces the formation of Phe ground-state dimers. CD was used to infer the conformation adopted by the polypeptides. For Phe:Asp ratios lower than 3, the polypeptides displayed no defined structure. The polypeptide with a Phe:Asp ratio of 3.0 was found to form an α–helix.

3.6. References:

1. Kwon, G. S.; Okano, T. *Adv*. *Drug Deliv*. *Rev*. **1996**, *21*, 107-116.
2. Kataoka, K.; Harada, A.; Nagasaki, Y. *Adv*. *Drug Deliv*. *Rev*. **2001**, *47*, 113-131.
3. Kopeček, J. *Eur*. *J*. *Pharma*. *Sci*. **2003**, *20*, 1-16.
4. Haag, R. *Angew*. *Chem*. *Int*. *Ed*. **2004**, *43*, 278-282.
5. Vonarbourg, A.; Passirani, C.; Saulnier, P.; Benoit, J.-P. *Biomaterials* **2006**, *27*, 4356-4373.
6. Duncan, R. *Nature Rev*. **2003**, *2*, 347-360.
7. Deming, T. J. *Adv*. *Drug Deliv*. *Rev*. **2002**, *54*, 1145-1155.
8. Discher, D. E.; Eisenberg, A. *Science* **2002**, *297*, 967-973.
9. Yokoyama, M.; Miyauchi, M.; Yamada, N.; Okano, T.; Sakurai, Y.; Kataoka, K.; Inoue, S. *J*. *Control*. *Rel*. **1990**, *11*, 269-278.
10. Francis, M. F.; Cristea, M.; Winnik, F. M. *Pure Appl*. *Chem*. **2004**, *76*, 1321-1335.
11. Matsusaki, M.; Hiwatari, K.-I.; Higashi, M.; Kaneko, T.; Akashi, M. *Chem*. *Lett*. **2004**, *33*, 398-399.
12. Sage, H. J.; Fasman, G. D. *Biochemistry* **1966**, *5*, 286-296.
13. Auer, H. E.; Doty, P. *Biochemistry* **1966**, *5*, 1708-1715.
14. DeTar, D. F.; Vajda, T. *J*. *Am*. *Chem*. *Soc*. **1967**, *89*, 998-1004.
15. Moses, J. P.; Satheeshkumar, K. S.; Murali, J.; Alli, D.; Jayakumar, R. *Langmuir* **2003**, *19*, 3413-3418.
16. Tirrell, J. G.; Tirrell, D. A. *Curr*. *Opin*. *Sol*. *State Mat*. *Sci*. **1996**, *1*, 407-411.
17. Langer, R.; Tirrell, D. A. *Nature* **2004**, *428*, 487-492.
18. Claracq, J.; Santos, S. F. C. R.; Duhamel, J.; Dumousseaux, C. ; Corpart, J.-M. *Langmuir* **2002**, *18*, 3829-3835.
19. Kwon, G. S.; Naito, M.; Yokoyama, M.; Okano, T.; Sakurai, Y.; Kataoka, K. *Pharma*. *Res*. **1995**, *12*, 192-195.
20. McDiarmid, R.; Doty, P. *J*. *Phys*. *Chem*. **1966**, *70*, 2620-2627.
21. Zito, T.; Seidel, C. *Eur*. *Phys*. *J*. *E* **2002**, *8*, 339-346.
22. Ulrich, S.; Laguecir, A.; Stoll, S. *J*. *Chem*. *Phys*. **2005**, *122*, 094911.
23. Bennett, E. L.; Niemann, C. *J*. *Am*. *Chem*. *Soc*. **1950**, *72*, 1804-1805.
24. Cantor, C. R.; Schimmel, P. R. *Biophysical Chemistry Part II*: *Techniques for the Study*

of Biological Structure and Function. W. H. Freeman and Company, New York, 1980, p 443.

25. Demchenko, A. P. *Ultraviolet Spectroscopy of Proteins*. Springer Verlag, New York, 1981, p 3.
26. Birks, J. B. *Photophysics of Aromatic Molecules*. Wiley: New York, 1970; p 301-371.
27. Saxena, V. P.; Wetlaufer, D. B. *Proc*. *Nat*. *Acad*. *Sci*. **1971**, *68*, 969-972.
28. Johnson, W. C. *Proteins*: *Struct*. *Func*. *Gen*. **1990**, *7*, 205-214.
29. Yamashita, O.; Yamane, T.; Ashida, T.; Yamashita, S.; Yamashita, T. *Polym*. *J*. **1979**, *11*, 763-774.
30. Peggion, E.; Cosani, A.; Terbojevich, M.; Borin, G. *Biopolymers* **1972**, *11*, 633-643.
31. Auer, H. E.; Doty, P. *Biochemistry* **1966**, *5*, 1716-1725.

Chapter 4

Characterization of the Self-Association of an Amphiphilic Polypeptide

4.1. Abstract

The behavior of an alternating polypeptide of aspartic acid and phenylalanine $(Asp_1Phe_1)_n$ was studied in solution by performing quenching and non-radiative energy transfer (NRET) fluorescence experiments. Dynamic light scattering (DLS) was used to complement the results obtained by fluorescence. The fluorescence quenching experiments where the chromophore pyrene was either covalently attached onto the polypeptide or physically bound to the polypeptide via hydrophobic interactions demonstrated that the chromophore was less accessible to its surrounding. Restricted accessibility of pyrene to the solvent was most pronounced when pyrene was not attached to the polypeptide since the fluorescence quenching experiments showed protective quenching. The absence of NRET between a naphthalene labeled $(Asp_1Phe_1)_n$ and a pyrene labeled $(Asp_1Phe_1)_n$ led to the conclusion that $(Asp_1Phe_1)_n$ generates essentially unimolecular polymeric micelles. The small amount of polypeptide aggregation was further confirmed from the substantial reduction in the light scattered by the filtered polypeptide solutions. The filtration experiments also demonstrated that molecular pyrene targets the hydrophobic domains generated by the few polypeptide aggregates present in solution.

4.2. Introduction

Amphiphilic polymers (APs) are polymers made up of hydrophilic and hydrophobic parts, which can self-assemble into objects which often have sizes in the nanometer range, such as micelles,[1,2] vesicles,[3] and fibers[4] in organic solvents or aqueous solutions. The self-assembly of APs into large polymeric structures has led to their use in numerous applications such as associative thickeners in paints,[5] crosslinking agents in smart gels,[6] or the building

blocks of polymeric micelles whose interior can be loaded with drugs.[7] Most of the studies on self-assembling systems and their applications have focused on hydrophobically modified polymers (HMPs).[8-12] The synthesis of these amphiphilic polymers can be achieved either by block copolymerization where one block is water–soluble poly(ethylene oxide) (PEO) and the other is not such as polystyrene (PS), poly(propylene oxide) (PPO), or poly(L-amino acids)[1,13] by grafting onto the water-soluble polymer backbone bulky hydrophobes such as long alkyl chains,[14] cholesteryl pendants,[15] or cholic acid,[16,17] or by random copolymerization of a water soluble monomer with a hydrophobic comonomer.[18,19]

The characterization of polymeric aggregates in solution is usually accomplished by a combination of several techniques such as fluorescence,[20,21] dynamic light scattering,[22] small angle X-ray scattering,[23] small angle neutron scattering,[24,25] electron microscopy,[4,26] and NMR.[27,28] Among these, fluorescence has been used extensively to gain structural information on polymeric aggregates at the molecular level.[20,21] This is due to the high sensitivity of fluorescence, the small size of the fluorescent probe which can report on molecular sized domains, the strong structural dependence of most fluorophores on their local environment, and the availability of a large number of fluorescence techniques which have been designed to probe almost all aspects of polymeric systems.[20,21] A variety of probes can be used, but pyrene has been coined as being "by far the most frequently used dye in fluorescence studies of labeled polymers".[29] Pyrene has been used to study amphiphilic polymers in aqueous solution by taking advantage of its hydrophobicity which enables its favourable partition in the hydrophobic domains generated by the APs, or by covalent labeling of the AP.

In comparison to the extensive research performed on APs, very little attention has

been paid to the self-assembly of APs having well defined repeat units of hydrophobic and hydrophilic monomer residues. This situation results certainly from the more demanding synthetic skills required to prepare such APs. One such study was carried out on the self-assembly of copolymers of styrene and maleic anhydride (SMA).[30] The alternating SMA copolymers were shown to associate in aqueous alkaline solutions into small spherical polymeric aggregates 3.4 nm in diameter. These aggregates exhibit hydrophobic microdomains made of the styrene monomers, which are stabilized by the carboxylate anions generated by the hydrolyzed maleic anhydride.

The interior of the SMA aggregates can solublize large quantities of hydrophobic compounds such as pyrene, anthracene, or phenanthrene.[30] The rate of release of these hydrophobic compounds from the hydrophobic microdomains of SMA is very slow, 10^3-10^4 times slower than that from typical surfactant micelles such as those of sodium dodecyl sulfate (SDS). The hydrophobic interior of the SMA aggregates was shown to be extremely rigid. The slow rates of release exhibited by the SMA aggregates would have made them ideal candidates as carriers for drug delivery applications had it not been for their lack of biocompatibility, which prevents their use in physiological environments. If the slow, controllable rate of release of hydrophobic compounds from the hydrophobic interior of SMA aggregates were due to the sequence of alternating hydrophobic and hydrophilic monomers, it would be worthwhile to undertake the synthesis of a biocompatible amphiphilic polymer where the hydrophobic and hydrophilic monomers could be incorporated into the backbone in a controlled manner. Such polymers could become a valuable addition to the arsenal of carriers used for drug delivery applications.[31]

In view of the inherent biocompatibility of polypeptides and the ability to control

their sequence via synthetic routes,[32-34] the structure of a polypeptide was designed with an alternating sequence of amino acids having a chemical structure that would mimic that of the styrene and maleic acid monomers constituting the SMA backbone. Phenylalanine (Phe) was chosen to replace styrene since both contain an aryl pendant. Maleic acid was substituted with an aspartic acid (Asp). The structure of the alternating polypeptide $(Asp_1Phe_1)_n$ is shown in Figure 4.1 together with that of SMA.

SMA **Polypeptide**

Figure 4.1. Comparison of the structure of SMA and $(Asp_1Phe_1)_n$.

Under basic conditions, $(Asp_1Phe_1)_n$ is negatively charged and is water-soluble. The ability of the hydrophobic Phe residues to induce the formation of hydrophobic domains intra- or intermolecularly was investigated by fluorescence quenching and non-radiative energy transfer (NRET). The fluorescence study was complemented by dynamic light scattering (DLS) experiments. The results obtained by the combination of these techniques suggest that $(Asp_1Phe_1)_n$ forms essentially unimolecular micelles generated through intra-molecular hydrophobic association of the hydrophobic monomer, Phe.

4.3. Experimental

UV-Vis absorption. All UV-Vis absorption spectra were obtained with a Hewlett Packard 8452A diode array spectrophotometer using an absorption cell with a 1 cm path length. The resolution of the spectrophotometer equals ± 2 nm.

Circular dichroism. CD spectra were acquired on a J 715 CD spectropolarimeter (Jasco) at 25 ^{o}C with a 0.1 cm path length cell, a 100 nm/min scan rate, and a 2 nm bandwidth. Spectra were an average of 10 scans from 190 to 250 nm.

Dynamic light scattering. Dynamic light scattering measurements were carried out on a Zeta Sizer, NanoZS (Malvern Instrument, England). The analysis was performed at a laser wavelength of 633 nm, a scattering angle of 173^{o}, and at a temperature of 25 ^{o}C. Solutions were filtered prior to data acquisition through a 0.2 μm pore size Supor® Membrane (Life Science) filter. For each sample, the mean diameter and standard deviation of the particles present in solution were calculated by applying the multimodal analysis.

Steady-state fluorescence measurements. The steady-state emission spectra were obtained using a Photon Technology International LS-100 steady-state fluorometer with a continuous xenon lamp. A fluorescence cell (VWR) with an inner cross section of 10×10 mm^2 was used in the right angle geometry and the samples were not deoxygenated. The emission spectra of the samples containing pyrene were acquired by exciting the solutions at their maximum absorption, either 338 nm when pyrene was present as a free probe or 346 nm when pyrene was covalently attached to the polypeptides. The intensity of the first peak of the pyrene monomer, I_1, was taken to be the intensity of the peak at 374 nm. The intensity of the third peak of the pyrene monomer, I_3, was taken to be the intensity of the peak at 385 nm (slit width = 1 nm). Polypeptides labeled with naphthalene for the energy transfer experiments

were excited at 290 nm where pyrene absorbs little.

Time-resolved fluorescence measurements. The fluorescence decay profiles were obtained by a time-correlated single photon counter manufactured by IBH Ltd. using a 5000F coaxial nanosecond flash lamp filled with H_2 gas. Samples were excited at either 338 nm or 344 nm, respectively (maximum absorption), depending on whether pyrene was used as a free probe or covalently attached to the polypeptide. The emission wavelength was set at 374 and 510 nm for the pyrene monomer and excimer, respectively. To reduce the noise stemming from stray scattered light, filters with a cut off wavelength at 370 nm and 495 nm were used to acquire the monomer and excimer decays, respectively. All samples were placed in a 10×10 mm^2 fluorescence cell (VWR). All decays were collected with the right angle geometry over 200-800 channels with a minimum of 20,000 counts taken at the maximum of both the monomer and excimer decays to ensure a high signal-to-noise ratio. Deoxygenated solutions of PPO [2,5–diphenyloxazole] in cyclohexane (τ = 1.42 ns) and BBOT [2,5–bis(5–*tert*-butyl–2–benzoxazolyl)thiophene] in ethanol (τ = 1.47 ns) were used as references for the monomer and excimer, respectively. The references were necessary to determine the true instrument response function of the IBH fluorometer according to the MIMIC method.[35] All measured decays were deconvoluted from the lamp profile and were fitted with a sum of three exponentials according to Equation 4.1 where the index x represents either the monomer (M) or the excimer (E).

$$i_x(t) = a_{x1}\exp(-t/\tau_{x1}) + a_{x2}\exp(-t/\tau_{x2}) + a_{x3}\exp(-t/\tau_{x3}) \quad x = M, E \tag{4.1}$$

The parameters of the fits were optimized using the Marquardt-Levenberg algorithm.[36] The

quality of the fits was established from the χ^2 values (< 1.30) and the random distribution around zero of the residuals and of the autocorrelation function of the residuals.

Reagents. Pyrene, 1-pyrenemethylamine hydrochloride, 1–pyrenebutyric acid *N*–hydroxy succinimide ester, 1–naphthalenemethylamine, (1–ethyl–3–(3–dimethylaminopropyl) carbodiimide hydrochloride (EDC), and nitromethane were all purchased from Sigma-Aldrich. THF and DMF (distilled in glass, Caledon), NaOH (BDH), HCl (reagent ACS grade, Fischer), methanol, anhydrous diethyl ether and acetone (all HPLC grade, EMD) were used as received. Milli-Q water with a resistivity of over 18 MΩ.cm was used to make all the aqueous solutions. Spectra/Por® 7 regenerated cellulose dialysis membranes having a cut-off value of 3,500 g/mol were used for dialysis. Pyrene was purified by recrystallization from ethanol three times, whereas 1–pyrenemethylamine ($PyMeNH_2$) was obtained from the neutralization of 1–pyrenemethylamine hydrochloride with NH_4OH in water, extraction into hexane, and washing and drying over NaOH pellets prior to use.[37]

Random labeling of polypeptides. A small amount of $(Asp_1Phe_1)_n$ (40 mg, 1.53×10^{-4} mole of Asp) was weighed in a 20 mL vial in which 8 mL of DMF was added. The solution was stirred. To this solution, 1.77 mg (7.65×10^{-6} mole) of $PyMeNH_2$ was added and stirred vigorously for approximately 10 min. An equivalent amount of EDC (1.47 mg, 7.65×10^{-6} mole) was added and the reaction was carried out under vigorous stirring for 5 hours.[28] The reaction mixture was transferred to a dialysis bag having a molecular weight cut-off of 3,500 MW and dialyzed against slightly acidic, basic, and neutral water in successive steps for 2 days each. The dialyzed solution was removed from the dialysis bag and water was removed under a stream of nitrogen. The solid obtained was dissolved in DMF and precipitated in diethyl ether and collected. This procedure was repeated 3-4 times and the solid obtained was

dried under vacuum yielding a sample of $(Asp_1Phe_1)_n$ randomly labeled with pyrene ($RPy–(Asp_1Phe_1)_n$).

Poly(aspartic acid) was also randomly labeled with pyrene to yield $RPy–Asp_n–229$ using a slightly modified procedure. After dialysis, the polypeptide is obtained in its salt form. Whereas the salt of $(Asp_1Phe_1)_n$ was soluble in DMF thanks to the hydrophobic Phe, poly(aspartic acid) was not. Consequently, poly(aspartic acid) was acidified with 1 M HCL before disolution in DMF and precipitation with diethyl ether. The same procedure used for pyrene labeling was followed to randomly label $(Asp_1Phe_1)_n$ and poly(aspartic acid) with 1-naphthalenemethylamine.

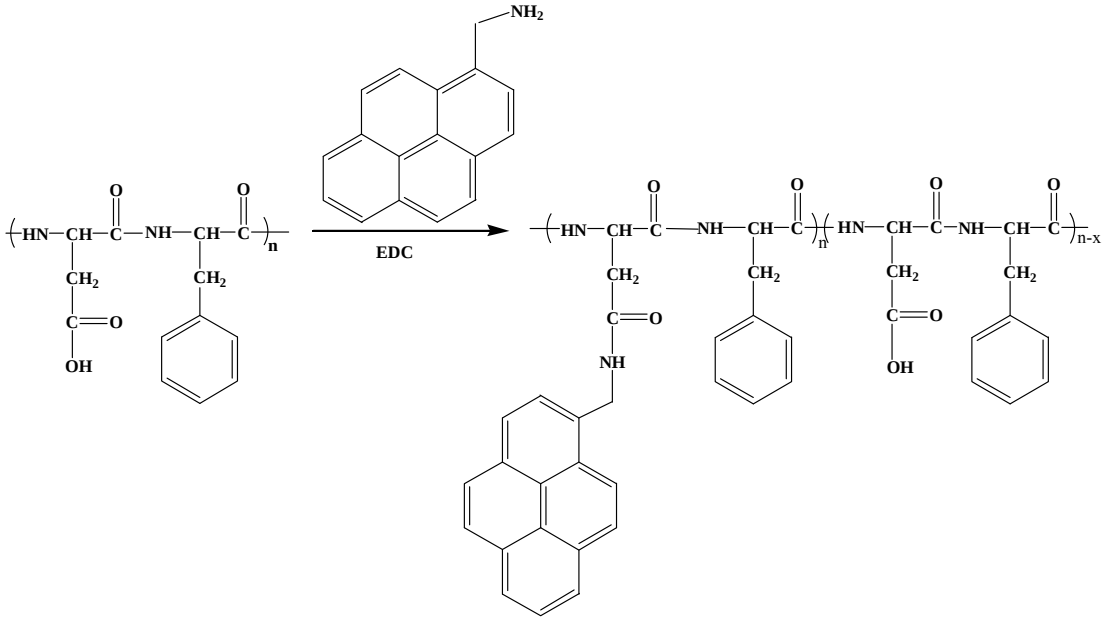

Figure 4.2. Random labeling of pyrene along the polypeptide chain

End labeling of the polypeptides. A solution of $(Asp_1Phe_1)_n$ (40 mg, 3.1×10^{-6} mole of chain ends as calculated from M_w given in Table 3.1), 1-pyrenebutyric acid N-hydroxy succinimide ester (3.6 mg, 9.3×10^{-6} mole) and $NaHCO_3$ (1.6 mg, 0.019 mole) in 8 mL of DMF was vigorously stirred at room temperature for 24 hours. The solution was transferred to a

dialysis bag with a 3500 MW cut-off and was dialyzed and purified as mentioned for the random labeling reaction to yield the pyrene end-labeled polypeptide (EPy–$(Asp_1Phe_1)_n$).

Determination of the pyrene and naphthalene contents. The pyrene content (λ_{py}) of the pyrene-labeled polypeptide was determined by measuring the absorbance of a carefully weighed amount of the labeled polypeptide in a known volume (V) of DMF. As DMF is a good solvent for pyrene, no significant pyrene-pyrene interactions are expected, resulting in negligible distortion of the pyrene absorbance. The pyrene concentration [Py] in mol.L^{-1} was calculated using the Beer-Lambert law given in Equation 4.2. The extinction coefficient of *N*–(1–pyrenemethyl)acrylamide (ε_{Py} = 40,000 mol^{-1}.L.cm^{-1} at 344 nm in DMF)[40] and 1–pyrenebutyric acid *N*-hydroxy succinimide ester in DMF (ε_{Py} = 38,000 mol^{-1}.L.cm^{-1} at 344 nm)[40] were used for RPy–$(Asp_1Phe_1)_n$ and EPy–$(Asp_1Phe_1)_n$, respectively.

$$\text{Absorbance} = \varepsilon_{Py}\,[Py]\,L \tag{4.2}$$

In Equation 4.2, L is the cell path length which equals 1 cm. The pyrene content, λ_{Py}, was calculated using Equation 4.3,

$$\lambda_{Py} = \frac{[Py]}{m/V} \tag{4.3}$$

where λ_{Py} is expressed in moles of pyrene per gram of polypeptide (mol.g^{-1}). To determine the naphthalene content (λ_{Np}) of RNp–$(Asp_1Phe_1)_n$, the extinction coefficient of 1–naphthalenemethylacetamide in DMF was used (ε_{Np} = 6,500 mol^{-1}.L.cm^{-1} at 284 nm).[40]

The chromophore content (λ_{Py} or λ_{Np}) of the polypeptide can be used to determine the fractions of labeled amino acids (X_{Total}) and aspartic acids (X_{Asp}).

$$X_{Total} = \frac{\lambda_D \left[xM_{Asp} + yM_{Phe} \right]}{(x+y)\left[1 + \lambda_D \left(M_{Asp} - M_{Asp-D} \right)\right]} \tag{4.4}$$

$$X_{Asp} = \frac{\lambda_D \left[xM_{Asp} + yM_{Phe} \right]}{x\left[1 + \lambda_D \left(M_{Asp} - M_{Asp-D} \right)\right]} \tag{4.5}$$

In Equations 4.4 and 4.5, x and y represent the molar fractions of Asp and Phe constituting the polypeptide, λ_D represents the chromophore content expressed in mol.g^{-1}, M_{Phe} and M_{Asp-D} are the molar mass of Phe (147 g.mol^{-1}) and chromophore-labeled Asp (328 g.mol^{-1} and 254 g.mol^{-1} for pyrene and naphthalene labeled Asp) incorporated in the polypeptide. The two values of 115 and 137 g.mol^{-1} for M_{Asp} were used depending on whether the polypeptide taken to measure the chromophore content was originally in its acid or salt form. More precisely, poly(aspartic acid) was used in its acid form whereas $(Asp_1Phe_1)_n$ was used in its salt form.

For the samples where pyrene was used as a non-covalent probe, the pyrene concentration was determined by adding a 0.1 M SDS solution to the polypeptide solution loaded with pyrene, measuring the absorbance of the solution, and applying Beer-Lambert law (Equation 4.2) knowing that the extinction coefficient of pyrene in SDS equals 42,600 mol^{-1}.L.cm^{-1} at 338 nm.[40] Table 4.1 gives the dye content of the labeled polypeptides.

Table 4.1. Pyrene and naphthalene contents (λ_{Py}, λ_{Np}) in moles of chromophore per gram of polymer and the molar fraction of labeled aspartic acids (X_{Asp}) and of amino acids (X_{Total}) in $(Asp_1Phe_1)_n$ and $(Asp)_n$ determined by UV-Vis absorption.

Sample	Chromophore content		
	λ (μmol/g)	X_{Total} mole%	X_{Asp} mole%
RPy–$(Asp)_n$–229*	229	2.8	2.8
RPy–$(Asp_1Phe_1)_n$–70	70	1.0	2.0
RPy–$(Asp_1Phe_1)_n$–132	132	1.9	3.8
RPy–$(Asp_1Phe_1)_n$–221	221	3.3	6.6
EPy–$(Asp_1Phe_1)_n$–44	44	–	1.2
RNp–$(Asp)_n$–180*	180	2.1	2.1
RNp–$(Asp_1Phe_1)_n$–195	195	2.8	5.7
RNp–$(Asp_1Phe_1)_n$–313	313	4.6	9.2

* For $(Asp)_n$, $X_{Total} = X_{Asp}$ since all amino acids are aspartic acid.

Preparation of the aqueous solutions of polypeptides. Polypeptide samples were prepared indirectly using DMF as the solvent for the solubilization of the polypeptides after which 0.01 M NaOH was added dropwise up to 30 wt% with vigorous stirring to induce the formation of the polypeptide aggregates.[41] The polypeptide solutions were transferred to dialysis bags and dialyzed against 0.01 M Na_2CO_3 solution at pH 9 for 2 days to remove all traces of DMF. Pyrene was added to the unlabeled polypeptide solution in DMF when pyrene was used as a free probe before being dialyzed against a 0.01 M Na_2CO_3 solution at pH 9 saturated with pyrene. Figure 4.3 shows the three different types of samples prepared with $(Asp_1Phe_1)_n$ and pyrene.

A-Molecular pyrene used as a probe

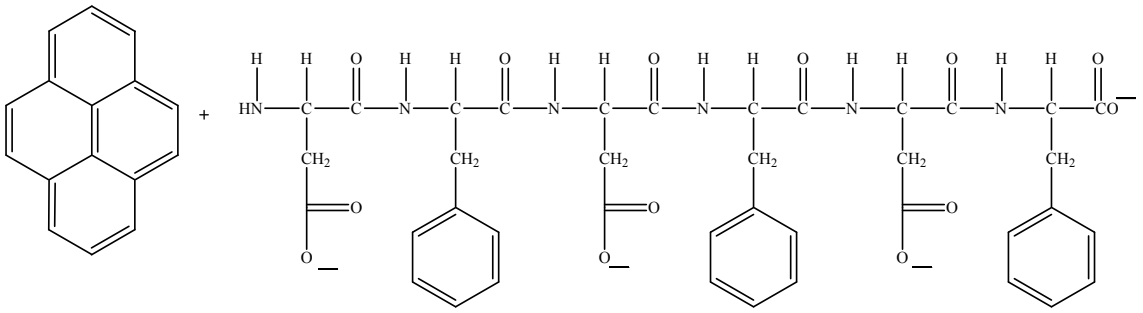

B-Polypeptide randomly labeled with pyrene: RPy–$(Asp_1Phe_1)_n$

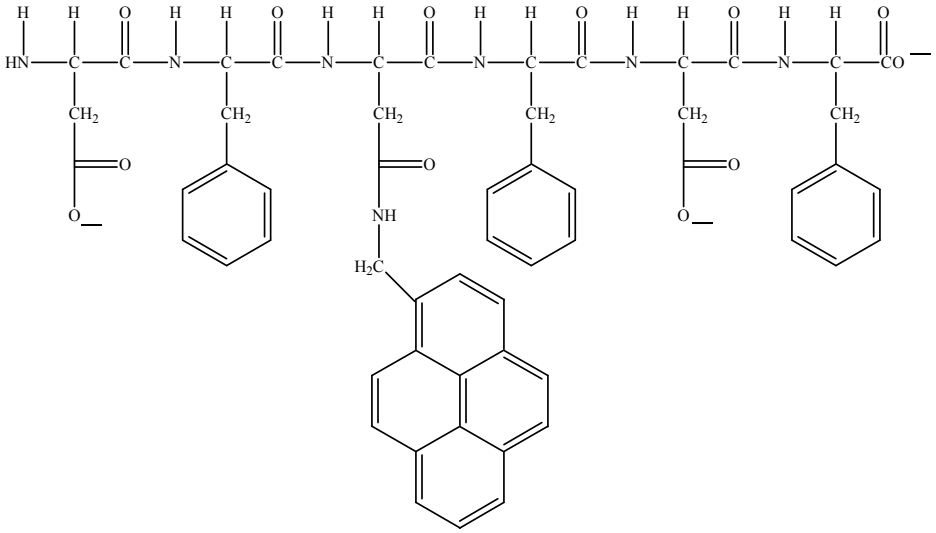

C-Polypeptide end-labeled with pyrene: EPy–$(Asp_1Phe_1)_n$

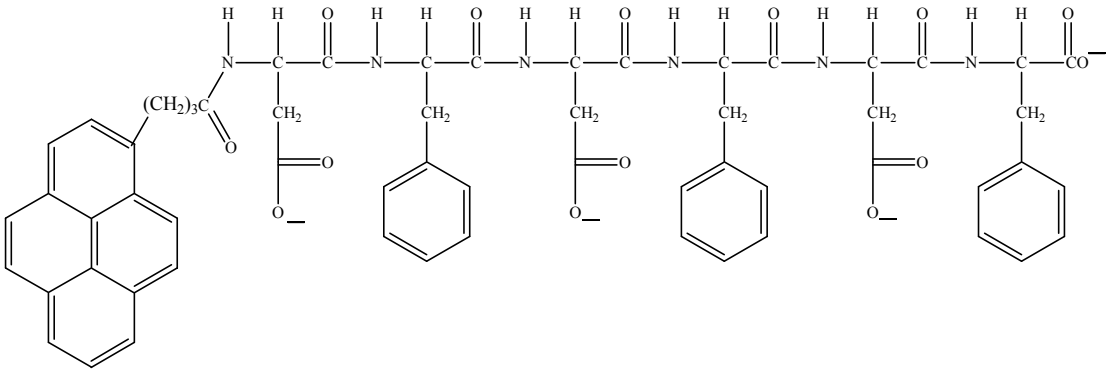

Figure 4.3. Samples prepared with $(Asp_1Phe_1)_n$ and pyrene

4.4. Results and Discussion

Most proteins and polypeptides have an intrinsic fluorescence caused by the presence of aromatic side chains. Out of the 20 naturally occurring amino acids, three bear aromatic groups. They are tryptophan, tyrosine, and phenylalanine. Tryptophan and tyrosine have very similar quantum yields, whereas the fluorescence of phenylalanine is so weak that it can only be observed in polypeptides lacking both tryptophan and tyrosine.[42] However the alternating polypeptide $(Asp_1Phe_1)_n$ has such a high phenylalanine content that it exhibits substantial fluorescence. Its photophysical properties and those of other polypeptides have been described in Chapter 3.

The conformations of polypeptides in solution have been studied extensively by circular dichroism (CD) since CD can assess whether a polypeptide exists as an α-helix, a β-sheet, or a random coil. The CD spectra of $(Asp_1Phe_1)_n$, RPy–$(Asp_1Phe_1)_n$–132, $(Asp)_n$, and RPy–$(Asp)_n$–229 were acquired in a 0.01 M Na_2CO_3 solution at pH 9, to determine the secondary structure of the polypeptides (Figure 4.4). The comparison was done to ensure that pyrene does not induce any drastic conformational change of the polypeptide.

Negatively charged poly(aspartic acid) at pH 9 is known to adopt a random coil conformation,[43] and a right handed α-helical conformation is observed for phenylalanine blocks present in copolymers of aspartic acid and phenylalanine in alkaline solutions.[44-46] The opposite effects conferred by aspartic acid and phenylalanine to the conformation of a polypeptide make it difficult to predict the conformation of $(Asp_1Phe_1)_n$ where both amino acids alternate. The CD spectra of the unlabeled and pyrene-labeled $(Asp_1Phe_1)_n$ are shown in Figure 4.4A. They are noisy and do not exhibit the expected features of an α-helix, a β-sheet, or a random coil (Figure 1.13) which suggests that the labeled and unlabeled $(Asp_1Phe_1)_n$

adopt no well defined conformation in aqueous solution. The CD spectrum of poly(L-aspartic acid) exhibits a minimum at 205 nm in Figure 4.4B, suggesting a random coil conformation. In both Figures 4.4A and B, the CD spectra of the pyrene-labeled polypeptides resemble that of the naked polypeptides, indicating that the pyrene label does not induce the formation of undesirable secondary structures for both $(Asp_1Phe_1)_n$ and $(Asp)_n$

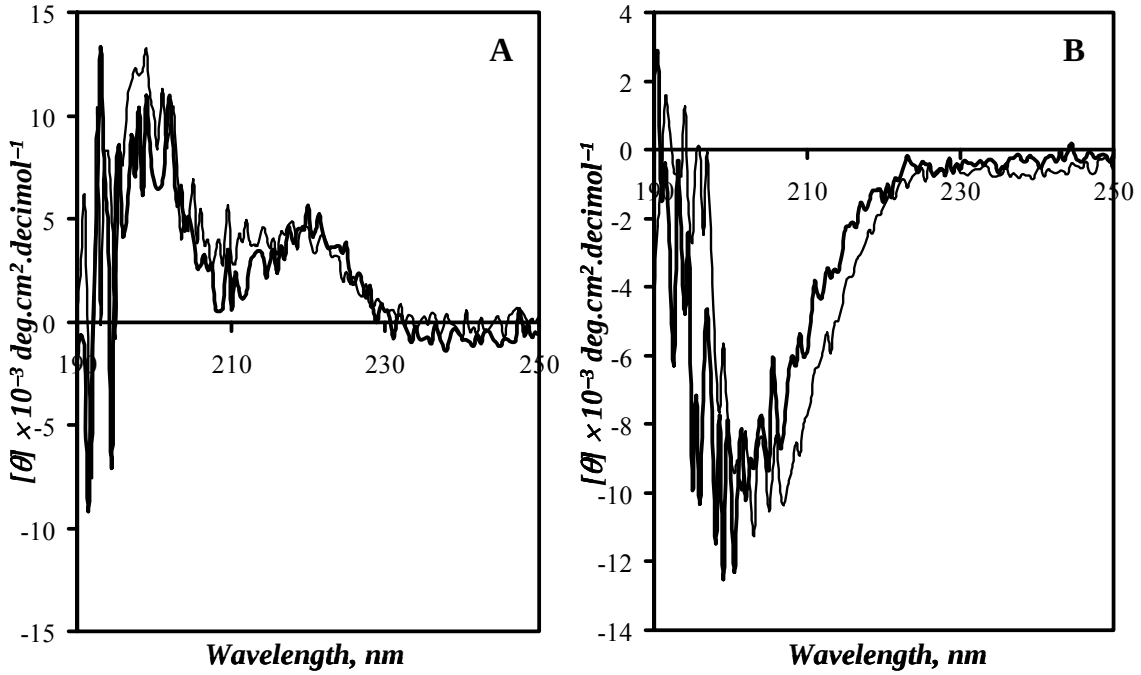

Figure 4.4. CD spectra of unlabeled (———) and labeled (▬▬▬) $(Asp_1Phe_1)_n$ (A) and $(Asp)_n$ (B) in a 0.01 M Na_2CO_3 solution at pH 9 in a 0.1 cm path length cell. $(Asp_1Phe_1)_n$, [*Polypeptide*] = 0.1 g/L and $(Asp)_n$, [*Polypeptide*] = 0.25 g/L. The labeled samples were RPy–$(Asp_1Phe_1)_n$–132, [*Polypeptide*] = 0.08 g/L; and RPy–$(Asp)_n$–229, [*Polypeptide*] = 0.2 g/L.

Since Dynamic Light Scattering (DLS) yields the hydrodynamic diameters of particles in solution, DLS experiments were conducted on the polypeptide solutions to investigate whether $(Asp_1Phe_1)_n$ would aggregate in solution. DLS experiments were carried

out on 0.05 g/L and 0.5 g/L solutions of $(Asp_1Phe_1)_n$, EPy–$(Asp_1Phe_1)_n$, RPy–$(Asp_1Phe_1)_n$, and $(Asp_1Phe_1)_n$ with molecular pyrene. The size distribution of the species present in the polypeptide solutions are represented in Figure 4.5A, B, and C using, respectively, the light scattering intensity, the number of particles, and the particle volume to determine the contribution of each species to the histograms. A summary of the peak diameters and standard deviations is provided in Table 4.2. The size distribution profile determined from the scattering intensities for $(Asp_1Phe_1)_n$, EPy–$(Asp_1Phe_1)_n$, and RPy–$(Asp_1Phe_1)_n$ exhibit two contributions: one peak in the 4-8 nm range attributed to individual polypeptide chains and a second peak centered around 130-160 nm depending on the polypeptide solution attributed to larger interchain polypeptide aggregates. In the presence of molecular pyrene, an additional peak centered around 20 nm is observed in the histograms. Unimodal size distributions are obtained for all samples when the histograms are calculated using numbers and volumes instead of scattering intensities, suggesting that a single species is present in solution. The diameter of this species is in the 3-7 nm range from the analysis based on the particle numbers, similar to the size expected from individual polypeptide chains.

The difference observed between the size distribution profiles obtained by numbers, volumes, and intensities can be rationalized by the fact that smaller particles scatter much less light than larger ones. Thus if a population of particles contains a small fraction of large particles, these large particles contribute a large fraction of the total light scattered by the solution. Consequently the presence of the large particles is detected from their contribution to the total light scattered, although they are present in too small a number to appear in a size histogram generated by either numbers or volumes. The DLS results suggest that $(Asp_1Phe_1)_n$ is present essentially as single chains and that a very small percentage of them form

interpolymeric/multichain aggregates.

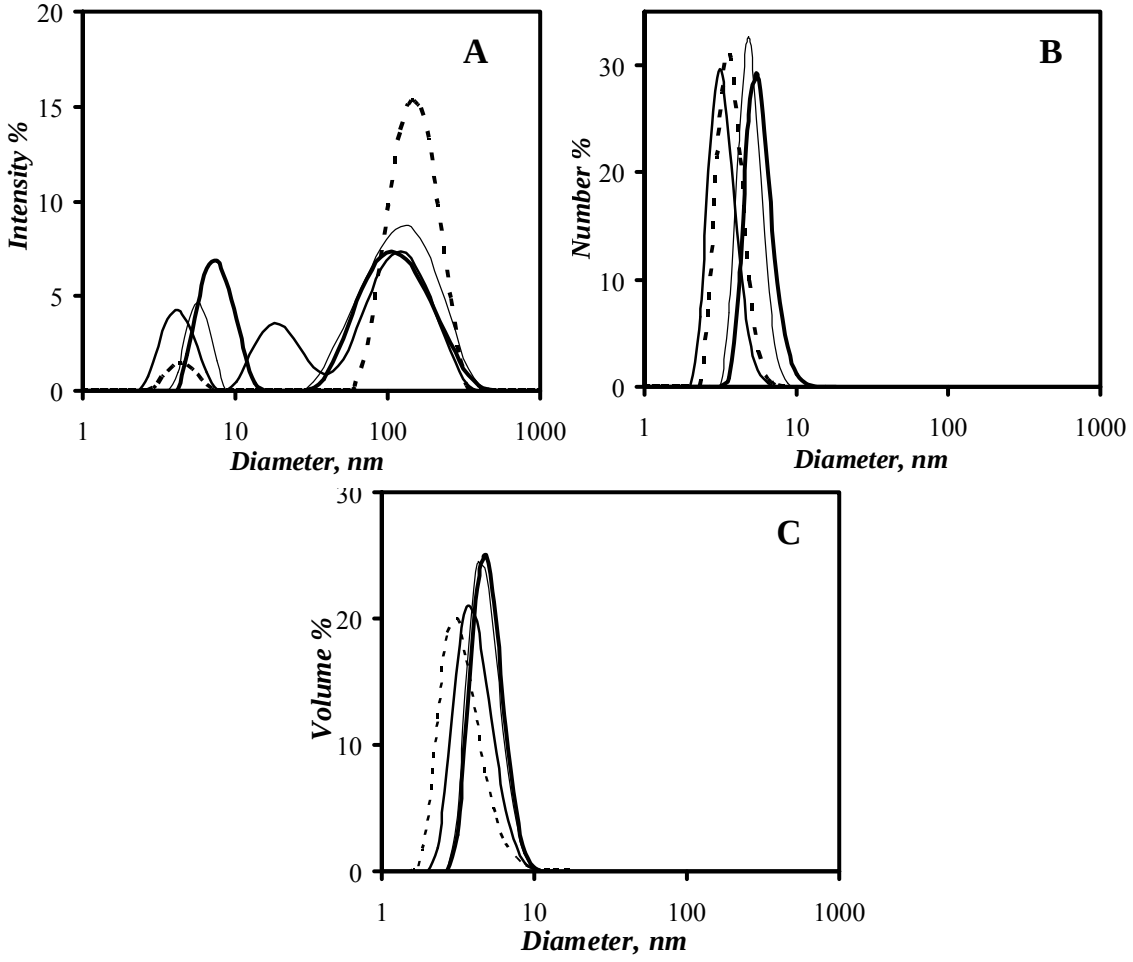

Figure 4.5. Particle size distribution determined by intensity (A), number (B), and volume (C) of $(Asp_1Phe_1)_n$ (——), EPy–$(Asp_1Phe_1)_n$–44 (·····), RPy–$(Asp_1Phe_1)_n$–132 (———), and $(Asp_1Phe_1)_n$ with molecular pyrene (———) in 0.01 M Na_2CO_3 at pH 9 and at a polypeptide concentration of 0.05 g/L.

Table 4.2. Peak diameter and their standard deviations for the alternating polypeptide samples.

Sample	Conc. g/L	Particle size (nm)		
		Number-average	Volume-average	Intensity-average
$(Asp_1Phe_1)_n$	0.05	5.8 ± 1.3	5.0 ± 1.2	7.7 ± 1.9 (31 %), 128.0 ± 67.1 (68 %)
	0.5	6.8 ± 1.0	5.1 ± 1.1	7.3 ± 0.8 (18 %), 105.2 ± 22.5 (21 %), 309.7 ± 51.3 (60 %)
$(Asp_1Phe_1)_n$ + molecular pyrene	0.05	3.4 ± 0.7	4.4 ± 4.1	4.3 ± 1.0 (17 %), 20.5 ± 6.8 (21 %), 130.1 ± 58.1 (61 %)
	0.5	2.9 ± 0.6	3.6 ± 2.6	3.8 ± 0.9 (14 %), 16.5 ± 5.3 (25 %), 135.3 ± 61.6 (59 %)
EPy–$(Asp_1Phe_1)_n$–44	0.05	3.7 ± 0.7	3.6 ± 1.1	4.5 ± 0.9 (5 %), 153.6 ± 50.2 (95 %)
	0.5	3.8 ± 0.7	4.2 ± 1.2	4.6 ± 0.9 (5 %), 45.7 ± 11.5 (8 %), 173.5 ± 51.8 (86 %)
RPy–$(Asp_1Phe_1)_n$–70	0.05	4.6 ± 1.0	5.0 ± 1.0	5.8 ± 1.2 (10 %), 154.0 ± 62.3 (90 %)
	0.5	4.5 ± 0.8	5.4 ± 1.2	5.3 ± 1.0 (8 %), 158.6 ± 58.6 (92 %)
RPy–$(Asp_1Phe_1)_n$–132	0.05	5.0 ± 0.9	4.9 ± 1.2	5.8 ± 0.9 (14 %), 134.2 ± 69.6 (86 %)
	0.5	4.4 ± 0.5	5.1 ± 1.1	5.2 ± 0.4 (10 %), 59.0 ± 9.8 (30 %), 229.7 ± 44.1 (60 %)
RPy–$(Asp_1Phe_1)_n$–221	0.05	4.2 ± 0.7	4.6 ± 1.5	4.8 ± 0.8 (9 %), 32.2 ± 6.3 (15 %), 142.5 ± 41.5 (75 %)
	0.5	3.6 ± 1.0	4.3 ± 1.0	6.0 ± 1.8 (15 %), 139.3 ± 55.5 (84 %)

To further support the conclusion reached by DLS that $(Asp_1Phe_1)_n$ is predominantly present as unimolecular micelles in 0.01 M Na_2CO_3 solutions at pH 9, fluorescence energy transfer experiments were carried out using the polypeptides labeled with pyrene (RPy–$(Asp_1Phe_1)_n$–70) and naphthalene (RNp–$(Asp_1Phe_1)_n$–313). The process of non-radiative energy transfer (NRET) involves the transfer of energy between an excited donor, naphthalene (Np), and a ground state acceptor, pyrene (Py),[47] as shown in Scheme 4.1. For energy transfer to take place, the emission of the donor must overlap with the absorption of the acceptor. Figure 4.6 shows the absorption and emission spectra of both naphthalene and pyrene and how the actual energy transfer takes place.

Scheme 4.1. Energy transfer between naphthalene and pyrene chromophores.

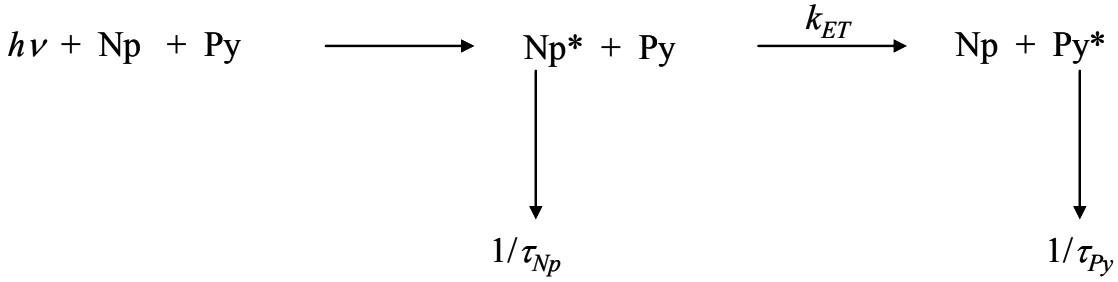

NRET occurs as a result of dipole-dipole interactions between the donor and the acceptor without emission of a photon.[47] The rate constant of energy transfer, k_{ET}, depends essentially on the distance between the two dyes,[48] as shown by Equation 4.6.

$$k_{ET} = \left(\frac{R_0}{r}\right)^6 \frac{1}{\tau_{Np}} \qquad (4.6)$$

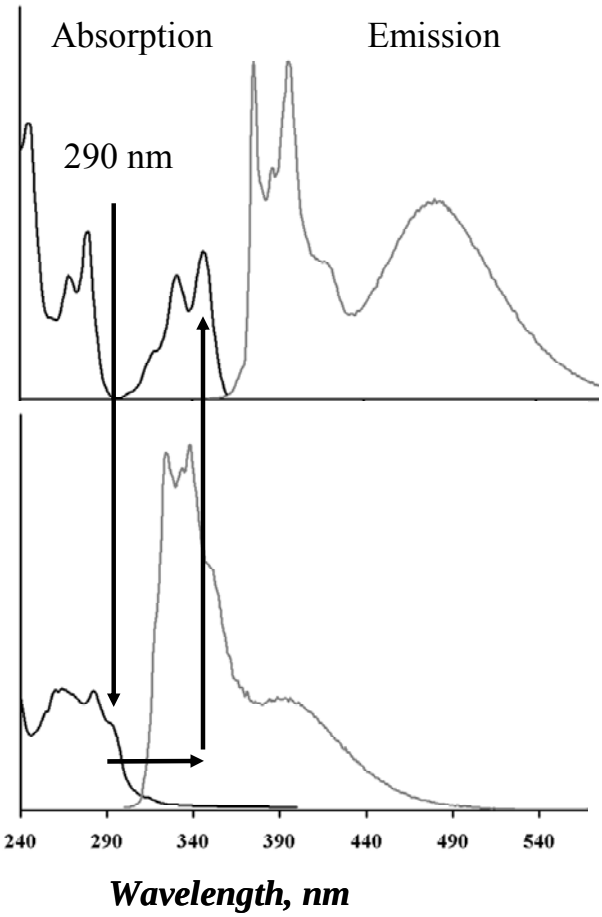

Figure 4.6. Absorption and emission spectra of pyrene (top) and naphthalene (bottom) for fluorescence NRET experiments.

In Equation 4.6, r is the distance between the donor (*Np*) and the acceptor (*Py*), R_o is the Förster radius which depends on the extent of overlap between the emission spectrum of the donor and the absorption spectrum of the acceptor and has been determined to equal 2.9 nm for the *Np*/*Py* pair,[49] and τ_{Np} is the lifetime of naphthalene. The NRET efficiency, E_{ET}, depends strongly on the distance between the donor and the acceptor and can be calculated from Equation 4.7.

$$E = \frac{R_0^{\,6}}{R_0^{\,6} + r^6} = 1 - \frac{I_{Np\,in\,mixture} / Abs(Np\,in\,mixture, \lambda_{ex})}{I^o_{Np} / Abs(Np, \lambda_{ex})} \qquad (4.7)$$

Here $I_{Np\ in\ mixture}$ and I^o_{Np} represent the fluorescence intensity of the donor in the presence and absence of the acceptor, respectively. In a NRET experiment, the donor is excited at a wavelength where the acceptor shows little or no absorption. In this study, naphthalene was selectively excited at 290 nm, where pyrene absorbs little. A 0.025 g/L solution of RNp–$(Asp_1Phe_1)_n$–313 and a 0.017 g/L solution of RPy–$(Asp_1Phe_1)_n$–70 were prepared with an optical density less than 0.05 at 290 nm. The solutions were excited at 290 nm and their steady-state fluorescence emission spectra were recorded. The solution for the NRET experiment was prepared by mixing RNp–$(Asp_1Phe_1)_n$–313 with RPy–$(Asp_1Phe_1)_n$–70 in DMF followed by dialysis in aqueous solution and adjusting the polypeptide concentration so that the OD at 290 nm takes a value lower than 0.05. The fluorescence spectrum of the mixture was recorded upon excitation of the solution at 290 nm. Similarly, solutions of labeled poly(L-aspartic acid) were prepared and their fluorescence emission spectra were acquired by exciting the solution at 290 nm. The fluorescence spectra of RNp–$(Asp_1Phe_1)_n$–313 (a), RPy–$(Asp_1Phe_1)_n$–70 (b), and the RNp–$(Asp_1Phe_1)_n$–313 + RPy–$(Asp_1Phe_1)_n$–70 mixture (d) are shown in Figure 4.7. The inset depicts the same experiment performed with RNp–$(Asp)_n$–180 and RPy–$(Asp)_n$–229.

The following precautions were taken when performing the NRET experiments. To avoid the inner-filter effect,[47] all experiments were conducted under conditions where the absorption did not exceed 0.1 across the absorption spectrum. The solution absorption was lower than 0.05 at 290 nm, the excitation wavelength. Since the accuracy of the

spectrophotometer is poor for absorptions below 0.1, concentrated solutions of the labeled polypeptides were prepared at a higher concentration and their absorption was recorded. The solutions were then diluted and the dilution factor was used to determine the absorption of the diluted polypeptide solution at 290 nm. Then the fluorescence spectrum of the diluted solution was acquired.

To obtain Figure 4.7, the absorptions of the chromophores needed to be taken into account. The solution of the Np–labeled polypeptide was taken as reference, spectrum a) in Figure 4.7. As shown in Figure 4.6, the absorption of pyrene at 346 nm can be easily determined since it is separated from the absorption of naphthalene. This is not the case for naphthalene whose absorption at 290 nm overlaps with that of pyrene. The absorption of the Np–labeled polypeptide in the mixture of Py– and Np–labeled polypeptides was obtained by subtracting the normalized absorption spectrum of the Py–labeled polypeptide from the absorption spectrum of the mixture. To obtain spectrum d) in Figure 4.7, the fluorescence spectrum of the solution containing the mixture of the Np– and Py–labeled polypeptides was multiplied by the factor p given in Equation 4.8.

$$p = \frac{Abs(Np, 290\,nm)}{Abs(Np - mix, 290\,nm)} \tag{4.8}$$

In Equation 4.8, the quantities *Abs*(*Np*, 290 nm) and *Abs*(*Np-mix*, 290 nm) represent the naphthalene absorption at 290 nm of the solution containing the Np-labeled polypeptide only and that of the solution containing the mixture, respectively. The fluorescence spectrum of the solution containing only the Py-labeled polypeptide (spectrum b) needed also to be

adjusted for changes in concentrations. It was multiplied by the factor *q* given in Equation 4.9 to yield the fluorescence spectrum b) in Figure 4.7.

$$q = \frac{Abs(Py - mix,\ 346\,nm)}{Abs(Py,\ 346\,nm)} \times p \qquad (4.9)$$

In Equation 4.9, the quantities *Abs*(Py, 346 nm) and *Abs*(Py-mix, 346 nm) represent the pyrene absorption at 346 nm of the solution containing the Py-labeled polypeptide only and that of the solution containing the mixture, respectively. The normalized fluorescence spectra a) and b) were then added to yield spectrum c) which was compared to the fluorescence spectrum of the mixture d).

In Figure 4.7, the fluorescence emission of naphthalene in the 320-330 nm range is the same for the Np-labeled polypeptide, alone or in the mixture. According to Equation 4.7, the resulting NRET efficiency equals zero implying that no energy transfer is taking place. Comparison of the fluorescence spectra c) and d) shows a small increase in the pyrene fluorescence in spectrum d) suggesting that residual energy transfer is occurring. From the inset of Figure 4.7, it can be seen that no energy transfer occurs for the labeled poly(aspartic acid) as there is no change in the fluorescence of either naphthalene or pyrene. $(Asp)_n$ being more hydrophilic than $(Asp_1Phe_1)_n$, the complete absence of NRET from RNp–$(Asp)_n$–180 to RPy–$(Asp)_n$–229 is reasonable since $(Asp)_n$ is expected to be present as individual polymer coils in solution.

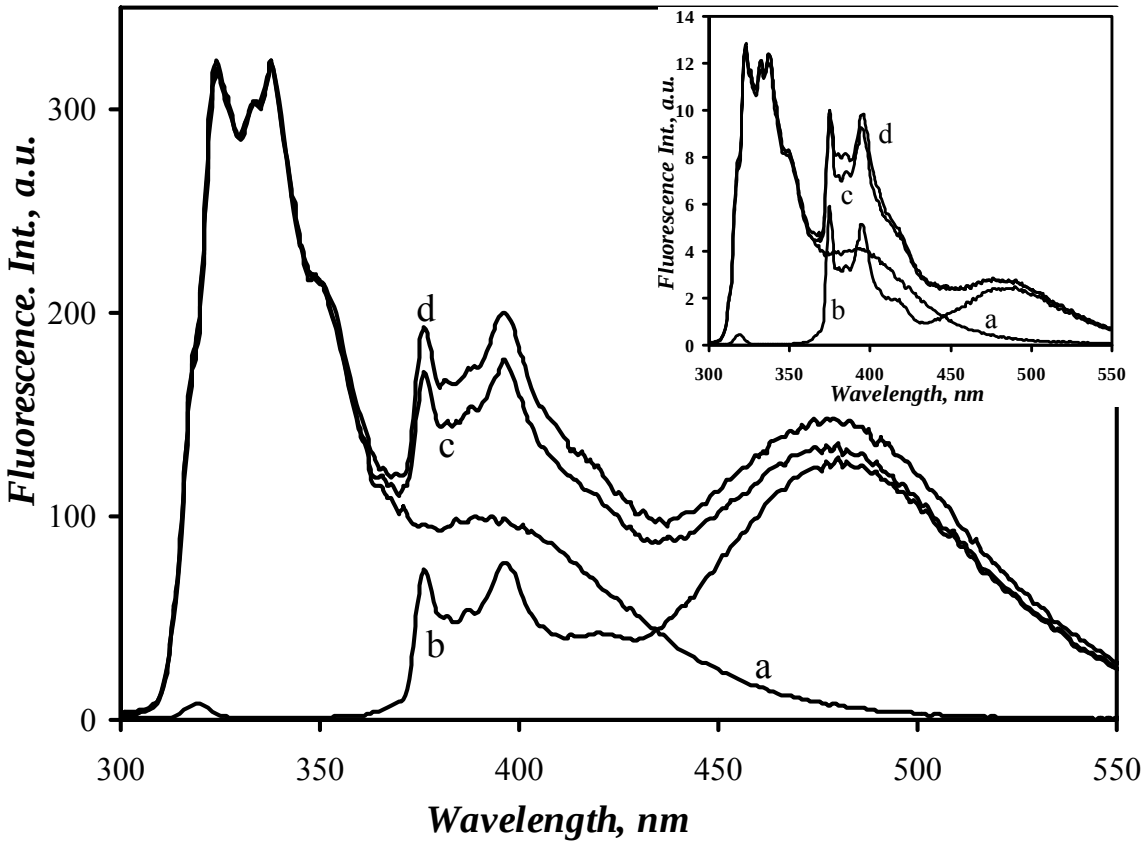

Figure 4.7. Fluorescence emission spectra of aqueous solutions of labeled polypeptides: a) RNp–$(Asp_1Phe_1)_n$–313, [*Polypeptide*] = 0.025 g/L; b) RPy–$(Asp_1Phe_1)_n$–70, [*Polypeptide*] = 0.017 g/L; c) sum of the two preceding spectra; and d) fluorescence emission spectrum of a mixture of the two singly labeled polypeptides, RNp–$(Asp_1Phe_1)_n$–313, [*Polypeptide*] = 0.025 g/L, RPy–$(Asp_1Phe_1)_n$–70, [*Polypeptide*] = 0.017 g/L; Inset: a) RNp–$(Asp)_n$–180, [*Polypeptide*] = 0.042 g/L; b) RPy–$(Asp)_n$–229, [*Polypeptide*] = 0.004 g/L; c) sum of the two precedent spectra; d) fluorescence spectrum of a mixture of the two singly labeled poly(aspartic acid)s, RNp–$(Asp)_n$–180, [*Polypeptide*] = 0.042 g/L, RPy–$(Asp)_n$–229, [*Polypeptide*] = 0.004 g/L. λ_{ex} = 290 nm, O.D ≤ 0.05 at 290 nm.

Since the Förster radius is around 3 nm for the Np/Py pair,[49] the quasi-absence of energy transfer observed for $(Asp_1Phe_1)_n$ in Figure 4.7 indicates that the naphthalene and pyrene chromophores in the RNp–$(Asp_1Phe_1)_n$ + RPy–$(Asp_1Phe_1)_n$ mixture are located at

distances larger than $2 \times R_o \sim 6$ nm, or larger than the average size of a single polypeptide estimated by DLS to range from 3 to 8 nm in Figure 4.5B. Consequently, the NRET experiments suggest that few interpolymeric aggregates are being formed, in agreement with the light scattering results.

Fluorescence techniques using pyrene as a hydrophobic fluorescent chromophore have frequently been used to determine the polarity of its surrounding environment in micellar and polymeric systems.[50,51] In this study, pyrene has been used both as a probe and a hydrophobic label to characterize the hydrophobic microdomains generated by $(Asp_1Phe_1)_n$. The I_1/I_3 ratio, where I_1 and I_3 are, respectively, the fluorescence intensities of the first and third peaks of the fluorescence spectrum of molecular pyrene, gives information about the polarity of the environment where pyrene is located. This ratio has been found to equal 1.66-1.80 for pyrene in water[50,51] and takes on lower values as the local environment of pyrene becomes less polar (I_1/I_3 = 1.10 for molecular pyrene in SDS micelles). A similar effect has been reported for pyrene labels although the dependence of the I_1/I_3 ratio with the environment polarity is somewhat reduced when compared to the pyrene molecule.[21] Recently the I_1/I_3 ratio of a poly(ethylene oxide) labeled at one end with a pyrenyl group (Py-PEO) has been found to equal 1.69 in a 0.1 M Na_2CO_3 solution at pH 9 and 1.38 when large quantities of sodium dodecyl sulphate (SDS) are added to the solution.[52] As the pyrenyl pendant of Py-PEO is being incorporated inside the SDS micelles, the I_1/I_3 ratio decreases. For the alternating polypeptide, the I_1/I_3 ratio was found to be 1.24 when pyrene was used as a probe and around 1.42 for the polypeptides where pyrene was randomly attached along the backbone. These results indicate that pyrene whether free in solution or covalently attached to the polypeptide is located in an apolar environment and that the polypeptide does generate

hydrophobic microdomains. The higher values of the I_1/I_3 ratios obtained for the labeled pyrenes is a direct result of the restriction in their mobilities which lowers their ability to target the hydrophobic microdomains generated by the polypeptide. Figure 4.8 shows the steady-state fluorescence emission spectra of the different polypeptide solutions. Very little pyrene excimer is observed for the end-labeled polypeptide and the sample where pyrene is used as a probe. The I_1/I_3 ratio of EPy–$(Asp_1Phe_1)_n$–44 was not taken into account since it has been reported that the pyrene label loses its sensitivity to the environment when it is connected to a polymer with a butyl linker.[21] All randomly labeled polypeptides show emission from the pyrene excimer which increases as the pyrene content increases, as expected.[53]

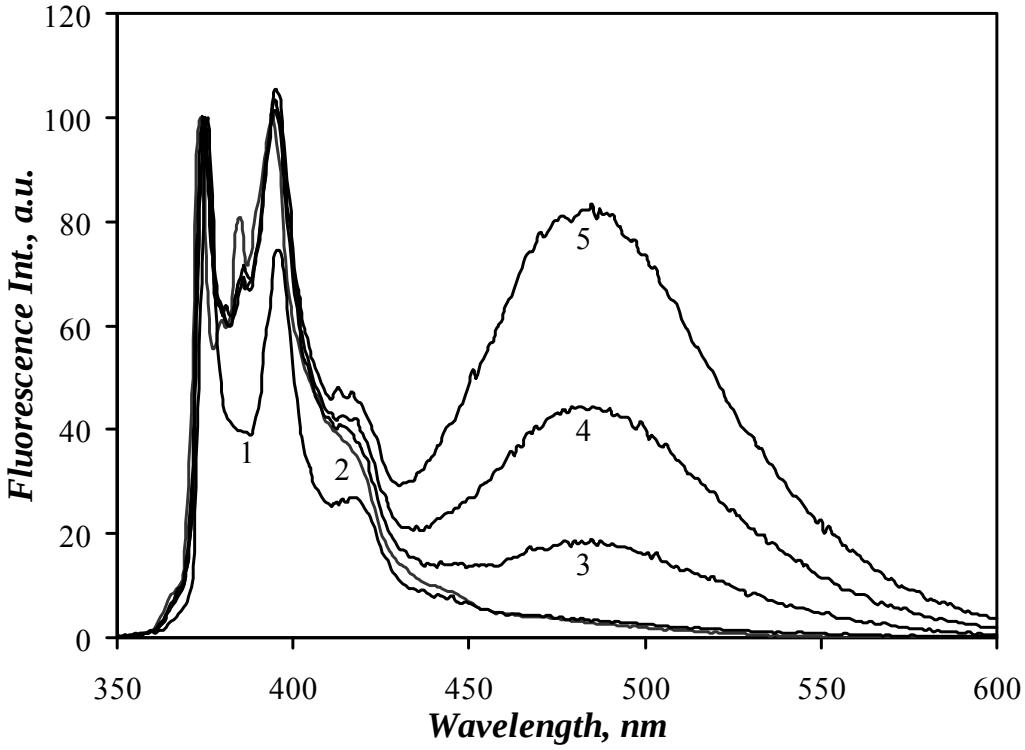

Figure 4.8. Steady-state emission spectra normalized at 375 nm: 1) [EPy–$(Asp_1Phe_1)_n$–44] = 0.32 g/L, λ_{ex} = 346 nm; 2) $(Asp_1Phe_1)_n$ + Py, [$(Asp_1Phe_1)_n$] = 1.5 g/L, [*Py*] = 1.7×10^{-5} M, λ_{ex} = 338 nm; 3) [RPy–$(Asp_1Phe_1)_n$–70] = 0.14 g/L, λ_{ex} = 346 nm; 4) [RPy–$(Asp_1Phe_1)_n$–132] = 0.54 g/L, λ_{ex} = 346 nm; 5) [RPy–$(Asp_1Phe_1)_n$–221] = 0.26 g/L, λ_{ex} = 346 nm.

The fluorescence decays of the pyrene monomer and excimer (Figure 4.9) were acquired for the solutions used in Figure 4.8. The decays could be fitted by a sum of three exponentials whose pre-exponential factors and decay times are listed in Tables 4.3 and 4.4 for the pyrene monomer and excimer, respectively.

Table 4.3. Summary of the pyrene monomer decay times and pre-exponential factors obtained for the polypeptide solutions

Sample	τ_{M1} (ns)	a_{M1}	τ_{M2} (ns)	a_{M2}	τ_{M3} (ns)	a_{M3}	$\langle\tau_0\rangle$ (ns)	χ^2
$(Asp_1Phe_1)_n$ + Py	8.6	0.26	118	0.35	299	0.38	157	1.10
EPy–$(Asp_1Phe_1)_n$–44	10.7	0.13	92	0.30	150	0.56	113	1.15
RPy–$(Asp_1Phe_1)_n$–70	17.5	0.16	78	0.16	176	0.68	135	1.18
RPy–$(Asp_1Phe_1)_n$–132	13.3	0.25	73	0.21	176	0.54	114	0.94
RPy–$(Asp_1Phe_1)_n$–221	10.0	0.26	57	0.23	172	0.51	104	1.00
RPy–$(Asp)_n$–229	7.1	0.09	53	0.16	128	0.75	105	1.08

The first entry of Table 4.3 indicates that when pyrene is used as a probe in the polypeptide solution, 38 % of all pyrene monomers emit with a 299 ns decay time. A decay time of 299 ns observed for pyrene in aerated polypeptide solution is rather long since pyrene dissolved in an aerated 0.01 M Na_2CO_3 pH 9 aqueous solution has a lifetime of 128 ns. Since the I_1/I_3 ratio suggests that pyrene is located in an environment less polar than water, these long-lived pyrenes are located inside the hydrophobic domains generated by the polypeptide chains. While inside these hydrophobic domains, pyrene is protected from the quenching of oxygen dissolved in the aqueous solution. Similarly long decay times were also observed for

pyrene dissolved in SMA aggregates.[30]

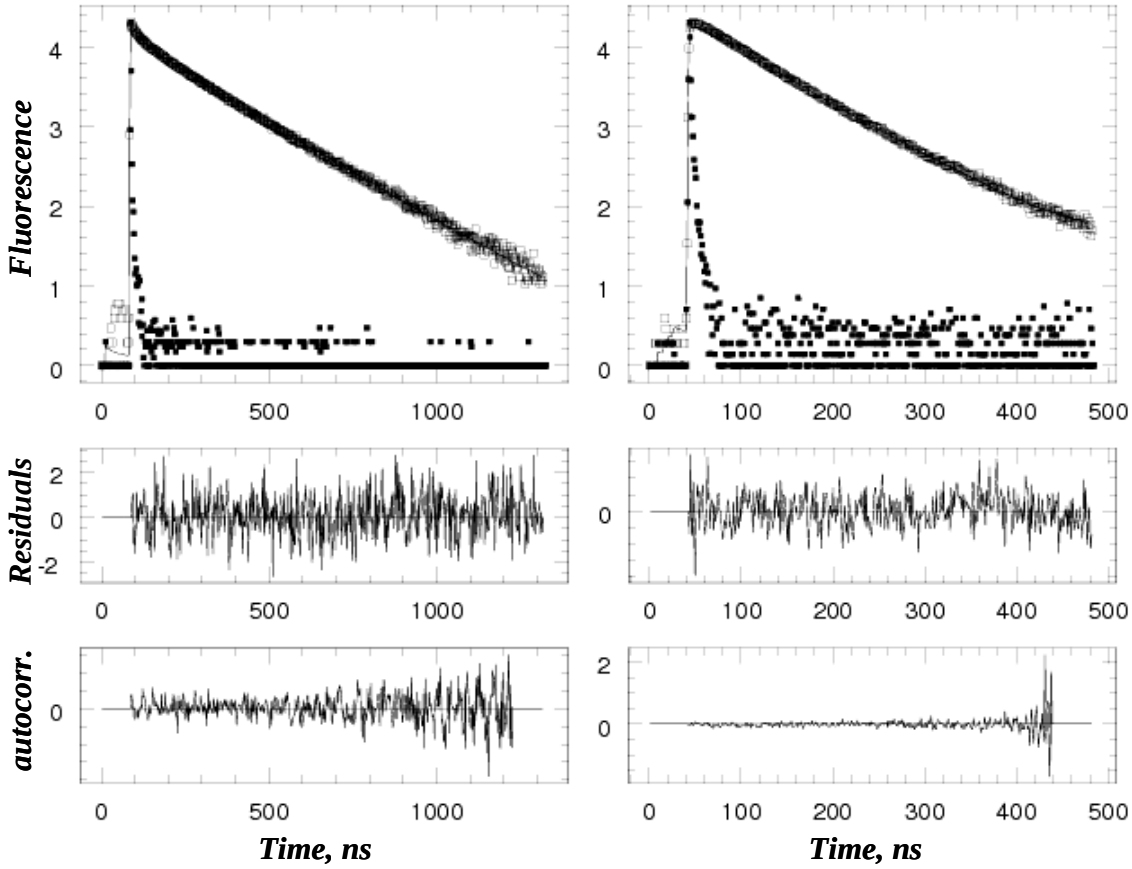

Figure 4.9. Monomer (left) and excimer (right) fluorescence decays of RPy–$(Asp_1Phe_1)_n$–132 in 0.01 M Na_2CO_3 solution at pH 9, [*Polypeptide*] = 0.54 g/L. The samples were excited at 346 nm. The monomer and excimer decays were acquired at 374 and 510 nm, respectively. The decays were fitted with a sum of exponentials. The χ^2 were 0.94 and 1.14 for the monomer and the excimer, respectively.

The fact that a hydrophobic organic molecule like pyrene can be incorporated inside and protected by the polypeptide suggests that $(Asp_1Phe_1)_n$ could be used as a potential carrier of hydrophobic drugs. Unfortunately only a small amount of pyrene (1.7×10^{-5} M) could dissolve molecularly in the 1.5 g/L polypeptide solution. Nevertheless, a pyrene concentration of 1.7×10^{-5} M is 24 times larger than the concentration of pyrene in water

(0.7×10^{-6} M)[54] so that the decay times τ_1 and τ_2 obtained with substantial pre-exponential factors a_{M1} and a_{M2} can not be attributed to pyrene in the aqueous solution. These shorter decaytimes are certainly due to pyrenes associated with the polypeptides but more exposed to the solvent. Also residual pyrene association into pyrene aggregates might be occurring leading to shorter decay times.

The fluorescence decays of the pyrene monomer of all pyrene-labeled polypeptides were also fitted with three exponentials. Poly(aspartic acid) being less hydrophobic than $(Asp_1Phe_1)_n$, it is expected to provide less protection from the solvent. This is indeed observed since all $(Asp_1Phe_1)_n$ samples labeled with 1-pyrenemethylamine (i.e. the "R" series in Table 4.3) have a substantially larger τ_3 decaytime (175 ns) than RPy–$(Asp)_n$–229 (τ_3 = 128 ns). The pyrene derivative bearing a butyl linker in EPy–$(Asp_1Phe_1)_n$–44 has a shorter natural lifetime and can not be compared with the polypeptides randomly labeled with longer-lived 1-pyrenemethylamine.[55]

The pyrene excimer can form via diffusional encounters between an excited pyrene and a ground-state pyrene, or by the direct excitation of ground-state pyrene aggregates.[20,21,53] In order to determine how the excimer of the pyrene-labeled polypeptides is formed, time-resolved fluorescence decays of the excimer of the randomly labeled polypeptides were acquired, since these are the only ones which give rise to excimer formation (Figure 4.8). A rise time is observed in the excimer decay if excimer formation occurs via diffusion whereas the rise time is absent when the excimer is formed from direct excitation of the pyrene ground-state aggregates. Figure 4.9 shows the excimer decay of RPy–$(Asp_1Phe_1)_n$–132. A very small rise time is visible at the beginning of the decays. Similarly short rise times were observed for the other two randomly labeled polypeptides.

The magnitude of the rise time is calculated using the pre-exponential factors obtained from the fits of the fluorescence decays. The negative pre-exponential factors are associated with the rise time and the positive ones with the decay. The ξ parameter being the ratio of the sum of the negative pre-exponential factors over the sum of the positive ones yields information about the process by which the excimer is formed. When excimer formation occurs via diffusional encounters only, ξ equals –1.0. ξ becomes more positive as more ground-state dimers are present. The ξ values listed in Table 4.4 suggest that excimer formation occurs mainly via direct excitation of pyrene ground-state dimers. The ξ ratio in Table 4.4 becomes less positive as the labeling level increases. The decrease of ξ with increasing pyrene content is certainly an analysis problem due to the second decaytime τ_2 becoming too close to the risetime τ_1. Nevertheless, for RPy–$(Asp_1Phe_1)_n$–70 and RPy–$(Asp_1Phe_1)_n$–132 where τ_{E1} and τ_{E2} are sufficiently well separated, a small rise time is observed indicating the formation of excimer by diffusion. Excimer formation by diffusion is enabled by the hydrophobic microdomains constituted of the Phe units of $(Asp_1Phe_1)_n$ that solubilize the pyrene label.

Table 4.4. Summary of the excimer decay times and the rise time calculated for the randomly labeled polypeptides.

Sample	τ_{E1} (ns)	a_{E1}	τ_{E2} (ns)	a_{E2}	τ_{E3} (ns)	a_{E3}	ξ	χ^2
RPy–$(Asp_1Phe_1)_n$–70	13	–0.23	50	0.88	84	0.35	–0.19	1.15
RPy–$(Asp_1Phe_1)_n$–132	18	–0.37	32	0.54	68	0.82	–0.27	1.14
RPy–$(Asp_1Phe_1)_n$–221	22	–0.75	29	0.98	70	0.77	–0.43	1.25
RPy–$(Asp)_n$–229	4.3	0.15	26	0.41	58	0.44	0.00	1.04

No rise time could be detected in the excimer decay of RPy–$(Asp)_n$–229 indicating that all pyrene excimer is generated via direct excitation of pyrene aggregates. The absence of hydrophobic aryl side chains in $(Asp)_n$ is certainly responsible for preventing the partial solubilization of the pyrenyl pendants achieved by the RPy–$(Asp_1Phe_1)_n$ samples. Consequently the formation of ground-state pyrene aggregates is favored with RPy–$(Asp)_n$–229 and no excimer is formed by diffusion. The same result has been reported for poly(L-glutamic acid) randomly labeled with 1-pyrenemethylamine.[56]

Steady-state and time-resolved fluorescence quenching experiments were carried out on the different types of pyrene solutions to further investigate the hydrophobic microdomains generated by the polypeptide. The polypeptide concentration for these solutions was approximately 0.15 g/L for the labeled polypeptides and 1.5 g/L for the solution where pyrene was molecularly dissolved. Nitromethane, CH_3NO_2, was used as a neutral water-soluble quencher of pyrene. Upon the addition of the quencher, the fluorescence intensity of the pyrene monomer decreases and the number-average lifetime shortens as shown in Figure 4.10 for the solution in which pyrene is molecularly dissolved.

The fluorescence spectra and decays shown in Figure 4.10 allow one to plot the ratios I_0/I and $<\tau_0>/<\tau>$ as a function of quencher concentration, $[Q]$. I_0 and I represent the fluorescence intensity of pyrene in the absence and presence of quencher, respectively. Similarly, $<\tau_0>$ and $<\tau>$ are the number-average lifetime of pyrene in the absence and presence of quencher, respectively. Quenching of pyrene results in a decrease of I and $<\tau>$. A plot of the I_0/I and $<\tau_0>/<\tau>$ ratios as a function of quencher concentration, $[Q]$, (equation 1.5 Chapter 1), is referred to as a Stern-Volmer plot.[47] These plots are shown in Figure 4.11.

The I_o/I and $<\tau_o>/<\tau>$ ratios do not overlap. This is a clear indication that static

quenching is occurring.[47] Static quenching occurs when a ground-state complex is formed between the chromophore and the quencher. Upon excitation of the chromophore, those chromophores which are complexed do not emit whereas those which are not complexed with the quencher can emit. Consequently, a steady-state fluorescence experiment reports on all chromophores present in solution, whereas a time-resolved fluorescence experiment reports only on those chromophores that can emit, i.e. are not complexed. The I_o/I ratio increases more steeply with [Q] than the $<\tau_o>/<\tau>$ ratio when static quenching is occurring, as observed in Figure 4.11. Since the $<\tau_o>/<\tau>$ ratio increases with [Q], it indicates that quenching of the excited pyrene occurs also via diffusion-controlled encounters with quencher molecules.

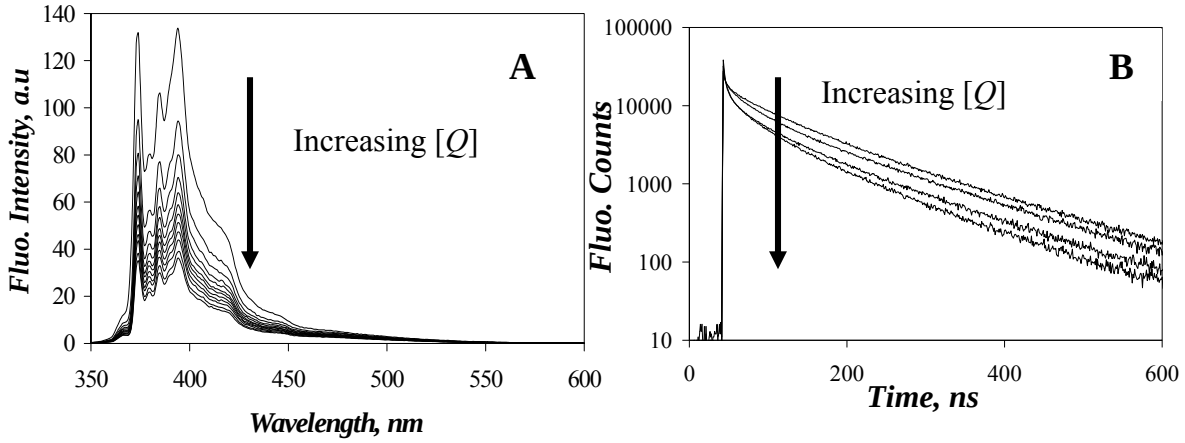

Figure 4.10. Nitromethane quenching of pyrene used as a probe by steady-state A) and time-resolved B) fluorescence for a range of nitromethane concentrations. λ_{ex} = 338 nm, [Py] = 1.7 × 10^{-5} M, [$(Asp_1Phe_1)_n$] = 1.5 g/L.

Another interesting feature of Figure 4.11 is that the $<\tau_o>/<\tau>$ ratio plateaus for high quencher concentrations. Since the $<\tau_o>/<\tau>$ ratio reports only on those pyrenes which are not complexed with nitromethane, the plateau observed in Figure 4.11 indicates that those

pyrenes which are not complexed with nitromethane can not be quenched when larger amounts of nitromethane are added. In other words, they are protected from quenching.[47]

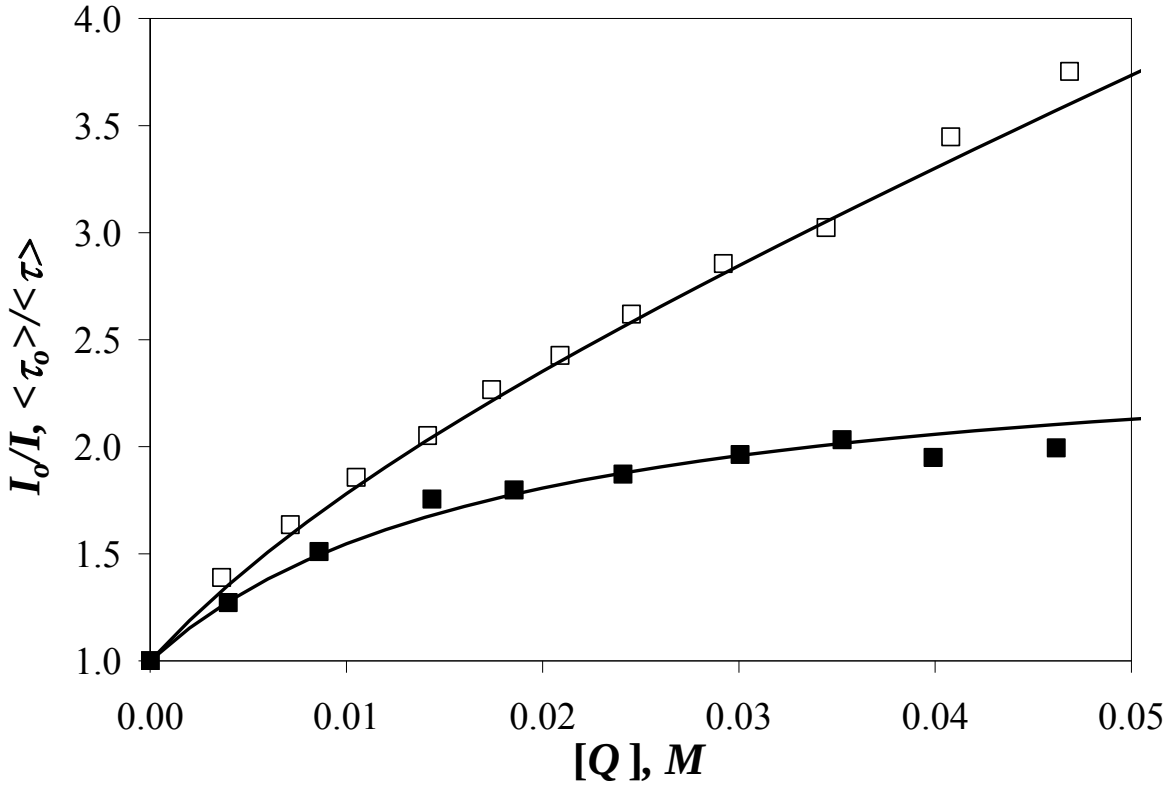

Figure 4.11. Stern-Volmer plot obtained by steady-state (□) and time-resolved (■) fluorescence with 1.7×10^{-5} M pyrene dissolved in 1.5 g/L of polypeptide in 0.01 M Na_2CO_3 solution at pH 9. λ_{ex} = 338 nm, λ_{em} = 374 nm.

The data shown in Figure 4.11 indicate that static, dynamic, and protective quenching are occurring concurrently. They are represented by Scheme 4.2 where α_1 and α_2 are the molar fractions of pyrenes which are protected and quenched diffusionally, respectively. The fraction $1 - \alpha_1 - \alpha_2$ represents those pyrenes which are complexed with nitromethane. The rate constant for dynamic quenching is k_Q whereas K_S is the equilibrium constant for the

formation of the complex between pyrene and nitromethane. Since no model could be found in the literature to analyze the data shown in Figure 4.11 according to Scheme 4.2, Equations 4.10 and 4.11 were derived as shown in the Appendix located in section 4.7, to yield the parameters $f_a = \alpha_2/(\alpha_1 + \alpha_2)$, k_Q, and K_S. Equations 4.10 and 4.11 were used to fit the trends shown in Figure 4.11.

Scheme 4.2. Pathways for dynamic, static, and protective quenching

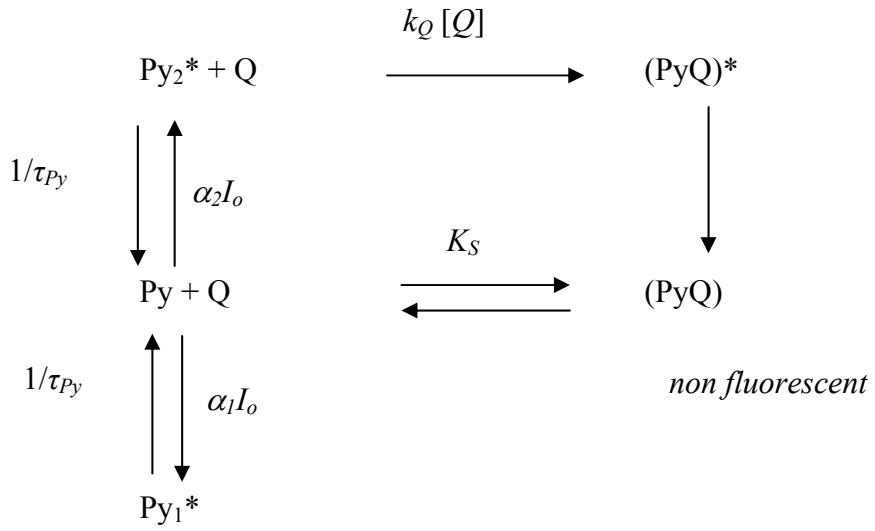

$$\frac{I_o}{I}\left(1 - f_a + \frac{f_a}{1 + k_Q\,\tau_{Py}\,[Q]}\right) = 1 + K_S[Q] \qquad (4.10)$$

$$\frac{<\tau_o>}{\Delta<\tau>} = \frac{1}{f_a} + \frac{1}{f_a k_Q \tau_{Py}} \times \frac{1}{[Q]} \qquad (4.11)$$

In Equations 4.10 and 4.11, f_a represents the fraction of accessible pyrenes that are quenched diffusionally by nitromethane. The quantity $\Delta<\tau>$ represents the difference $<\tau_o> -$

$<\tau>$. The brackets for $<\tau_o>$ and $<\tau>$ indicate that the number-average lifetime is being used. First the data obtained by time-resolved fluorescence were used to plot the ratio $<\tau_o>/\Delta<\tau>$ as a function of $1/[Q]$. Fit of this plot with a straight line according to Equation 4.11 yielded f_a and k_Q. These parameters where used in Equation 4.10 with the I_o/I ratios obtained by steady-state fluorescence to yield K_S. As very often done when the pyrene monomer with no quencher exhibits a multiexponential decay, the lifetime of pyrene, τ_{Py}, in Equations 4.10 and 4.11 was approximated by $<\tau_o>$.[30]

When this analysis was applied to the data shown in Figure 4.11, f_a, k_Q, and K_S were found to equal 0.60, 0.92×10^9 $M^{-1}.s^{-1}$, and 15.8 M^{-1}, respectively. An f_a value of 0.60 implies that 40 % of all non-complexed pyrenes are not accessible to the quenchers in the solution. This result agrees with the fact that 38 % of all non-complexed pyrenes emit with a lifetime of 299 ns (see a_{M3} for the "$(Asp_1Phe_1)_n$ + Py" entry in Table 4.3), much longer than the 128 ns lifetime of pyrene in the 0.01 M Na_2CO_3 pH 9 solution. The quenching rate constant, k_Q, for the solution of $(Asp_1Phe_1)_n$ and pyrene is 10 times smaller than that of pyrene by nitromethane in the 0.01 M Na_2CO_3 solution at pH 9 found experimentally to equal 9.5×10^9 $M^{-1}.s^{-1}$.

Quenching studies were also carried out for the end-labeled and the randomly labeled $(Asp_1Phe_1)_n$, and for the randomly labeled poly(aspartic acid) using both steady-state and time-resolved fluorescence measurements. The results are reported in the form of Stern-Volmer plots shown in Figure 4.12. A striking difference is observed for the labeled $(Asp_1Phe_1)_n$ samples which do not exhibit the protective quenching found when pyrene is used as a molecular probe (f_a = 1.0). All the plots are linear, indicating that efficient quenching of pyrene takes place and the main process of quenching is via diffusional

encounters of pyrene with nitromethane. As a result the data shown in Figure 4.12 were fitted according to the classic Stern-Volmer Equations 4.12 and 4.13.[47] A small amount of static quenching also takes place as slight differences are observed between the slopes of the straight lines obtained by steady-state and time-resolved fluorescence. A linear Stern-Volmer plot is also observed for the labeled poly(aspartic acid) which means that diffusional quenching is taking place.

$$\frac{I_o}{I} = 1 + k_Q < \tau_o > [Q] \tag{4.12}$$

$$\frac{< \tau_o >}{< \tau >} = 1 + k_Q < \tau_o > [Q] \tag{4.13}$$

The quenching parameters k_Q and f_a listed in Table 4.5 indicate that the quenching of pyrene is more efficient when pyrene is covalently attached to the polypeptide than when it is used as a free probe. It would seem that the polypeptide is able to generate a few hydrophobic microdomains that can accommodate some free pyrene molecules which are protected from quenching by nitromethane. However once the pyrene is attached onto the polypeptide, it also locates itself inside the microdomains generated by Phe, as suggested by the I_1/I_3 ratio value of 1.42 lower than that of 1.69 found for Py–PEO in aqueous solution,[52] but those hydrophobic domains are unable to protect efficiently the pyrenyl pendants from being quenched. The pyrene labels are more exposed to the quencher and efficient quenching is taking place.

The quenching rate constant, k_Q, of the pyrene-labeled $(Asp_1Phe_1)_n$ is decreased to a

third of its value obtained for the quenching of pyrene in aqueous solution. This reduction in k_Q is due in part to a loss in mobility of the pyrenyl pendants upon attachment onto the polypeptide. The k_Q values obtained for the pyrene-labeled $(Asp_1Phe_1)_n$ are about half that obtained for RPy–$(Asp)_n$–229. It suggests that $(Asp_1Phe_1)_n$ provides some relative protection against quenching when compared to $(Asp)_n$. Nevertheless, that protection is not sufficient to induce protective quenching as was observed for the $(Asp_1Phe_1)_n$ + Py solution. The similar k_Q values found for the polypeptides labeled either at the end (EPy–$(Asp_1Phe_1)_n$–44) or randomly suggest that the entire chain is similarly exposed to the solvent.

The different techniques used to describe the $(Asp_1Phe_1)_n$ species present in solution fall into two main categories. They can be classified depending on whether they are biased toward observing large structures in solution or not. Experiments carried out by DLS and analyzed with scattering intensity are biased toward probing larger species (Figures 4.5A). The NRET experiments carried out with the fluorescently labeled polypeptides (Figure 4.7) as well as the DLS experiments analyzed by numbers or volumes (Figures 4.5B and C) provide a number-averaged representation of the species present in solution. If most macromolecules are not aggregated, these experiments report the absence of aggregation as found experimentally for $(Asp_1Phe_1)_n$ (Figures 4.5B, 4.5C, 4.7). The results observed by DLS and fluorescence are certainly consistent with a situation where residual polypeptide aggregation occurs in solution but where the majority of polypeptides are isolated.

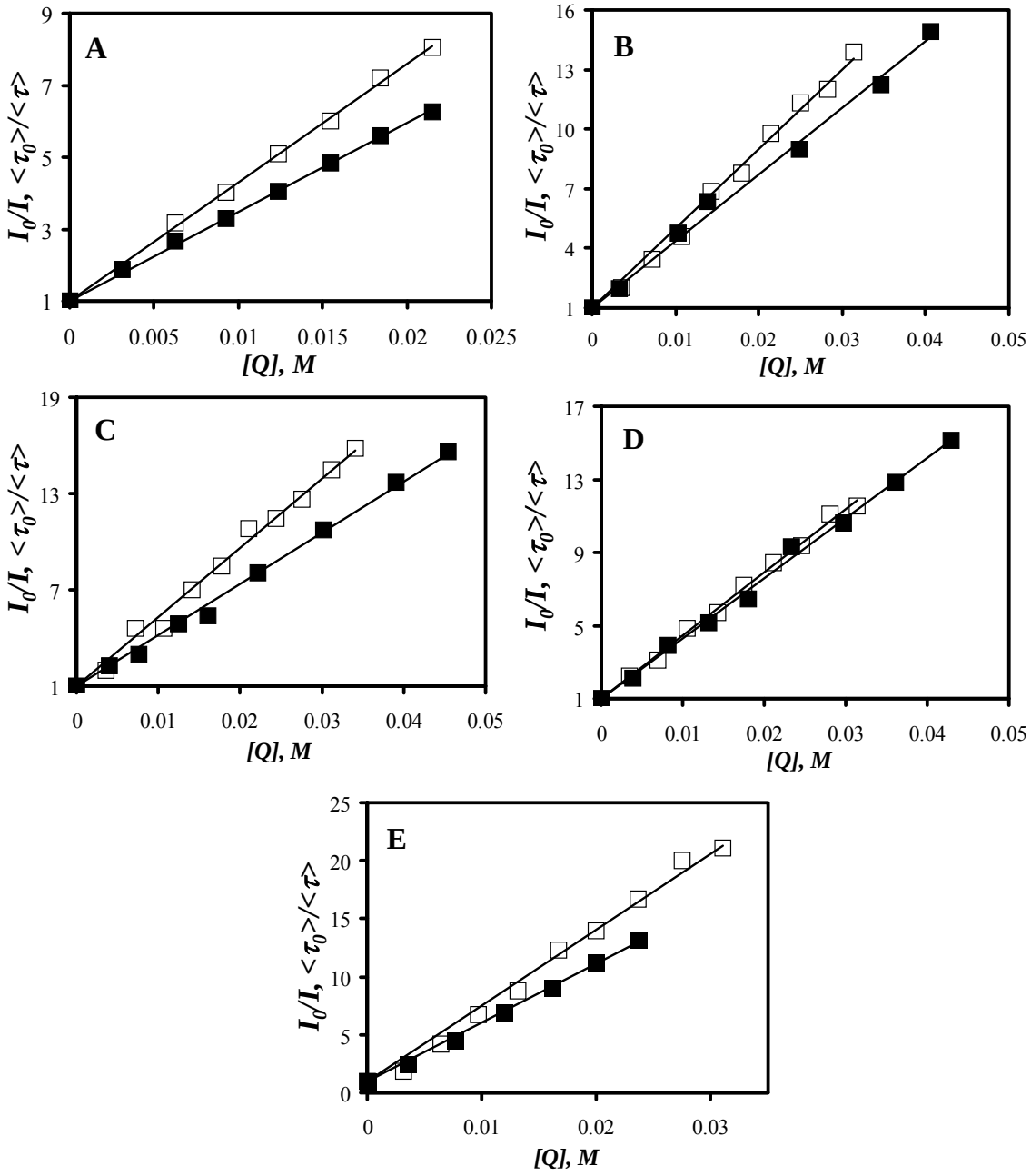

Figure 4.12. Stern-Volmer plots obtained for the labeled polypeptides by steady-state (□) and time-resolved (■) fluorescence. A) EPy–$(Asp_1Phe_1)_n$–44, [*Polypeptide*] = 0.32 g/L [*Py*] = 1.41×10^{-5} M; B) RPy–$(Asp_1Phe_1)_n$–70, [*Polypeptide*] = 0.14 g/L, [*Py*] = 9.52×10^{-6} M; C) RPy–$(Asp_1Phe_1)_n$–132, [*Polypeptide*] = 0.54 g/L, [*Py*] = 7.18×10^{-5} M; D) RPy–$(Asp_1Phe_1)_n$–221, [*Polypeptide*] = 0.26 g/L, [*Py*] = 5.83×10^{-5} M; E) RPy–$P(Asp)_n$–229, [*Polypeptide*] = 0.15 g/L, [*Py*] = 3.44×10^{-5} M in 0.01 M Na_2CO_3 solution at pH 9, λ_{ex} = 346 nm, λ_{em} = 374 nm.

Table 4.5. Summary of parameters retrieved from the analysis with Equations 4.8-4.11 of the steady-state and time-resolved fluorescence quenching trends shown in Figures 4.11 and 4.12.

Sample	$<\tau_0>$ ns	K_S M^{-1}	$10^{-9} \times k_Q$ $M^{-1}s^{-1}$ (SS)	$10^{-9} \times k_Q$ $M^{-1}s^{-1}$ (TR)	f_a
Na_2CO_3 solution	128	n.a.	9.82 ± 0.05	n.a.	n.a.
$(Asp_1Phe_1)_n$ + Py	157	15.8 ± 0.3	n.a.	0.92 ± 0.05	0.61 ± 0.01
RPy–$(Asp)_n$–229	105	11.8 ± 1.1	6.23 ± 0.13	4.82 ± 0.06	1.00
EPy–$(Asp_1Phe_1)_n$–44	113	16.7 ± 2.1	2.91 ± 0.03	2.19 ± 0.18	1.00
RPy–$(Asp_1Phe_1)_n$–70	135	6.5 ± 1.0	2.80 ± 0.05	2.51 ± 0.09	1.00
RPy–$(Asp_1Phe_1)_n$–132	113	12.5 ± 1.9	3.81 ± 0.06	2.82 ± 0.04	1.00
RPy–$(Asp_1Phe_1)_n$–221	104	1.8 ± 0.7	3.34 ± 0.04	3.18 ± 0.05	1.00

To further test the validity of these conclusions, the following experiment was conducted. A 0.05 g/L solution of $(Asp_1Phe_1)_n$ was prepared and the light scattering and fluorescence intensities of the solution were determined before and after the solution was filtered through 20 nm pores. The scattering and fluorescence intensities obtained before and after filtration are shown in Figure 4.13. Filtering the $(Asp_1Phe_1)_n$ solution had a major effect on the scattering intensity which was reduced by 75 %. It indicates that the large polypeptide aggregates were filtered out. On the other hand, filtering did not affect much the intrinsic fluorescence intensity of the polypeptide, demonstrating that the aggregates involve a small proportion of all polypeptides.

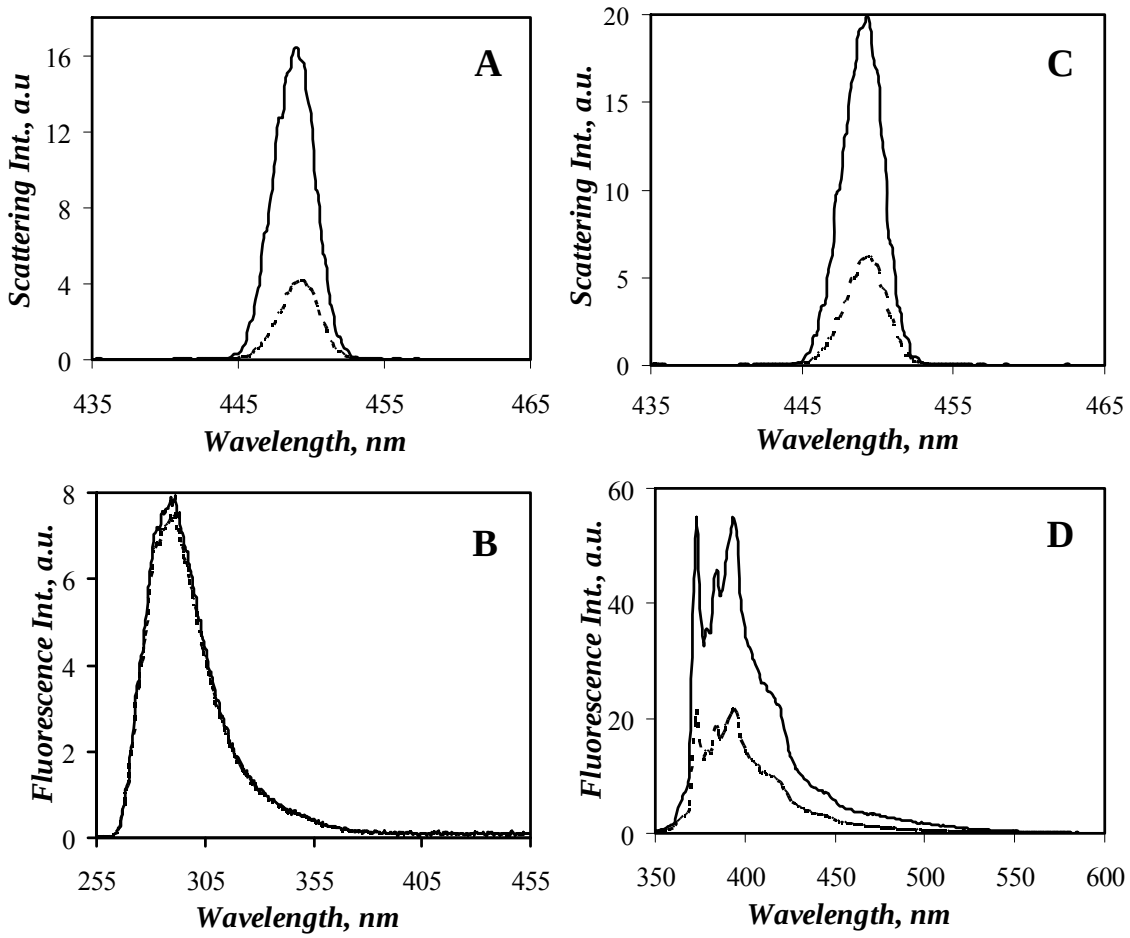

Figure 4.13. (A) Light scattering intensity (λ_{ex} = λ_{em} = 450 nm) and (B) fluorescence emission spectra (λ_{ex} = 255 nm) of $(Asp_1Phe_1)_n$ before (——) and after (– – –) filtration of 0.05 g/L solutions $(Asp_1Phe_1)_n$; (C) Light scattering intensity (λ_{ex} = λ_{em} = 450 nm) and (D) fluorescence emission spectra (λ_{ex} = 338 nm) before (——) and after (– – –) filtration of 0.05 g/L solutions $(Asp_1Phe_1)_n$ + Py in 0.01 M Na_2CO_3.

A similar experiment helps rationalize why the results of the fluorescence quenching experiments obtained with $(Asp_1Phe_1)_n$ and molecular pyrene are so different from those obtained with the pyrene-labeled $(Asp_1Phe_1)_n$ (cf. Figures 4.11 and 4.12). Filtering the $(Asp_1Phe_1)_n$ + Py solutions results in a substantial decrease of light scattering (Figure 4.13C) and pyrene fluorescence (Figure 4.13D). It suggests that molecular pyrene targets the

hydrophobic pockets provided by the polypeptide aggregates. The situation is different for the pyrene-labeled polypeptides where the pyrene label is confined to a single chain since the polypeptides have shown little tendency to aggregate (Figures 4.5B and C, Figure 4.7). There the pyrene labels are not free to target the hydrophobic domains generated by the few polypeptide aggregates. They are more accessible to the solvent and no protective quenching is observed (Figure 4.12).

In summary, using pyrene as a molecular probe provides information about the polypeptide aggregates (Figure 4.11), as does DLS analyzed with light scattering intensities (Figure 4.5A). Covalently attaching a chromophore onto the polypeptide enables the study of the overall polypeptide population, as do NRET (Figure 4.7) and DLS analyzed with particle volumes or numbers (Figures 4.5B and C). The combined use of different types of fluorescence and DLS experiments results in a detailed description of the $(Asp_1Phe_1)_n$ solutions.

4.5. Conclusions

CD, DLS, and various fluorescence techniques have been employed to investigate the solution properties of the amphiphilic polypeptide $(Asp_1Phe_1)_n$. Those were compared to the solution properties of $(Asp)_n$. CD spectra (Figure 4.4) show that $(Asp_1Phe_1)_n$ exhibits no defined secondary structure and that labeling of $(Asp_1Phe_1)_n$ or $(Asp)_n$ with a chromophore does not affect the CD spectra of the polypeptides. $(Asp_1Phe_1)_n$ forms predominantly unimolecular micelles in the 0.01 M Na_2CO_3 solution at pH 9 as shown by DLS which detects the presence of particles 3-7 nm in diameter (Figures 4.5B and C). The quasi-absence of fluorescence NRET between the Np- and Py-labeled polypeptides also supports the

formation of unimolecular micelles (Figure 4.7). The presence of some hydrophobic microdomains was revealed by both the low value of the I_1/I_3 ratio and the long decay time of pyrene. Molecular pyrene in solution targets those hydrophobic domains generated by the few polypeptide aggregates which are compact enough to lead to protective quenching (Figure 4.11). Quenching experiments carried out on the labeled polypeptides show no evidence of protective quenching (Figure 4.12). Instead the quenching process appears to be diffusion controlled. This is expected from individual polymer coils which do not offer sufficient protection against quenching.

4.6. References and Notes:

1. Kwon, G. S.; Forrest, M. L. *Drug Devel. Res*. **2006**, *67*, 15-22.
2. Pedersen, J. S.; Svaneborg, C. *Curr. Opin. Colloid Interface Sci*. **2002**, *7*, 158-166.
3. Discher, D. E.; Eisenberg, A. *Science* **2002**, *297*, 967-973.
4. Raez, J.; Tomba, J. P.; Manners, I.; Winnik, M. A. *J. Am. Chem. Soc.* **2003**, *125*, 9546-9547.
5. Jenkins, R. D.; Bassett, D. R.; Shay, G. D.; Smith, D. E.; Argyropoulos, J. N.; Loftus, J. E. *PCT Int*. *Appl*. **1993**, 115 WO 93/24544.
6. Warriner, H. E.; Idziak, S. H. J.; Slack, N. L.; Davidson, P.; Safinya, C. R. *Science* **1996**, *271*, 969 – 973.
7. Kataoka, K.; Harada, A.; Nagasaki, Y. *Adv*. *Drug Deliv*. *Rev*. **2001**, *47*, 113-131.
8. *Polymers in Aqueous Media: Performance through Association*. Ed. J. E. Glass; ACS Advances in Chemistry Series 223; 1989.
9. *Hydrophilic Polymers: Performance with Environmental Acceptance*. Ed. J. E. Glass; ACS Advances in Chemistry Series 248; 1996.
10. *Associative Polymers in Aqueous Media*. Ed. J. E. Glass; ACS Advances in Chemistry Series 765; 2000.
11. *Polymer-Surfactant Systems*. Kwak, J. C.; Surfactant Science Series 77; Marcel Decker; New York, 1998.
12. Winnik, M. A.; Yekta, A. *Curr. Opin. Colloid Interface Sci.* **1997**, *2*, 424-436.
13. Talingting, M. R.; Munk, P.; Webber, S. E.; Tuzar, Z. *Macromolecules* **1999**, *32*, 1593-1601.
14. Anghel, D. F.; Toca-Herrera, J. L.; Winnik, F. M.; Rettig, W.; v. Klitzing, R. *Langmuir* **2002**, *18*, 5600-5606.
15. Akiyoshi, K.; Deguchi, S.; Moriguchi, N.; Yamaguchi, S.; Sunamoto, J *Macromolecules* **1993**, *26*, 3062-3068.
16. Lee, K. Y.; Jo, W. H.; Kwon, I. C.; Kim, Y.; Jeong, S. Y. *Macromolecules*, **1998**, *31*, 378-383.
17. Nichifor, M.; Lopes, A.; Carpov, A.; Melo, E. *Macromolecules*, **1999**, *32*, 7078-7085.
18. Volpert, E.; Selb, J.; Candau, F. *Macromolecules* **1996**, *29*, 1452-1463.
19. Yusa, S.-I.; Kakimoto, K.; Yamamoto, T.; Morishima, Y. *Macromol. Rapid Commun.*

2001, *22*, 253-256.

20. Winnik, F. M.; Regismond, S. T. A. *Colloids Surf. A: Phys. Eng. Asp.* **1996**, *118*, 1-39.
21. Duhamel, J. in *Molecular Interfacial Phenomena of Polymers and Biopolymers*. Ed. P. Chen, CRC Press, 2005; pp 214-248.
22. Chassenieux, C.; Nicolai, T.; Durand, D. *Macromolecules* **1997**, *30*, 4952-4958.
23. Abrahnsén-Alami, S.; Alami, E.; François, J. *J. Colloid Interface Sci.* **1996**, *179*, 20-33.
24. Séréno, Y.; Aznar, R.; Porte, G.; Berret, J.-F.; Calvet, D.; Collet, A.; Viguier, M. *Phys. Rev. Lett.* **1998**, *81*, 5584-5587.
25. Beaudoin, E.; Borisov, O.; Lapp, A.; Billon, L.; Hiorns, R. C.; François, J. *Macromolecules* **2002**, *35*, 7436-7447.
26. Shen, H.; Eisenberg, A. *J. Phys. Chem. B.* **1999**, *103*, 9473-9487.
27. Persson, K.; Wang, G.; Olofsson, G. *J. Chem. Soc. Faraday Trans.* **1994**, *90*, 3555-3562.
28. Zhang, K.; Xu, B.; Winnik, M. A.; Macdonald, P. M. *J. Phys. Chem.* **1996**, *100*, 9834-9841.
29. Winnik, F. M. *Chem. Rev.* **1993**, *93*, 587-614.
30. Claracq, J.; Santos, S. F. C. R.; Duhamel, J.; Dumousseaux, C.; Corpart, J. *Langmuir*. **2002**, *18*, 3829-3835.
31. Senter, P. D.; Kopecek, J. *Mol. Pharm.* **2004**, *1*, 395-398.
32. Kovacs, J.; Giannotti, R.; Kapoor, A. *J. Am. Chem. Soc.* **1966**, *88*, 2282-2292.
33. DeTar, D. F.; Gouge, M.; Honsberg, W.; Honsberg, U. *J. Am. Chem. Soc.* **1967**, *89*, 988-998.
34. DeTar, D. F.; Vajda, T. *J. Am. Chem. Soc.* **1967**, *89*, 998-1004.
35. James, D. R.; Demmer, D. R. M.; Verrall, R. E.; Steer, R. P. *Rev. Sci. Instrum.* **1983**, *54*, 1121-1130.
36. Press, W. H.; Flannery, B. P.; Teukolsky, S. A.; Vetterling, W. T. *Numerical Recipes. The Art of Scientific Computing (Fortran Version)*; Cambridge University Press: Cambridge, 1992.
37. Nemeth, S.; Jao, T.-C.; Fendler, J. H. *Photochem. Photobiol. A: Chem*. **1994**, *78*, 229-235.
38. Zhang, L.; Yu, K.; Eisenberg, A. *Science* **1996**, *272*, 1777-1779.

39. Hongwei, S.; Zhang, L.; Eisenberg, A. *J. Am. Chem. Soc.* **1999**, *121*, 2728-2740.
40. This extinction coefficient was determined in the laboratory.
41. Kwon, G. S.; Naito, M.; Yokoyama, M.; Okano, T.; Sakurai, Y.; Kataoka, K. *Pharma. Res.* **1995**, *12*, 192-195.
42. Demchenko, A. P. *Ultraviolet Spectroscopy of Proteins*. Springer Verlag, New York, 1981, p 3.
43. McDiarmid, R.; Doty, P. *J. Phys. Chem.* **1966**, *70*, 2620-2627.
44. Sage, H. J.; Fasman, G. D. *Biochemistry* **1966**, *5*, 286-296.
45. Auer, H. E.; Doty, P. *Biochemistry* **1966**, *5*, 1708-1715.
46. Auer, H. E.; Doty, P. *Biochemistry* **1966**, *5*, 1716-1725.
47. Lakowicz, J. R. *Principles of Fluorescence Spectroscopy, 2nd Ed*. Kluwer Academic/Plenum Publishers: New York, 1999.
48. Stryer, L.; Haugland, R. P. *Proc. Natl. Acad. Sci.* **1967**, *58*, 719-726.
49. Berlman, I. B. *Energy Transfer Parameters of Aromatic Compounds*; Academic Press: New York, 1973.
50. Kalyanasundaran, K.; Thomas, J. K. *J. Am. Chem. Soc.* **1977**, *99*, 2039-2044.
51. Dong, D. C.; Winnik, M. A. *Can. J. Chem.* **1984**, *62*, 2560-2565.
52. Siu, H.; Duhamel, J. *Macromolecules* **2006**, *39*, 1144-1155.
53. Birks, J. B. *Photophysics of Aromatic Molecules*; Wiley: New York, 1970; p 351.
54. Yekta, A.; Duhamel, J.; Brochard, P.; Adiwidjaja, H.; Winnik, M. A. *Macromolecules* **1993**, *26*, 1829-1836.
55. Mathew, A. K.; Duhamel, J.; Gao, J. *Macromolecules* **2001**, *34*, 1454-1469.
56. Duhamel, J.; Kanagalingam, S.; O'Brien, T.; Ingratta, M. *J. Am. Chem. Soc.* **2003**, *125*, 12810-12822.

4.7. Appendix

Scheme A1: Photophysical processes undergone by a chromophore *D* subject to static, protective, and dynamic quenching.

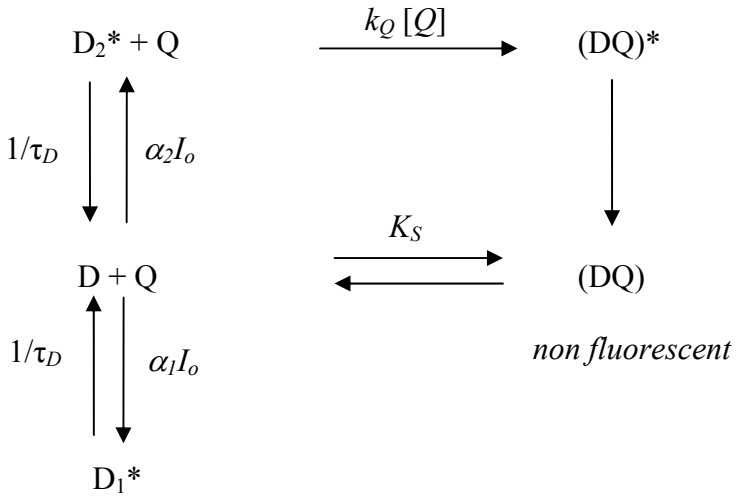

Scheme A1 states that a fraction $(1 - \alpha_1 - \alpha_2)$ of chromophores *D* associate with the quencher *Q* with an association constant K_S, a fraction α_1 of the chromophores *D* are not quenched, and a fraction α_2 of the chromophores *D* are quenched by diffusion with a quenching rate constant k_Q. According to Scheme A1, the following equations can be derived.

$$\frac{d[D_1^*]}{dt} = \alpha_1 I_0 - \frac{1}{\tau_D}[D_1^*] \qquad \text{(A1)}$$

$$\frac{d[D_2^*]}{dt} = \alpha_2 I_0 - \left(\frac{1}{\tau_D} + k_Q[Q]\right)[D_2^*] \qquad \text{(A2)}$$

$$K_S = \frac{[DQ]}{[D][Q]} = \frac{1-\alpha_1-\alpha_2}{(\alpha_1+\alpha_2)[Q]} \qquad \text{(A3)}$$

$$f_a = \frac{\alpha_2}{\alpha_1 + \alpha_2} \tag{A4}$$

In Equations A1 and A2, I_o represents the concentration of chromophores D absorbing a photon per unit time. If the solution is excited with a short pulse of light as done during a time-resolved fluorescence experiment, Equations A1 and A2 can be integrated to yield:

$$[D_1^*] = [D_1^*]_0 \exp\left(-\frac{t}{\tau_D}\right) \tag{A5}$$

$$[D_2^*] = [D_2^*]_0 \exp\left(-t\left(\frac{1}{\tau_D} + k_Q[Q]\right)\right) \tag{A6}$$

Integration of Equations A5 and A6 over time yields Equations A7 and A8, respectively.

$$Int_{D_1} = (1 - f_a)[D^*]_0 \tau_D \tag{A7}$$

$$Int_{D_2} = f_a[D^*]_0 \frac{\tau_D}{1 + k_Q \tau_D [Q]} \tag{A8}$$

In Equations A7 and A8, D^* represents the chromophores which do not form a complex with the quencher and can be detected by time-resolved fluorescence. Equations A7 and A8 can be rearranged into Equation A9 where $I_{TR} = Int_{D1} + Int_{D2}$ and the "o" subscript indicates that no quencher is present in solution.

$$\frac{I_{TRo}}{I_{TRo} - I_{TR}} = \frac{I_{TRo}}{\Delta I_{TR}} = \frac{1}{f_a} \frac{1 + k_Q \tau_D [Q]}{k_Q \tau_D [Q]} = \frac{1}{f_a} + \frac{1}{f_a k_Q \tau_D} \frac{1}{[Q]} \tag{A9}$$

According to Equation A9, a plot of $I_{TRo}/\Delta I_{TR}$ as a function of $[Q]^{-1}$ yields a straight line with

a slope $(f_a k_Q \tau_D)^{-1}$ and an intercept $(f_a)^{-1}$. Since the lifetime of the chromophore τ_D can be determined independently, Equation A9 allows one to estimate the fraction of accessible chromophores f_a and the rate constant for diffusion quenching k_Q.

Experimentally, the fluorescence decays of the chromophore with and without quencher are acquired and fitted with a sum of exponentials. Integration of the fluorescence decays yields the quantities I_{TR} and I_{TRo} which can be used in Equation A9.

Under steady-state irradiation of the solution, the derivatives with respect to time in Equations A1 and A2 equal 0 leading to Equations A10 and A11.

$$[D_1^*] = \alpha_1 \tau_D I_0 \tag{A10}$$

$$[D_2^*] = \frac{\alpha_2 \tau_D I_0}{1 + k_Q \tau_D [Q]} \tag{A11}$$

Equations A3 and A4 can be used to find an expression of α_1 and α_2.

$$\alpha_2 = \frac{f_a}{1 + K_S [Q]} \tag{A12}$$

$$\alpha_1 = \frac{1 - f_a}{1 + K_S [Q]} \tag{A13}$$

Equations A10-A13 can be rearranged into Equation A14.

$$\frac{I_{SSo}}{I_{SS}}\left(1-f_a+\frac{f_a}{1+k_Q\tau_D[Q]}\right)=1+K_S[Q] \qquad \text{(A14)}$$

In Equation A14, the quantities I_{SSo} and I_{SS} represent the fluorescence intensity of the solution without and with quencher. The parameters f_a and k_Q have been determined by conducting time-resolved fluorescence experiments using Equation A9. Plotting the left-hand side of Equation A14 as a function of quencher concentration resulted in a straight line whose slope equals K_S.

Table A-1. Pre-exponential factors and decay times of the fluorescence decays of 1.5 g/L of $(Asp_1Phe_1)_n$ solution with 1.7×10^{-5} M pyrene quenched by nitromethane.

$[Q]$, M	τ_{M1} (ns)	a_{M1}	τ_{M2} (ns)	a_{M2}	τ_{M3} (ns)	a_{M3}	$<\tau_0>$ (ns)	χ^2
0.0000	8.6	0.26	118.15	0.35	299.4	0.38	157.3	1.10
0.003978	18.2	0.39	93.6	0.28	271.6	0.33	123.0	1.22
0.008607	13.0	0.45	87.9	0.26	257.9	0.29	103.5	1.07
0.01436	9.7	0.47	81.6	0.27	249.8	0.25	89.0	1.15
0.018549	9.2	0.47	78.0	0.28	243.1	0.25	87.0	1.07
0.024091	9.0	0.46	76.5	0.29	238.3	0.24	83.5	1.27
0.030059	8.0	0.45	68.6	0.30	231.0	0.24	79.6	1.19
0.035262	7.4	0.47	69.0	0.30	229.34	0.23	76.9	1.17
0.039896	9.0	0.45	72.5	0.32	230.22	0.23	80.1	1.14
0.046174	8.2	0.45	69.6	0.32	227.71	0.23	78.4	1.28

Table A-2. Pre-exponential factors and decay times of the fluorescence decays of 0.15 g/L of EPy–$(Asp_1Phe_1)_n$–44 quenched by nitromethane.

[*Q*], M	τ_{M1} (ns)	a_{M1}	τ_{M2} (ns)	a_{M2}	τ_{M3} (ns)	a_{M3}	$\langle\tau_0\rangle$ (ns)	χ^2
0.00000	10.7	0.13	91.8	0.30	150.0	0.56	113.0	1.15
0.00312	12.5	0.10	56.4	0.78	122.6	0.12	60.1	1.16
0.00620	19.1	0.22	42.0	0.70	114.0	0.08	42.5	1.04
0.00931	22.0	0.56	40.8	0.39	113.4	0.05	34.1	1.17
0.01238	15.7	0.50	31.7	0.49	110.0	0.05	28.0	0.88
0.01543	14.7	0.67	33.2	0.28	109.8	0.04	23.3	1.19
0.01843	13.0	0.73	30.7	0.23	102.4	0.04	20.2	1.07
0.02150	12.0	0.78	31.1	0.18	102.7	0.03	18.1	1.18

Table A-3. Pre-exponential factors and decay times of the fluorescence decays of 0.15 g/L of RPy–$(Asp_1Phe_1)_n$–70 quenched by nitromethane.

[*Q*], M	τ_{M1} (ns)	a_{M1}	τ_{M2} (ns)	a_{M2}	τ_{M3} (ns)	a_{M3}	$\langle\tau_0\rangle$ (ns)	χ^2
0.00000	17.5	0.16	77.6	0.16	175.7	0.68	134.6	1.18
0.00330	11.8	0.16	59.1	0.48	105.0	0.36	68.0	1.25
0.01035	10.4	0.21	29.0	0.71	69.0	0.08	28.3	1.01
0.01380	8.0	0.26	22.8	0.68	59.0	0.06	21.1	1.25
0.02480	3.5	0.23	15.5	0.69	42.7	0.08	15.0	1.22
0.03470	5.2	0.38	12.6	0.56	35.2	0.06	11.0	1.04
0.04060	2.7	0.29	9.8	0.65	29.5	0.06	9.0	0.93

Table A-4. Pre-exponential factors and decay times of the fluorescence decays of 0.15 g/L of RPy–$(Asp_1Phe_1)_n$–132 quenched by nitromethane.

[*Q*], M	τ_{M1} (ns)	a_{M1}	τ_{M2} (ns)	a_{M2}	τ_{M3} (ns)	a_{M3}	$\langle\tau_0\rangle$ (ns)	χ^2
0.00000	13.3	0.25	73.1	0.21	175.9	0.54	113.4	0.94
0.00396	9.6	0.25	49.8	0.54	95.6	0.21	49.4	1.01
0.00758	10.2	0.25	39.5	0.61	81.2	0.14	38.0	1.05
0.01240	8.0	0.27	25.0	0.65	61.0	0.08	23.3	1.03
0.01610	7.5	0.28	22.7	0.64	56.5	0.081	21.2	1.11
0.02220	5.9	0.36	16.5	0.59	45.1	0.05	14.1	0.98
0.03020	4.0	0.32	11.2	0.59	30.0	0.09	10.6	1.2
0.03900	3.1	0.38	9.8	0.56	28.8	0.06	8.3	1.09
0.04540	3.3	0.50	10.0	0.47	31.3	0.03	7.2	1.26

Table A-5. Pre-exponential factors and decay times of the fluorescence decays of 0.15 g/L of RPy–$(Asp_1Phe_1)_n$–221 quenched by nitromethane.

[*Q*], M	τ_{M1} (ns)	a_{M1}	τ_{M2} (ns)	a_{M2}	τ_{M3} (ns)	a_{M3}	$\langle\tau_0\rangle$ (ns)	χ^2
0.00000	10.0	0.26	57.4	0.23	172.2	0.51	103.6	1.00
0.00392	9.4	0.26	46.7	0.47	91.3	0.27	49.0	1.00
0.00813	7.8	0.28	28.5	0.60	60.9	0.12	26.6	1.10
0.01320	9.5	0.33	21.8	0.57	47.5	0.10	20.1	1.10
0.01800	9.6	0.46	19.4	0.49	47.2	0.05	16.0	0.98
0.0233	2.6	0.28	11.3	0.60	27.7	0.13	11.1	1.02
0.02708	2.4	0.27	9.4	0.62	24.4	0.11	9.2	1.11
0.03610	2.6	0.32	8.8	0.59	22.9	0.09	8.1	1.34
0.04290	1.7	0.33	7.4	0.58	20.2	0.10	6.8	1.29
0.02290	2.1	0.28	11.7	0.57	29.5	0.14	11.4	1.06
0.02970	2.0	0.26	9.2	0.56	22.9	0.18	9.8	0.94

Chapter 5

Effect of Polypeptide Sequence on Polypeptide Self-Assembly

5.1. Abstract

The behaviour of five polypeptides prepared from aspartic acid and phenylalanine $(Asp_xPhe_y)_n$ with different sequences was studied in solution by fluorescence quenching and non-radiative energy transfer (NRET) fluorescence experiments. Dynamic (DLS) and static (SLS) light scattering studies were used to complement the results obtained. The fluorescence quenching experiments conducted with the chromophore pyrene used as a free probe, physically bound to the polypeptides via hydrophobic interactions, demonstrated that the chromophore was less accessible to its surrounding for the sequences having a higher hydrophobic character, $(Asp_1Phe_1)_n$, $(Asp_1Phe_2)_n$, and $(Asp_1Phe_3)_n$. Protective quenching was also observed for those randomly labeled polypeptides where the phenylalanine content was high whereas pyrene was found to be fully exposed to the quencher for the polypeptides having more hydrophilic sequences. No NRET was observed between a naphthalene and a pyrene labeled polypeptide for the polypeptide sequences which were richer in the hydrophilic monomer, aspartic acid, whereas energy transfer was seen to take place in the more hydrophobic sequences of the polypeptides. This observation led to the conclusion that those sequences with a higher content of aspartic acid essentially generate unimolecular polymeric micelles, whereas those with a higher content of phenylalanine, generate polymeric aggregates which offer some protection to the hydrophobic cargo. The presence of these polymeric aggregates was also confirmed by DLS and SLS studies.

5.2. Introduction

Water-soluble polymers containing hydrophobic segments are known to undergo spontaneous self-association of their hydrophobic groups in aqueous solution leading to the

generation of hydrophobic microdomains.[1-4] These hydrophobic interactions are affected by changes in the polymer concentration, temperature, ionic strength, or pH.

The hydrophobic domains thus created are capable of encapsulating by hydrophobic association hydrophobic cargos such as ink pigments or hydrophobic drugs which are then protected from their surroundings. These modified polymers are used in various technological formulations such as associative thickeners in paints and coatings,[5-7] colloidal stabilizers in food products, and drug carriers.[8-10]

The hydrophobic groups of these water-soluble polymers can be incorporated in different manners, either during the polymerization resulting in the blocky or random incorporation of the hydrophobes or after the polymerization by covalent attachment onto the water-soluble polymer backbone using already available functional groups or after functionalization of the polymer backbone.[2,11] Such polymers are broadly referred to as hydrophobically modified water-soluble polymers (HMWSPs).[1-3]

The hydrophilic backbone of HMWSPs can be either neutral such as poly(ethylene oxide) (PEO),[12,13] poly(*N*–vinylcaprolactam) (PVCL),[14,15] and poly(*N*–isopropylacrylamide) (PNIPAM),[16-19] or charged such as poly(sodium–2–(acrylamido)–2-methylpropanesulphonate) (PAMPS).[20-24] Apart from those already mentioned, a wide range of water-soluble biopolymers such as hydroxycellulose (HEC)[25] or poly(aspartic acid)[26,27] can be hydrophobically modified by attaching alkyl chains[23,26-28] and cholestryl pendants[24,29,30] either along the backbone or at the polymer chain ends.[13,18]

The solution properties of the HMWSPs depend on the hydrophobic microdomains produced through the association of their hydrophobic parts. These interactions depend on both the distribution of the hydrophobic segments along the polymer backbone[21,31,32] and the

rigidity and bulkiness of the hydrophobic groups.[20] The hydrophobic microdomains generated by HMWSPs can occur via intra– or intermolecular association. Intramolecular associations result in the formation of unimolecular polymeric micelles whereas polymeric aggregates are obtained via intermolecular associations.[24,30,33,34]

One much less studied feature is the effect that the position of the hydrophobes along the chain has on the association of the HMWSP.[35] Recently Duhamel et al.[36] have investigated the hydrophobic microdomains generated by a series of copolymers of styrene and maleic anhydride (SMAs) using several fluorescence techniques. The reactivity ratios of styrene and maleic anhydride are such that these two monomers tend to copolymerize in a strongly alternating fashion.[37] The hydrophobic character of the SMAs could be increased either by increasing the content of the styrene monomer or by lowering the degree of ionization of the copolymers. The ability of these SMAs to encapsulate large amounts of hydrophobic compounds such as pyrene, phenanthrene, anthracene, and dipyme and release them in a controlled manner by adjusting the SMA degree of ionization would have made them very attractive as carriers of hydrophobic drugs were it not for their non-biocompatibility.

To circumvent the non-biocompatibility issue, a series of polypeptides built with well-defined sequences of phenylalanine (Phe) and aspartic acid (Asp) were prepared, namely $(Asp_3Phe_1)_n$, $(Asp_2Phe_1)_n$, $(Asp_1Phe_1)_n$, $(Asp_1Phe_2)_n$, and $(Asp_1Phe_3)_n$. Phe and Asp were chosen since they bear, respectively, a phenyl pendent and a carboxylic acid, chemical features which mimic those found in the SMAs. Furthermore the synthetic procedure used to prepare the $(Asp_xPhe_y)_n$ polypeptides ensures that the hydrophobic (Phe) and hydrophilic (Asp) monomers are incorporated in a controlled manner in the polypeptide, as found in the

strongly alternating SMAs.[38-40] In this work, self-association of these polypeptides in a 0.01 M Na_2CO_3 solution at pH 9 was studied using dynamic light scattering and several fluorescence techniques.

5.3. Experimental

UV-Vis absorption. All UV-Vis absorption spectra were recorded on a Hewlett Packard 8452A diode array spectrophotometer with a resolution of ± 2 nm, using an absorption cell with a 1 cm path length.

Circular dichroism. CD spectra were acquired at 25 ^{o}C on a J 715 CD spectropolarimeter (Jasco) with a 0.1 cm path length cell, a 100 nm/min scan rate, and a 2 nm bandwidth. Spectra were averaged over 10 scans from 190 to 250 nm.

Dynamic light scattering. Dynamic light scattering measurements were carried out on a Zeta Sizer, NanoZS (Malvern Instrument, England). The analysis was performed at a laser wavelength of 633 nm, a scattering angle of 173^{o}, and at a temperature of 25 ^{o}C. For each sample, the mean diameter and standard deviation of the particles present in solution were calculated by applying the multimodal analysis. Solutions were filtered prior to data acquisition through a 0.2 μm pore size Supor® Membrane (Life Science) filter.

Steady-state fluorescence measurements. The steady-state emission spectra were obtained using a Photon Technology International LS-100 steady-state fluorometer with a continuous xenon lamp using a square fluorescence cell (VWR) with an inner cross section of 10×10 mm^2. The samples were not deoxygenated. The emission spectra of the samples were acquired by exciting the solutions at 338 nm when pyrene was present as a free probe and at 346 nm when pyrene was covalently attached to the polypeptides. To determine the I_1/I_3 ratio

used to evaluate the polarity of the local environment surrounding pyrene, the intensity of the first peak of the pyrene monomer, I_1, was taken to be the intensity of the peak at 374 nm. The intensity of the third peak of the pyrene monomer, I_3, was taken to be the intensity of the peak at 385 nm. Polypeptides labeled with naphthalene for the energy transfer experiments were excited at 290 nm where pyrene absorption is low and phenylalanine does not absorb (Figure 3.1).

Time-resolved fluorescence measurements. The fluorescence decay profiles were acquired on a time-correlated single photon counter manufactured by IBH Ltd. using a 5000F coaxial nanosecond flash lamp filled with H_2 gas. The excitation and the emission wavelengths were 338 nm and 374 nm, respectively, for pyrene used as a free probe and 344 nm and 374 nm, respectively, when covalently attached. The emission wavelength for the excimer decays was set at 510 nm. Cut off filters of 370 nm and 495 nm were used to reduce the noise from stray scattered light for the monomer and excimer decays, respectively. Reference decay curves of deoxygenated solutions of PPO in cyclohexane and BBOT in ethanol were also obtained for the monomer and excimer, respectively, in order to determine the actual response of the IBH fluorometer according to the MIMIC method.[41] All acquired decays were fitted with a sum of three exponentials according to Equation 5.1 where x represents either the monomer (M) or the excimer (E).

$$i_x(t) = a_{x1}\exp(-t/\tau_{x1}) + a_{x2}\exp(-t/\tau_{x2}) + a_{x3}\exp(-t/\tau_{x3}) \quad x = M, E \tag{5.1}$$

The Marquardt-Levenberg algorithm[42] was used to optimize the parameters of the fits. The quality of the fits was determined from the χ^2 values (< 1.30) and the random distribution

around zero of the residuals and of the autocorrelation function of the residuals.

Reagents. Pyrene, 1-pyrenemethylamine hydrochloride, 1–pyrenebutyric acid *N*–hydroxy succinimide ester, 1–naphthalenemethylamine, (1–ethyl–3–(3–dimethylaminopropyl) carbodiimide hydrochloride (EDC), and nitromethane were all purchased from Sigma-Aldrich. THF and DMF (distilled in glass, Caledon), NaOH (BDH), HCl (reagent ACS grade, Fischer), methanol, anhydrous diethyl ether and acetone (all HPLC grade, EMD) were used as received. Milli-Q water with a resistivity of over 18 MΩ.cm was used to make all the aqueous solutions. Spectra/Por membranes having a cut-off value of 3,500 g/mol were used for dialysis. Both pyrene and 1–pyrenemethylamine ($PyMeNH_2$) were purified prior to usage as mentioned in Chapter 4.

Labeling of polypeptides: The synthesis of the polypeptides has been described in Chapter 2. The polypeptides were labeled randomly with either 1-pyrenemethylamine or 1-naphthalenemethylamine. The end-labeling of the polypeptides was carried out by using 1–pyrenebutyric acid *N*–hydroxy succinimide ester. The labeling procedure and purification procedure is outlined in Chapter 4. The chromophore content of the polypeptides, given in Table 5.1, was determined by UV–Vis absorption. Pyrene concentrations for samples containing pyrene as a non-covalent probe were obtained through a 0.1 M SDS solution where the extinction coefficient of pyrene in SDS micelles was experimentally found to be 42,600 $mol^{-1}.L.cm^{-1}$ at 338 nm.

As done in Chapter 4, the fractions of labeled amino acids (X_{Total}) and aspartic acids (X_{Asp}) for a given polypeptide were determined with Equations 5.2 and 5.3.

$$X_{Total} = \frac{\lambda_D \left[x M_{Asp} + y M_{Phe} \right]}{(x+y)\left[1 + \lambda_D \left(M_{Asp} - M_{Asp-D} \right)\right]} \qquad (5.2)$$

$$X_{Asp} = \frac{\lambda_D \left[x M_{Asp} + y M_{Phe} \right]}{x\left[1 + \lambda_D \left(M_{Asp} - M_{Asp-D} \right)\right]} \qquad (5.3)$$

In Equations 5.2 and 5.3, the chromophore content is given by λ_D ($D = Py$ or Np for pyrene or naphthalene, respectively) and is expressed in mol.g^{-1}, x and y represent the molar fractions of, respectively, Asp and Phe in the polypeptide of sequence $(Asp_xPhe_y)_n$, and the molar masses M_{Phe}, $M_{Asp\text{-}Py}$, and $M_{Asp\text{-}Np}$ were taken equal to 147 g.mol^{-1}, 328 g.mol^{-1}, and 254 g.mol^{-1} for Phe, the pyrene labeled Asp, and the naphthalene labeled Asp, respectively. Depending on whether the polypeptide was weighed in its acid or salt form for the characterization of the chromophore content, a value of 115 or 137 g.mol^{-1} was used for M_{Asp}. In practice, the polypeptides $(Asp_3Phe_1)_n$ and $(Asp_2Phe_1)_n$ were acidified before chromophore content determination, whereas the polypeptides $(Asp_1Phe_1)_n$, $(Asp_1Phe_2)_n$, and $(Asp_1Phe_3)_n$ were used in their salt form.

The description of the polypeptides was done according to the following nomenclature. The unlabeled polypeptides were referred to as $(Asp_xPhe_y)_n$, where Asp and Phe stand for aspartic acid and phenylalanine, respectively, and x and y represent the numbers of each amino acid in the particular polypeptide sequence. For the labeled polypeptides RPy(Np)–$(Asp_xPhe_y)_n$–N and EPy–$(Asp_xPhe_y)_n$–N, R and E refer to a random or an end-chain incorporation of the chromophore and N represents the chromophore content of the labeled polypeptide expressed in μmol of chromophore per gram of polypeptide. Py

and Np stand for the pyrene and naphthalene chromophores, respectively.

Table 5.1. Pyrene (λ_{Py}) and naphthalene contents (λ_{Np}) in μmoles of chromophore per gram of polymer and the total molar fraction X_{Total} of labeled $(Asp_xPhe_y)_n$ and $(Asp)_n$ determined by UV-Vis absorption.

Sample	Chromophore content		Sample	Chromophore content	
	λ (μmol/g)	X_{Total} mole%		λ (μmol/g)	X_{Total} mole%
RPy–$(Asp)_n$–229	229	2.8	RNp–$(Asp_3Phe_1)_n$–232	232	2.9
RPy–$(Asp_3Phe_1)_n$–195	195	2.5	RNp–$(Asp_3Phe_1)_n$–335	335	4.3
RPy–$(Asp_3Phe_1)_n$–245	245	3.2	RNp–$(Asp_2Phe_1)_n$–115	115	1.5
RPy–$(Asp_2Phe_1)_n$–56	56	0.7	RNp–$(Asp_2Phe_1)_n$–120	120	1.5
RPy–$(Asp_2Phe_1)_n$–176	176	2.3	RNp–$(Asp_1Phe_1)_n$–195	195	2.8
RPy–$(Asp_2Phe_1)_n$–322	322	4.3	RNp–$(Asp_1Phe_1)_n$–313	313	4.6
RPy–$(Asp_1Phe_1)_n$–70	70	1.0	RNp–$(Asp_1Phe_2)_n$–149	149	2.2
RPy–$(Asp_1Phe_1)_n$–132	132	1.9	RNp–$(Asp_1Phe_2)_n$–223	223	3.3
RPy–$(Asp_1Phe_1)_n$–221	221	3.3	RNp–$(Asp_1Phe_3)_n$–103	103	1.5
RPy–$(Asp_1Phe_2)_n$–45	45	0.7	RNp–$(Asp_1Phe_3)_n$–155	155	2.3
RPy–$(Asp_1Phe_2)_n$–97	97	1.4	EPy–$(Asp_3Phe_1)_n$–26	26	0.3
RPy–$(Asp_1Phe_2)_n$–131	131	1.9	EPy–$(Asp_2Phe_1)_n$–15	15	0.2
RPy–$(Asp_1Phe_3)_n$–72	72	1.1	EPy–$(Asp_1Phe_1)_n$–44	44	0.6
RPy–$(Asp_1Phe_3)_n$–104	104	1.5	EPy–$(Asp_1Phe_2)_n$–13	13	0.2
RNp–$(Asp)_n$–180	180	2.1	EPy–$(Asp_1Phe_3)_n$–91	91	1.3

Preparation of the aqueous polypeptide solutions. The aqueous solutions of all the polypeptides unlabeled, labeled, and those using molecular pyrene as a probe were prepared in a solution of 0.01 M Na_2CO_3 at pH 9 through dialysis by an indirect method as explained in Chapters 3 and 4.

5.4. Results and Discussion

The conformation of polypeptides containing residues of L-aspartic acid and L-phenylalanine have been examined in Chapter 3, where it was established from the CD spectra of the four sequences $(Asp_3Phe_1)_n$, $(Asp_2Phe_1)_n$, $(Asp_1Phe_1)_n$, and $(Asp_1Phe_2)_n$ that they do not show any well-defined conformation. The polypeptide sequence having the most hydrophobic character, $(Asp_1Phe_3)_n$, adopts an α-helical conformation.[43] The polypeptides were then labeled randomly with pyrene, a hydrophobic chromophore, in order to study their solution properties by fluorescence. The CD spectra of the randomly labeled polypeptides were also obtained in order to determine whether any conformational change takes place after this modification. Figure 5.1 A and B illustrate the effect if any that pyrene labeling has on the secondary structure of the polypeptides. It is easily discernable that these polypeptides undergo no noticeable conformational change after this modification, which suggests that labeling the polypeptides with small amounts of the hydrophobic chromophore pyrene does not affect substantially the behavior of the polypeptides in aqueous solution.

The $(Asp_xPhe_y)_n$ polypeptides are HMWSPs. As such they are expected to associate and form polypeptide aggregates in aqueous solution. Polymeric aggregates have been widely characterized using dynamic light scattering which provides the hydrodynamic diameters and the relative amounts of the various species present in solution. Hence DLS experiments were performed on the $(Asp_xPhe_y)_n$ polypeptides to investigate their ability to associate via hydrophobic interactions. It was already shown in Chapter 4 that the alternating polypeptide $(Asp_1Phe_1)_n$ is primarily present as unimolecular micelles in solution. It is therefore expected that out of the five polypeptide sequences, those with a lower hydrophobic character i.e. $(Asp_3Phe_1)_n$ and $(Asp_2Phe_1)_n$ where the phenylalanine content is less than 50 mol% would

also exist as single chains in solution and generate intramolecular hydrophobic domains. Intermolecular association, resulting in polymeric aggregates is more likely for the polypeptide sequences having a larger percentage of the hydrophobic monomer phenylalanine, i.e. $(Asp_1Phe_2)_n$ and $(Asp_1Phe_3)_n$. The increased number of hydrophobic pendants along with the decreased solubility of these sequences both favors the formation of large interpolymeric particles. The DLS experiments were carried out for the different polypeptide sequences, in their unlabeled form as well as the labeled form and for the solutions where pyrene was present as a molecular probe. Two sets of solutions with polypeptide concentrations 0.05 g/L and 0.5 g/L were investigated.

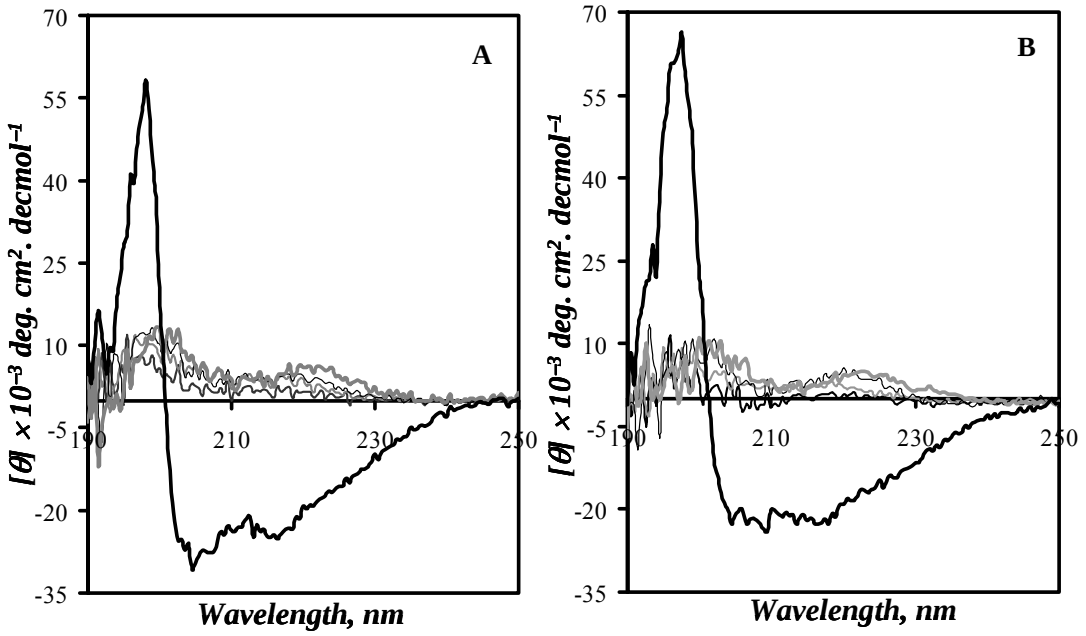

Figure 5.1. CD spectra of (A) unlabeled and (B) labeled polypeptides. (——) $(Asp_3Phe_1)_n$, $(Asp_2Phe_1)_n$ (——), $(Asp_1Phe_1)_n$ (——), $(Asp_1Phe_2)_n$ (——), $(Asp_1Phe_3)_n$ (——). The concentration of the unlabeled polypeptide was 0.1 g/L. For the labeled polypeptides RPy—$(Asp_3Phe_1)_n$—195, RPy—$(Asp_2Phe_1)_n$—176, RPy—$(Asp_1Phe_1)_n$—132, RPy—$(Asp_1Phe_2)_n$—131, and RPy—$(Asp_1Phe_3)_n$—104, the polypeptide concentrations were 0.10 g/L, 0.13 g/L, 0.08 g/L, 0.13 g/L, and 0.08 g/L respectively. All polypeptide solutions were prepared in a 0.01 M Na_2CO_3 solution at pH 9 in a 0.1 cm cell.

The size distribution of the species observed in the solutions of the two extreme polypeptide sequences, namely the most hydrophilic sequence $(Asp_3Phe_1)_n$ and the most hydrophobic sequence $(Asp_1Phe_3)_n$, are represented in Figure 5.2 using, respectively, light scattering intensity (A and D), the number of particles (B and E), and the particle volume (C and F). The contribution of each species is given by these histograms and a summary of the peak diameters and standard deviations is given in Table A-1 in the Appendix.

The size distribution profiles obtained with light scattering intensity (Figures 5.2 A and D) confirm that more than one species is present in solution for both polypeptide sequences. This result indicates the coexistence of single chains as well as polymeric aggregates in solution. For the hydrophilic sequence $(Asp_3Phe_1)_n$, two contributions are observed in the size distribution profile of the labeled polypeptides whereas a third peak is present for the unlabeled sample. The first peak to the left which is attributed to the individual polymeric chains is in the 3-5 nm range and the second and more intense peak in the 95-150 nm range depending on the polypeptide sample indicates the presence of polymeric aggregates. The unlabeled polypeptide solution has an additional peak centered at 16 nm. For the hydrophobic sequence $(Asp_1Phe_3)_n$, the diameters range between 9-10 nm and 100-190 nm for the peaks representing single chains and polymeric aggregates, respectively. Despite some differences in the size distribution profiles, all profiles exhibit similar features for all polypeptides (see Table A-1). The profiles obtained with the scattering intensity exhibit two major peaks, one in the 3-10 nm range and a second one in the 100-200 nm range. The profiles obtained by number and volume exhibit a single peak in the 2-8 nm range. The different outlook of the size distribution profiles obtained by using on the one hand scattering intensity, and on the other hand number and volume is due to the extreme sensitivity of light

scattering to the presence of large objects. As a result, a small concentration of large particles can be probed by light scattering (Figures 5.2 A and D), although these particles constitute a negligible fraction of the overall population (Figures 5.2 B, C, E and F). Subtle differences in the particle size listed in Table A-6 are difficult to assess accurately since changes in the hydrodynamic volume can be due to a variety of effects ranging from electrostatic repulsion of the negatively charged backbone leading to coil expansion, a hydrophobic collapse of the coil due to the Phe content, a conformational change from random coil to extended α-helix. However, the DLS experiments do confirm the existence of a small concentration of polypeptide aggregates regardless of the polypeptide sequence.

The DLS experiments showed that all $(Asp_xPhe_y)_n$ polypeptides are capable of forming aggregates regardless of the polypeptide sequence. This result was somewhat surprising because the ability of these polypeptides to form aggregates was expected to depend on the hydrophobic character of the polypeptide. However the extreme sensitivity of DLS towards large particles led us to suspect that DLS would not be sensitive enough to determine the effect that subtle changes in the polypeptide hydrophobic content would have on the relative ability of each polypeptide sequence to generate polypeptide aggregates. To obtain this information, a series of fluorescence experiments was conducted.

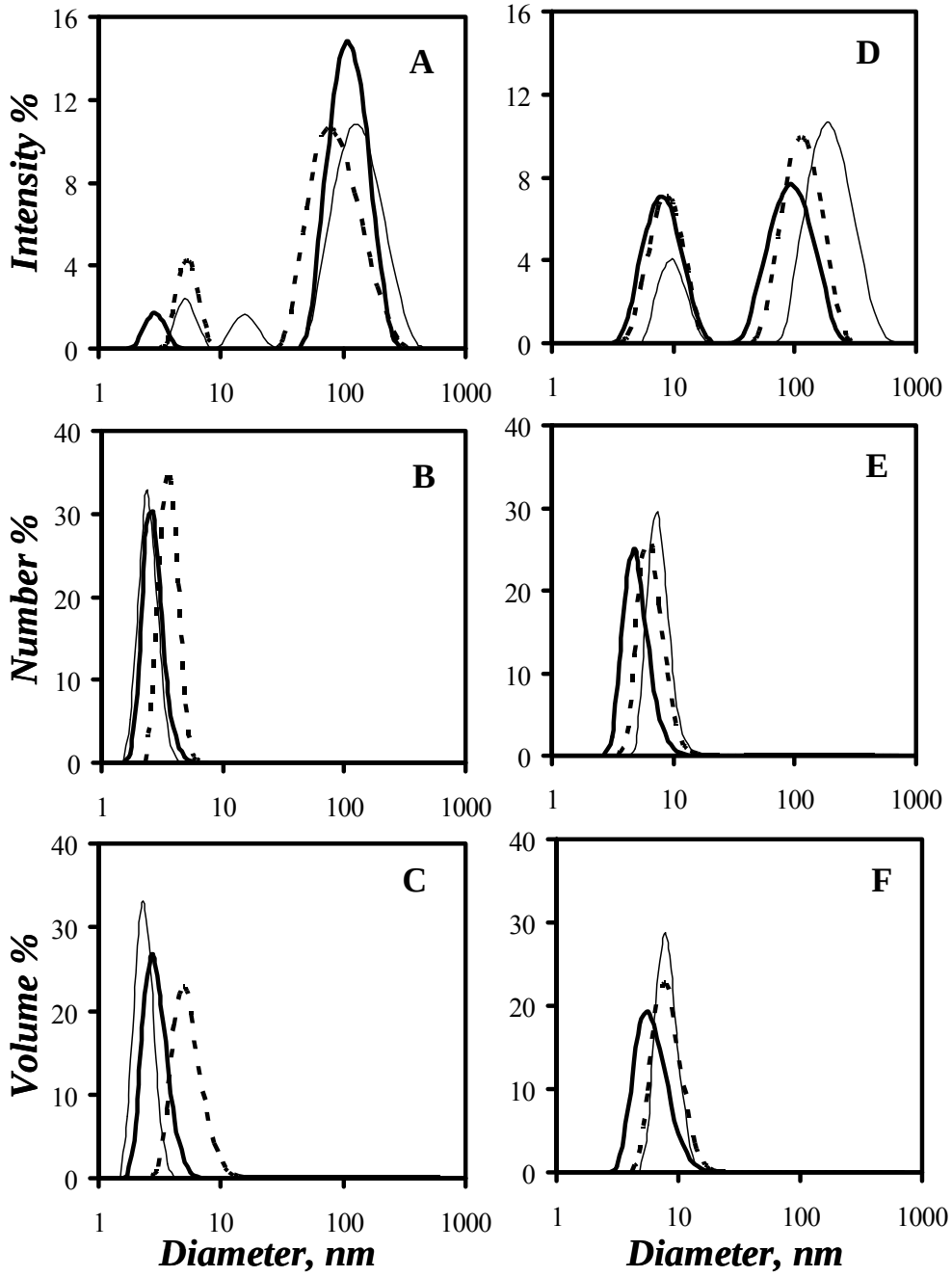

Figure 5.2. Particle size distribution by intensity (A), number (B), and volume (C) for $(Asp_3Phe_1)_n$, and intensity (D), number (E), and volume (F) for $(Asp_1Phe_3)_n$. (———) unlabeled polypeptides, (———) end-labeled polypeptides and (– – – –) randomly labeled polypeptides. [*Polypeptide*] = 0.05 g/L in 0.01 M Na_2CO_3 solution at pH 9.

Fluorescence energy transfer is a simple but powerful tool for detecting the presence or absence of polymeric aggregates.[17,20,22,23,25] It has been frequently used for this purpose by utilizing naphthalene and pyrene as donor/acceptor pair.[44] The process of non radiative energy transfer (NRET) takes place as a result of dipole-dipole interactions between the excited donor, naphthalene (*Np*), and the ground-state acceptor, pyrene (*Py*), and hence does not involve photon emission. The emission of the donor molecule (*Np*) must overlap the absorption of the acceptor molecule (*Py*) in order for energy transfer to actually take place. Also, the acceptor should show little or no absorption at the wavelength where the donor is excited.

The efficiency of energy transfer E_{ET} is strongly dependent on the distance between the donor and the acceptor molecules (d_{DA}). Its expression was given in Equation 4.7 in Chapter 4. The strong dependency of E_{ET} with d_{DA} means that energy transfer occurs only if the donor and acceptor molecules are close to each other. Fluorescence energy transfer experiments were performed using the polypeptides labeled with pyrene RPy–$(Asp_xPhe_y)_n$ and naphthalene RNp–$(Asp_xPhe_y)_n$. Those polypeptides which exist predominantly as individual chains should exhibit no energy transfer from naphthalene to pyrene whereas those which are able to form polymeric aggregates would have the two molecules Np and Py close enough for NRET to occur.[45]

NRET experiments were carried out for solutions of all the polypeptide sequences with the naphthalene (RNp–$(Asp_xPhe_y)_n$) and pyrene (RPy–$(Asp_xPhe_y)_n$) labeled polypeptides by selectively exciting naphthalene at 290 nm where pyrene and phenylalanine have little to no absorption. The polypeptide solutions were prepared with polypeptide concentrations in the 0.04–0.07 g/L range and with optical density (OD) of less than 0.05.

The solutions for the NRET experiment were prepared by mixing RNp–$(Asp_xPhe_y)_n$ and RPy–$(Asp_xPhe_y)_n$ in DMF followed by dialysis and then adjusting the polypeptide concentrations so that the OD be below 0.05 for each solution. The steady-state fluorescence emission spectra of all solutions were recorded by exciting at 290 nm. Table 5.2 lists the samples used for the NRET experiments along with the polypeptide concentrations and the naphthalene and pyrene contents for each solution.

Table 5.2. Polypeptide samples used for NRET

Sample	Polypeptide conc. (g/L)	λ (μmol/g)	Chromophore conc. (μM)
RNp–$(Asp_3Phe_1)_n$–232	0.049	232	11.4
RPy–$(Asp_3Phe_1)_n$–195	0.004	195	0.9
RNp–$(Asp_2Phe_1)_n$–115	0.052	115	5.9
RPy–$(Asp_2Phe_1)_n$–176	0.008	176	1.5
RNp–$(Asp_1Phe_1)_n$–313	0.025	313	7.8
RPy–$(Asp_1Phe_1)_n$–70	0.017	70	1.2
RNp–$(Asp_1Phe_2)_n$–149	0.047	149	7.0
RPy–$(Asp_1Phe_2)_n$–97	0.012	97	1.3
RNp–$(Asp_1Phe_3)_n$–103	0.048	103	4.9
RPy–$(Asp_1Phe_3)_n$–72	0.017	72	1.3

Figure 5.3 shows the NRET experiments which were conducted with $(Asp_3Phe_1)_n$ and $(Asp_1Phe_3)_n$. The same procedure used to obtain Figure 4.7 in Chapter 4 was applied. In Figure 5.3, the fluorescence emission spectrum c) was obtained by summing the fluorescence spectra a) and b). The spectra a) and b) are, respectively, the fluorescence spectra of RNp–$(Asp_xPhe_y)_n$ and RPy–$(Asp_xPhe_y)_n$ whose intensities were scaled to account for the differences of the naphthalene concentration in the RNp–$(Asp_xPhe_y)_n$ solution and the

mixture of RNp–$(Asp_xPhe_y)_n$ and RPy–$(Asp_xPhe_y)_n$ and the differences of the pyrene concentration in the RPy–$(Asp_xPhe_y)_n$ solution and the mixture of RNp–$(Asp_xPhe_y)_n$ and RPy–$(Asp_xPhe_y)_n$. The fluorescence spectrum c) was then compared to d) which is the fluorescence spectrum of the RPy–$(Asp_xPhe_y)_n$ and RNp–$(Asp_xPhe_y)_n$ mixture. Whereas spectra c) and d) overlap in Figure 5.3A, they do not in Figure 5.3B. In Figure 5.3B, the fluorescence intensity of naphthalene and pyrene in the mixture are decreased and increased, respectively. This result is a hallmark that intermolecular NRET is taking place.

A more quantitative description of the extent of NRET is obtained from the NRET efficiency (E_{ET}) which can be calculated with Equation 4.5. To do so, the fluorescence intensity of naphthalene for both the Np–labeled polypeptide alone or in the mixture is integrated between 320 and 330 nm. E_{ET} was measured for each polypeptide sequence and is listed in Table 5.3. The efficiency of NRET was found to equal zero for the more hydrophilic sequences $(Asp_3Phe_1)_n$, $(Asp_2Phe_1)_n$, and $(Asp_1Phe_1)_n$. However the more hydrophobic sequences $(Asp_1Phe_2)_n$, and $(Asp_1Phe_3)_n$ had non zero E_{ET}. The NRET efficiencies listed in Table 5.3 indicate that as the content of the hydrophobic monomer (Phe) increases in the polypeptide sequence, the ability of the polypeptide to generate polymeric aggregates is enhanced. The energy transfer efficiency given in Table 5.3 increases from zero for the first three polypeptide sequences to 16 % and 34 % for the $(Asp_1Phe_2)_n$ and $(Asp_1Phe_3)_n$ sequences.

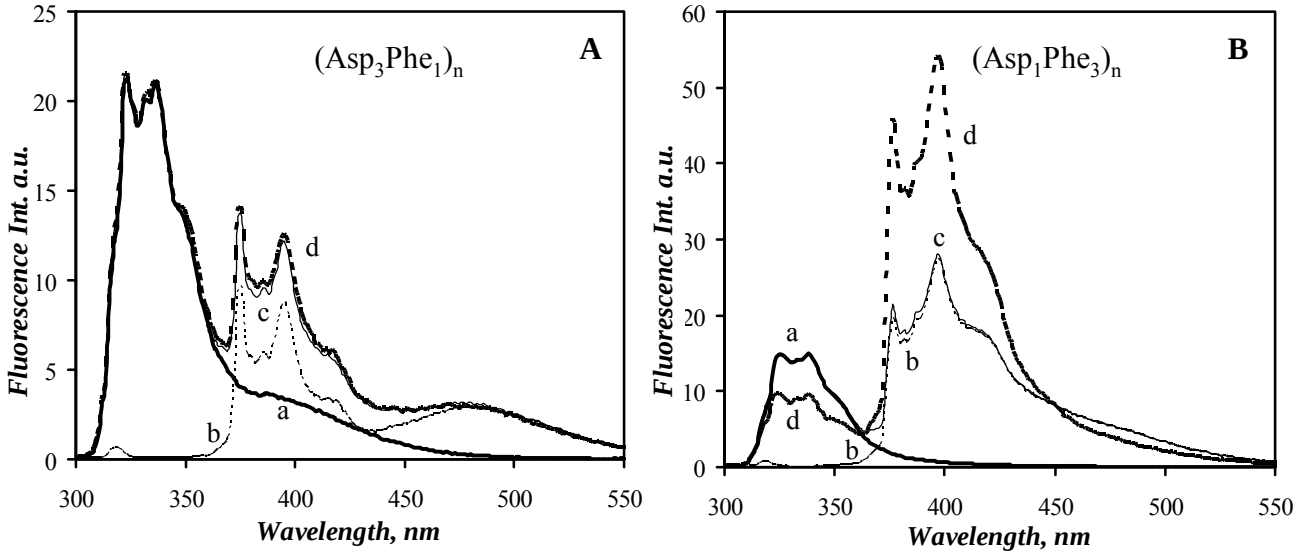

Figure 5.3. Fluorescence emission spectra obtained for (A) a) RNp–$(Asp_3Phe_1)_n$–232, [*Polypeptide*] = 0.049 g/L; b) RPy–$(Asp_3Phe_1)_n$–195, [*Polypeptide*] = 0.004 g/L; c) sum of the two precedent spectra; and d) fluorescence emission spectrum of a mixture of the two singly labeled polypeptides, RNp–$(Asp_3Phe_1)_n$–232, [*Polypeptide*] = 0.049 g/L and RPy–$(Asp_3Phe_1)_n$–195, [*Polypeptide*] = 0.004 g/L; and (B) a) RNp–$(Asp_1Phe_3)_n$–103, [*Polypeptide*] = 0.048 g/L; b) RPy–$(Asp_1Phe_3)_n$–72, [*Polypeptide*] = 0.017 g/L; c) sum of the two precedent spectra; and d) fluorescence emission spectrum of a mixture of the two singly labeled polypeptides, RNp–$(Asp_1Phe_3)_n$–103, [*Polypeptide*] = 0.032 g/L and RPy–$(Asp_1Phe_3)_n$–72, [*Polypeptide*] = 0.016 g/L. λ_{ex} = 290 nm, O.D ≤ 0.05 at 290 nm.

Table 5.3. Fluorescence energy transfer efficiency (E_{ET}) for the polypeptide sequences

Sample	E_{ET} %
$(Asp_3Phe_1)_n$	0
$(Asp_2Phe_1)_n$	0
$(Asp_1Phe_1)_n$	0
$(Asp_1Phe_2)_n$	16
$(Asp_1Phe_3)_n$	34

The sensitivity of pyrene to the polarity of its microenvironment has led to its use to probe the hydrophobic microdomains generated by a wide variety of micellar and polymeric systems.[5,26,37] Pyrene has been used both as a free probe and a hydrophobic label. The relative intensities of the monomer peaks I_1 and I_3 in the pyrene fluorescence emission spectrum vary with the polarity of the solvent.[46,47] Hence the ratio I_1/I_3 is a useful parameter in establishing the location of pyrene in a heterogeneous system. The I_1/I_3 ratio of pyrene takes a value of 1.66-1.80 in water[46,47] but this value decreases in an apolar environment such as in the hydrophobic cores of SDS micelles where it takes a value of 1.10. Changes in the I_1/I_3 ratio are also observed for 1-pyrenemethyl derivatives, although the magnitude of these changes is smaller that that found for pyrene. The intra– and intermolecular hydrophobic associations leading to the generation of the hydrophobic microdomains with the polypeptide sequences $(Asp_3Phe_1)_n$, $(Asp_2Phe_1)_n$, $(Asp_1Phe_1)_n$, $(Asp_1Phe_2)_n$, and $(Asp_1Phe_3)_n$ were characterized using pyrene both as a free probe and as a hydrophobic label. The steady-state emission spectra of pyrene used as a free probe in the three hydrophobic polypeptide sequences $(Asp_1Phe_1)_n$, $(Asp_1Phe_2)_n$, and $(Asp_1Phe_3)_n$ is shown in Figure 5.4. The I_1/I_3 ratios were found to be 1.24, 1.20, and 1.24 for, respectively, $(Asp_1Phe_1)_n$, $(Asp_1Phe_2)_n$, and $(Asp_1Phe_3)_n$, clearly indicative of pyrene being located in an apolar environment. It was not possible to solubilize large quantities of pyrene in any of the polypeptides having more hydrophilic sequences. In fact, the two most hydrophilic sequences only solubilized the same amount of pyrene as that found in a saturated 0.01 M Na_2CO_3 aqueous solution ($\sim 4.0 \times 10^{-7}$ M). Very little emission of pyrene excimer was observed for all polypeptides.

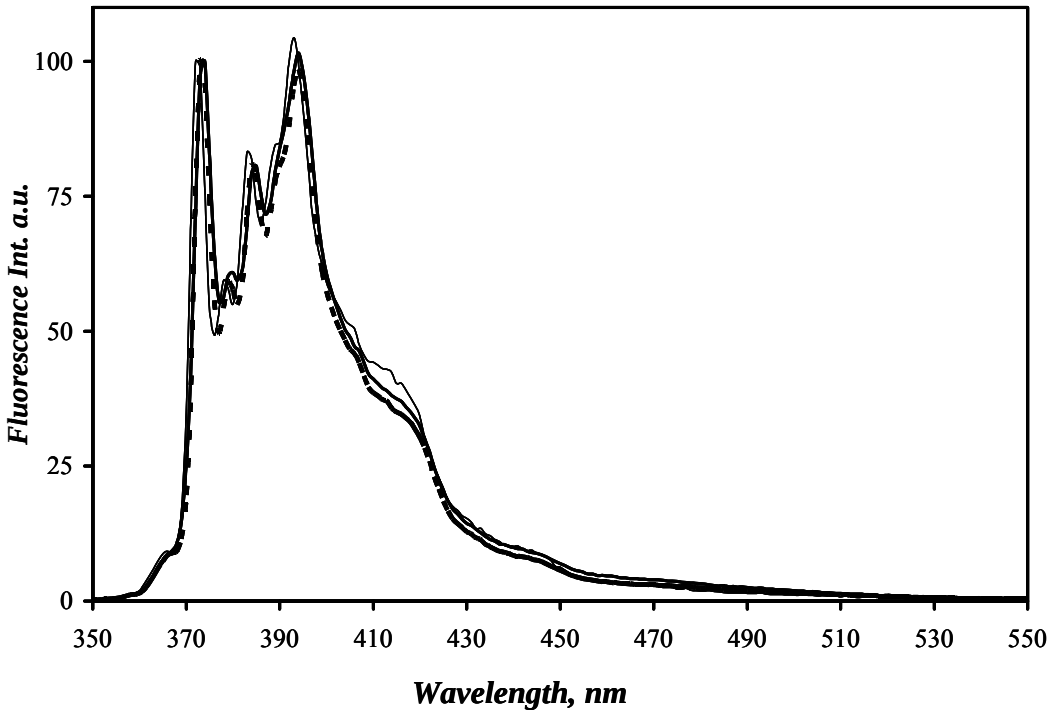

Figure 5.4. Steady-state emission spectra obtained for pyrene as a free probe. (———) $(Asp_1Phe_1)_n$, [*Polypeptide*] = 1.50 g/L, [*Py*] = 1.75×10^{-5} M, (———) $(Asp_1Phe_2)_n$, [*Polypeptide*] = 1.44 g/L, [*Py*] = 2.22×10^{-6} M, and (– – – –) $(Asp_1Phe_3)_n$, [*Polypeptide*] = 1.84 g/L, [*Py*] = 5.13×10^{-6} M. λ_{ex} = 338 nm. Polypeptides in 0.01 M Na_2CO_3 solution at pH 9.

A representative steady-state fluorescence emission spectrum obtained for each of the randomly labeled polypeptide sequences is presented in Figure 5.5. For these pyrene labeled polypeptides, the I_1/I_3 ratio increases from 1.29 to 1.66 as the polypeptide sequence becomes richer in the aspartic acid, the hydrophilic monomer (see inset in Figure 5.5). These values are similar to the I_1/I_3 ratios of 1.69 and 1.38 found for a poly(ethylene oxide) labeled at one end with 1-pyrenemethanol in basic aqueous solution and 3.5 mM SDS basic aqueous solution, respectively.[5] This result suggests that pyrene is located inside the hydrophobic microdomains generated by the polypeptides having a more hydrophobic sequence but is

more exposed to the polar aqueous phase for the more hydrophilic polypeptides.[48] For the end-labeled polypeptides, the I_1/I_3 ratios were not taken into consideration since the pyrene label is known to lose its sensitivity to the polarity of its environment when it is connected to a polymer through a butyl linker.[48]

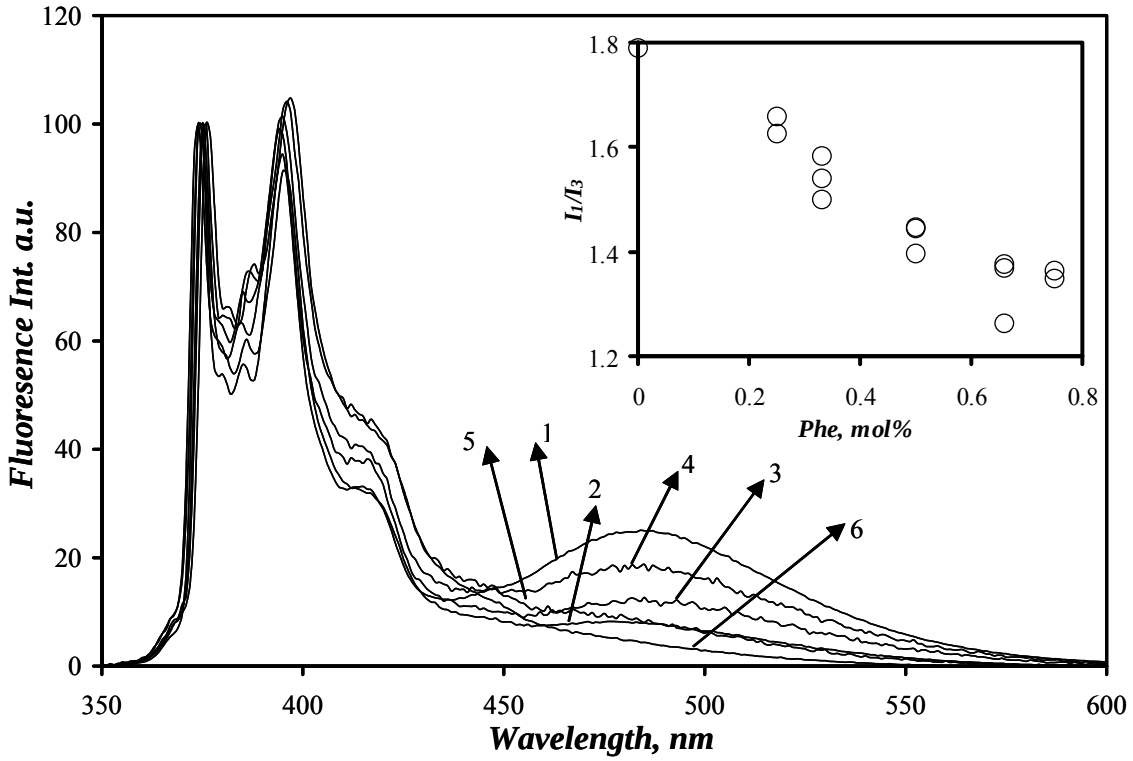

Figure 5.5. Steady-state emission spectra obtained for randomly labeled polypeptides. 1) RPy–$(Asp)_n$–229, [*Polypeptide*] = 0.12 g/L, λ_{ex} = 344 nm; 2) RPy–$(Asp_3Phe_1)_n$–195, [*Polypeptide*] = 0.14 g/L, λ_{ex} = 344 nm; 3) Py–$(Asp_2Phe_1)_n$–56, [*Polypeptide*] = 0.30 g/L, λ_{ex} = 344 nm; 4) Py–$(Asp_1Phe_1)_n$–70, [*Polypeptide*] = 0.14 g/L, λ_{ex} = 346 nm; 5) RPy–$(Asp_1Phe_2)_n$–97, [*Polypeptide*] = 0.09 g/L, λ_{ex} = 346 nm; 6) RPy–$(Asp_1Phe_3)_n$–72, [*Polypeptide*] = 0.29 g/L, λ_{ex} = 346 nm. Inset: Change in I_1/I_3 ratio as a function of Phe content in the polypeptides for the polypeptides randomly labeled with pyrene listed in Table 5.1. Polypeptides in 0.01 M Na_2CO_3 solutions at pH 9.

The results obtained with the I_1/I_3 ratios indicate that for the $(Asp_1Phe_1)_n$, $(Asp_1Phe_2)_n$, and $(Asp_1Phe_3)_n$ polypeptides, pyrene is located in an apolar environment

whether it is introduced as a free probe in the solution or covalently attached to the polypeptide. These sequences have the ability to form hydrophobic microdomains and interpolymeric aggregates, as indicated by DLS and NRET especially for those sequences having the highest Phe content.

The extent of excimer formation for a pyrene-labeled polymer is reflected by the I_E/I_M ratio, the ratio of the excimer fluorescence intensity over that of the monomer. The I_E/I_M ratio of the polypeptides randomly labeled with pyrene was calculated and is plotted in Figure 5.6A as a function of pyrene content. As the pyrene content of a labeled polypeptide increases, so does the I_E/I_M ratio. However the magnitude of that increase depends strongly on the polypeptide sequence. This statement is illustrated by fitting arbitrarily the I_E/I_M ratios plotted as a function of pyrene content in Figure 5.6A with a straight line and plotting the slope of the line as a function of phenylalanine content in Figure 5.6B. Figure 5.6B shows a marked increase in excimer formation as the Phe content of the polypeptides increases up to 50 mol% followed by a marked decrease of excimer formation for polypeptides having a larger Phe content. These results can be rationalized by invoking the coiling index.[49] The I_E/I_M ratio has been referred to as the coiling index as it decreases as the polymer switches from a coiled to an extended conformation. At pH 9, the polypeptides with an Asp-rich sequence, namely $(Aps_3Phe_1)_n$ and $(Asp_2Phe_1)_n$, adopt an extended conformation due to electrostatic repulsion along the negatively charged polypeptide backbone and their I_E/I_M ratio is small. As the Phe content of the polypeptide increases, the charge density of the polypeptide decreases and stronger hydrophobic interactions take place resulting in a less extended conformation of the polypeptide coil. The I_E/I_M ratio increases up to a Phe content of 50 mol%. As the Phe content is increased further, not only are the pyrene pendants

separated by longer stretches of Phe, but the polypeptide adopts an extended α–helical conformation (see CD signal for $(Asp_1Phe_3)_n$ in Figure 5.1B) resulting in a decrease of the coiling index. The I_E/I_M ratio decreases.

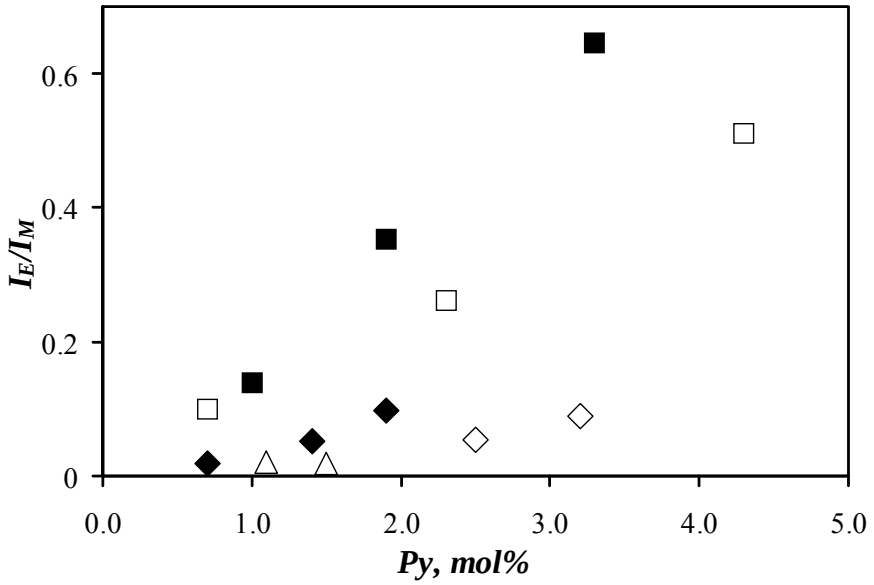

Figure 5.6A. Pyrene I_E/I_M ratios calculated for the randomly labeled polypeptides (◇) $(Asp_3Phe_1)_n$, (□) $(Asp_2Phe_1)_n$, (■) $(Asp_1Phe_1)_n$, (◆) $(Asp_1Phe_2)_n$, and (△) $(Asp_1Phe_3)_n$. I_M integrated between 373-377 nm and I_E integrated between 500-530 nm. Polypeptides in 0.01 M, Na_2CO_3 solution at pH 9.

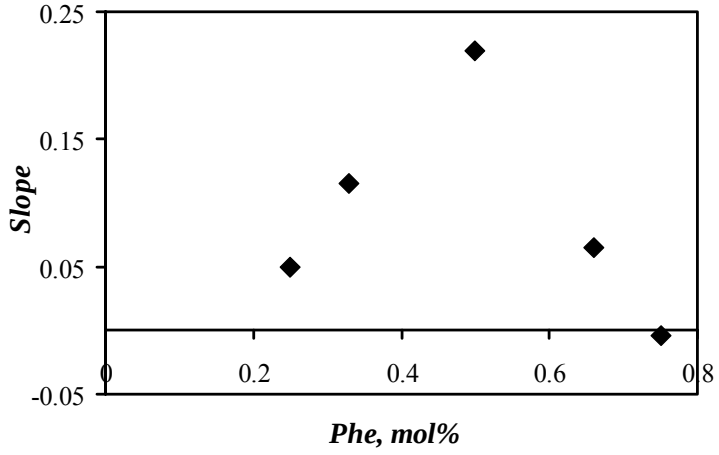

Figure 5.6B. Slopes calculated from Figure 5.6A for the randomly labeled polypeptides as a function of phenylalanine content in mol%. Polypeptides in 0.01 M Na_2CO_3 solution at pH 9.

To gain more insight into the nature of the hydrophobic microdomains generated by the polypeptides, the decays of pyrene either covalently attached to the polypeptides or physically bound to the polypeptides were acquired. The decay times for the pyrene monomer and excimer, when formed, were determined for the polypeptides in aqueous solution by fitting the fluorescence decays with a sum of three exponentials. The pre-exponential factors and decay times retrieved from this analysis are listed in Tables 5.4 and 5.5 for the pyrene monomer and excimer, respectively.

The decay times for pyrene used as a free probe are listed in the first three rows of Table 5.4 for the sequences having a phenylalanine content larger than or equal to 50 mol %. For these three polypeptides, a long decay time τ_{M3} of 299 ns, 309 ns, and 314 ns is obtained. Those pyrenes emitting with a ~300 ns decay time can not be located in the aqueous solution since pyrene has a lifetime of 128 ns in aerated 0.01 M Na_2CO_3 aqueous solution at pH 9. Those long-lived pyrene monomers are located in the hydrophobic microdomains generated by the polypeptides where they are protected from oxygen quenching. A similar protection has been reported for numerous other polymeric systems,[22,50] including SMA polymeric aggregates.[36] The fraction of long-lived pyrenes increases from 0.38 to 0.60 as the Phe content of the polypeptide increases. The increase in the decay time τ_{M3} as a function of Phe content was also observed for the randomly labeled polypeptides, for which the more hydrophobic sequence resulted in a τ_{M3} decay time much larger than the one obtained for RPy–$(Asp)_n$ where the pyrene label is fully exposed to the aqueous solution (I_1/I_3 = 1.79 and τ_{M3} = 128 ns). As found for the fluorescence experiments where pyrene is added to the polypeptide solution as a free probe, the long-lived pyrene found for the RPy–$(Asp_xPhe_y)_n$ polypeptides must be located inside the hydrophobic microdomains formed by the more

hydrophobic polypeptide sequences. These pyrenes are thus protected from the quenching of the oxygen dissolved in the aqueous solutions. This is not the case for the Asp–rich polypeptides which show shorter decay times for pyrene resulting from its quenching by either dissolved oxygen or the formation of pyrene excimer.

The ability of these polypeptides, especially those with the more hydrophobic character, to encapsulate hydrophobic pyrene seems to suggest that they could be used as potential carriers for hydrophobic drugs. However as already mentioned above, only a small amount of free pyrene could be solubilized by the polypeptides having the sequences $(Asp_1Phe_1)_n$, $(Asp_1Phe_2)_n$, and $(Asp_1Phe_3)_n$. If these polypeptides were used to carry hydrophobic drugs, one might consider attaching the hydrophobic drug covalently onto the polypeptides having a more hydrophobic sequence.

Polypeptides end-labeled with 1–pyrenebutanoic acid had shorter decay times than their counterparts randomly labeled with 1-pyrenemethylamine. This is due to the 1–pyrenebutyl chromophore having a shorter lifetime than the 1–pyrenemethyl chromophore.[51] However the same trend is shown by the EPy–$(Asp_xPhe_y)_n$ polypeptides in that the decay time τ_{M3} increases with increasing phenylalanine content of the polypeptide sequence. This again suggests that the pyrenes are able to incorporate themselves inside the hydrophobic microdomains of these polypeptides.

Table 5.4. Summary of the pyrene monomer decay times and pre-exponential factors obtained for the polypeptides solutions in 0.01 M Na_2CO_3 at pH 9.

Sample	τ_{M1} (ns)	a_{M1}	τ_{M2} (ns)	a_{M2}	τ_{M3} (ns)	a_{M3}	$<\tau_0>$ (ns)	χ^2
$(Asp_1Phe_1)_n$ + Py	9	0.26	118	0.35	299	0.38	157	1.10
$(Asp_1Phe_2)_n$ + Py	11	0.17	122	0.40	309	0.42	181	1.13
$(Asp_1Phe_3)_n$ + Py	12	0.16	130	0.24	314	0.60	222	0.97
RPy–$(Asp)_n$–229	7	0.09	53	0.16	128	0.75	105	1.08
RPy–$(Asp_3Phe_1)_n$–195	17	0.14	99	0.20	146	0.66	119	1.14
RPy–$(Asp_2Phe_1)_n$–56	–	–	35	0.16	149	0.84	131	1.18
RPy–$(Asp_1Phe_1)_n$–70	17	0.16	78	0.16	176	0.68	135	1.18
RPy–$(Asp_1Phe_2)_n$–97	20	0.14	104	0.30	240	0.56	168	1.05
RPy–$(Asp_1Phe_3)_n$–72	26	0.11	117	0.34	226	0.56	169	1.05
EPy–$(Asp_3Phe_1)_n$–26	7	0.07	85	0.20	114	0.72	99	1.03
EPy–$(Asp_2Phe_1)_n$–15	6	0.10	63	0.05	114	0.85	101	1.03
EPy–$(Asp_1Phe_1)_n$–44	11	0.13	92	0.30	150	0.56	113	1.15
EPy–$(Asp_1Phe_2)_n$–13	9	0.11	92	0.19	186	0.69	147	1.02
EPy–$(Asp_1Phe_3)_n$–91	6	0.12	85	0.22	180	0.66	138	1.04

The ability of pyrene to form an excimer has been used to characterize numerous polymeric systems.[5,6,12,37,52-54] The formation of a pyrene excimer can occur either via diffusional encounters of an excited pyrene and a ground-state pyrene or by the direct excitation of ground-state pyrene aggregates.[52] The former process results in the appearance of a rise time at the beginning of the excimer decay profile while the latter process yields no such rise time. The excimer decays were fitted with a sum of exponentials. The amount of excimer formed either via diffusion or by direct excitation of ground-state pyrene aggregates

can be evaluated from the value of the ratio ξ of the sum of the negative pre-exponential factors to the sum of the positive pre-exponential factors. This ratio equals −1.0 when the excimer is exclusively produced via diffusional encounters and takes more positive values when the excimer formation occurs by direct excitation of ground-state pyrene aggregates.

As excimer formation was only observed for those polypeptides which were randomly labeled with 1−pyrenemethylamine, excimer fluorescence decays were acquired only with their solutions. The decays were fitted with a sum of three exponentials. The ξ values were determined and are listed in Table 5.5. According to those ξ values, excimers formed by the polypeptides having hydrophilic sequences, namely $(Asp_3Phe_1)_n$ and $(Asp_2Phe_1)_n$, are produced through the direct excitation of ground-state pyrene aggregates. However those formed by pyrene labels attached to the more hydrophobic polypeptides show a very small rise time, indicating that some excimers are formed by the diffusional encounters of pyrene labels. This is certainly a consequence of the presence of hydrophobic microdomains generated by the phenylalanines which solubilize the hydrophobic pyrene.

To further characterize the hydrophobic microdomains generated by the polypeptides sequences, steady-state and time-resolved fluorescence quenching experiments were performed. From the I_1/I_3 ratios and the long decay time of the pyrene monomer, it was concluded that the polypeptides $(Asp_1Phe_1)_n$, $(Asp_1Phe_2)_n$, and $(Asp_1Phe_3)_n$ generate hydrophobic microdomains that can solubilize pyrene and provide protection from the solution whereas in solutions of the more hydrophilic polypeptides $(Asp_3Phe_1)_n$ and $(Asp_2Phe_1)_n$, most pyrenes are exposed to the aqueous phase. If these conclusions are correct, a fraction of the pyrenes associated with the hydrophobic polypeptides should be inaccessible to an external quencher introduced to the solution. To this end, fluorescence quenching

experiments were conducted on the polypeptides using pyrene as the probe and nitromethane as a neutral water–soluble quencher of pyrene.

Table 5.5. Summary of the excimer decay times and pre-exponential factors calculated for the randomly labeled polypeptides.

Sample	τ_{E1} (ns)	a_{E1}	τ_{E2} (ns)	a_{E2}	τ_{E3} (ns)	a_{E3}	ξ	χ^2
RPy–$(Asp)_n$–229	4	0.15	26	0.41	58	0.44	0.00	1.04
RPy–$(Asp_3Phe_1)_n$–195	30	0.53	56	0.46	–	–	0.00	1.19
RPy–$(Asp_3Phe_1)_n$–245	28	0.47	53	0.53	–	–	0.00	1.20
RPy–$(Asp_2Phe_1)_n$–56	41	0.77	68	0.23	–	–	0.00	1.17
RPy–$(Asp_2Phe_1)_n$–176	35	0.43	58	0.57	–	–	0.00	1.26
RPy–$(Asp_2Phe_1)_n$–322	30	0.30	54	0.70	–	–	0.00	1.19
RPy–$(Asp_1Phe_1)_n$–70	13	–0.23	50	0.88	84	0.35	–0.19	1.15
RPy–$(Asp_1Phe_1)_n$–132	18	–0.37	32	0.54	68	0.82	–0.27	1.14
RPy–$(Asp_1Phe_1)_n$–221	22	–0.75	29	0.98	70	0.77	–0.43*	1.25
RPy–$(Asp_1Phe_2)_n$–45	3	0.26	71	0.62	168	0.13	0.00	1.02
RPy–$(Asp_1Phe_2)_n$–97	32	–0.17	64	0.90	142	0.28	–0.14	1.13
RPy–$(Asp_1Phe_2)_n$–131	15	–0.26	66	0.90	127	0.35	–0.21	1.08
RPy–$(Asp_1Phe_3)_n$–72	30	–0.03	68	0.79	152	0.24	–0.03	1.04
RPy–$(Asp_1Phe_3)_n$–104	13	–0.11	67	0.82	143	0.28	–0.10	1.05

∗The decay times τ_{E1} and τ_{E2} are too close to yield a reliable ξ value.

With the addition of nitromethane, the excited pyrene is quenched which is observed by the decrease of the pyrene fluorescence intensity in the fluorescence spectra and by the shortening of the pyrene number-average decay times in the fluorescence decays.[36] These

results are presented in the form of Stern-Volmer plots where the ratios I_0/I and $<\tau_0>/<\tau>$ are plotted as a function of quencher concentrations [Q], as illustrated in Figure 5.7 for pyrene used as a free probe for the $(Asp_1Phe_2)_n$ and $(Asp_1Phe_3)_n$ polypeptide sequences. Here I_0 and I represent the fluorescence intensity of the pyrene monomer in the absence and presence of quencher, respectively.[36] Similarly, $<\tau_0>$ and $<\tau>$ are, respectively, the number-average decay times of pyrene in the absence and presence of the quencher.

The Stern–Volmer plots obtained by steady-state and time-resolved fluorescence do not overlap, implying that there is an additional quenching process. Such trends are a clear indication that static quenching is taking place, due to the formation of a ground-state complex between the chromophore and the quencher.[55] This chromophore-quencher complex does not fluoresce upon excitation and only those chromophores which are not complexed emit. In steady-state fluorescence experiments all chromophores are taken into consideration whereas time-resolved fluorescence experiments only probe those chromophores which are not complexed. Hence the I_0/I ratio increases more steeply with increasing quencher concentration than the $<\tau_0>/<\tau>$ ratio does. The ratio $<\tau_0>/<\tau>$ also increases with [Q] demonstrating that diffusional quenching of pyrene is taking place. However the $<\tau_0>/<\tau>$ ratio is observed to plateau at higher quencher concentrations. This leveling off suggests that the quencher is unable to quench some of the pyrenes by diffusion. These pyrenes are said to be protected from diffusional quenching.[54] Similar results were obtained for $(Asp_1Phe_1)_n$ when pyrene was introduced as a free probe (Chapter 4).

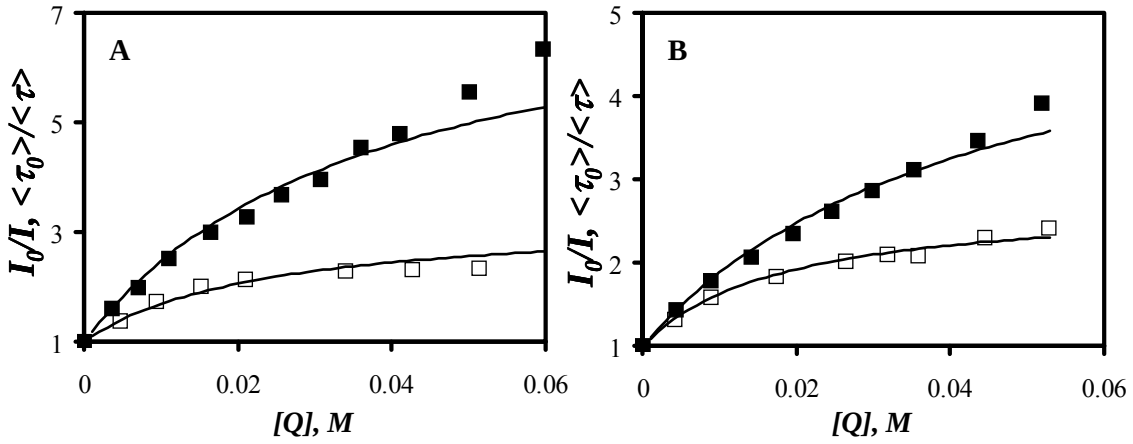

Figure 5.7. Stern-Volmer plots obtained by steady-state (■) and time-resolved (□) fluorescence for A) $(Asp_1Phe_2)_n$, [*Py*] = 2.2 × 10^{-6} M, [*Polypeptide*] = 1.44 g/L and B) $(Asp_1Phe_3)_n$, [*Py*] = 5.1 × 10^{-6} M, [*Polypeptide*] = 1.84 g/L. Polypeptides in 0.01 M Na_2CO_3 solution at pH 9. λ_{ex} = 338 nm, λ_{em} = 374 nm.

As already discussed in Chapter 4 for $(Asp_1Phe_1)_n$, quenching of pyrene by nitromethane in aqueous solutions of polypeptides is both dynamic and static. These photophysical processes were described in Scheme 4.2 where the equations accounting for them were derived. Modified Stern-Volmer plots were obtained for the time-resolved fluorescence measurements carried out with the $(Asp_1Phe_1)_n$, $(Asp_1Phe_2)_n$, and $(Asp_1Phe_3)_n$ polypeptide sequences by plotting the ratio $<\tau_0>/\Delta<\tau>$ as a function of 1/[*Q*]. Straight lines were obtained for these plots as suggested by Equation 4.11 in Chapter 4 and the parameters f_a, the fraction of accessible pyrenes and k_Q, the quenching rate constant, were determined. Equation 4.11 yielded K_S, the equilibrium constant for complex formation between pyrene and nitromethane. Table 5.6 lists these parameters obtained for the $(Asp_1Phe_1)_n$, $(Asp_1Phe_2)_n$, and $(Asp_1Phe_3)_n$ polypeptide sequences. The quenching rate constants k_Q for all three polypeptide sequences using pyrene as a free probe were found to be ~10 times smaller than

that determined for pyrene in 0.01 M Na_2CO_3 solution at pH 9 ($k_Q = 9.8 \times 10^9$ M^{-1} s^{-1}). The f_a values obtained for these polypeptide sequences indicate that ~60 % of the pyrenes are accessible for quenching by nitromethane whereas ~40 % of the pyrenes solubilized by the hydrophobic domains are protected from the quencher and are still able to emit regardless of quencher concentration. This fraction is somewhat similar to the pre-exponential factors a_{M3} determined for the polypeptides $(Asp_1Phe_1)_n$, $(Asp_1Phe_2)_n$, and $(Asp_1Phe_3)_n$, which indicates that ~40-60 % of the pyrenes are long-lived. This is a clear indication that these polypeptides generate hydrophobic microdomains which are able to encapsulate pyrene in such a way as to protect it from its surroundings and hence quenching by nitromethane.

Table 5.6. Summary of parameters determined for quenching of pyrene dissolved in polypeptides.

Sample	K_S M^{-1}	$10^{-9} \times k_Q$ M^{-1} s^{-1}	$<\tau_0>$ ns	$<\tau_L>$ ns	f_a
$(Asp_1Phe_1)_n$ + Py	15.8 ± 0.3	0.92 ± 0.05	157	299	0.61 ± 0.01
$(Asp_1Phe_2)_n$ + Py	26.9 ± 0.4	1.27 ± 0.11	181	309	0.63 ± 0.01
$(Asp_1Phe_3)_n$ + Py	12.6 ± 0.2	0.68 ± 0.02	222	314	0.64 ± 0.01

Quenching experiments were also performed for all the labeled polypeptides and all polypeptide sequences using both steady-state and time-resolved fluorescence. The Stern-Volmer plots obtained for the $(Asp_3Phe_1)_n$ and $(Asp_1Phe_3)_n$ sequences by steady-state and time-resolved fluorescence measurements for the end-labeled and randomly labeled polypeptides are presented in Figure 5.8 (A–D). The first significant difference between these plots is the absence of protective quenching for the more hydrophilic sequence (A and

B) as indicated by the linear increase for the I_0/I and $<\tau_0>/<\tau>$ ratios as a function of quencher concentration. This is observed when efficient quenching of pyrene takes place and the main process for quenching is diffusion–controlled. There is also a small amount of static quenching shown by the slight difference between the plots obtained from the steady-state and time-resolved fluorescence measurements for both the end-labeled and randomly labeled polypeptides. The more hydrophobic sequence $(Asp_1Phe_3)_n$ exhibits some protective quenching since the $<\tau_0>/<\tau>$ ratio starts to plateau at higher quencher concentrations. The extent of protective quenching is however less for the labeled polypeptides than for the polypeptide solutions where pyrene was present as a free probe. Furthermore the pyrene labels are more exposed to the solvent since the fraction of pyrenes accessible to the quencher is ~90 % for both the end-labeled and the randomly labeled polypeptide solutions for the $(Asp_1Phe_2)_n$ and $(Asp_1Phe_3)_n$ sequences. Therefore only a small fraction (~10 %) is found to be protected from quenching by nitromethane. Static quenching is also taking place in these polypeptides. The quenching rate constant k_Q decreases from 6.1×10^9 M^{-1} s^{-1} to 0.7×10^9 M^{-1} s^{-1} as the hydrophobic character of the polypeptides increases. The parameters k_Q and f_a are listed in Table 5.7.

The results obtained for the quenching experiments carried out using steady-state and time-resolved fluorescence for all the polypeptide sequences using pyrene as a free probe and pyrene covalently attached to the polypeptide (both end-labeled and randomly labeled) are illustrated in Figure 5.9. Here the quenching rate constant k_Q is plotted as a function of the phenylalanine content of the polypeptide sequences and compared to the k_Q value of pyrene in 0.01 M Na_2CO_3 solution at pH 9 obtained by steady-state fluorescence. The k_Q value obtained for a Phe content equal to 0.0 mol% corresponds to that of RPy–$(Asp)_n$–229. The

value of the quenching rate constant, k_Q, obtained for molecular pyrene dissolved in 0.01 M Na_2CO_3 solution at pH 9 is clearly the highest at 9.8×10^{9} M^{-1} s^{-1} as shown by the horizontal line in Figure 5.9 used as a reference. Starting from $(Asp)_n$ with zero phenylalanine content and moving to the far right for $(Asp_1Phe_3)_n$ with 75 mol% phenylalanine content, the quenching rate constant, k_Q, shows a steady decrease in its value as the Phe content of the polypeptide sequence increases up to a Phe content of 66 mol%, above which it levels off for the $(Asp_1Phe_2)_n$ and $(Asp_1Phe_3)_n$ sequences.

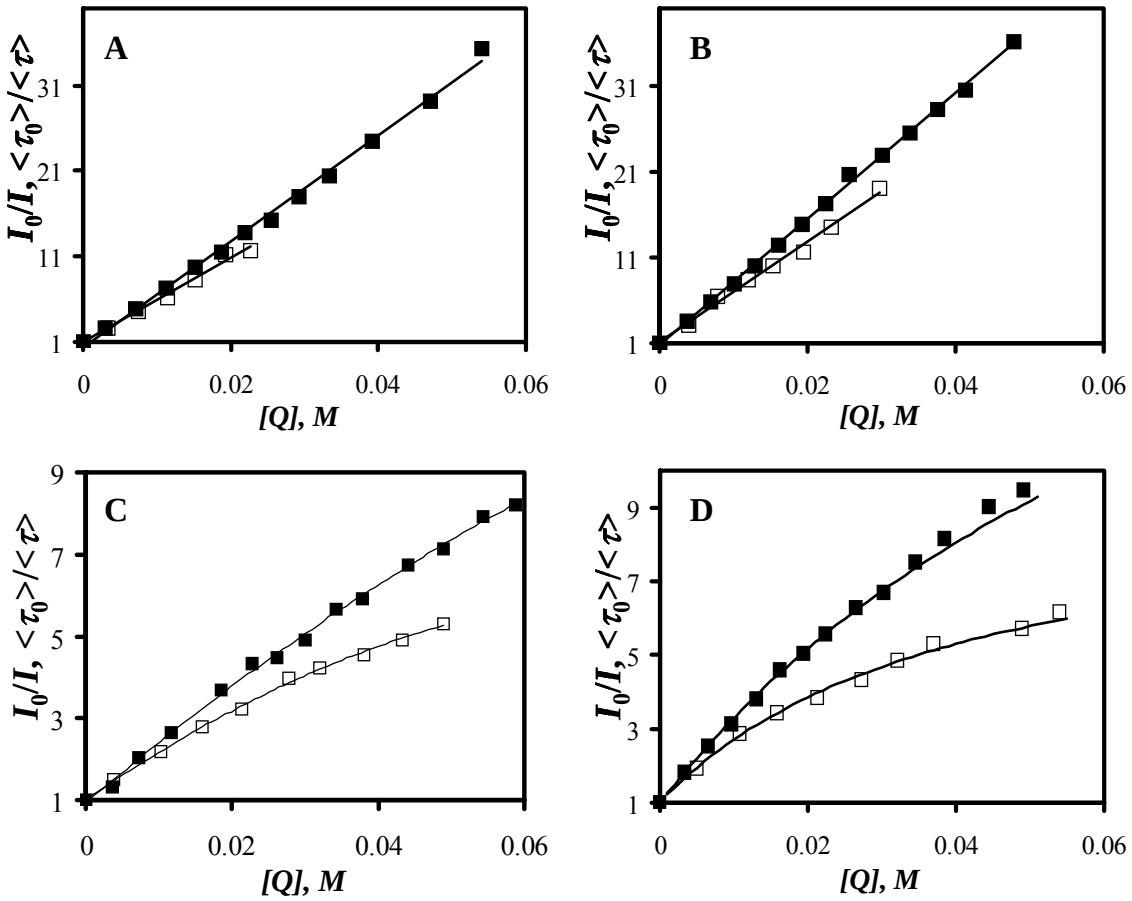

Figure 5.8. Stern–Volmer plots obtained for pyrene labeled polypeptides: by steady-state (■) and time-resolved (□) fluorescence. (A) EPy–$(Asp_3Phe_1)_n$–26, [*Polypeptide*] = 1.0 g/L; (B) RPy–$(Asp_3Phe_1)_n$–195, [*Polypeptide*] = 0.14 g/L; (C) EPy–$(Asp_1Phe_3)_n$–91, [*Polypeptide*] = 1.1 g/L; and (D) RPy–$(Asp_1Phe_3)_n$–72, [*Polypeptide*] = 0.29 g/L; λ_{ex} = 346 nm, λ_{em} = 374 nm. Polypeptides solutions in 0.01 M Na_2CO_3 at pH 9.

Table 5.7. Parameters obtained from the quenching experiments.

Sample	$<\tau_0>$ ns	K_S M^{-1}	$10^{-9}\times k_Q$ $M^{-1}s^{-1}$ (SS)	$10^{-9}\times k_Q$ $M^{-1}s^{-1}$ (TR)	f_a
Na_2CO_3 solution	128	n.a.	9.82 ± 0.05	n.a.	n.a.
RPy–$(Asp)_n$–229	105	11.8 ± 1.1	6.23 ± 0.13	4.82 ± 0.06	1.00
EPy–(Asp_3Phe_1)–26	99	4.9 ± 0.3	6.06 ± 0.07	5.05 ± 0.15	1.00
RPy–$(Asp_3Phe_1)_n$–195	119	0.2 ± 0.3	6.12 ± 0.03	4.97 ± 0.10	1.00
RPy–$(Asp_3Phe_1)_n$–245	102	6.9 ± 1.0	6.63 ± 0.06	5.27 ± 0.14	1.00
EPy–(Asp_2Phe_1)–15	101	19.4 ± 2.3	6.40 ± 0.06	4.62 ± 0.10	1.00
RPy–(Asp_2Phe_1)–56	131	0.3 ± 0.9	4.72 ± 0.08	4.66 ± 0.19	1.00
RPy–(Asp_2Phe_1)–176	117	4.6 ± 2.0	4.72 ± 0.33	4.21 ± 0.22	1.00
RPy–(Asp_2Phe_1)–322	111	0.3 ± 1.1	4.55 ± 0.09	4.41 ± 0.13	1.00
$(Asp_1Phe_1)_n$ + Py	157	15.8 ± 0.3	n.a.	0.92 ± 0.05	0.61 ± 0.01
EPy–(Asp_1Phe_1)–44	127	16.7 ± 2.1	2.91 ± 0.03	2.19 ± 0.18	1.00
RPy–(Asp_1Phe_1)–70	135	6.5 ± 1.0	2.80 ± 0.05	2.51 ± 0.09	1.00
RPy–(Asp_1Phe_1)–132	113	12.5 ± 1.9	3.81 ± 0.06	2.82 ± 0.04	1.00
RPy–(Asp_1Phe_1)–221	104	1.8 ± 0.7	3.34 ± 0.04	3.18 ± 0.05	1.00
$(Asp_1Phe_2)_n$ + Py	181	26.9 ± 0.4	n.a.	1.27 ± 0.11	0.63 ± 0.01
EPy–(Asp_1Phe_2)–13	147	12.2 ± 0.9	n.a.	0.98 ± 0.03	0.88 ± 0.01
RPy–(Asp_1Phe_2)–45	190	4.1 ± 0.4	n.a.	0.90 ± 0.01	0.92 ± 0.00
RPy–(Asp_1Phe_2)–97	168	10.1 ± 0.5	n.a.	0.85 ± 0.02	0.90 ± 0.01
RPy–(Asp_1Phe_2)–131	156	8.0 ± 0.3	n.a.	0.77 ± 0.02	0.91 ± 0.00
$(Asp_1Phe_3)_n$ + Py	222	12.6 ± 0.2	n.a.	0.68 ± 0.02	0.64 ± 0.01
EPy–(Asp_1Phe_3)–91	138	18.7 ± 1.1	n.a.	0.67 ± 0.17	0.91 ± 0.09
RPy–(Asp_1Phe_3)–72	169	16.0 ± 0.5	n.a.	1.40 ± 0.03	0.90 ± 0.00
RPy–(Asp_1Phe_3)–104	140	26.3 ± 2.3	n.a.	0.91 ± 0.05	0.91 ± 0.02

The quenching results indicate that for the labeled polypeptide having a Phe content smaller than 50 mol%, efficient quenching is observed and linear Stern–Volmer plots are obtained. The alternating polypeptide $(Asp_1Phe_1)_n$ shows a mixed situation where protective quenching is observed when pyrene is dissolved as a free probe as found for the more

hydrophobic sequences and no protective quenching is observed when pyrene is covalently attached onto the polypeptide, as found for the more hydrophilic sequences. The values of the quenching rate constants are nearly 10 times smaller for all the solutions of the $(Asp_1Phe_2)_n$ and $(Asp_1Phe_3)_n$ polypeptides than for the $(Asp_3Phe_1)_n$ and $(Asp_2Phe_1)_n$ polypeptides which are richer in the Asp monomer. The polypeptide sequences $(Asp_1Phe_2)_n$ and $(Asp_1Phe_3)_n$ exhibit some protective quenching along with both dynamic and static quenching. A fraction of the pyrenes locate themselves in the hydrophobic microdomains generated by these two polypeptides and the domains enable these pyrenes to avoid being quenched by the water-soluble quencher. The extent of protective quenching is higher when pyrene is present as a free probe than when it is covalently attached to the polypeptide. This observation suggests that when pyrene is used as a free probe, it has the freedom to access those more hydrophobic microdomains generated by the polypeptides, whereas when pyrene is covalently attached onto the polypeptide, its freedom of motion is restricted which prevents pyrene to diffuse towards the hydrophobic domains. Consequently, a smaller fraction of the pyrenes attached covalently onto the polypeptide is protected from quenching.

From the quenching results, the conclusions can be drawn that in the presence of the polypeptides $(Asp_3Phe_1)_n$ and $(Asp_2Phe_1)_n$ which are richer in Asp, pyrene quenching occurs predominantly by diffusion with a small amount of static quenching. The absence of protective quenching indicates the absence of hydrophobic microdomains since the pyrene labels are fully exposed to the quencher molecule. The protective quenching observed for the polypeptide $(Asp_1Phe_2)_n$ and $(Asp_1Phe_3)_n$ richer in Phe demonstrates the ability of these polypeptides to associate and generate hydrophobic microdomains which are able to encapsulate the chromophore pyrene whether it is present as a free molecule or as a

hydrophobic pendant. The alternating polypeptide falls between these two extremes as it shows the presence of hydrophobic microdomains evident by the occurrence of protective quenching when pyrene is used as a free probe. However these hydrophobic microdomains are not present in sufficient amount to accommodate pyrene once it has been chemically bonded to the polypeptide.

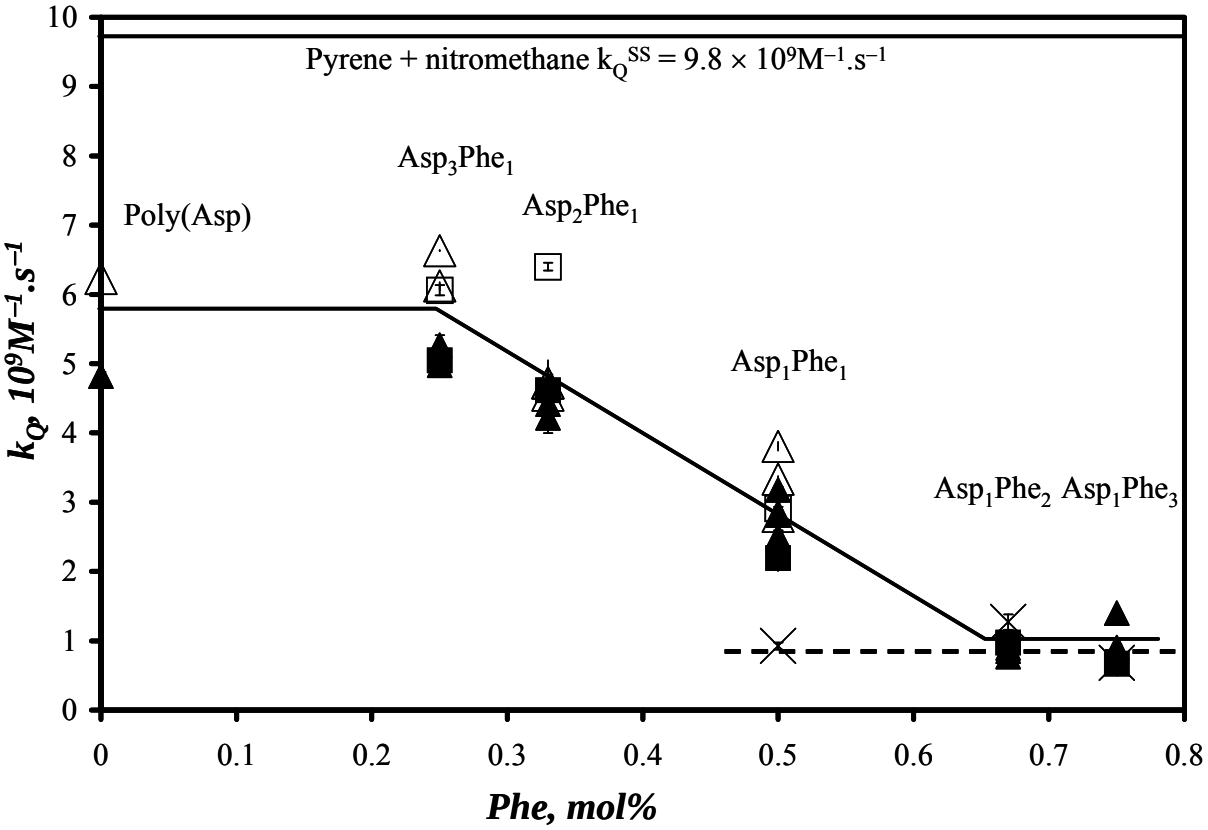

Figure 5.9. Plot of the quenching rate constant k_Q as a function of the phenylalanine content in the polypeptide sequences. (×) k_Q for pyrene as a free probe determined by time-resolved fluorescence. k_Q for the end-labeled polypeptides obtained by steady-state (□) and time-resolved (■) fluorescence. k_Q for the randomly labeled polypeptides obtained by steady-state (△) and time-resolved (▲) fluorescence. Polypeptides in 0.01 M Na_2CO_3 solution at pH 9.

These results complement those obtained by the DLS and NRET studies. The DLS

study indicated that all polypeptides sequences led to the presence of single chains and polypeptide aggregates. However no conclusion could be drawn regarding the extent of aggregation as a function of the Phe content of the polypeptides. Such conclusions could be drawn by conducting the fluorescence experiments. No NRET was observed from the Np labeled polypeptide to the Py labeled polypeptide for the more hydrophilic polypeptide sequences. NRET occurred from the Np–labeled polypeptide to the Py–labeled polypeptide for both the $(Asp_1Phe_2)_n$ and $(Asp_1Phe_3)_n$ sequences. The stronger associations generated by these polypeptides were further confirmed by the evidence of protective quenching which indicated that pyrene was able to bury itself deep inside the hydrophobic domains to avoid the quencher molecule present in the aqueous phase.

Although evidence for polypeptide aggregation was obtained for $(Asp_1Phe_2)_n$ and $(Asp_1Phe_3)_n$ from the fluorescence energy transfer and quenching experiments in agreement with the DLS results, the fluorescence measurements detected no polypeptide aggregates for the $(Asp_3Phe_1)_n$ and $(Asp_2Phe_1)_n$ polypeptides, disagreeing with the DLS study. The different observation made with the two techniques, fluorescence and light scattering, results certainly from the difference in what the two techniques probe. The fluorescence measurements provide a number-average representation of the species present in solution, whereas light scattering is more heavily weighed towards the larger species present in solution. To assess how those differences could affect the results presented in this thesis, additional experiments were performed on the unlabeled polypeptide solutions and those where pyrene was dissolved as a free molecule. Polypeptide solutions having polypeptide concentrations of 0.05 g/L were prepared for all sequences. The light scattering and emission intensities were determined using excitation wavelengths of 450 nm and 255 nm, respectively. For the

samples containing pyrene, the emission spectra of pyrene were also recorded with an excitation wavelength of 338 nm. The polypeptide solutions were then filtered using a 20 nm pore size filter paper and the fluorescence experiments were repeated on the filtered solutions. Figure 5.10 gives the scattering and fluorescence intensities of the polypeptide sequences $(Asp_3Phe_1)_n$ and $(Asp_1Phe_3)_n$ before and after filtration, whereas the light scattering and pyrene fluorescence intensities obtained for "$(Asp_1Phe_3)_n$ + Py" before and after filtration, are presented in Figure 5.12.

The light scattering intensities for both the $(Asp_3Phe_1)_n$ and $(Asp_1Phe_3)_n$ sequences presented in Figure 5.10A and C show a substantial decrease after filtration. The decrease was larger for the hydrophobic sequence (85 %) than for the hydrophilic sequence (45 %). This decrease suggests that large particles were present in solutions which were removed after filtration, suggesting the existence of polymeric aggregates for both sequences as inferred from the DLS results. However no such decrease is observed in the fluorescence emission intensity for $(Asp_3Phe_1)_n$ after filtration as demonstrated by Figure 5.10B, whereas a 35 % decrease in the fluorescence emission occurs for the $(Asp_1Phe_3)_n$ polypeptide sequence in Figure 5.10D. Since the fluorescence intensity is directly related to the polypeptide concentration, a decrease in the fluorescence signal indicates that some of the $(Asp_1Phe_3)_n$ polypeptide was filtered out. From this simple experiment, it can be deduced that $(Asp_3Phe_1)_n$ mainly exists as individual chains in solution whereas the more hydrophobic polypeptide $(Asp_1Phe_3)_n$ is generating polymeric aggregates to a larger extent. Similar results to those found for $(Asp_3Phe_1)_n$ were obtained for the $(Asp_2Phe_1)_n$ and $(Asp_1Phe_1)_n$ sequences confirming their existence mainly as single chains. A small decrease ~10 % is observed for the fluorescence emission intensity for $(Asp_1Phe_2)_n$ sequence confirming its ability to form

polymeric aggregates, but to a lower extent than found for the $(Asp_1Phe_3)_n$ sequence. Figure 5.11 summarizes these results.

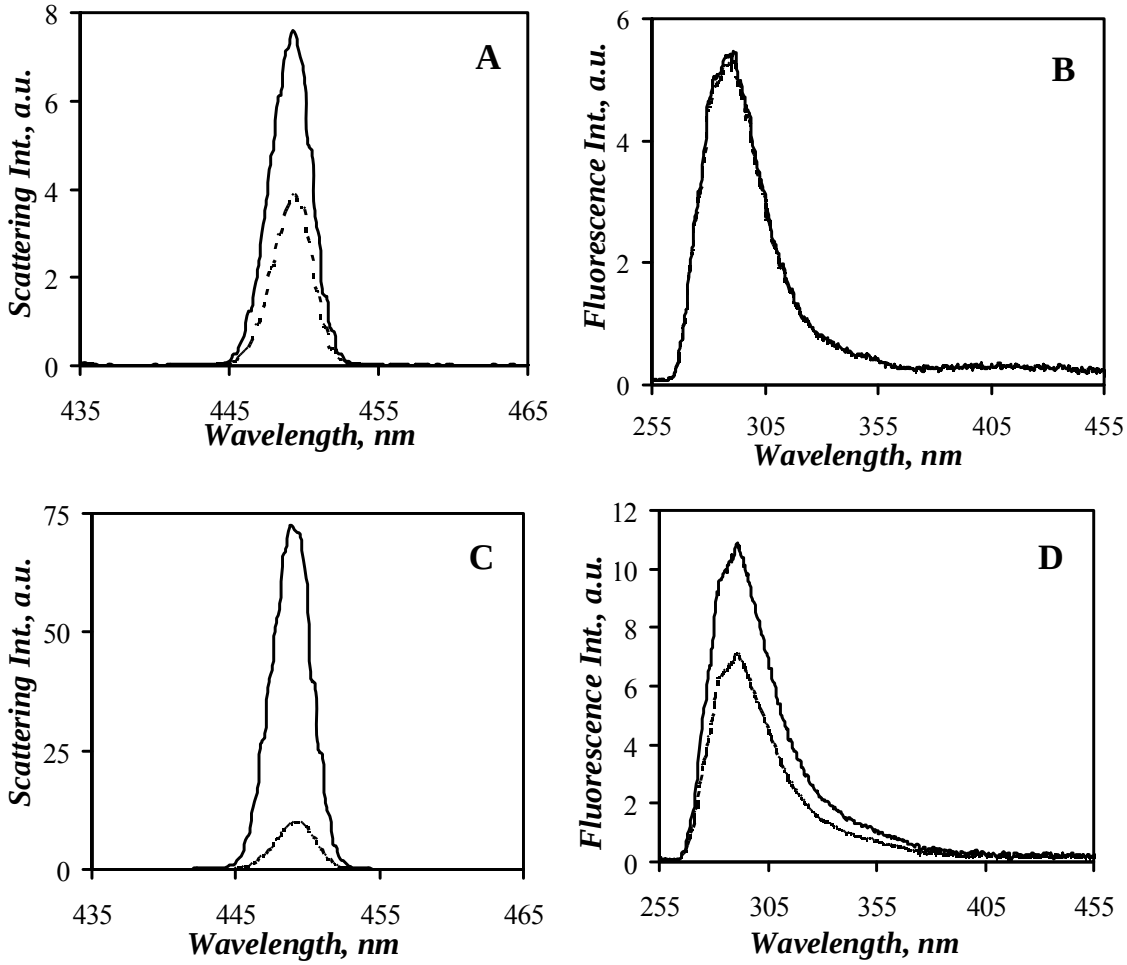

Figure 5.10. (A) Light scattering intensity (λ_{ex} = λ_{em} = 450 nm) and (B) fluorescence emission spectra (λ_{ex} = 255 nm) before (————) and after (– – – – ·) filtration of the $(Asp_3Phe_1)_n$ solution. (C) Light scattering intensity (λ_{ex} = λ_{em} = 450 nm) and (D) fluorescence emission spectra (λ_{ex} = 255 nm) before (————) and after (– – – – ·) filtration of the $(Asp_1Phe_3)_n$ solution. [*Polypeptide*] = 0.05 g/L in 0.01 M Na_2CO_3 solutions at pH 9.

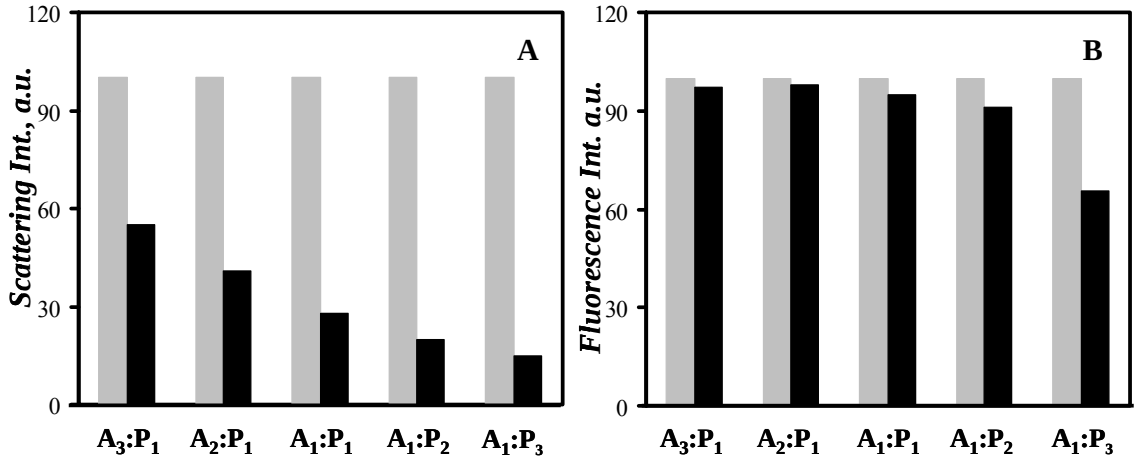

Figure 5.11. (A) Light scattering intensity (λ_{ex} = λ_{em} = 450 nm), (B) fluorescence intensity (λ_{ex} = 255 nm and λ_{em} = 292 nm) for $(Asp_xPhe_y)_n$. Grey bars: unfiltered solutions, Black bars: filtered solutions. A = Asp and P = Phe; [*Polypeptides*] = 0.05 g/L in 0.01 M Na_2CO_3 solution at pH 9.

For polypeptide solutions where pyrene was used as a probe, a decrease of more than 50 % of the light scattering intensity is found in Figure 5.12B for all three sequences. This decrease in light scattering is accompanied by a larger than 60 % decrease of the pyrene emission after filtration of the polypeptide solutions. This was observed for all three polypeptide sequences, the decrease being larger for the more hydrophobic sequences. These results suggest that pyrene targets specifically the hydrophobic domains provided by the polypeptide aggregates which are removed through filtration.

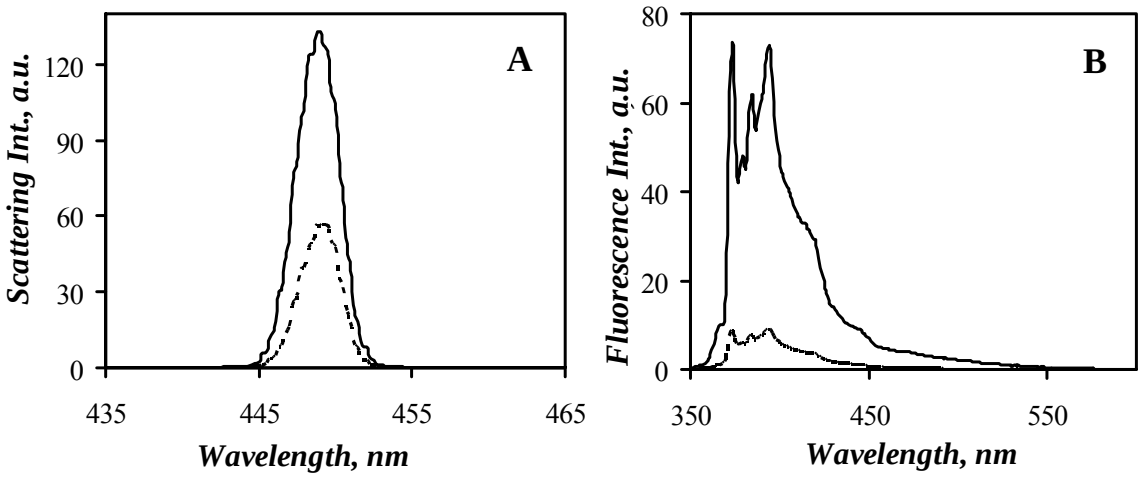

Figure 5.12. (A) Light scattering intensity, $\lambda_{ex} = \lambda_{em}$ =450 nm and (B) fluorescence emission spectra (λ_{ex} = 338 nm) before (————) and after (– – – – ·) filtration of 0.05 g/L solution of $(Asp_1Phe_3)_n$ + Py in 0.01 M Na_2CO_3 at pH 9.

The effect observed on the self-association of a polypeptide in aqueous solution as its character is gradually changed from hydrophilic to hydrophobic by adjusting the polypeptide sequence $(Asp_3Phe_1)_n$, $(Asp_2Phe_1)_n$, $(Asp_1Phe_1)_n$, $(Asp_1Phe_2)_n$, and $(Asp_1Phe_3)_n$, can be investigated in extensive detail by the combined use of DLS and various fluorescence techniques such as NRET and fluorescence quenching. Using pyrene as a free probe, the presence and absence of hydrophobic microdomains and polymeric aggregates could be established by DLS, the pyrene I_1/I_3 ratio, the pyrene decay times, and the fluorescence quenching experiments. Covalently attaching chromophores onto the polypeptides provided another means for characterizing the formation of the polypeptide aggregates by carrying out fluorescence NRET experiments.

5.5. Conclusions

The effect that the sequence of a polypeptide has on its solution properties was investigated for five different polypeptide sequences, namely $(Asp_3Phe_1)_n$, $(Asp_2Phe_1)_n$, $(Asp_1Phe_1)_n$, $(Asp_1Phe_2)_n$, and $(Asp_1Phe_3)_n$. CD, DLS, and several fluorescence techniques were used to characterize these polypeptides. CD spectra (Figure 5.1) for the polypeptides before and after labeling with pyrene indicated no substantial change in their conformation after modification. It was also noted that the first four sequences show no clear conformation. The $(Asp_1Phe_3)_n$ polypeptide was observed to adopt an α-helical conformation which was maintained even after pyrene labeling. The DLS performed in Figure 5.2, suggested that all polypeptide sequences generated a mixture of single chains and polypeptide aggregates. Fluorescence energy transfer experiments (Figure 5.3) performed using polypeptides singly labeled with naphthalene as the donor molecule and pyrene as the acceptor molecule confirm the existence of polypeptide aggregates only for those sequences richer in Phe, namely $(Asp_1Phe_2)_n$ and $(Asp_1Phe_3)_n$. On the other hand, no polypeptide aggregates could be found by NRET for the sequences with a lower Phe content. The I_1/I_3 ratios and the pyrene monomer decay times determined for the polypeptides using pyrene as a probe also demonstrate the presence of hydrophobic pockets for the polypeptide having a Phe content of 50 % and above. For the randomly labeled polypeptides, the ratio takes on higher values and the pyrene decay times become shorter as the polypeptides become richer in the Asp monomer. The extensive quenching studies carried out (Figures 5.7-5.9) showed that pyrene attached to the hydrophilic polypeptides undergoes diffusional quenching by an external quencher, whereas protective quenching is observed for the more hydrophobic sequences. For the polypeptide solutions where pyrene is used as a probe, protective quenching was

observed for the three sequences $(Asp_1Phe_1)_n$, $(Asp_1Phe_2)_n$, and $(Asp_1Phe_3)_n$. Thus the overall picture that emerges suggests that, those polypeptide sequences which are richer in the Asp monomer do not undergo intermolecular associations. The $(Asp_3Phe_1)_n$ and $(Asp_2Phe_1)_n$ polypeptides exist as individual polymer chains and do not provide hydrophobic microdomains to the pyrene labels. The more hydrophobic polypeptide sequences are able to generate hydrophobic microdomains both through intra– and intermolecular hydrophobic interactions. Pyrene present as either a free probe or a hydrophobic label is able to associate with these hydrophobic domains which provide sufficient protection against quenching by a water-soluble quencher such as nitromethane.

5.6. References:

1. *Polymers in Aqueous Media : Performance through Association*. Ed. J. E. Glass; ACS Advances in Chemistry Series 223; 1989.
2. *Hydrophilic Polymers : Performance with Environmental Acceptance*. Ed. J. E. Glass; ACS Advances in Chemistry Series 248; 1996.
3. *Associative Polymers in Aqueous Media*. Ed. J. E. Glass; ACS Advances in Chemistry Series 765; 2000.
4. *Polymer-Surfactant Systems*. Kwak, J. C.; Surfactant Science Series 77; Marcel Decker; New York, 1998.
5. Siu, H.; Duhamel, J. *Macromolecules* **2006**, *39*, 1144-1155.
6. Kumacheva, E.; Rharbi, Y.; Winnik, M. A.; Guo, L.; Tam, K. C.; Jenkins, R. D. *Langmuir* **1997**, *13*, 182-186.
7. Yekta, A.; Xu, B.; Duhamel, J.; Adiwidjaja, H.; Winnik, M. A. *Macromolecules* **1995**, *28*, 956-966.
8. Uhrich, K. E. *Chem*. *Rev*. **1999**, *99*, 3181-3198.
9. Francis, M. F.; Cristea, M.; Winnik, F. M. *Pure Appl*. *Chem*. **2004**, *76*, 1321-1335.
10. Kataoka, K.; Harada, A.; Nagasaki, Y. *Adv*. *Drug Deliv*. *Rev*. **2001**, *47*, 113-131.
11. *Water-soluble polymers: synthesis, solution properties, and applications*. Pub. Washinton, DC: ACS Symposium Series 467; 1991.
12. Duhamel, J.; Yekta, A.; Hu, Y. Z.; Winnik, M. A. *Macromolecules* **1992**, *25*, 7024-7030.
13. Beaudoin, E.; Borisov, O.; Lapp, A.; Billon, L.; Hiorns, R. C.; François, J. *Macromolecules* **2002**, *35*, 7436-7447.
14. Laukkanen, A.; Hietala, S.; Maunu, S. L.; Tenhu, H. *Macromolecules* **2000**, *33*, 8703-8708.
15. Kjøniksen, A.; Laukkanen, A.; Galant, C.; Knudsen, K. D.; Tenhu, H.; Nyström, B. *Macromolecules* **2005**, *38*, 948-960.
16. Kujawa, P.; Goh, C. C. E.; Calvet, D.; Winnik, F. M. *Macromolecules* **2001**, *34*, 6387-6395.
17. Kujawa, P.; Liu, R. C. W.; Winnik, F. M. *J*. *Phys*. *Chem*. *B* **2002**, *106*, 5578-5585.
18. Barros, T. C.; Adronov, A.; Winnik, F. M.; Bhone, C. *Langmuir* **1997**, *13*, 6089-6094.

19. Miyazawa, K; Winnik, F. M. *J*. *Phys*. *Chem*. *B* **2003**, *107*, 10677-10682.
20. Morishima, Y.; Nomura, S.; Ikeda, T.; Seki, M.; Kamachi, M. *Macromolecules* **1995**, *28*, 2874-2881.
21. Hashidzume, A.; Mizusaki, M.; Yoda, K.; Morishima, Y. *Langmuir* **1999**, *15*, 4276-4282.
22. Yamamoto, H.; Mizusaki, M.; Yoda, K.; Morishima, Y. *Macromolecules* **1998**, *31*, 3588-3594.
23. Mizusaki, M.; Morishima, Y.; Winnik, F. M. *Macromolecules* **1999**, *32*, 4317-4326.
24. Yusa, S. –I.; Kamachi, M.; Morishima, Y. *Langmuir* **1998**, *14*, 6059-6067.
25. Nishikawa, K.; Yekta, A.; Pham, H. H.; Winnik, M. A.; Sau, A. C. *Langmuir* **1998**, *14*, 7119-7129.
26. Madoka, S.; Hashidzume, A.; Morishima, Y.; Nakato, T.; Tomida, M. *Macromolecules* **2000**, *33*, 7884-7892.
27. Kang, H. S.; Yang, S. R.; Kim, J.; Han, S.; Chang, I. *Langmuir* **2001**, *17*, 7501-7506.
28. Nichifor, M.; Lopes, S.; Bastos, M.; Lopez, A. *J*. *Phys*. *Chem*. *B* **2004**, *108*, 16463-16472.
29. Taniguchi, I.; Akiyoshi, K.; Sunamoto, J. *Macromol*. *Chem*. *Phys*. **1999**, *200*, 1386-1392.
30. Akiyoshi, K.; Deguchi, S.; Moriguchi, N.; Yamaguchi, S.; Sunamoto, J. *Macromolecules* **1993**, *26*, 3062-3068.
31. Yusa, S. –I.; Sakakibara, A.; Yamamoto, M.; Morishima, Y. *Macromolecules* **2002**, *35*, 10182-10188.
32. Taniguchi, I.; Akiyoshi, K.; Sunamoto, J. *Macromol*. *Chem*. *Phys*. **1999**, *200*, 1554-1560.
33. Kramer, M.; Welch, C. G.; Steger, J. R.; McCormick, C. L. *Macromolecules* **1995**, *28*, 5248-5254.
34. Hu, Y.; Kramer, M. C.; Boudreaux, C. J.; McCormick, C. L. *Macromolecules* **1995**, *28*, 7100-7106.
35. Garnier, G.; Duskova-Smrckova, M.; Vyhnalkova, R.; van de Ven, T. G. M.; Revol, J. *Langmuir* **2000**, *16*, 3757-763.
36. Claracq, J.; Santos, S. F.C R.; Duhamel, J.; Dumousseaux, C.; Corpart, J. *Langmuir*

2002, *18*, 3829-3835.

37. *Polymer Handbook*, Brandrup, J.; Immergut, E. H.; Grulke, E. A. 4th Ed. New York, Wiley, 1999.
38. Kovacs, J.; Giannotti, R.; Kapoor, A. *J. Am. Chem. Soc.* **1966**, *88*, 2282-2292.
39. DeTar, D. F.; Gouge, M.; Honsberg, W.; Honsberg, U. *J. Am. Chem. Soc.* **1967**, *89*, 988-998.
40. DeTar, D. F.; Vajda, T. *J. Am. Chem. Soc.* **1967**, *89*, 998-1004.
41. James, D. R.; Demmer, D. R. M.; Verrall, R. E.; Steer, R. P. *Rev. Sci. Instrum.* **1983**, *54*, 1121-1130.
42. Press, W. H.; Flannery, B. P.; Teukolsky, S. A.; Vetterling, W. T. *Numerical Recipes. The Art of Scientific Computing (Fortran Version)*; Cambridge University Press: Cambridge, 1992.
43. a) Auer, H. E.; Doty, P. *Biochemistry* **1966**, *5*, 1708-1715. b) Auer, H. E.; Doty, P. *Biochemistry* **1966**, *5*, 1716-1723.
44. Winnik, F. M. *Polymer* **1990**, *31*, 2125-2134.
45. Mizusaki, M.; Kopek, N.; Morishima, Y.; Winnik, F. M. *Langmuir* **1999**, *15*, 8090-8099.
46. Kalyanasundaran, K.; Thomas, J. K. *J. Am. Chem. Soc.* **1977**, *99*, 2039-2044.
47. Dong, D. C.; Winnik, M. A. *Can. J. Chem.* **1984**, *62*, 2560-2565.
48. Duhamel, J. in *Molecular Interfacial Phenomena of Polymers and Biopolymers*. Ed. P. Chen, CRC Press, 2005; pp 214-248.
49. Kramer, C.; Somasundaran, P. *Langmuir* **2002**, *18*, 9357-9361.
50. Suwa, M.; Hashidzume, A.; Morishima, Y.; Nakato, T.; Tomida, M. *Macromolecules* **2000**, *33*, 7884-7892.
51. Mathew, A. K.; Duhamel, J.; Gao, J. *Macromolecules* **2001**, *34*, 1454-1469.
52. Birks, J. B. *Photophysics of Aromatic Molecules*; Wiley: New York, 1970; p 351. Winnik,
53. F. M.; Regismond, S. T. A. *Colloids Surf. A: Phys. Eng. Asp.* **1996**, *118*, 1-39.
54. Akiyoshi, K.; Kang, E.; Kurumada, S.; Sunamoto, J. *Macromolecules* **2000**, *33*, 3244-3249.
55. Lakowicz, J. R. *Principles of Fluorescence Spectroscopy, 2nd Ed*. Kluwer

Academic/Plenum Publishers: New York, 1999.

5.7. Appendix

Table A-1. Peak diameters and their standard deviations for the four polypeptides sequences, $(Asp_3Phe_1)_n$, $(Asp_2Phe_1)_n$, $(Asp_1Phe_2)_n$ and $(Asp_1Phe_3)_n$.

Sample	Conc. g/L	Particle size (nm)		
		Number-average	Volume-average	Intensity-average
$(Asp_3Phe_1)_n$	0.05	2.5 ± 0.4	2.6 ± 0.5	5.3 ±0.9 (7 %), 16.1 ± 0.4 (6%), 144.2 ± 63.3 (85 %)
	0.5	2.3 ± 0.4	2.4 ± 0.4	4.6 ± 0.7 (12 %), 172.5 ± 63.8 (87 %)
EPy–$(Asp_3Phe_1)_n$–26	0.05	2.2 ± 0.4	2.3 ± 0.4	2.4 ± 0.3 (6 %), 94.7 ± 18.0 (94 %)
	0.5	2.7 ± 0.5	2.9 ± 0.6	2.9 ± 0.5 (5 %), 117.1 ± 40.5 (94 %)
RPy–$(Asp_3Phe_1)_n$–195	0.05	5.2 ± 1.1	3.7 ± 0.6	2.5 ± 0.4 (6 %), 19.6 ± 4.7 (13 %), 237.1 ± 122.4 (79 %)
	0.5	3.6 ± 0.7	4.7 ± 0.9	2.8 ± 0.4 (15 %), 108.0 ± 38.0 (84 %)
RPy–$(Asp_3Phe_1)_n$–245	0.05	6.3 ± 1.5	4.1 ± 0.9	4.6 ± 0.7 (13 %), 172.7 ± 63.8 (86 %)
	0.5	6.8 ± 1.4	5.5 ± 1.7	5.3 ± 0.9 (6 %), 16.1 ± 3.4 (7 %), 144.1 ± 63.3 (85 %)
$(Asp_2Phe_1)_n$	0.05	3.4 ± 0.7	2.3 ± 1.1	4.2 ± 8 (28 %), 125.0 ± 55.6 (71 %)
	0.5	2.2 ± 0.4	2.4 ± 0.5	2.6 ± 0.4 (7 %), 105 ± 46.0 (92 %)
EPy–$(Asp_2Phe_1)_n$–15	0.05	3.5 ± 0.7	4.4 ± 1.0	4.4 ± 0.6 (8 %), 98.2 ± 30.6 (91 %)
	0.5	4.5 ± 0.9	4.7 ± 0.9	4.2 ± 0.8 (6 %), 145.4 ± 76.2 (93 %)
RPy–$(Asp_2Phe_1)_n$–56	0.05	3.4 ± 0.7	2.2 ± 1.3	4.2 ± 0.8 (28 %), 124.9 ± 55.6 (71 %)
	0.5	2.2 ± 0.4	4.2 ± 0.7	2.1 ± 0.4 (5 %), 118.0 ± 55.1 (94 %)
RPy–$(Asp_2Phe_1)_n$–176	0.05	5.3 ± 1.2	3.8 ± 0.7	6.9 ± 1.4 (33 %), 168.6 ± 81.1 (66 %)
	0.5	5.5 ± 1.1	4.5 ± 0.8	2.5 ± 0.5 (6 %), 131.4 ± 77.3 (93 %)
RPy–$(Asp_2Phe_1)_n$–322	0.05	5.5 ± 1.3	3.7 ± 0.5	7.3 ± 1.2 (18 %), 149.7 ± 37.8 (81 %)
	0.5	6.8 ± 1.4	4.9 ± 0.5	2.6 ± 0.4 (7 %), 105.3 ± 46.0 (92 %)
$(Asp_1Phe_1)_n$	0.05	5.8 ± 1.3	5.0 ± 1.2	7.7 ± 1.9 (31 %), 128.0 ± 67.1 (68 %)
	0.5	6.8 ± 1.0	5.1 ± 1.1	7.3 ± 0.8 (18 %), 105.2 ± 22.5 (21 %), 309.7 ± 51.3 (60 %)
$(Asp_1Phe_1)_n$ + molecular pyrene	0.05	3.4 ± 0.7	4.4 ± 4.1	4.3 ± 1.0 (17 %), 20.5 ± 6.8 (21 %), 130.1 ± 58.1 (61 %)
	0.5	2.9 ± 0.6	3.6 ± 2.6	3.8 ± 0.9 (14 %), 16.5 ± 5.3 (25 %), 135.3 ± 61.6 (59 %)
EPy–$(Asp_1Phe_1)_n$–44	0.05	3.7 ± 0.7	3.6 ± 1.1	4.5 ± 0.9 (5 %), 153.6 ± 50.2 (95 %)
	0.5	3.8 ± 0.7	4.2 ± 1.2	4.6 ± 0.9 (5 %), 45.7 ± 11.5 (8 %), 173.5 ± 51.8 (86 %)

RPy–$(Asp_1Phe_1)_n$–70	0.05	4.6 ± 1.0	5.0 ± 1.0	5.8 ± 1.2 (10 %), 154.0 ± 62.3 (90 %)
	0.5	4.5 ± 0.8	5.4 ± 1.2	5.3 ± 1.0 (8 %), 158.6 ± 58.6 (92 %)
RPy–$(Asp_1Phe_1)_n$–132	0.05	5.0 ± 0.9	4.9 ± 1.2	5.8 ± 0.9 (14 %), 134.2 ± 69.6 (86 %)
	0.5	4.4 ± 0.5	5.1 ± 1.1	5.2 ± 0.4 (10 %), 59.0 ± 9.8 (30 %), 229.7 ± 44.1 (60 %)
RPy–$(Asp_1Phe_1)_n$–221	0.05	4.2 ± 0.7	4.6 ± 1.5	4.8 ± 0.8 (9 %), 32.2 ± 6.3 (15 %), 142.5 ± 41.5 (75 %)
	0.5	3.6 ± 1.0	4.3 ± 1.0	6.0 ± 1.8 (15 %), 139.3 ± 55.5 (84 %)
$(Asp_1Phe_2)_n$	0.05	4.1 ± 0.8	3.7 ± 0.8	3.7 ± 1.7 (21 %), 107.7 ±56.1 (77%)
	0.5	3.7 ± 0.7	3.4 ± 0.8	4.3 ± 0.9 (38 %), 111.3 ± 43.0 (61 %)
$(Asp_1Phe_2)_n$ + molecular pyrene	0.05	3.1 ± 0.5	3.2 ± 0.6	3.0 ± 0.6 (11 %), 25.3 ± 5.7 (10 %), 211.8 ± 74.8 (77 %)
	0.5	3.5 ± 0.6	3.7 ± 0.6	3.6 ± 0.5 (14 %), 42.9 ± 12.1 (13 %), 240.0 ± 106.2 (71 %)
EPy–$(Asp_1Phe_2)_n$–13	0.05	3.8 ± 0.7	3.5 ± 1.3	4.5 ± 0.7 (9%), 115.0 ± 35.5 (90 %)
	0.5	3.4 ± 0.7	3.8 ± 0.9	4.3 ± 0.9 (5 %), 24.9 ± 6.4 (7%), 162.6 ± 80.0 (86 %)
RPy–$(Asp_1Phe_2)_n$–45	0.05	3.4 ± 0.7	4.6 ± 1.2	6.3 ± 1.0 (23 %), 137.5 ± 43.1 (76 %)
	0.5	3.4 ± 0.7	4.6 ± 0.9	3.9 ± 1.1 (36 %), 143.3 ± 114.5 (63 %)
RPy–$(Asp_1Phe_2)_n$–97	0.05	3.7 ± 0.7	4.8 ± 1.2	6.4 ± 1.1 (13 %), 212.3 ± 107.7 (86 %)
	0.5	3.3 ± 0.7	4.8 ± 1.2	4.1 ± 0.9 (39%), 117.8 ± 75.6 (58 %)
RPy–$(Asp_1Phe_2)_n$–131	0.05	7.1 ± 1.3	4.7 ± 1.1	4.4 ± 0.8 (19 %), 152.6 ± 60.8 (80 %)
	0.5	3.7 ± 0.7	4.5 ± 1.2	4.2 ± 0.7 (37 %), 115.4 ± 42.2 (58 %)
$(Asp_1Phe_3)_n$	0.05	7.7 ± 1.7	7.4 ± 1.8	9.6 ± 2.2 (28 %), 169.9 ± 87.8 (69 %)
	0.5	6.6 ± 1.1	7.3 ± 2.7	8.7 ± 2.5 (24 %), 155.8 ± 41.1 (75 %)
$(Asp_1Phe_3)_n$ + molecular pyrene	0.05	4.5 ± 1.2	3.4 ± 0.6	9.9 ± 4.1 (34 %), 219.6 ± 148.0 (65 %)
	0.5	5.0 ± 1.4	5.8 ± 4.1	10.6 ± 5.5 (353 %), 264.0 ± 195.5 (64 %)
EPy–$(Asp_1Phe_3)_n$–91	0.05	4.7 ± 1.2	5.8 ± 3.7	8.6 ± 2.9 (44 %), 100.5 ± 39.5 (55 %)
	0.5	5.1 ± 1.4	6.3 ± 2.1	8.6 ± 3.5 (43 %), 132.2 ± 71.3 (56 %)
RPy–$(Asp_1Phe_3)_n$–72	0.05	7.7 ± 1.7	7.4 ± 2.1	10.3 ± 2.6 (29 %), 171.4 ± 66.1 (70 %)
	0.5	8.0 ± 1.6	7.2 ± 2.1	8.2 ± 1.6 (22 %), 147.6 ± 36.6 (77 %)
RPy–$(Asp_1Phe_3)_n$–104	0.05	6.3 ± 1.4	7.9 ± 2.5	10.1 ± 2.4 (18 %), 213.9 ± 89.1 (78 %)
	0.5	6.4 ± 1.4	8.3 ± 2.3	9.3 ± 2.6 (24 %), 174.3 ± 65.2 (75 %)

Table A-2. Pre-exponential factors and decay times of the fluorescence decays of 1.0 g/L of EPy–(Asp_3Phe_1)–26 quenched by nitromethane.

[*Q*], M	τ_{M1} (ns)	a_{M1}	τ_{M2} (ns)	a_{M2}	τ_{M3} (ns)	a_{M3}	$\langle\tau_0\rangle$ (ns)	χ^2
0.00000	7	0.07	85	0.20	114	0.72	99	1.03
0.00333	23	0.19	42	0.81	–	–	38	1.19
0.00741	14	0.32	25	0.67	–	–	22	1.22
0.01141	15	0.91	27	0.09	–	–	16	1.23
0.01522	10	0.70	16	0.30	–	–	12	1.12
0.01924	2	0.15	9	0.71	15	0.14	9	1.15
0.02277	6	0.35	9	0.38	12	0.27	8	1.29

Table A-3. Pre-exponential factors and decay times of the fluorescence decays of 0.17 g/L of RPy–(Asp_3Phe_1)–195 quenched by nitromethane.

[*Q*], M	τ_{M1} (ns)	a_{M1}	τ_{M2} (ns)	a_{M2}	τ_{M3} (ns)	a_{M3}	$\langle\tau_0\rangle$ (ns)	χ^2
0.00000	17	0.14	99	0.20	146	0.66	119	1.14
0.00385	15	0.17	42	0.70	51	0.12	38	1.13
0.00781	2	0.21	13	0.18	26	0.61	18	1.09
0.01198	3	0.19	15	0.54	21	0.27	14	1.04
0.01530	2	0.18	13	0.64	18	0.18	12	1.14
0.01940	5	0.29	12	0.71	–	–	10	1.23
0.02320	2	0.20	9	0.63	14	0.17	8	1.18
0.02980	1	0.23	7	0.67	12	0.10	6	1.21

Table A-4. Pre-exponential factors and decay times of the fluorescence decays of 0.29 g/L of RPy–(Asp_3Phe_1)–245 quenched by nitromethane.

[*Q*], M	τ_{M1} (ns)	a_{M1}	τ_{M2} (ns)	a_{M2}	τ_{M3} (ns)	a_{M3}	$\langle\tau_0\rangle$ (ns)	χ^2
0.00000	5	0.16	41	0.14	136	0.70	102	0.99
0.00325	3	0.15	18	0.17	46	0.68	35	1.20
0.00655	4	0.16	12	0.28	30	0.56	23	1.22
0.00984	2	0.17	9	0.21	21	0.61	15	0.92
0.01330	2	0.15	8	0.23	16	0.62	12	1.18
0.02020	2	0.16	7	0.27	12	0.56	9	1.08

TableA-5. Pre-exponential factors and decay times of the fluorescence decays of 0.51 g/L of EPy–(Asp_2Phe_1)–15 quenched by nitromethane.

[*Q*], M	τ_{M1} (ns)	a_{M1}	τ_{M2} (ns)	a_{M2}	τ_{M3} (ns)	a_{M3}	$<\tau_0>$ (ns)	χ^2
0.00000	6	0.10	63	0.05	114	0.85	101	1.03
0.00352	4	0.13	38	0.8	65	0.08	36	1.18
0.01070	2	0.17	19	0.5	30	0.33	20	1.03
0.01600	2	0.21	14	0.75	30	0.05	12	1.20
0.02570	2	0.24	9	0.75	37	0.01	8	1.09
0.03550	2	0.27	7	0.72	37	0.01	6	1.22

TableA-6. Pre-exponential factors and decay times of the fluorescence decays of 1.38 g/L of RPy–(Asp_2Phe_1)–56 quenched by nitromethane.

[*Q*], M	τ_{M1} (ns)	a_{M1}	τ_{M2} (ns)	a_{M2}	τ_{M3} (ns)	a_{M3}	$<\tau_0>$ (ns)	χ^2
0.00000	35	0.16	150	0.84	–	–	131	1.18
0.00343	18	0.19	62	0.81	–	–	54	0.97
0.00683	14	0.24	32	0.76	–	–	27	1.14
0.01050	7	0.15	21	0.83	41	0.03	19	1.17
0.01480	1	0.24	9	0.32	17	0.44	11	1.2
0.02430	3	0.26	9	0.70	17	0.04	8	0.92
0.03550	4	0.52	8	0.48	–	–	6	1.26

TableA-7. Pre-exponential factors and decay times of the fluorescence decays of 0.46 g/L of RPy–(Asp_2Phe_1)–176 quenched by nitromethane.

[*Q*], M	τ_{M1} (ns)	a_{M1}	τ_{M2} (ns)	a_{M2}	τ_{M3} (ns)	a_{M3}	$<\tau_0>$ (ns)	χ^2
0.00000	6	0.14	49	0.15	153	0.71	117	1.03
0.00517	7	0.16	33	0.71	48	0.13	31	0.95
0.00973	6	0.14	18	0.40	25	0.45	19	0.94
0.01380	8	0.28	18	0.71	38	0.01	15	0.97
0.01820	2	0.10	11	0.42	17	0.48	13	1.08
0.02516	2	0.11	6	0.28	11	0.61	9	0.98
0.03210	2	0.19	7	0.47	10	0.33	7	0.91
0.03660	1	0.09	4	0.35	8	0.56	6	0.90

TableA-8. Pre-exponential factors and decay times of the fluorescence decays of 0.36 g/L of RPy–(Asp_2Phe_1)–322 quenched by nitromethane.

[*Q*], M	τ_{M1} (ns)	a_{M1}	τ_{M2} (ns)	a_{M2}	τ_{M3} (ns)	a_{M3}	$<\tau_0>$ (ns)	χ^2
0.00000	13	0.17	62	0.17	151	0.65	111	0.94
0.00389	6	0.16	34	0.37	57	0.47	40	1.20
0.00727	3	0.11	15	0.29	30	0.61	23	1.20
0.01120	5	0.18	18	0.76	31	0.06	16	0.93
0.02120	2	0.22	11	0.64	17	0.13	10	1.08

TableA-9. Pre-exponential factors and decay times of the fluorescence decays of 1.4 g/L of $(Asp_1Phe_2)_n$ solution with 2.2×10^{-6} M pyrene quenched by nitromethane.

[*Q*], M	τ_{M1} (ns)	a_{M1}	τ_{M2} (ns)	a_{M2}	τ_{M3} (ns)	a_{M3}	$<\tau_0>$ (ns)	χ^2
0.0000	11	0.17	122	0.40	310	0.42	181	1.13
0.00469	22	0.41	105	0.26	290	0.33	132	1.11
0.00935	13	0.48	99	0.26	276	0.26	104	1.14
0.01510	11	0.49	88	0.27	265	0.23	90	1.05
0.02090	9	0.50	85	0.29	263	0.21	84	1.28
0.03390	9	0.48	78	0.31	254	0.20	79	1.22
0.04260	9	0.47	73	0.33	247	0.20	78	1.29
0.05140	10	0.46	71	0.34	244	0.20	77	1.13

TableA-10. Pre-exponential factors and decay times of the fluorescence decays of 0.35 g/L of EPy–(Asp_1Phe_2)–13 quenched by nitromethane.

[*Q*], M	τ_{M1} (ns)	a_{M1}	τ_{M2} (ns)	a_{M2}	τ_{M3} (ns)	a_{M3}	$<\tau_0>$ (ns)	χ^2
0.00000	9	0.11	92	0.19	186	0.69	147	1.02
0.00359	21	0.13	81	0.51	168	0.35	103	1.14
0.00837	24	0.31	74	0.47	161	0.22	77	1.07
0.01270	18	0.33	58	0.45	144	0.22	64	1.07
0.01940	11	0.36	46	0.44	133	0.19	49	1.03
0.02920	10	0.43	40	0.40	124	0.16	40	1.09
0.36300	9	0.47	37	0.38	122	0.15	37	1.03
0.04850	9	0.53	38	0.36	125	0.11	32	1.03
0.05830	9	0.50	39	0.37	127	0.13	35	1.06
0.07400	8	0.54	35	0.34	119	0.11	29	1.23

TableA-11. Pre-exponential factors and decay times of the fluorescence decays of 0.33 g/L of RPy–(Asp_1Phe_2)–45 quenched by nitromethane.

[*Q*], M	τ_{M1} (ns)	a_{M1}	τ_{M2} (ns)	a_{M2}	τ_{M3} (ns)	a_{M3}	$<\tau_0>$ (ns)	χ^2
0.00000	84	0.30	–	–	236	0.70	190	1.20
0.00585	28	0.19	88	0.53	188	0.27	103	1.00
0.01590	23	0.39	67	0.48	167	0.13	62	1.09
0.02430	18	0.47	59	0.43	156	0.10	49	1.20
0.03520	16	0.53	53	0.39	153	0.08	41	1.16
0.04520	14	0.50	45	0.41	139	0.08	36	1.10
0.05550	12	0.54	41	0.38	132	0.08	32	1.12
0.06930	10	0.56	36	0.36	120	0.08	28	1.11

TableA-12. Pre-exponential factors and decay times of the fluorescence decays of 0.11 g/L of RPy–(Asp_1Phe_2)–97 quenched by nitromethane.

[*Q*], M	τ_{M1} (ns)	a_{M1}	τ_{M2} (ns)	a_{M2}	τ_{M3} (ns)	a_{M3}	$<\tau_0>$ (ns)	χ^2
0.00000	20	0.14	104	0.30	240	0.56	169	1.05
0.00634	19	0.18	79	0.52	177	0.29	96	0.95
0.01270	22	0.28	68	0.54	162	0.18	72	0.98
0.01990	17	0.33	56	0.53	148	0.15	57	1.15
0.02920	17	0.43	55	0.46	147	0.10	48	1.07
0.03810	15	0.48	49	0.43	138	0.10	41	1.19
0.04710	13	0.47	42	0.43	126	0.10	35	1.03
0.05700	13	0.51	40	0.40	123	0.08	33	1.04
0.06670	11	0.51	36	0.40	113	0.09	30	0.99

Table A-13. Pre-exponential factors and decay times of the fluorescence decays of 0.33 g/L of RPy−(Asp_1Phe_2)−131 quenched by nitromethane.

[*Q*], M	τ_{M1} (ns)	a_{M1}	τ_{M2} (ns)	a_{M2}	τ_{M3} (ns)	a_{M3}	$<\tau_0>$ (ns)	χ^2
0.00000	16	0.15	91	0.29	232	0.55	156	1.07
0.00365	11	0.16	76	0.39	190	0.45	117	1.04
0.00752	17	0.21	72	0.50	163	0.29	87	1.03
0.01460	15	0.25	58	0.51	140	0.23	65	1.11
0.02160	15	0.33	52	0.51	133	0.16	53	1.18
0.02880	12	0.35	46	0.51	125	0.14	45	1.05
0.03500	11	0.34	41	0.52	118	0.13	40	0.99
0.04120	12	0.41	41	0.48	119	0.11	38	1.01
0.04780	11	0.43	42	0.45	120	0.10	36	1.18
0.05440	11	0.45	38	0.45	114	0.10	33	1.07
0.06100	9	0.43	34	0.46	104	0.11	31	1.02
0.06730	10	0.47	34	0.44	104	0.10	30	1.09
0.07580	9	0.51	34	0.41	108	0.08	27	0.98
0.08340	9	0.52	34	0.40	107	0.07	26	1.24
0.09000	7	0.46	27	0.44	91	0.10	24	1.08

Table A-14. Pre-exponential factors and decay times of the fluorescence decays of 1.50 g/L of $(Asp_1Phe_3)_n$ solution with 5.1×10^{-6} M pyrene quenched by nitromethane.

[*Q*], M	τ_{M1} (ns)	a_{M1}	τ_{M2} (ns)	a_{M2}	τ_{M3} (ns)	a_{M3}	$<\tau_0>$ (ns)	χ^2
0.00000	12	0.16	130	0.24	314	0.60	222	0.97
0.00412	19	0.27	117	0.28	285	0.46	167	1.05
0.00890	16	0.30	107	0.31	270	0.38	141	1.09
0.01734	14	0.34	101	0.35	260	0.31	121	1.06
0.02630	12	0.35	94	0.37	252	0.28	109	1.24
0.03180	12	0.35	86	0.36	242	0.29	105	1.15
0.03570	13	0.34	91	0.38	249	0.27	106	1.29
0.04440	13	0.35	82	0.40	236	0.25	96	1.18
0.05270	13	0.37	82	0.40	235	0.23	92	1.10

Table A-15. Pre-exponential factors and decay times of the fluorescence decays of 1.1 g/L of EPy–(Asp_1Phe_3)–91 quenched by nitromethane.

[*Q*], M	τ_{M1} (ns)	a_{M1}	τ_{M2} (ns)	a_{M2}	τ_{M3} (ns)	a_{M3}	$<\tau_0>$ (ns)	χ^2
0.00000	6	0.12	85	0.22	180	0.66	138	1.04
0.00388	6	0.14	69	0.46	147	0.40	91	1.09
0.01036	16	0.23	55	0.54	128	0.23	63	1.12
0.01581	14	0.32	50	0.51	121	0.16	49	1.00
0.02139	12	0.34	43	0.51	113	0.15	43	1.13
0.02775	10	0.40	38	0.48	106	0.12	35	1.11
0.03193	11	0.42	36	0.45	102	0.12	33	1.21
0.03812	10	0.46	34	0.43	99	0.11	30	1.23
0.04339	11	0.52	35	0.39	101	0.09	28	1.25
0.04895	9	0.51	32	0.40	96	0.09	26	0.99

Table A-16. Pre-exponential factors and decay times of the fluorescence decays of 0.36 g/L of RPy–(Asp_1Phe_3)–72 quenched by nitromethane.

[*Q*], M	τ_{M1} (ns)	a_{M1}	τ_{M2} (ns)	a_{M2}	τ_{M3} (ns)	a_{M3}	$<\tau_0>$ (ns)	χ^2
0.00000	26	0.11	118	0.34	226	0.56	169	1.05
0.00498	31	0.28	80	0.50	182	0.21	87	1.10
0.01078	22	0.44	62	0.40	160	0.15	59	1.10
0.01590	17	0.48	55	0.39	151	0.13	49	1.10
0.02130	16	0.55	56	0.34	147	0.11	44	1.06
0.02720	14	0.56	51	0.34	142	0.10	39	0.92
0.03220	12	0.59	48	0.32	136	0.09	35	1.05
0.03700	11	0.59	46	0.32	135	0.08	32	1.03
0.04900	9	0.58	39	0.33	126	0.09	30	1.20
0.05400	9	0.60	39	0.32	124	0.08	27	1.21

Table A-17. Pre-exponential factors and decay times of the fluorescence decays of 0.26g/L of RPy−(Asp_3Phe_1)−104 quenched by nitromethane.

[*Q*], M	τ_{M1} (ns)	a_{M1}	τ_{M2} (ns)	a_{M2}	τ_{M3} (ns)	a_{M3}	$<\tau_0>$ (ns)	χ^2
0.00000	21	0.10	12	0.31	228	0.59	140	1.06
0.00549	25	0.20	72	0.55	178	0.24	87	1.08
0.01070	21	0.38	59	0.45	159	0.17	61	1.06
0.01610	19	0.49	58	0.37	153	0.14	52	1.01
0.02140	16	0.53	55	0.35	149	0.12	46	1.12
0.02640	13	0.52	48	0.36	140	0.11	39	1.18
0.03180	13	0.57	49	0.34	142	0.10	37	1.09
0.03770	11	0.57	45	0.33	135	0.10	34	1.02
0.04670	9	0.58	40	0.32	125	0.10	30	1.09
0.05900	7	0.54	30	0.35	106	0.11	26	1.20

Chapter 6

Concluding Remarks and Future work

6.1. Summary of accomplished work

The ability of amphiphilic polymers to spontaneously self-assemble in aqueous solution due to weak hydrophobic interactions has received considerable attention over the past years.[1] Their self-assembly can be used to better control the rheology of solutions[1,2] and to generate various morphologies such as micelles, vesicles, rods, large compound micelles or large compound vesicles.[3] The properties of amphiphilic polymers in solution depend largely on their molecular structure and on the balance between the hydrophilic and hydrophobic segments or groups. This has sparked a great deal of interest in the synthesis of amphiphilic polymers tailor-made for specific applications. One of their most important property, which is of main interest to this work, is their ability to solubilize insoluble molecules, which makes them suitable as carriers of hydrophobic cargo.[4,5] Thus amphiphilic polymers are of interest not only for their industrial applications but also in biomedicine as well.

The motivation for this work came from a research project carried out in our laboratory where the alternating copolymers of styrene and maleic anhydride (SMA)[6] were found to self-assemble in aqueous alkaline solution. Their ability to solubilize and release hydrophobic molecules such as pyrene, phenanthrene, and anthracene was studied using fluorescence. The results obtained confirmed that they were suitable as carriers of hydrophobic cargo. However SMAs are not biocompatible and thus can not be used as carriers for hydrophobic drugs under physiological conditions. The ideal situation is to use biomolecules such as amino acids that are available for constructing amphiphilic polypeptides. Thus the aim of this thesis was to synthesize and characterize a series of amphiphilic polypeptides with well-defined sequences consisting of aspartic acid (Asp) as

the hydrophilic monomer and phenylalanine (Phe) as the hydrophobic monomer. These amino acids have a chemical structure similar to that of SMAs. The resulting polypeptides show a gradual increase from a hydrophilic to hydrophobic character and are expected to undergo self-assembly with increasing facility.

The first goal of this thesis was the synthesis of these polypeptides. The approach was to prepare five polypeptides, $(Asp_3Phe_1)_n$, $(Asp_2Phe_1)_n$, $(Asp_1Phe_1)_n$, $(Asp_1Phe_2)_n$, and $(Asp_1Phe_3)_n$, going from an Asp rich polypeptide with a hydrophilic character to increasingly hydrophobic polypeptides. The synthesis of the polypeptides was carried out using the classical solution method[7] utilizing a minimum number of steps. For polymerization purposes, either a tetrapeptide active ester consisting of four amino acids arranged in the required sequence or a tripeptide active ester having three amino acids in the required sequences were prepared. For the alternating polypeptide, the "tetrapeptide monomer" was prepared by extending from its amino end by the aminolysis of the Boc–Asp(OBzl)–OSu ester with the free H–Phe–OH using DCC (dicyclohexylcarbodiimide) as the coupling agent. The Boc group was removed with trifluoroacetic acid (TFA). Each subsequent amino acid addition went through an activation, a coupling and a deprotection step eventually resulting in Boc–Asp(OBzl)–Phe–Asp(OBzl)–Phe–OH. This procedure ensured minimum racemization throughout the synthesis. The Boc-tetrapeptide was then activated with *N*–hydroxysuccinimide (HOSu) and the Boc group removed before polymerization. All "peptide monomers" were prepared in a similar manner. The intermediates and the "peptide monomers" were obtained in good yields and high purity as observed by their sharp melting points and single spots on TLC. ^{1}H NMR for each intermediate and peptide monomer was obtained and the chemical shifts obtained agreed well with those expected. The molecular

weight values of the peptide monomers obtained from mass spectrometry were also as expected.

The polymerization was carried out in DMSO using triethylamine. The benzyl protecting group of the Asp side-chain was finally removed after completing the polymerization. ^{1}H NMR spectra were acquired for the polypeptides before and after the final removal of the benzyl group. The absolute weight-average molecular weight (M_W) of the polypeptides was obtained using static light scattering (SLS).

The photophysical properties of the polypeptides of the series $(Asp_xPhe_y)_n$ were investigated in aqueous solution at pH 9. All subsequent experiments for the polypeptides were performed in aqueous solutions of 0.01 M Na_2CO_3 at pH 9 which ensured that all the polypeptides were fully ionized and hence under the same conditions. The UV-Vis experiments resulted in absorbance peaks at 254, 260, and 264 nm due to phenylalanine (Phe). These absorption peaks are red shifted by 2 nm compared to those observed for Phe (252, 258, and 262 nm). A linear increase was observed for the absorbance of the polypeptide solutions as the Phe content of the polypeptide increased. The molar extinction coefficients for the polypeptides was found to equal 230 ± 15 $L.cm^{-1}$ per mole of Phe in the polypeptide but similar to that found for Phe-rich polypeptides.[8] This is slightly higher than that determined for Phe (202 $L.mol^{-1}.cm^{-1}$ in 0.1 M NaCl solution) which maybe due to the formation of ground-state dimers of the hydrophobic Phe as a result of its high local concentration in the polypeptides. Similarly the fluorescence intensity of the polypeptides showing a peak maximum at 290 nm increased linearly with the Phe content of the polypeptide. The peak maximum for Phe was at 281 nm. The fine structure obvious in the Phe fluorescence spectrum is lost once it is bound to the polypeptide, certainly due to the

hydrophobic interactions leading to ground-state Phe dimers. The lifetimes obtained for the polypeptides were also found to be dependent on the Phe content of the polypeptides and increased with increasing Phe content. They were also longer-lived than Phe. The circular dichroism spectra obtained for the polypeptides revealed that except for the $(Asp_1Phe_3)_n$ polypeptide which adopts an α–helical conformation, the other polypeptides show no evidence of any clear secondary structure. These results suggest that the photophysical properties of the polypeptides $(Asp_3Phe_1)_n$, $(Asp_2Phe_1)_n$, $(Asp_1Phe_1)_n$, $(Asp_1Phe_2)_n$, and $(Asp_1Phe_3)_n$ are strongly affected by the Phe content of the polypeptides and the intensity of these properties increases as the polypeptides become richer in Phe.

The examination of the associative properties in solution of the alternating polypeptide $(Asp_1Phe_1)_n$, the polypeptide with a molecular structure similar to that of the alternating SMAs, was the third task undertaken in this thesis. The results obtained were compared to the solution properties of $(Asp)_n$ which is a random coil in a 0.01 M Na_2CO_3 solution at pH 9. The polypeptide was studied in its various forms, with pyrene dissolved as a molecular probe, randomly labeled with 1–pyrenemethylamine, and end-labeled with 1–pyrenebutyric acid at the amino end. Circular dichroism spectra obtained for both the unlabeled and randomly labeled $(Asp_1Phe_1)_n$ and $(Asp)_n$ resulted in no change in the CD spectra before and after the labeling indicating that this modification does not affect the polypeptide conformation. The particle size distribution obtained by dynamic light scattering DLS, indicated the formation of polypeptide aggregates when the light scattering data were analyzed using light scattering intensities. However no aggregate could be found when using the numbers or volumes to analyse the DLS data. Non-radiative energy transfer (NRET) experiments were performed using naphthalene and pyrene as the donor/acceptor pair to

confirm the existence of the polypeptide aggregates suggested by the DLS intensity profiles. No NRET was observed to take place between a naphthalene labeled polypeptide and a pyrene labeled polypeptide. This result agrees with the number and volume profiles obtained by DLS and suggests that the alternating polypeptide is essentially present as individual chains.

The I_1/I_3 ratio which equals 1.24 when pyrene is present as a free probe and 1.42 when they are randomly labeled with pyrene indicated a hydrophobic microenvironment for the pyrene implying the presence of hydrophobic microdomains in $(Asp_1Phe_1)_n$. The long lifetime of 299 ns obtained for pyrene used as a free probe also points to the existence of these hydrophobic domains since such a long lifetime in aerated aqueous solution is only possible when pyrene is protected from quenching by the atmospheric oxygen. Clear evidence of protective quenching was observed for pyrene used as a free probe in fluorescence quenching experiments carried out using nitromethane as a water-soluble quencher. The results showed that around 40 % of the pyrene molecules are not accessible to the quencher and are long-lived. Protective quenching was absent for both the randomly labeled and the end-labeled $(Asp_1Phe_1)_n$ demonstrating that pyrene is more accessible to the quencher, when pyrene is covalently attached to the polypeptide, preventing pyrene to target the hydrophobic microdomains. Static light scattering and fluorescence emission spectra obtained for the unlabeled polypeptide before and after filtration using a 20 nm pore size filter showed a large decrease in the scattering intensity which further substantiates the presence of polymeric aggregates. However only a negligible decrease is observed in the fluorescence emission spectra of the polypeptide after filtration which confirms the results obtained from NRET and fluorescence quenching studies that the alternating polypeptide is

essentially present as individual chains.

The final task involved the investigation of the effect of the polypeptide sequence on the associative properties of the polypeptides. Five polypeptides having well-defined repeating sequences with increasing hydrophobic character, $(Asp_3Phe_1)_n$, $(Asp_2Phe_1)_n$, $(Asp_1Phe_1)_n$, $(Asp_1Phe_2)_n$, and $(Asp_1Phe_3)_n$ were studied. It was expected that as the hydrophobicity of the polypeptide would increase, so would their ability to self-assemble and generate hydrophobic microdomains. From the CD spectra it was deduced that only $(Asp_1Phe_3)_n$ exhibited a clear conformation, that of an α–helix, whereas the other polypeptides did not show any obvious conformation. This α–helical conformation was retained even after $(Asp_1Phe_3)_n$ was randomly labeled with 1-pyrenemethylamine. No change was observed in the CD spectra of the other polypeptides after their labeling. The particle size distribution of the polypeptide solutions obtained from the analysis of the DLS data with light scattering intensity pointed towards the presence of polymeric aggregates for all polypeptides regardless of their sequences. However the number and volume profiles indicated that only single polymeric chains were present in solutions for these polypeptides. The absence of NRET for the $(Asp_3Phe_1)_n$, $(Asp_2Phe_1)_n$, and $(Asp_1Phe_1)_n$ polypeptides confirmed the presence of unimolecular micelles observed in the number and volume profiles by DLS experiments. Energy transfer between a naphthalene labeled polypeptide and a pyrene labeled polypeptide was detected for the two most hydrophobic polypeptides, $(Asp_1Phe_2)_n$ and $(Asp_1Phe_3)_n$, with an energy transfer efficiency of 16 % and 30 %, respectively. The existence of NRET strongly suggests that these two polypeptides are able to undergo intermolecular hydrophobic association to generate polymeric aggregates.

Pyrene was used as a free probe for only the $(Asp_1Phe_1)_n$, $(Asp_1Phe_2)_n$, and

$(Asp_1Phe_3)_n$ polypeptides since it could not be solubilized in the solutions of the more hydrophilic polypeptides. The I_1/I_3 values which equal 1.24, 1.20, and 1.24 and the long decay times of 299, 309, and 314 ns observed for pyrene in, respectively, $(Asp_1Phe_1)_n$, $(Asp_1Phe_2)_n$, and $(Asp_1Phe_3)_n$, confirmed the ability of these polypeptides to generate hydrophobic microdomains capable of encapsulating and protecting pyrene. The randomly labeled polypeptides show that the I_1/I_3 ratio gradually decreased from 1.69 to 1.29 as the polypeptides became richer in Phe. The decay times also show the same trend. As the Phe content increases, the polypeptides are more able to generate hydrophobic domains which are targeted by the hydrophobic pyrenes. Little pyrene excimer was observed for polypeptide solutions where pyrene was used as a free probe or for the end-labeled polypeptides. Formation of excimers was only seen for the randomly labeled polypeptides and their I_E/I_M ratios were determined. The I_E/I_M ratios were found to be dependent on the polypeptide sequence with the highest values obtained for the $(Asp_1Phe_1)_n$ alternating polypeptide. The lower excimer formation observed for the hydrophilic polypeptides $(Asp_3Phe_1)_n$ and $(Asp_2Phe_1)_n$ was rationalized from their extended coil conformation due to electrostatic repulsion from the negatively charged aspartate ions whereas the α–helical conformation adopted by the $(Asp_1Phe_3)_n$ polypeptide would reduce excimer formation due to the extended conformation adopted by the polypeptides.

The fluorescence quenching studies showed evidence of protective quenching for the hydrophobic polypeptides $(Asp_1Phe_2)_n$ and $(Asp_1Phe_3)_n$ whether pyrene was used as a free probe or covalently attached onto the polypeptide randomly or at the end. Diffusional quenching observed for both the randomly labeled and end-labeled hydrophilic polypeptides indicated that pyrene was exposed to the quencher. The quenching rate constant k_Q decreased

as the polypeptides became richer in Phe, leveling off for the $(Asp_1Phe_2)_n$ and $(Asp_1Phe_3)_n$ polypeptides. This result agrees with the NRET experiments since NRET only occurs for the two most hydrophobic polypeptides. The emission spectra for the polypeptides acquired before and after filtration showed a strong decrease in scattering intensity and a small to modest decrease in the emission intensity reaching a maximum value of 35 % for the $(Asp_1Phe_3)_n$ polypeptide. These results confirm those obtained by NRET and fluorescence quenching that $(Asp_3Phe_1)_n$, $(Asp_2Phe_1)_n$, and $(Asp_1Phe_1)_n$ are predominantly present as individual chains whereas $(Asp_1Phe_2)_n$ and $(Asp_1Phe_3)_n$ have the ability to generate polymeric aggregates via interpolymeric hydrophobic associations.

This thesis has demonstrated the power of fluorescence techniques in characterizing the associative behaviour of hydrophobically modified polypeptides in aqueous solution. The ability of the polypeptides to associate either intra- or intermolecularly via hydrophobic interactions and the hydrophobic microdomains thus generated have been investigated comprehensively using fluorescence energy transfer together with fluorescence quenching.

6.2. Future work

If the polypeptide aggregates encountered in this work for the $(Asp_1Phe_2)_n$ and $(Asp_1Phe_3)_n$ polypeptides are to be used for drug delivery applications, their stability must be tested upon dilution, since diluting a solution of polypeptide aggregates should lead to their dissociation. Further fluorescence experiments can be carried out to investigate these effects. Fluorescence energy transfer experiments could be conducted with a solution of Py labeled $(Asp_1Phe_3)_n$ and a solution of Np labeled $(Asp_1Phe_3)_n$ that has already been shown to yield NRET. The solution will be diluted ten folds with a 0.01 M Na_2CO_3 solution at pH 9 and the

fluorescence emission of either Np or Py can be monitored over time to observe whether any change is occurring. A decrease in the efficiency of NRET would point towards the dissociation of these polypeptide aggregates upon dilution. These experiments will also provide the time scale over which dissociation takes place.

Pyrene has been used as a model for hydrophobic drugs to demonstrate the ability of hydrophobically modified polymers to solubilize and release hydrophobic cargos into cell mimics such as liposomes. Duhamel et al.[9] have demonstrated that microcrystals of pyrene can be stabilized by EAK16 II, an oligopeptide made up of glutamic acid (E), alanine (A), and lysine (K). The peptide is constituted of 16 amino acids arranged in a sequence that alternates the negatively charged glutamic acids and the positively charged lysines separated by a hydrophobic alanine. EAK16 II has been shown to exhibit a hydrophilic and hydrophobic surface when it adopts a β-sheet upon self-assembly into highly stable peptide aggregates. The release behavior of pyrene from EAK16 II into membrane bilayers made up of the egg phosphatidylcholine (EPC) vesicles was studied using fluorescence over time. From the release profiles obtained, it was shown that EAK16 II can be used as a potential carrier for a hydrophobic cargo. It would be interesting to investigate how the polypeptides $(Asp_xPhe_y)_n$ that exhibits a more hydrophobic character than EAK16 II would behave in similar conditions. It would be expected that the polypeptides richer in Phe would be better able to stabilize pyrene crystals since they have already been shown to take up pyrene through hydrophobic associations. They are also able to form polymeric aggregates thus providing a larger surface for pyrene crystals to be adsorbed onto.

Replacing phenylalanine with a more hydrophobic amino acid such as tryptophan (Trp) might deserve investigation. The higher hydrophobicity of Trp would be expected to

facilitate hydrophobic associations and the generation of a greater number of hydrophobic microdomains both intra- and intermolecularly. The higher hydrophobicity of Trp may make it possible to load a higher amount of a hydrophobic cargo like our reference, pyrene, into these polypeptides as it was not possible to load any significant amount of pyrene into the $(Asp_xPhe_y)_n$ polypeptides. This would make the $(Asp_xTrp_y)_n$ polypeptides better candidates for their potential use as carriers of hydrophobic cargo. The ability of these polypeptides to self-assemble into aggregates can be established by using the fluorescence techniques outlined in this thesis. The results would be compared with those already obtained with the $(Asp_xPhe_y)_n$ polypeptides.

The polypeptides investigated in this thesis are negatively charged in their basic or neutral aqueous solution. Polypeptides containing lysine (Lys) instead of aspartic acid, $(Lys_xPhe_y)_n$, would operate in acidic aqueous solutions. $(Lys_xPhe_y)_n$ polypeptides with an either random or alternating sequence have been synthesized by Arfmann et al.[10] However their associative behaviour has not been examined. This can be done using fluorescence as has been shown for the $(Asp_xPhe_y)_n$ polypeptides. A more complex system could be developed by combining the two families of $(Asp_xPhe_y)_n$ and $(Lys_xPhe_y)_n$ polypeptides into a series of $(Asp_xPhe_yLys_z)_n$ polypeptides. This would enable the associative behavior of the polypeptides to be studied over the entire pH range. Such polypeptides would exhibit self-assembling properties similar to those encountered with the EAK peptide family. Such polypeptides could also stabilize pyrene crystals in solution as EAK16 II with its alternating pairs of negatively charged and positively charged repeating units does.[9] Fluorescence can be used to provide a comprehensive characterization of the self-assembly of these polypeptides.

Interaction of DNA with polycations such as poly(lysine) are used to increase the

efficiency of transformation of cells with plasmids and to prevent its splitting by cell nucleases.[11,12] Since the base pairs of DNA are comprised of aromatic groups it would be useful to study their interaction with a hydrophobically modified poly(lysine) either with phenylalanine $(Lys_xPhe_y)_n$ or tryptophan, $(Lys_xTrp_y)_n$. The association would be expected to proceed via two mechanisms. First strong electrostatic interactions would take place between the positively charged lysine of the polypeptide and the negatively charged DNA phosphates. Second $\pi-\pi$ stacking should occur between the Phe or Trp residues of the polypeptides and the DNA bases. The efficiency of stacking might depend on the spacing between two consecutive phenylalanine or tryptophan residues.

6.3. References:

1. *Hydrophilic Polymers : Performance with Environmental Acceptability* Ed. J. E. Glass; ACS Advances in Chemistry Series 248; 1996.
2. Yekta, A.; Duhamel, J.; Adiwidjaja, H.; Brochard, P.; Winnik, M. A. *Langmuir* **1993**, *9*, 881-883.
3. Förster, S.; Plantenberg, T. *Angew. Chem. Int. Ed*. **2002**, *41*, 688-714.
4. Lavasanifar, A.; Samuel, J.; Kwon, G. S. *Adv. Drug Deliv*. *Rev*. **2002**, *54*, 169-190.
5. a) Kataoka, K.; Harada, A.; Nagasaki, Y. *Adv. Drug Deliv. Rev*. **2001**, *47*, 113-131. b) Kwon, G. S.; Naito, M.; Kataoka, K.; Yokoyama, M.; Sakuri, Y.; Okano, T. *Coll. Surf. B: Biointerfaces* **1994**, *2*, 429-424. c) Yokoyama, M.; Miyauchi, M. ; Yamada, N.; Okano, T.; Sakuri, Y.; Kataoka, K.; Inoue, S. *J. Control. Rel.* **1990**, *11*, 269-278.
6. Claracq, J.; Santos, S. F. C. R.; Duhamel, J. ; Dumousseaux, C. ; Corpart, J. –M. *Langmuir*, **2002**, *18*, 3829-3835.
7. Fukushima, Y. *Polym. Bull.* **2000**, *45*, 237-244.
8. Auer, H. E.; Doty, P. *Biochemistry* **1966**, *5*, 1708-1715.
9. Keyes-Baig, C.; Duhamel, J.; Fung, S. –Y.; Bezaire, J.; Chen, P. *J*. *Am*. *Chem*. *Soc*. **2004**, *126*, 7522-7532.
10. Seipke, G.; Arfmann, H. –A.; Wagner, K. G. *Biopolymers* **1974**, *13*, 1621-1633.
11. Zhou, Y.; Li, Y. *Biophysical Chem*. **2004**, *107*, 273-281.
12. Akitaya, T.; Seno, A.; Nakai, T.; Hazemoto, N.; Murata, S.; Yoshikawa, K. *Biomacromolecules* **2007**, *8*, 273-278.